Agr polymorphisms and exotoxin production in *Staphylococcus aureus*

Dr. Tim John Sloan

BMedSci (Hons), BMBS, DTM&H, MSc.

Thesis submitted to the University of Nottingham

for the degree of Doctor of Philosophy

January 2014

Declaration

Unless otherwise stated, all work presented here is my own and has not been submitted for any other degree at the University of Nottingham or any other institute of learning.

Dr. Tim Sloan

January 2014

Abstract

Staphylococcus aureus is a highly successful human pathogen capable of colonising and spreading easily between humans while causing a wide range of infections, including life threatening bacteraemias, endocarditis and pneumonia. Virulence gene expression is regulated primarily by the staphylococcal accessory gene regulator (*agr*) in a cell density-dependent manner termed quorum sensing. Strains of *S. aureus,* particularly community-associated methicillin resistant *S. aureus* (CA-MRSA), carrying the genes for a pore forming exotoxin, the Panton Valentine Leukocidin (PVL), have been spreading worldwide over the last 10 to 15 years. As high level production of exotoxins has been implicated in the success of the CA-MRSA clone USA300, a collection of PVL producing clinical isolates from Nottingham were studied with the aim of understanding why PVL production might vary between strains.

Sequence typing of the Nottingham strain collection revealed that high PVL producing ST22 *agr* group 1 and low PVL producing ST30 *agr* group 3 strains were the most common types. PVL production was stimulated by addition of the type specific exogenous autoinducing peptide (AIP), which activates the *agr* sensor AgrC, and inhibited by the AgrC antagonist (ala^5)AIP-1 if added before a critical cell population density was reached. Analysis of the *pvl* promoter identified predicted binding sites for RNA polymerase and the SarA protein family of regulators. Promoter pull down experiments confirmed the binding of several staphylococcal regulators to both the *agr* and *pvl* promoters including SarA, SarS, Rot and MgrA indicating that these are likely to play a role in the regulation of PVL production.

Analysis of the *agr* locus of high and low PVL producing strains found that a low PVL producing ST22 *agr* group 1 strain TS13 had a single nucleotide polymorphism (SNP) conferring an N267I substitution in the cytoplasmic domain region of *agrC* not present in a high PVL producing ST22 strain TS14. Whole genome sequencing of these strains revealed them to be closely related to each other, differing by less than 200 SNPs across their core genomes. While not possessing an SCC*mec* element, they carried phages encoding *pvl* and the immune evasion complex (IEC) comprising staphylokinase, the chemotaxis inhibitory protein (CHIPS) and the staphylococcal complement inhibitor (SCIN).

AgrC N267I reduced sensitivity to AIP in a bioluminescent reporter for *agr* which responds to but does not produce AIP. Introducing AgrC N267I into an *agr* reporter which both produces and senses AIP resulted in delayed autoinduction. This appeared to explain the delay in AIP autoinduction observed in TS13 as compared with TS14 with resulting low PVL production. Other naturally occurring *agrC* cytoplasmic mutations including T247I and I311T/A343T reduced AIP sensitivity and were associated with delayed autoinduction and reduced exotoxin production.

PVL production is closely regulated by *agr* with expression mediated by several staphylococcal regulators in a cell population density dependent manner. Mutations in *agrC* occur naturally, delay autoinduction, can have a marked impact on exotoxin production and may be a form of adaptation to niches where high level *agr* expression is not required.

Acknowledgements

I've been fortunate to have had an extraordinary amount of support and input from many different people in order to complete this study. In particular, Professor Paul Williams has been a constant source of guidance, ideas and encouragement from beginning to end. Professor Richard James first captured my interest on the subject of PVL *S. aureus* and his thoughtful comments and insights have been invaluable.

The laboratory work was challenging at times and I think parts of this project would not have been possible without the input of Victoria Steele and Ewan Murray, who were always willing to delay whatever they were doing to help me. In the early stages, Alan Cockayne devoted a sizeable portion of his time towards getting me started and Kome Otokunefor's typing of my clinical strains was also a great help in making sense of the collection. I am also incredibly grateful to Hardeep Naghra for her input with the whole genome sequencing analysis. I learned a great deal from her and would have spent considerably longer analysing the sequence data without her guidance and expertise. For discussions, data sharing and providing clinical strains I'd like to thank Ruth Massey and colleagues. The data derived from collaborating with her group came to form an essential component of the latter stages of my lab work.

Through the various trials and tribulations of PhD study, family and friends have shared the highs and the lows. My wife Em has undoubtedly kept me going when I would otherwise have ground to a halt, having already been through the experience herself. My three children Raph, Nina and Caleb, the latter two arriving part way through, make all the hard work worthwhile. Finally I am grateful for the touches of providence experienced along the way, bringing fresh insight and energy when I needed it most.

Abbreviations

°C	degree centigrade
aa	amino acid
agr	accessory gene regulator
AIP	autoinducing peptide
Amp	ampicillin
AMP	antimicrobial peptide
BHI	brain heart infusion
BLAST	basic local alignment search tool
bp	base pair
CA-MRSA	community associated methicillin resistant *Staphylococcus aureus*
CC	clonal complex
cDNA	copy deoxyribonucleic acid
CHIPS	chemotaxis inhibitory protein
Cm	chloramphenicol
CT	cycle threshold
dH_2O	deionised water
DMSO	dimethyl sulfoxide
DNA	deoxyribonucleic acid
dNTP	deoxyribonucleotide triphosphate
EC_{50}	median effective concentration (required to induce a 50% effect)
EDTA	ethylenediaminetetraacetic acid
Ery	erythromycin
FASTA	'fast all' file format
g	gram
gDNA	genomic DNA
h	hour
HA-MRSA	hospital associated methicillin resistant *Staphylococcus aureus*
HPK	histidine protein kinase
Kan	kanamycin
kb	kilobases
kDa	kiloDalton
kV	kilovolt
L	liter
LB	Lysogeny Broth
M	molar
mA	milliampere
Mb	megabases
MALDI	matrix-assisted laser desorption/ionization
mg	milligram
min	minutes
ml	milliliters
MLST	multi locus sequence type
mm	millimeters
mM	millimolar
MSCRAMM	microbial surface components recognizing adhesive matrix molecules
MSSA	methicillin sensitive *Staphylococcus aureus*
mRNA	messenger ribonucleic acid

MRSA	methicillin resistant *Staphylococcus aureus*
ng	nanogram
NLRP3	NLR family, pyrin domain-containing 3
o/n	overnight
OD_{600}	optical density at a wavelength of 600 nanometers
ORF	open reading frame
PAGE	polyacrylamide gel electrophoreses
PBS	phosphate buffer saline
PBST	phosphate buffer saline tween20
PCR	polymerase chain reaction
PEG	polyethylene glycol
PET	positron emission tomography
PSM	phenol soluble modulin
PVL	Panton Valentine leukocidin
QS	quorum sensing
RLU	relative light units
RNA	ribonucleic acid
RR	response regulator
RT-PCR	reverse transcriptase polymerase chain reaction
rpm	revolutions per minute
s	seconds
SCC	staphylococcal cassette chromosome
SCIN	staphylococcal complement inhibitor
SDS	sodium dodecyl sulfate
SNP	single nucleotide polymorphism
SPECT	single-positron emission computed tomography
SSTI	skin and soft tissue infection
ST	sequence type
TCS	two component system
TEMED	N,N,N',N'-tetramethylethylenediamine
Tet	tetracycline
TSB	tryptic soy broth
TSST-1	toxic shock syndrome toxin 1
U	units
UV	ultraviolet
V	Volt
% vol/vol	percent volume per volume
% wt/vol	percent weight pr volume
µF	microFarad
µg	microgram
µl	microliter
µm	micrometer
µM	micromolar

Table of contents

1 Introduction

1.1 *Staphylococcus aureus*

1.1.1 Cell structure and phylogeny

Staphylococcus aureus, a member of the family Staphylococcaceae, belongs to the phylum Firmicutes, a diverse collection of Gram positive organisms traditionally classified as having low GC content (Figure 1.1).

Analysis of signature insertions in the sequences of a number of important conserved genes, including DNA gyrase and RNA polymerase, between phyla suggests that the Firmicutes were one of the earliest eubacterial groupings to develop. Both the Firmicutes and the Archaea lack many signature insertions in conserved genes which are present in other, particularly Gram negative, eubacterial phyla (Griffiths & Gupta, 2004).

As geological data suggests that the early atmosphere of the earth did not contain oxygen, anaerobic Firmicutes such as the Clostridia were probably the earliest members of the phylum to develop. The great oxygenation event is believed to have occurred approximately 2.5 to 3 billion years ago as a consequence of the activity of photosynthesizing cyanobacteria and would have presumably enabled the development of the facultatively anaerobic and aerobic members of the class Bacilli (Crowe *et al*, 2013; Holland, 2006).

The thickened cell wall characteristic of the Firmicutes and other Gram positive bacteria gives the bacterial cell a protective structure against environmental hazards, such as osmotic and shearing forces, that would otherwise damage the cell membrane and destroy the cell. The cell wall also facilitates cell division and inhibits uncontrolled uptake of foreign DNA. The simpler Gram positive cell structure with a single inner membrane is believed to have been the

precursor of the double membrane structure characteristic of Gram negative bacteria (Errington, 2013).

Figure 1.1 The phylum Firmicutes

A diagrammatic representation of the phylum Firmicutes tracing the subgroupings which contain the staphylococci. Selected families, genera and species are shown within the order Bacillales. Groupings are displayed according to the latest information available on the Names for Life website (http://doi.namesforlife.com/10.1601/tx.3874, accessed 16th November 2013).

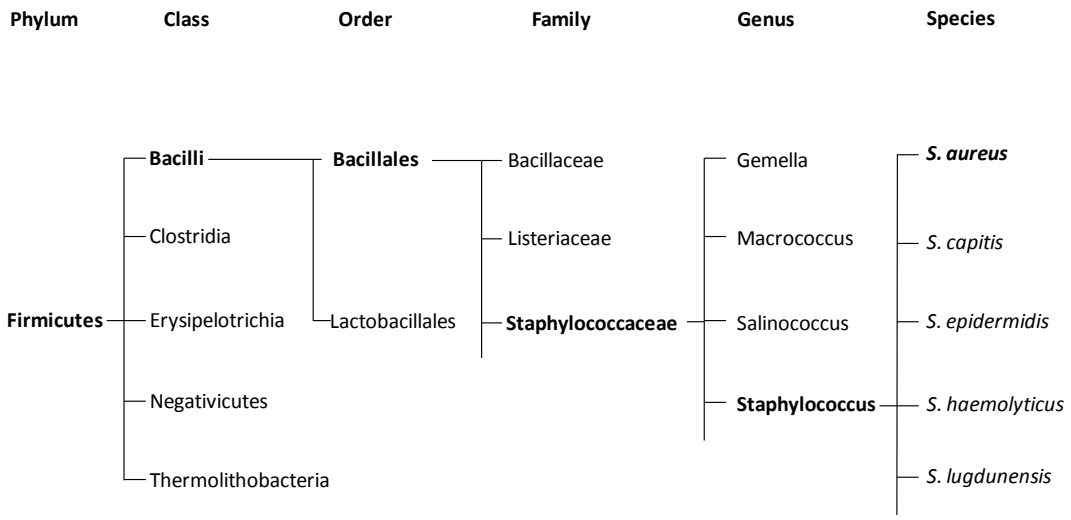

1.1.2 Overview of staphylococcal virulence factors and clinical features

Although the ancestral forms of the class Bacilli are understood to have existed long before the emergence of multicellular eukaryotic organisms, the staphylococci have nonetheless become highly adapted to host colonization. *Staphylococcus epidermidis* is a ubiquitous colonizer of human skin, while *S. aureus* is carried persistently by around 20 % and intermittently by 30 % of healthy people (Sakwinska *et al*, 2009; Wertheim *et al*, 2005).

Staphylococcal virulence is dependent on a diverse array of virulence factors giving the bacteria capacity for colonization, tissue destruction and invasion, immune evasion, and long term survival. The stepwise acquisition of virulence genes has facilitated the ongoing spread and survival of staphylococci in human and animal populations.

To adhere to mucosal and other epithelial surfaces such as the anterior nares, axillae, oropharynx and perineum, *S. aureus* uses a number of cell surface bound adhesive proteins termed MSCRAMMS (Microbial Surface Components Recognising Adhesive Matrix Molecules). These are anchored to the cell wall peptidoglycan by sortase and enable binding to a number of different molecules such as fibronectin (FnbA), fibrinogen (ClfA) and collagen (Cna) (Foster & Höök, 1998). Colonisation of the anterior nares in particular is facilitated by clumping factor B binding to epithelial cells, with the recently characterized SasX protein also having a role in some CA-MRSA strains (Li *et al*, 2012; Wertheim *et al*, 2008). The capacity to spread quickly from inanimate surfaces to host surfaces and back again is essential for staphylococcal dissemination, either through direct contact or sometimes aerosolisation. Hand hygiene initiatives, screening, isolation and decolonization aimed at reducing MRSA infections in hospitals during the last 15 to 20 years appear to have been very effective in limiting this surface contact reliant spread (Coia *et al*, 2006). As *S. aureus* can colonise a host for prolonged periods without causing infections unless certain circumstances permit, it is generally considered to be an opportunistic pathogen.

Progression from colonisation to disease is usually dependent on breaches of the physical barrier provided by intact skin through abrasions, surgery or hair follicle trauma such that bacteria can invade into tissue directly or via the bloodstream to establish abscesses (Cheng *et al*, 2011). Once in the bloodstream, MSCRAMMs are understood to play a vital role in endothelial adherence, along with wall teichoic acid (WTA) and a secreted, non-anchored, adhesive protein, the extracellular adherence protein (Eap) (Edwards & Massey, 2011). Endovascular infections such as endocarditis are initiated by adherence to, often damaged, endothelium mediated by the fibronectin binding proteins with subsequent accumulation of fibrin, erythrocytes, platelets and other cellular debris forming vegetations (Beynon *et al*, 2006; Que *et al*, 2005).

Following endothelial adherence at organ sites and other tissues, extravasation occurs via a number of mechanisms including endocytosis, transport within professional phagocytes and perhaps paracytosis by interfering with tight junctions between cells (Edwards & Massey, 2011). Staphylococci are notorious for their capacity to survive within various cell types, even neutrophils, through inhibition of phagosome lysosome fusion, neutralization of phagosome contents by staphyloxanthin, resistance to lysozyme and subsequent escape into the cell cytoplasm (Clauditz *et al*, 2006; Foster, 2005; Gresham *et al*, 2000). Once bacteria have gained access to tissues, *S. aureus* has a veritable arsenal of enzymes which can destroy surrounding cells and structures including proteases, lipases, hyaluronidase, nuclease, Staphylokinase and haemolysins (Burlak *et al*, 2007). Iron scavenging and uptake is also essential at this stage to meet the nutritional requirements of the pathogen (Skaar *et al*, 2004). The inflammation generated by cell damage would then generate a wider immune response, resulting in the influx of neutrophils to the site.

Staphylococci are experts in immune evasion and subversion, presumably reflecting an ancient and lengthy conflict between host and pathogen. As mentioned already, *S. aureus* is adept at

survival within neutrophils, however, numerous other strategies are employed to prevent phagocytosis happening in the first place. The prophage encoded virulence factors CHIPS (Chemotaxis inhibitory protein) and SCIN (Staphylococcal complement inhibitor) interfere with chemotaxis (de Haas *et al*, 2004; Rooijakkers *et al*, 2005a) and complement activation respectively. Clumping factor A triggers staphylococcal agglutination and adherence to fibrin, presumably making opsonisation and phagocytosis more difficult (Higgins *et al*, 2006). Protein A binds to the Fc region of IgG conferring additional antiphagocytic protection by providing a 'camouflage' of ineffectively bound immunoglobulins (Peterson *et al*, 1977). Capsular polysaccharide is also well characterized for its antiphagocytic properties (Thakker *et al*, 1998). In addition to these defensive strategies, some strains of *S. aureus* are capable of directly lysing neutrophils through production of leukocidins and phenol soluble modulins – these will be discussed in more detail later in section 1.2.

While evasion of the immune response gives bacteria more time to replicate and disseminate throughout the host, subversion of the immune response is a more pernicious strategy which directly contributes to clinical syndromes. The best known example of this is the toxic shock syndrome toxin 1 (TSST-1), although similar toxic shock syndromes can be caused by the other pyrogenic toxin superantigens (PTSAgs) such as the staphylococcal enterotoxins. Superantigens interfere with antigen presentation to cause a pathogenic 'cytokine storm' which leads to the fever, haemodynamic instability and the characteristic widespread blanching rash associated with toxic shock (Dinges *et al*, 2000).

Abscess formation appears to be another form of immune subversion relying, in part, on the immune response. Developing abscesses appear to be made up of a central nidus of replicating Staphylococci surrounded by a fibrin deposit, promoted by coagulase and clumping factor A and an outer ring of necrotic neutrophils (Cheng *et al*, 2011). Bacterial replication will continue within an abscess capsule until rupture and dissemination of bacteria into the bloodstream or

skin surface occurs, thus continuing the cycle. Abscess formation is the central component of many of the disease processes associated with *S. aureus* including skin and soft tissue infections, cavitating pneumonia, osteomyelitis and other end organ abscesses such as in the kidneys and brain. The capacity for the bacteria to continually metastasize and disseminate back into the bloodstream at a later time is associated with recurrent infections. Bacterial endocarditis is a notorious source of continual bacteraemia and frequently occurs in conjunction with infections at other sites such as septic arthritis, discitis and infected pulmonary emboli (Beynon *et al*, 2006).

As discussed above, staphylococci will tend to persist at former abscess sites through forming biofilms within cellular debris or surviving within host cells. Biofilm formation promotes long-term bacterial survival by providing protection from the immune system and inhibiting penetration of antibiotics (O'Neill *et al*, 2008). Biofilms are particularly problematic in the context of implanted prosthetic devices as once an infection is established these are virtually impossible for the immune system to sterilize. Examples of infections associated with prosthetic material include joint and heart valve replacements, intravenous and intraperitoneal catheters and cardiac pacing systems.

Viewed as a whole, *S. aureus* is an extremely versatile pathogen with an impressive arsenal of virulence factors. Able to respond to virtually every facet of the innate immune system, the bacteria can quickly gain access to a variety of niches in the host from where it is difficult to eradicate.

1.1.3 Antimicrobial resistance

Over the past three decades *S. aureus* has gained notoriety in the public consciousness largely by virtue of the rising prevalence of methicillin resistant hospital-acquired infections during the 1980s and 1990s (Boyce & Causey, 1982; Johnson, 1998; Witte, 2004). The loss of efficacy of the beta-lactam group of antibiotics has presented an awkward therapeutic challenge as the traditional intravenous alternative vancomycin suffers from both reduced bactericidal activity and a narrow therapeutic window (Pope & Roecker, 2007; Rybak *et al*, 2009), with increasing resistance also reported (Cunha, 2005; Sakoulas & Moellering, 2008). Although extremely dangerous in immunocompromised patients, usually due to co-morbidities, recent surgery or indwelling prosthetic devices, these strains have previously not presented a significant threat outwith this context; clinical studies comparing bacteraemia due to healthcare associated methicillin resistant *S. aureus* (HA-MRSA) and methicillin sensitive *S. aureus* (MSSA) have tended to suggest that worse outcomes in HA-MRSA bacteraemia derive from extended hospitalisation, treatment and host factors as opposed to differences in innate bacterial virulence (Harbarth *et al*, 1998; Hershow *et al*, 1992; Melzer *et al*, 2003; Wolkewitz *et al*, 2011).

Methicillin resistance is the result of the insertion of a mobile genetic element, the staphylococcal resistance cassette SCC*mec,* encoding several genes of unknown origin possibly transferred from another bacterial species (Ito *et al*, 1999). The *mecA* gene encodes a modified penicillin binding protein PBP2' which has low affinity for the penicillinase resistant beta lactam antibiotics routinely used to treat *S. aureus* infections such as flucloxacillin (Matsuhashi *et al*, 1986). Insertion of SCC*mec* is dependent on site-specific recombinases called cassette chromosome recombinases A and B (CcrA and CcrB) which recognize a unique sequence within the *orfX* gene (Katayama *et al*, 2000). The SCC*mec* element itself contains an insertion site allowing for integration of multiples copies of SCC*mec.*

Several SCC*mec* allotypes have been recognised which vary in terms of total size of the cassette, sequence differences in the recombinases genes, genes immediately adjacent to *mecA* and additional genetic material, including resistance genes for other antibiotics (Hiramatsu, 1995). Many of the HA-MRSA strains originally spreading in hospitals harbour SCC*mec* types I to III. By contrast, an emerging phenomenon of Community-acquired MRSA (CA-MRSA) has been recognised which have a smaller staphylococcal chromosomal cassette type, usually IV, but also V and VI, containing *mecA*, but often lack the multi-drug resistance of hospital strains (Ma *et al*, 2002; Vandenesch *et al*, 2003).

1.2 Panton Valentine Leukocidin

1.2.1 Clinical associations with PVL

If the 1980s and 1990s were marked by the rise of HA-MRSA, the emerging threat posed by *S. aureus* over the last 10 years has been due to an increase in virulent strains originating in community settings, often causing disease in young immunocompetent people. The two aspects to this trend which have been extensively studied are the emergence of CA-MRSA and the potential association with a phage-encoded pore forming toxin, the Panton Valentine leukocidin (PVL).

The genes encoding the two components of the PVL toxin *lukS-PV* and *lukF-PV* are carried on bacteriophages, insert into well-defined sites in the bacterial chromosome, and are transcribed from a single promoter (Kaneko *et al*, 1998). As the PVL genes are phage-borne they have not only spread rapidly by clonal expansion of successful CA-MRSA clones but are also capable of spreading between lineages by horizontal gene transfer.

The precise role of PVL in the pathogenesis of CA-MRSA and more generally in *S. aureus* infections has been the subject of much debate. This body of literature has been complicated by the extraordinary success in the United States of a single PVL positive CA-MRSA clone, designated USA300 by pulsed field gel electrophoresis. A study of 1055 representative isolates collected nationally in the US between 2004 and 2006 revealed clonal expansion of USA300 from 12 % of clinically isolated *S. aureus* to 38 % (O'Hara *et al*, 2012). In a multicenter study of presentation to emergency departments, USA300 was the pathogen isolated most commonly from skin and soft tissue infections (SSTIs) (Moran *et al*, 2006). USA300 has been associated with necrotising pneumonia and is now epidemic in the United States (Hidron *et al*, 2009; Klevens *et al*, 2007). Having begun as a community problem, USA300 has also spread into American hospitals, becoming an important cause of surgical wound infections and hospital acquired pneumonias (Pasquale *et al*, 2013).

Due to the rise of USA300, elucidating the unique role of PVL, which is carried by the majority of CA-MRSA and a significant reservoir of MSSA strains, has proven difficult. The clearest epidemiological association with *S. aureus* carrying the PVL genes appears to be SSTIs; a recent meta-analysis found a clear association of PVL with SSTIs but not invasive infections. Patients with PVL positive infections were also more likely to require surgery (Shallcross *et al*, 2013). A seven year study of skin infections presenting to a dermatology department in France found that 97 out of 225 (42.5 %) Staphylococcal SSTIs were caused by PVL positive strains, with a strong association with folliculitis (Del Giudice *et al*, 2011). In a large multicenter trial of complicated SSTI, PVL positive USA300 was the most common strain isolated. Abscesses caused by PVL strains were larger but resolved faster following drainage (Bae *et al*, 2009). A study of SSTIs caused by MSSA in the Bronx area of New York found that 36 % of these were PVL positive and had similar outcomes to PVL positive CA-MRSA strains, with PVL infections being more likely to require incision and drainage (Kaltsas *et al*, 2011).

Apart from SSTIs the other associations have been with osteomyelitis in children and necrotising pneumonia. The meta-analysis by Shallcross *et al* (2013) also indicated that osteomyelitis caused by PVL positive strains could be associated with increased morbidity. Furthermore, a study comparing bone and joint infections in children caused by PVL positive and PVL negative *S. aureus* found that long-term complications, prolonged treatment and requirement for surgical drainage were all associated with PVL (Dohin *et al*, 2007).

An early case series published by the Staphylococcal Pathogenesis Group in Lyon, France, noted that *S. aureus* causing necrotising pneumonia in previously immunocompetent people were PVL positive (Gillet *et al*, 2002). These cases were characterised by an influenza-like prodrome, haemoptysis, leucopoenia and rapid disease progression, with a high mortality rate. Although the numbers of cases of life-threatening necrotising pneumonia are infrequent and sporadic, there have been numerous other case reports of similar clinical cases associated with PVL. In a

recent study of 148 cases of necrotising pneumonia due to PVL, patients had a 40 % overall mortality, rising to 75 % if they had leucopoenia at presentation, with a median survival of 4 days (Khanafer *et al*, 2013). Leucopoenia was associated with co-infection with influenza. Molecular analysis of a collection of post-mortem lung tissue from 66 cases of necrotising pneumonia showed the majority of cases were PVL positive (Denison *et al*, 2013).

Aside from the clinical syndromes discussed above, there may be other potential associations with PVL that have not yet been recognised, particularly in uncommon infections. A study of patients presenting to an ophthalmology department in the UK found that 9 out of 95 strains of *S. aureus* causing keratitis over the study period were PVL positive. The PVL positive cases were associated with worse outcomes and need for surgery (Sueke *et al*, 2013).

While the rise of PVL in the United States is clearly due to clonal expansion of USA300, reports by the United Kingdom Health Protection Agency (HPA) noted a rising incidence of PVL positive strains in the UK, both MRSA and MSSA, which typically cause recurrent SSTIs and occasionally more severe disease (Ellington *et al*, 2009).

1.2.2 CA-MRSA virulence

CA-MRSA, while particularly problematic in the United States, is now a worldwide problem. Elsewhere in the world, PVL positive CA-MRSA clones have been extremely successful in certain countries; the European clone ST80-MRSA-IV is highly prevalent in Greece (Vourli *et al*, 2009), while in Australia, although CA-MRSA strains have been present for some time, the highly virulent 'Queensland' clone ST93-MRSA-IV is now predominant in Eastern Australia and an important cause of osteomyelitis, septic arthritis and necrotising pneumonia (Nimmo & Coombs, 2008). The ST30-MRSA-IV Southwest Pacific Clone emerged from Asia but is also prevalent in other parts of the world (Chen *et al*, 2013). While the vast majority of CA-MRSA strains encode the genes for the Panton Valentine Leukocidin (PVL), this may not always be the case (Otter *et al*, 2009).

Research has focused on why emerging CA-MRSA clones have been so successful over a short period of time. Compared to HA-MRSA, the smaller SCC*mec* elements, usually type IV, carried by CA-MRSA strains are understood to reduce the fitness burden (Collins *et al*, 2010). Strains which are predominantly circulating in the community would not necessarily benefit from multiple resistance genes as their antibiotic exposure will be lower than in hospital settings.

In addition to the PVL genes, the success of USA300 and other CA-MRSA has been attributed to a combination of the smaller SCCmec element, enhanced expression of core genome virulence determinants and acquisition of other mobile genetic elements (MGEs) such as the arginine catabolic mobile element (ACME) (Otto, 2013). Eukaryotic cells produce polyamines, including spermidine and spermine, from arginine which are toxic to *S. aureus.* The function of ACME in promoting colonisation and persistence is two-fold; ACME encoded *speG* converts spermidine and spermine to non-toxic acetylated forms, while the arginine deaminase system (ACME-arc) produces ammonia from arginine breakdown, enabling *S. aureus* to survive the low pH environment of the skin surface (Joshi *et al*, 2011; Thurlow *et al*, 2013). Core genome virulence

determinants which could enhance virulence through over expression include alpha-haemolysin and the phenol soluble modulins (PSMs). PSMs are amphipathic peptides which are pore forming and could have detergent-like damaging effects on membranes, particularly at high concentrations (Vandenesch *et al*, 2012).

1.2.3 Continuing global spread of PVL positive strains

As PVL is not routinely screened for, comprehensive data on the prevalence of PVL positive *S. aureus* is not available. A review of the literature over the past year, however, appears to indicate ongoing global spread of PVL in both MSSA and CA-MRSA strains.

A study of 142 Spanish children with SSTIs caused by *S. aureus* found that 46 (32 %) of isolates were PVL positive of which 33 were MSSA (Barrios López *et al*, 2013). A Lebanese study of nasal carriage in schoolchildren found a PVL positivity rate of around 15 %, with 60 % of children presenting with abscesses carrying a PVL positive strain (Beyrouthy *et al*, 2012). In one study from Benin, out of 136 SSTI and osteomyelitis isolates, only 25 % were MRSA but 70 % were PVL positive, presumably reflecting a local outbreak (Sina *et al*, 2013).

Elsewhere in the world, high rates of PVL were reported in studies of SSTIs in China and Australia, and also a study of bacteraemia in India, in which 16 % of isolates were PVL positive (Bennett *et al*, 2013; Eshwara *et al*, 2013; Zhao *et al*, 2012).

PVL positive strains have been previously noted to spread rapidly in situations where there is frequent close contact between individuals such as in schools, prisons, sports facilities and homes (Klevens *et al*, 2007). The spread of PVL in military settings is also a largely unrecognised but potentially important problem. A recent study of clinically isolated *S. aureus* at Camp Bastion, Afghanistan, found 41 % of isolates were PVL positive (Johnstone & Matheson, 2013).

Either through association with CA-MRSA or successful locally circulating strains of MSSA, it appears as though PVL is continually spreading around the world. As this virulence factor is likely here to stay and will be encountered frequently in clinical settings, it is imperative that we gain as clear an understanding as possible about its role in staphylococcal pathogenesis and spread.

1.2.4 Mechanism of action of PVL

PVL is not a recently discovered protein toxin; it was initially identified by Van deVelde in 1894, characterised by its ability to lyse human neutrophils and subsequently associated with skin and soft tissue infections by Sir Philip Panton and Francis Valentine in 1932 (Boyle-Vavra & Daum, 2007; Panton *et al*, 1932). PVL is a member of a family of bi-component pore forming leukocidins along with gamma haemolysin, LukED and LukAB. All of these toxins have so-called fast and slow components, characterised by electrophoretic mobility. Gamma haemolysin is a slight exception to this rule in that it has two interchangeable slow components; HlgA and HlgC, which combine with one fast component HlgB. The slow components usually bind to the cell membranes first, forming a hetero-octamer with four F and four S subcomponents (Vandenesch *et al*, 2012) (Figure 1.2). The formation of membrane pores by the established toxin structure leads to efflux of cell contents, particularly ions (Meunier *et al*, 1995). *In vitro* studies have demonstrated that PVL exhibits a concentration dependent effect, ranging from the induction of cell apoptosis to frank necrosis (Genestier *et al*, 2005). Across cell types and animal species, PVL has particular affinity for human neutrophils (Löffler *et al*, 2010).

In addition to direct cell lysis through membrane pore formation, other potential effects of PVL have been postulated. There is some evidence to suggest that PVL enhances inflammation by binding to leukocytes and stimulating the NLRP3 (NLR family, pyrin domain-containing 3) pathway, a cascade of responses which leads to the upregulation of inflammatory cytokines, particularly interleukin 1β (Holzinger *et al*, 2012). In a study of PVL effects on osteoblasts, the toxin inhibited cell proliferation, inducing apoptosis and inflammation (Jin *et al*, 2013). If the bacteria are phagocytosed, PVL appears to play a role in endosomal escape, intracellular replication and triggering apoptosis from within the cell (Chi *et al*, 2013). Direct stimulation of inflammatory pathways and release of inflammatory granules from neutrophils may explain the severity of pneumonia observed in conjunction with influenza. Epithelial and ciliary damage by

influenza reduces staphylococcal clearance and attracts neutrophils which are then lysed, creating a vicious cycle of inflammation (Niemann *et al*, 2012).

1.2.5 Animal model data

In an attempt to define the contribution of PVL to *S. aureus* infections, particularly with CA-MRSA strains, various animal models have been employed with conflicting results. Some of the early studies appeared to indicate that PVL did not influence pathogenesis at all, generating some controversy.

One of the earliest mouse studies involved the inoculation of purified recombinant PVL toxin into the lungs of mice, which appeared sufficient to induce haemorrhagic necrosis (Labandeira-Rey *et al*, 2007). In addition, a laboratory strain RN6390 complemented with a plasmid containing the *lukSF-PV* genes caused necrotising pneumonia in the same model where as an isogenic PVL negative strain did not. In contrast, other studies using clinical strains such as USA300 with isogenic *lukSF-PV* knockouts in mouse models of skin infection and pneumonia did not demonstrate any difference in disease severity or outcome (Bubeck Wardenburg *et al*, 2008; Voyich *et al*, 2006). This led to much speculation as to the validity of the study by Labandeira-Rey and whether their results using laboratory strains could be extrapolated to clinical infections (Villaruz *et al*, 2009). As the strain causing necrotising pneumonia contained a multi-copy plasmid expressing high levels of PVL, an alternative explanation is that a very high toxin concentration was required to cause the observed pathology. MSSA and MRSA strains that exhibited higher production of PVL caused larger abscesses and worse inflammation than lower producing strains in a mouse skin infection model (Varshney *et al*, 2010).

Figure 1.2 The Panton Valentine Leukocidin

PVL is secreted by *S. aureus* as two subcomponents, LukS-PV and LukF-PV, which form a hetero-octamer on the cell membrane of polymorphonuclear neutrophils (PMNs). The resulting formation of membrane pores leads to efflux of cell contents and cell death. In addition to impairing the innate immune response to staphylococci, neutrophil lysis also contributes to tissue inflammation and necrosis through the release of inflammatory mediators or reactive oxygen species (ROS). Adapted from Boyle-Vavra and Daum (2007).

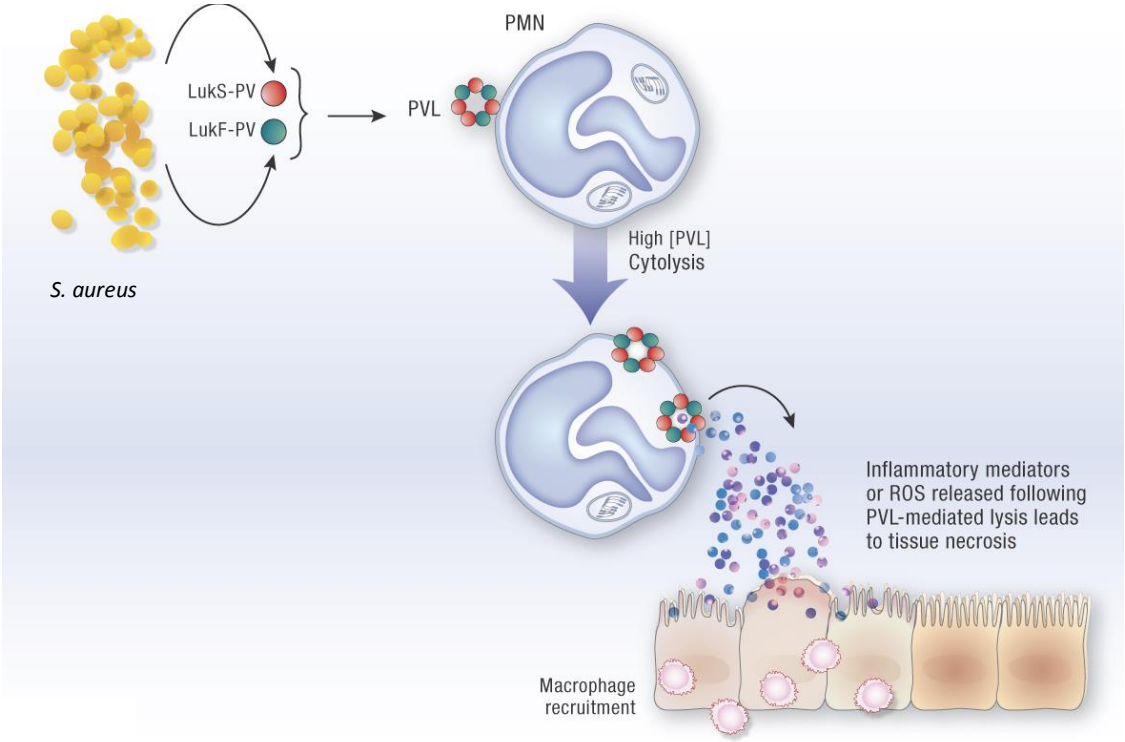

Contributing to the growing debate about the importance of PVL and the pathogenicity of USA300 in particular, Li and colleagues published an analysis of the genetic evolution of CC8 CA-MRSA (Li *et al*, 2009b). In this paper, they noted that USA300 appeared to have developed from its parent strain USA500 through acquisition of mobile genetic elements, including a phage containing the *lukSF* genes. However through comparison of these two strains with other epidemic MRSA clones, it was noted that both USA300 and USA500 exhibited increased expression of the accessory gene regulator (*agr)*, alpha haemolysin and phenol soluble modulins (PSMs), as well as heightened capacity to lyse neutrophils and erythrocytes, and cause dermonecrosis in mice. They concluded that the enhanced virulence of USA300 resulted from greater exotoxin expression, probably due to higher activity of *agr* and other staphylococcal regulators, rather than the acquisition of the *lukSF-PV* genes, which USA500 does not possess. They failed to explain however, why it is USA300, not USA500 which is currently epidemic in the United States, or concede that increased regulatory activity in USA300 is also likely to result in increased PVL expression in addition to the other exotoxins. As mentioned previously, other *agr* regulated exotoxins including alpha-haemolysin, which is produced by many clinical strains of *S. aureus*, and the cytolytic PSMs are considered as alternative virulence factors in CA-MRSA infections (Bubeck Wardenburg *et al*, 2007; Wang *et al*, 2007). It seems likely that these toxins work in concert with PVL; Hongo and colleagues demonstrated that PVL induced lysis of neutrophils was enhanced by the presence of PSMs (Hongo *et al*, 2009). A recent study has also suggested that perhaps increased expression of these toxins in CA-MRSA is due to a modification of the *agr* regulon, the magnitude of the downstream effects of *agr* expression, rather than being solely due to increased *agr* expression (Cheung *et al*, 2011).

While the mouse models summarized above have produced conflicting data, it has since been observed that mouse neutrophils have reduced susceptibility to PVL when compared with the neutrophils of humans and other animal species, such as rabbits, casting doubt on whether these data could be extrapolated to human infections (Löffler *et al*, 2010). While PVL can act

directly on membranes at high concentrations, the toxin appears to target the human complement receptor C5a, allowing it to trigger apoptosis at low concentrations and explaining the species specific effects observed (Spaan *et al*, 2013).

A series of rabbit models have given a clearer indication that PVL contributes to outcomes of staphylococcal infections. A rabbit osteomyelitis model comparing USA300 with an isogenic PVL knockout demonstrated that infections lasted longer and were associated with greater bony deformity and tissue injury with the PVL positive strain (Crémieux *et al*, 2009). A similar study involving a rabbit model of pneumonia and similar isogenic USA300 PVL positive and negative strains also demonstrated enhanced lung necrosis and worse survival rates in the PVL positive group (Diep *et al*, 2010). A follow-up study demonstrated a role for linezolid in treatment, suppressing PVL production and improving outcomes (Diep *et al*, 2013).

Results of rabbit models have not however been unanimous. In a rabbit abscess model, outcomes were improved, with smaller abscesses, in rabbits infected with alpha-haemolysin or PSM alpha knockouts, while no effect was observed with a PVL knockout mutant (Kobayashi *et al*, 2011). In a study comparing different CA-MRSA clones, SSTIs in a rabbit model were of comparable size between PVL positive and negative strains, although larger in strains which expressed high levels of alpha-haemolysin and phenol soluble modulins (Li *et al*, 2010). Another rabbit model of SSTI however did report a difference in abscess size between a PVL positive strain and isogenic PVL knockout mutant (Lipinska *et al*, 2011).

1.2.6 The importance of gene expression

Weighing up the evidence available to date from *in vitro* and animal studies, it would appear that both the presence of the PVL toxin genes and the strain background have a role to play in defining the severity of PVL-associated infections. The observation that USA300 exhibits high level *agr* expression, and a greater sensitivity of toxin expression to changes in *agr,* when compared with other strains *in vitro* and in animal models is interesting for two reasons; the mechanism behind this difference in *agr* expression is not fully understood and, furthermore, uncovering this may shed significant light on the role of this and other regulators in staphylococcal pathogenesis. While targeting specific virulence factors like PVL with vaccines or monoclonal antibody therapy has been suggested as one approach to treating severe staphylococcal infections, pinpointing and interfering with key staphylococcal regulators responsible for multiple virulence factors is a compelling strategy for reducing the burden of staphylococcal disease.

1.3 Regulation of virulence in *S. aureus*

1.3.1 Two component signal transduction systems and quorum sensing

Two component systems (TCSs) are widespread in bacteria and enable recognition of environmental and cytoplasmic signals coupled to an intracellular response. This coupling usually involves a histidine protein kinase (HPK) which is autophosphorylated at a histidine residue in response to the stimulus and then transfers this phosphate to a response regulator (RR) (Grebe & Stock, 1999). This basic pattern can be complicated by the involvement of additional components such as other sensors or multiple phosphate transfer steps. TCSs fulfil a plethora of functions including control of chemotaxis, sporulation, exoprotein production, nutrient uptake, metabolism and environmental stress responses (Stock *et al*, 1989).

1.3.1.1 TCSs in *S. aureus*

S. aureus has a number of TCSs; in the sequenced strain N315, 16 putative TCS have been identified, interacting with each other as well as regulating target genes independently (Cheung *et al*, 2004; Matsuo *et al*, 2010; Novick, 2003) (Table 1.1). The function of TCSs in *S. aureus* include those involved in autolysis regulation and antimicrobial peptide (AMP) resistance, homeostasis, oxidative, thermal, pH and membrane stress responses, quorum sensing and virulence gene regulation (Novick & Jiang, 2003). This is an important consideration when attempting to relate *in vitro* gene regulation to the context of *in vivo* infection where a multitude of environmental variables exist.

There are a number of these systems whose primary function is in resisting AMPs or other antibiotics. BraRS is responsible for resistance to bacitracin and also the lantibiotics nisin and nukacin ISK-1 through sensing inhibition of or binding to membrane anchored lipid II in conjunction with BraDE (Hiron *et al*, 2011). GraRS senses the presence of cationic AMPs and

confers resistance to them through modifying cell wall teichoic acids, increasing their positive charge. GraRS is also activated in response to oxidative or thermal stress, possibly due to its role in modifying cell wall components and has been linked to downstream effects on cell wall biosynthesis and virulence gene regulation (Falord *et al*, 2011). VraDE is activated by coordinated expression of BraRS and GraRS and acts as a detoxification module, particularly for bacitracin resistance (Kawada-Matsuo *et al*, 2013). VraRS responds to inhibition of cell wall biosynthesis through the action of cell wall active antibiotics such as vancomycin or cationic AMPs. VraRS is involved in regulating a number of cell wall related pathways including cell wall biosynthesis and protein folding (Pietiäinen *et al*, 2009).

Overlapping with antimicrobial resistance, are those systems which control autolysin genes in response to cell wall or membrane disturbance. WalKR, also known as YycGF, senses disturbance to cell wall integrity through changes in osmotic pressure, including the action of lysostaphin, and controls peptidoglycan biosynthesis and turnover with downstream control of several autolysin genes including AtlA and LytM (Dubrac *et al*, 2007). ArlRS and LytRS also sense changes in cell wall or membrane integrity and regulate murein hydrolases. As autolysins are also involved in adherence to surfaces, these systems also play a role in biofilm formation (Brunskill & Bayles, 1996; Fournier & Hooper, 2000; Sharma-Kuinkel *et al*, 2009).

TCSs have been identified with important homeostatic functions for iron, potassium and nitrogen. The Heme-sensor system HssRS plays an important part in iron homeostasis by preventing excess accumulation of intracellular heme. High concentrations of extracellular heme lead to upregulation of the heme efflux system HrtAB thus ensuring that intracellular levels are controlled (Torres *et al*, 2007). KdpDE is primarily understood to be involved in K^+ homeostasis, directly regulating a K^+ pump. It also appears to have a much wider role, not only sensing changes in osmolarity and coordinating response to osmotic stress, but also having a number of downstream effects on virulence genes including cell surface proteins and exotoxins

(Freeman *et al*, 2013). It could therefore be considered as part of the wider stress response and may have a role to play in response to phagocytosis. NreBC is activated in low oxygen conditions and regulates nitrate reductases and transporters, enabling nitrate respiration in oxygen depleted environments (Schlag *et al*, 2008). Although not well characterized, YhcSR is also thought to play a role in nitrate respiration (Sun *et al*, 2005).

SrrAB responds to both hypoxia and nitrosative stress caused by nitrous oxide. Downstream regulation of genes involved in cytochrome biosynthesis, nitrous oxide detoxification, anaerobic metabolism and production of polysaccharide intracellular adhesin (PIA) results in adaptation to these stress conditions (Kinkel *et al*, 2013; Pragman *et al*, 2004). PIA production is understood to be important for protection against non-oxidative neutrophil killing mechanisms (Ulrich *et al*, 2007).

Table 1.1 Two component systems in *S. aureus*

A summary of 13 of the 16 putative TCSs which have been characterised in *S. aureus*. The histidine kinase and response regulator pairings are shown (HK followed by RR), with the principal signals, functions and key references. Several of the TCSs are known by more than one name. AMP = antimicrobial peptide. AIP = autoinducing peptide

Name	Signal	Functions	References
ArlRS	Cell wall /membrane integrity	Autolysis regulation, biofilm formation	Fournier & Hooper (2000)
AgrCA	AIP	Quorum sensing, virulence gene regulation	Novick *et al* (1995)
BraRS/ NsaRS	AMPs	AMP resistance	Hiron *et al* (2011)
GraRS/ ApsRS	Cationic AMPs, membrane charge	AMP resistance, oxidative and thermal stress response	Falord *et al* (2011)
HssRS	Haem	Iron homeostasis	Torres *et al* (2007)
KdpDE	K^+, osmolarity	Potassium transport, osmotic stress response	Freeman *et al* (2013)
LytRS	Cell wall /membrane integrity	Autolysis regulation, biofilm formation	Brunskill & Bayles (1996)
NreBC	Oxygen depletion	Nitrate respiration, anaerobic growth	Schlag *et al* (2008)
SaeRS	Hydrogen peroxide, pH, osmolarity	Virulence regulation, oxidative stress response	Geiger *et al* (2008) Jeong *et al* (2012)
SrhRS/ SrrAB	Oxygen depletion, nitrous oxide	Hypoxic and nitrosative stress response	Kinkel *et al* (2013) Pragman *et al* (2004)
VraRS	AMPs, cell wall active antibiotics	AMP, antibiotic resistance	Pietiäinen *et al* (2009)
WalKR/ YycFG	Osmotic pressure, lysostaphin	Cell wall turnover, autolysis, biofilm formation	Dubrac *et al* (2007)
YhcSR	Nitrate	Control of cell growth, nitrate respiration	Sun *et al* (2005)

1.3.1.2 The SaeRS TCS

SaeRS is thought to fulfill an integral role in virulence gene expression *in vivo,* responding to cell membrane perturbation due to changes in pH, oxidative stress and osmolarity, particularly useful in coordinating a response to phagocytes (Geiger *et al*, 2008). SaeRS is under the control of two promoters. The P3 promoter lies immediately upstream of SaeRS and is repressed by SaeR, creating a negative feedback mechanism such that the Sae locus will return to a steady state following upregulation. Further upstream, the P1 promoter controls transcription of both SaePQ and SaeRS, is activated by *agr* but repressed by SigB (Geiger *et al*, 2008). SaePQ form a complex with SaeS, promoting phosphatase activity and resetting the TCS to a resting state (Jeong *et al*, 2012). While SaeRS activation initially results in the upregulation of both cell surface protein and exotoxin genes, SaePQ enables differential activation of these genes as the exotoxin gene promoters have higher affinity for phosphorylated SaeR and so respond to lower concentrations. This gives SaeRS two 'modes' of action depending on which promoter is activated, enabling upregulation of both sets of virulence genes by P3, or primarily exotoxin genes by P1 (Jeong *et al*, 2012). SaeRS therefore regulates virulence genes in a coordinated manner with *agr* while retaining the flexibility to upregulate both exotoxin and cell surface protein genes. The capacity to respond to environmental signals and membrane damage represent an important mechanism for high level induction of virulence genes *in vivo*.

1.3.1.3 Quorum sensing

When the signal recognised by TCSs is produced by the bacteria, cell density dependent signal accumulation occurs through a positive feedback loop, a phenomenon known as 'quorum sensing' (QS) (Williams *et al*, 2000). In several Gram negative bacteria, *N*-acyl homo-serine lactones act as this signal, diffusing through cell membranes and binding to intracellular receptors (Withers *et al*, 2001). In Gram positive bacteria, small post-translationally modified peptides fulfil this role by binding to cell surface receptors (Winzer & Williams, 2001). QS systems can control various subsets of genes depending on the organism. In *Bacillus subtilis* and *Streptococcus pneumoniae,* QS systems regulate genetic competence while in other bacteria such as *Lactococcus lactis*, the production of antimicrobial peptides are controlled by QS (Kleerebezem *et al*, 1997). In *S. aureus*, the accessory gene regulator (*agr)* QS system regulates a large number of genes, including those associated with exotoxin expression, cell surface proteins and metabolism (Novick, 2003).

As global regulation of toxin expression could be an important determinant of severity in PVL associated infections, particularly in CA-MRSA, a summary of the current understanding of the most important regulatory systems in *S. aureus*; principally *agr,* and the staphylococcal accessory regulator SarA and its homologues, are presented below, followed by specific details pertaining to the toxins of interest described above.

1.3.2 The accessory gene regulator (*agr*)

1.3.2.1 Mechanism of action and function

agr is pivotal to gene regulation in *S. aureus*, allowing for the coordinated expression of a multitude of genes involved in toxin production, adhesion, cell metabolism and growth (Recsei *et al*, 1986). *agr* consists of two operons controlled by divergent promoters *agr*P2 and *agr*P3 which initiate respectively the transcription of RNAII, responsible for density dependent signaling, and RNAIII, the effector RNA, which in turn stimulates or represses a host of other genes (Janzon *et al*, 1989; Novick *et al*, 1995) (Figure 1.3). RNAIII, which also encodes the toxin delta-haemolysin, was first identified as restoring an *agr* regulatory phenotype to an *agr* null mutant and is one of the first examples of target gene regulation by RNA through an antisense mechanism (Morfeldt *et al*, 1995; Novick *et al*, 1993). The RNAII transcript encodes four genes *agrBDCA* conferring functions in signal generation, release and detection. AgrB, a transmembrane peptidase, processes the AgrD propeptide, resulting in the secretion of small auto inducing peptides (AIPs) (Qiu *et al*, 2005; Saenz *et al*, 2000). These possess an endocyclic ring of between 7 and 9 amino acids in length with a central cysteine residue (Mayville *et al*, 1999). The AIPs, bind to the transmembrane histidine kinase receptor AgrC, resulting in phosphorylation of intracellular AgrA which has strong affinity for the P2 promoter immediately activating it, and weaker affinity for P3 (Koenig *et al*, 2004; Lina *et al*, 1998). The result is a positive feedback loop in which accumulation of AIP leads to further AIP production and eventual activation of P3 when a threshold concentration is reached. There are four *agr* groups in *S. aureus*, each with a different AIP sequence and corresponding AgrC receptor where the AIP of one group will only activate its cognate AgrC receptor while inhibiting heterologous AgrCs (Ji *et al*, 1997).

As the upregulation of *agr* depends on an accumulation of AIP, a classical QS pattern is observed where simultaneous release of AIP by a dense group of cells results in coordinated gene

regulation. This is normally observed *in vitro* during the transition from exponential to stationary phase (Ji *et al*, 1995), but is also understood to occur during an infection as bacteria growing within a confined space such as an abscess or hair follicle will undergo this transition quickly; producing toxins enabling tissue destruction and metastasis to other body sites (Loughman *et al*, 2009). *agr* expression by internalised bacteria occurs within the host endosome shortly before escape (Qazi *et al*, 2001).

Figure 1.3 The accessory gene regulator

The accessory gene regulator (*agr*) (A) in *S. aureus* encodes a quorum sensing system whereby the AgrD propeptide is post-translationally modified and exported by AgrB in the form of a cyclic thiolactone autoinducing peptide (AIP). AgrC, a histidine protein kinase, is autophosphorylated in response to AIP with subsequent phosphotransfer to the response regulator AgrA. AgrA binds to the *agr*P2 and *agr*P3 promoters resulting in positive feedback of AIP production and transcription of the regulatory mRNA RNAIII when an activation threshold is reached. RNAIII upregulates exotoxin gene expression and downregulates cell surface protein expression, both directly and through modifying the translation of other regulators such as the repressor of toxin (*rot*). Adapted from Rutherford and Bassler (2012).

The structure of the *agr* group 1 peptide AIP-1 is shown in B. Substituting the 5th amino acid, an aspartate, for an alanine (marked with an arrow) results in a cross-group AgrC antagonist (ala^5)AIP-1 (McDowell *et al*, 2001). Adapted from Jensen *et al* (2008).

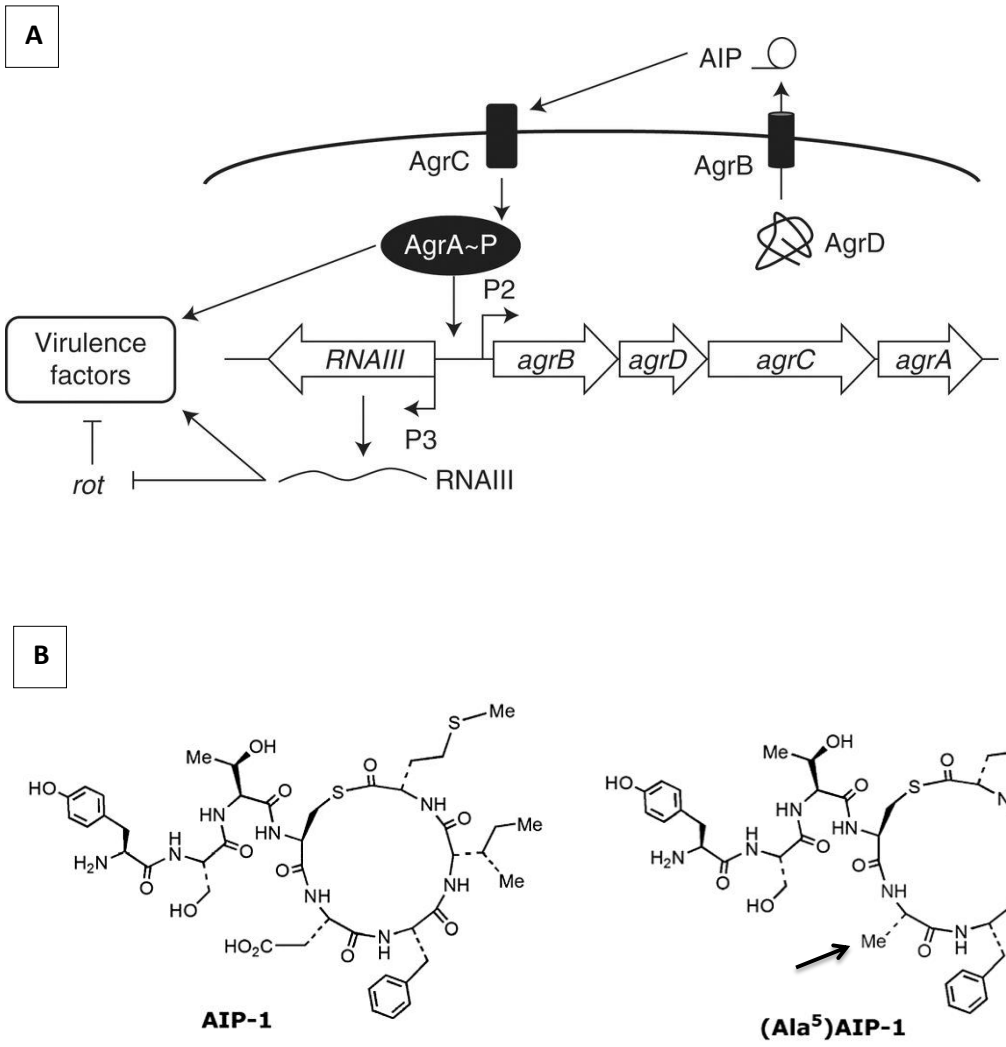

1.3.2.2 Role in pathogenesis

The *agr* system has demonstrated clinical importance. *agr* mutants have reduced capacity to cause abscesses as compared with the wild type when tested in various murine and rabbit models including septic arthritis, skin abscess, osteomyelitis and endocarditis (Abdelnour *et al*, 1993; Cheung *et al*, 1994; Cheung *et al*, 2011; Gillaspy *et al*, 1995). Although *agr* mutants are recovered from clinical specimens, they tend to be from chronic infections such as in cystic fibrosis and device-related infections where the bacteria often survive within a biofilm (Goerke & Wolz, 2004). The phenotype of an *agr* mutant is characterised by low to absent production of exotoxins, with corresponding upregulation of protein A and other cell surface associated proteins (Recsei *et al*, 1986). As toxin production, and therefore toxin-mediated pathology, appears to be heavily reliant on a functional *agr*, therapeutic interference with *agr* has been considered as a strategy for treating acute infections. The co-inoculation of a type I strain with type II AIP prevented abscess formation, demonstrating the potential merit of this approach (Wright *et al*, 2005a). Through substitution of the endocyclic aspartate for an alanine in AIP-1, a cross group inhibitory AIP has been developed with activity in the nanomolar range (Chan *et al*, 2004; McDowell *et al*, 2001) (Figure 1.3B). Conversely, inhibition of agr has been shown to enhance initial biofilm development (Vuong *et al*, 2000), which could theoretically exacerbate or predispose to chronic or device-related staphylococcal infection where biofilms play a major role, an effect which has been observed in S. epidermidis *agr* mutants (Vuong *et al*, 2004); further *in vivo* modelling data is required to investigate this possibility.

1.3.3 The Sar protein family

While *agr*P2 and *agr*P3 primarily respond to activation by a phosphorylated AgrA, other regulatory proteins also bind and modulate their function, predominantly members of the *S. aureus* regulator SarA protein family (Cheung & Projan, 1994; Chien & Cheung, 1998). The regions of the *agr*P2 and *agr*P3 promoters to which SarA in particular bind have been well characterised through a variety of methods (Chien & Cheung, 1998; Sterba *et al*, 2003). As SarA interaction activates these promoters, this influences the threshold concentration of AIP required for *agr*P3 activation and subsequent RNAIII transcription. *agr* activity, in turn, alters the transcription of SarA and a number of SarA homologues, described below, creating complex regulatory networks which allow the bacteria to respond to different environmental pressures. The integrated, layered network of regulation between *agr*, Sar proteins and other regulators is summarised in Figure 1.4.

The SarA protein family consists of a number of related regulatory proteins, some of which have only been recently identified. All of these proteins are understood to share in common a winged helical structure, believed to be important for their DNA binding function (Liu *et al*, 2006). SarA is a 124-residue protein which forms a dimeric structure with a single DNA binding domain (Liu *et al*, 2006). Some of the family, such as the 250-residue protein SarS, are larger and contain two domains within a single monomeric structure (Cheung *et al*, 2008). MgrA is similar to SarA but shares a greater percentage of its sequence with a regulatory protein found in Gram negative bacteria, MarR (Ingavale *et al*, 2005). The family can therefore be divided into three groups; the single domain proteins SarA, SarR, SarT, SarV, SarX and Rot, the double domain proteins SarS, SarU and SarY and the MarR homologs, MgrA and SarZ (Cheung *et al*, 2008) (Figure 1.5).

Figure 1.4 Integrated virulence gene regulation in *S. aureus*

The *agr* quorum sensing system integrates with the Sar proteins to form a regulatory network enabling coordinated gene regulation in response to cell density and other environmental signals. While *agr* is primarily activated by AIP through quorum sensing, it is also upregulated by SarA, SarU and downregulated by SigB. *agr* expression can also be altered following the activation of various TCSs (e.g. SrrAB) in response to environmental signals, although this may also be mediated by Sar proteins such as SarR and SarA. RNAIII inhibits the translation of Rot and SarT mRNA while promoting exotoxin gene translation. Repression of SarT and Rot result in reduced activation of SarS and cell surface protein gene expression (e.g. *spa*) but derepression of exotoxin genes (e.g. *hla*) and SarU. SaeRS can upregulate exotoxin genes directly in response to environmental signals, particularly oxidative stress. Many of the Sar proteins, including SarZ and SarA, can also bind directly to target gene promoters to alter gene transcription.

Adapted from Felden *et al* (2011) and Cheung *et al* (2008).

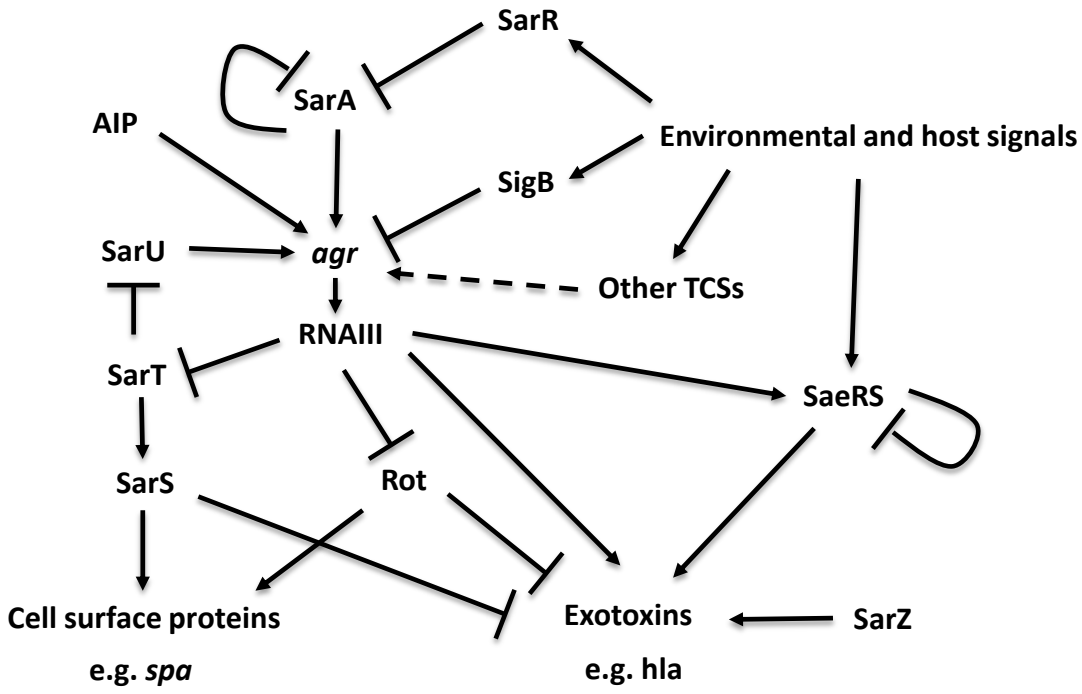

Figure 1.5 Structural comparison of members of the SarA protein family

The SarA protein family can be grouped into 3 depending on protein structure. The single domain proteins such as SarA and SarR dimerise to form a winged-helix structure, with each dimer consisting of 5 α-helixes and 3 β-strands. The double domain proteins, including SarS and SarU, have a monomeric structure consisting of two homologous but non-identical halves (labelled below as SarS1 and SarS2), also forming a similar winged-helix. MgrA and SarZ have an asymmetrical structure and share greater sequence similarity with the MarR-like regulatory proteins found in Gram negative bacteria. Adapted from Cheung *et al* (2008).

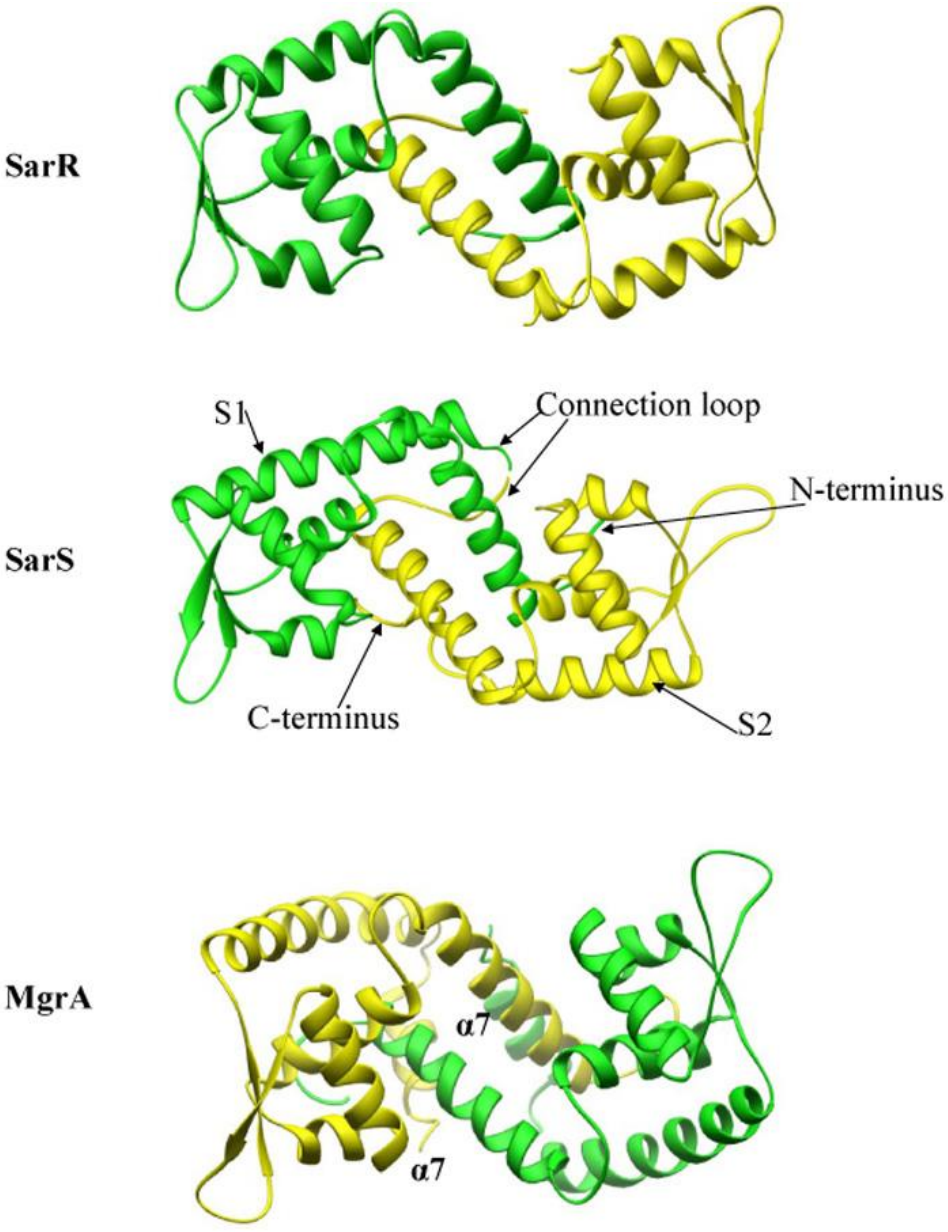

1.3.3.1 SarA

The *sarA* locus was initially identified in a transposon mutant exhibiting numerous changes in the expression of extracellular and cell wall associated proteins (Cheung *et al*, 1992). SarA regulates target genes by directly binding to their promoter regions and also indirectly by modulating *agr* activity as described above (Liu *et al*, 2006). While the interplay of SarA and other regulators is extremely complicated, the overall impact of SarA activity appears to be to enhance post-exponential exotoxin expression (Cheung *et al*, 2004). SarA is expressed *in vivo* and appears to play an important role in pathogenesis; in a rabbit model of endocarditis an *agr/sar* double mutant was more attenuated than an *agr* single mutant (Cheung *et al*, 1994).

1.3.3.2 Other SarA homologs

The other SarA homologs have both overlapping and divergent functions, combining together to form a regulatory network. SarS primarily upregulates protein A expression while acting as a repressor of exotoxin expression (Tegmark *et al*, 2000). SarS expression is dependent on SarT which is, in turn repressed by RNAIII and SarA; SarS therefore acts divergently but in coordinated equilibrium with *agr* (Cheung *et al*, 2004).

Rot (repressor of toxin) was initially identified by screening a transposon mutant library in an *agr* null background for restoration of exotoxin and protease expression (McNamara *et al*, 2000). It has a similar function to SarS, also acting in an opposing manner to the classical paradigm of the *agr* response*;* repressing toxin genes while upregulating cell surface proteins (Saïd-Salim *et al*, 2003). RNAIII can bind to the *rot* transcript, preventing its translation (Geisinger *et al*, 2006). Furthermore mutation of *rot* in an *agr* null strain restored virulence in a rabbit model of endocarditis, suggesting suppression of *rot* may be a key feature of the *agr* response *in vivo* (McNamara & Bayer, 2005).

The MarR homolog MgrA is involved in autolysis regulation – an MgrA mutant exhibited increased autolysis (Ingavale *et al*, 2005). In addition, MgrA also displays similar function to the *agr* response, upregulating expression of exotoxin genes (Luong *et al*, 2006). As MgrA has only been identified relatively recently, the significance of this co-regulation of autolysis and virulence genes is not fully understood but raises interesting questions about the impact of the bacterial stress response on virulence, and the interplay between antibiotic resistance and bacterial virulence *in vivo.*

Genome analysis is continuing to reveal transcriptional factors with homology to existing Sar proteins. SAUSA300_2452 was identified by analysing the USA300 genome and found to share close homology with SarZ and MgrA, with several other MarR like proteins also identified elsewhere in the genome (Ibarra *et al*, 2013).

1.3.4 The sigma factor SigB

The sigma factor SigB is a key component of the staphylococcal stress response and in a normal strain background will repress *agr* activity, particularly following exposure to environmental stresses (Cheung *et al*, 1999). The laboratory strain NCTC8325-4 has a deletion in the *rsbU* gene which encodes a positive regulator of SigB. An *rsbU* restored derivative SH1000 exhibited reduced exotoxin production, presumably due to SigB mediated inhibition of *agr* expression (Horsburgh *et al*, 2002). A mutation in the genes for a kinase *pknB*, a positive regulator of *sigB*, in clinical strains, including USA300, resulted in the opposite effect; *agr* activity and consequently exotoxin production were upregulated in response to environmental stress, enhancing virulence in a murine skin abscess model (Tamber *et al*, 2010).

1.3.5 Regulation of specific toxins

Of the three exotoxins principally implicated in the pathogenesis of CA-MRSA and other PVL associated infections, the regulation of alpha haemolysin is the best understood. It can be considered as the classical example of exotoxin regulation in *S. aureus*, usually used as an indicator of exotoxin expression in the studies of staphylococcal regulators referred to above. Expression of alpha haemolysin was linked to bacterial growth as early as 1971 and subsequently found to be primarily regulated by *agr* via RNAIII (Duncan & Cho, 1971; Recsei *et al*, 1986).

By contrast, the regulation of PVL has not been comprehensively investigated, although there is reasonable evidence to suggest that *agr* plays an important role (Bronner *et al*, 2000; Cheung *et al*, 2011). A number of studies have examined the effect of antibiotic exposure on PVL expression since sub-inhibitory concentrations of beta-lactam antibiotics provoke an increase in transcription of the *lukSF-PV* genes (Dumitrescu *et al*, 2007) as has previously been observed for alpha haemolysin (Ohlsen *et al*, 1998). Protein synthesis inhibitors appear to suppress translation but not transcription of several toxin genes, including *lukSF-PV* (Stevens *et al*, 2007). The full mechanism for beta-lactam-mediated induction of toxin is currently unknown; however a more recent study employing strains carrying mutations in key regulators identified a potential role for both SarA and Rot (Dumitrescu *et al*, 2011). As the strain used in this study, RN6390, carries a mutation in *rsbU* which results in the phenotype of a *sigB* mutant, this finding should be interpreted with caution. The mechanism proposed by Dumitrescu *et al* (2007) is that SarA and Rot are recruited following antibiotic binding to specific PBPs, notably PBP1, with the involvement of the autolysis regulatory system as a potential intermediary step. As, unlike alpha haemolysin and PSMs, the *lukSF-PV* genes are carried on a phage, Wirtz *et al* (2009) were able to induce PVL toxin expression through stimulation of phage replication by mitomycin C, although this did not occur in USA300 as the prophage appeared to have a defect resulting in failed excision. The potential for PVL upregulation beyond the activity of core staphylococcal

regulators is an interesting prospect; expression of the *lukSF-PV* genes as measured by RT-PCR of pus from drained abscesses was greater than could be explained by *agr* activity alone, although interaction with human neutrophils appeared to increase *pvl* expression independently of *agr,* explaining some of this discrepancy (Loughman *et al*, 2009).

Cheung and colleagues demonstrated that the genes for PSMs beta, *psm*β1 and *psm*β2, are expressed more than 60 fold greater in a wild type USA300 strain over an *agr* mutant (Cheung *et al*, 2011). This effect was more dramatic than changes observed in RN6390 or the HA-MRSA strain 252, and was suggested as a contributing factor to the virulence of USA300. The PSMs are regulated through an *agr* dependent but RNAIII independent mechanism, with the promoter instead responding directly to binding of phosphorylated AgrA (Queck *et al*, 2008). As the recurring theme with all three of these toxins is the regulation of expression by *agr* and related regulators, this does lend itself to a potential unifying theory of pathogenesis where both high level strain specific and induced *in vivo* activity of major regulators is important.

1.4 Study aims

The recent global spread of PVL producing CA-MRSA and MSSA is a threat to public health and so, it is incumbent on us to gain a clearer understanding as to why these strains are so successful. The balance of the literature indicates a role for the PVL toxin, other cytolytic toxins such as the PSMs and global regulation of virulence factors. Much of the research so far has focused on CA-MRSA, particularly USA300, with comparatively little known about PVL expression in MSSA strains. Although PVL expression is known to be, at least partially, regulated by *agr*, a comprehensive understanding of PVL toxin regulation is lacking.

The aims of this study are as follows:

- To determine whether PVL toxin expression varies in locally circulating MSSA strains and to explore why this variation occurs.
- To gain a better understanding of how *agr* regulates PVL expression and to determine, whether there is a potential role for quorum sensing inhibitors in managing PVL associated infections.
- To study locally successful MSSA isolates in detail through whole genome sequencing, placing them in context with globally important lineages.

2 Materials and Methods

2.1 Growth media and antibiotics

Unless otherwise stated, all media were prepared using distilled water and sterilised by autoclaving for 20 min at 6.9 kPa, 121 ^{o}C.

2.1.1 Brain heart infusion (BHI)

Brain heart infusion (Oxoid)	37 g/L

Bacteriological agar No. 1 (1.5 % (w/v)) was added to prepare BHI agar.

2.1.2 CYGP

Casamino acids (Becton Dickinson)	10 g/L
Yeast extract (Oxoid)	10 g/L
Glucose (Sigma)	5 g/L
Sodium chloride (Fisher scientific)	5.9 g/L

A 1.5 M stock solution of β-glycerophosphate (Sigma) was prepared in deionised water, filter sterilised and added to the media at a concentration of 40 ml/L before use.

2.1.3 Lysogeny Broth (LB)

Tryptone (Oxoid)	10 g/L
Yeast extract (Oxoid)	5 g/L
Sodium chloride (Fisher scientific)	10 g/L

Bacteriological agar No. 1 (1.5 % (w/v)) was added to prepare LB agar.

2.1.4 Tryptone soya broth (TSB)

Tryptone soya broth (Oxoid)	30 g/L

Bacteriological agar No. 1 (1.5 % (w/v)) was added to prepare tryptone soya agar.

2.1.5 LK

Tryptone (Oxoid)	10 g/L
Yeast extract (Oxoid)	5 g/L
KCl	16 g/L

2.1.6 Antibiotics

Growth media for *E. coli* were supplemented as required with: carbenicillin (Cb) at 50 µg/ml, ampicillin (Amp) at 50 µg/ml or kanamycin (Kan) at 50 µg/ml. Growth media for *S. aureus* were supplemented with: erythromycin (Ery) at 10 µg/ml, chloramphenicol (Cm) at 10 µg/ml or tetracycline (Tet) at 10 µg/ml.

2.2 Bacterial strains and plasmids

2.2.1 Bacterial strains

2.2.1.1 S. aureus

Strains of *S. aureus* used in this study are listed in Table 2.1. Strains were kept at -80 ^{o}C in glycerol stocks for long-term storage or at -4 ^{o}C on BHI agar for short term storage.

For standard growth, strains were grown aerobically in BHI or CYGP broth at 37 ^{o}C with shaking at 250 rpm. Optical density was measured at 600 nm (OD_{600}), using a Jenway 6705 spectrophotometer.

2.2.1.1.1 Sourcing of clinical strains

Clinical isolates were collected from the Clinical Microbiology Laboratory at Queen's Medical Centre (Nottingham University Hospitals NHS Trust). Once identified by the clinical laboratory, isolates were stored on nutrient agar slopes (Oxoid). Isolates were retrieved from slopes by plating on Columbia agar (Oxoid) and grown overnight at 37 ^{o}C.

Clinical strains were also provided by collaborators at Bath University (Ruth Massey, Maisem Laabei) or ordered from NARSA (Network for Antimicrobial Resistance in *Staphylococcus aureus*, Virginia, United States).

2.2.1.1.2 Growth with exogenous AIPs

Specific AIPs (AIP-1, AIP-2, AIP-3) and *agr* inhibitors, including the global inhibitor (ala^{5})AIP-1 (McDowell *et al*, 2001), were provided by Dr. Weng Chan, Centre for Biomolecular Sciences, University of Nottingham. For *agr* activation and inhibition experiments, 100 nM of the desired AIP was added to the culture medium prior to inoculation unless stated otherwise.

Table 2.1 *S. aureus* laboratory strains used in the study

Name	Genotype	Source
RN4220	8325-4 restriction negative derivative *rsbU-*	(Kreiswirth *et al*, 1983)
ROJ48	RN4220 Δagr::*ErmB agr*P3-*lux* Tet^R Erm^R	(Jensen *et al*, 2008)
ROJ143	ROJ48 pAgrC1agrA	(Jensen *et al*, 2008)
ROJ154	ROJ48 pAgrC3agrA	Rasmus Jensen (Unpublished)
TS112	ROJ48 pAgrC-N267I	This work
TS113	ROJ48 pAgrC-I311T	This work
TS114	ROJ48 pAgrC-Y251F	This work
TS115	ROJ48 pAgrC-A343T	This work
TS119	ROJ48 pAgrC-N267I-Y251F	This work
TS120	ROJ48 pAgrC-I311T-A343T	This work
TS143	ROJ48 pAgrC-L245A	This work
TS144	ROJ48 pAgrC-F264A	This work
TS145	ROJ48 pAgrC-N308A	This work
TS152	ROJ48 pAgrC-T247I	This work
CYL12349	RN4220 *attB2* pYL112Δ19	(Lei *et al*, 2012)
MY15	ROJ48 *attB2*::*P2agrC1agrA*	Maho Yokoyama (Unpublished)
MY20	ROJ48 *attB2*::*P2agrC1agrA* AgrC-N267I	Maho Yokoyama (Unpublished)
BH1CC ΔmecA	BH1CC ΔmecA::Tet^R	(Rudkin *et al*, 2012)

Tet^R = Tetracycline resistance. Erm^R = Erythromycin resistance.

Table 2.2 *S. aureus* clinical isolates used in the study

Name	Characteristics and clinical details if known	*agr* group	Source
TS1	ST1518 MSSA spa t1941 PVL+ Fatal necrotising pneumonia	1	NUH NHS Trust
TS2	ST772 MRSA spa t657 PVL+ Thigh abscess	2	NUH NHS Trust
TS3	MRSA PVL- Perineal wound	4	NUH NHS Trust
TS4	MRSA PVL- Recurrent boils	1	NUH NHS Trust
TS5	ST772 MSSA spa t657 PVL+ Axillary boil	2	NUH NHS Trust
TS6	ST22 MSSA spa t6642 PVL+ Wound infection following hip surgery	1	NUH NHS Trust
TS7	ST30 MSSA spa t021 PVL+ Nasal carriage	3	NUH NHS Trust
TS8	ST772 MSSA spa t657 PVL+ Facial abscess	2	NUH NHS Trust
TS9	ST22 MSSA spa t6642 PVL+ Wound infection following hip surgery	1	NUH NHS Trust
TS10	MSSA PVL- Abdominal wound infection	1	NUH NHS Trust
TS11	MSSA PVL- Dialysis fistula infection and recurrent bacteraemia	2	NUH NHS Trust
TS12	ST30 MSSA spa t021 PVL+ Wound infection	3	NUH NHS Trust
TS13	ST22 MSSA spa t005 PVL+ Leg abscess	1	NUH NHS Trust
TS14	ST22 MSSA spa t005 PVL+ Leg ulcer	1	NUH NHS Trust
TS15	ST30 MSSA spa t021 PVL+ Recurrent boils	3	NUH NHS Trust
TS16	ST30 MSSA spa t021 PVL+ Thigh abscess	3	NUH NHS Trust
TS17	ST22 MSSA spa t852 PVL+ Nasal carriage	1	NUH NHS Trust
TS18	ST22 MSSA spa t005 PVL+ Foot wound	1	NUH NHS Trust
TS19	ST22 MSSA spa t310 PVL+ Back abscess	1	NUH NHS Trust
TS20	ST22 MSSA spa t005 PVL+ Knee bursitis	1	NUH NHS Trust
TS21	ST88 MSSA spa t6769 Empyema	3	NUH NHS Trust
TS22	MSSA PVL- Recurrent bacteraemia	2	NUH NHS Trust
TS23	ST22 MSSA spa t6642 PVL+ Cellulitis and bacteraemia in an IVDU	1	NUH NHS Trust

TS24	ST22 MSSA spa t005 PVL+ Cellulitis on foot and bacteraemia	1	NUH NHS Trust
TS25	ST22 MSSA spa t6642 PVL+ Severe pneumonia following a viral illness	3	NUH NHS Trust
TS27	MRSA PVL+ Recurrent boils	1	NUH NHS Trust
TS31	MSSA PVL+ Necrotising pneumonia	1	NUH NHS Trust
TS32	MSSA PVL+ Prostatic abscess	1	NUH NHS Trust
TS33	MSSA PVL+ Bacteraemia associated with prostatic abscess	1	NUH NHS Trust
SANOT01	MRSA PVL+ Aortic root abscess	3	NUH NHS Trust
NRS123	MW2/USA400 CC1 Type IVa MRSA PVL+	3	NARSA
NRS133	NCTC8325 MSSA	1	NARSA
NRS162	ST30 MSSA	3	NARSA
NRS255	CC80 Type IV MRSA	3	NARSA
NRS384	USA300 CC8 Type IVa MRSA	1	NARSA
TW20	ST20	1	Ruth Massey
HU24	ST239 AgrC-I311T-A343T	1	Ruth Massey
IU12	ST239 AgrC-I311T	1	Ruth Massey
DEU9	ST239 AgrC-I311T-A343T	1	Ruth Massey
BH1CC	CC8 type II MRSA	1	(O'Neill *et al*, 2008)
ICP5014	ST239	1	Ruth Massey
ICP5062	ST239 AgrC-T247I	1	Ruth Massey

MSSA = Methicillin sensitive *S. aureus*. MRSA = Methicillin resistant *S. aureus*. NUH = Nottingham University Hospitals. CC = Clonal complex. ST = Sequence type. PVL = Panton-Valentine Leukocidin. IVDU = intravenous drug user.

2.2.1.2 E. coli

TOP10 *E. coli (*F- *mcr Δ*(*mrr-hsdRMS-mcrBC*) ϕ 80 *lacZ ΔM15 ΔlacX74 recA1 deoR araD139 Δ*(*ara-leu*) *7697 galK rpsL* (Str^R) *endA1 nupG*) (Invitrogen) was used for plasmid manipulation and propagation. Growth conditions were similar to *S. aureus* except that LB broth was used as the growth medium.

2.2.2 Plasmids

Plasmids used in this study are listed in Table 2.3.

Table 2.3 Plasmids used in this study

Name	Genotype	Source
pSK5630	pSK1 *rep* and *par rrnBT1 bla cat* Cm^R	(Grkovic *et al*, 2003)
pSKermP2	pSK5630 *ermB* P2*agr* Erm^R, Cm^R	(Jensen *et al*, 2008)
pAgrC1agrA	pSKermP2 *agrC1 agrA* Erm^R, Cm^R	(Jensen *et al*, 2008)
pAgrC3agrA	pSKermP2 *agrC3 agrA* Erm^R, Cm^R	Rasmus Jensen (Unpublished)
pAgrC-N267I	pAgrC1agrA AgrC-N267I	This work
pAgrC-I311T	pAgrC1agrA AgrC-I311T	This work
pAgrC-Y251F	pAgrC1agrA AgrC-Y251F	This work
pAgrC-A343T	pAgrC1agrA AgrC-A343T	This work
pAgrC-N267I-Y251F	pAgrC1agrA AgrC-N267I-Y251F	This work
pAgrC-I311T-A343T	pAgrC1agrA AgrC-I311T-A343T	This work
pAgrC-L245A	pAgrC1agrA AgrC- L245A	This work
pAgrC-F264A	pAgrC1agrA AgrC- F264A	This work
pAgrC-N308A	pAgrC1agrA AgrC- N308A	This work
pAgrC-T247I	pAgrC1agrA AgrC- T247I	This work
pLL102	Derivative of pCL25 carrying *attP2* Tet^R	(Lei *et al*, 2012)
pEJM5	pLL102 Tet^R , Kan^R	Ewan Murray (Unpublished)
pEJM6	pEJM5 *P2agrC1agrA* Tet^R, Kan^R	Ewan Murray (Unpublished)
pMYP3	pLL102 *P2agrC1agrA* AgrC-N267I Tet^R, Kan^R	Maho Yokoyama (Unpublished)

Tet^R = Tetracycline resistance. Erm^R = Erythromycin resistance. Cm^R = Chloramphenicol resistance. Kan^R = Kanamycin resistance.

2.3 DNA purification techniques

2.3.1 Genomic DNA preparation

Genomic DNA was extracted from *S. aureus* as follows: 500 µl of overnight culture was centrifuged at 17,000 x g for 5 min and the supernatant discarded. 5 µl lysostaphin 5 mg/ml (Sigma), 5 µl RNase 1 mg/ml (Qiagen) and 180 µl enzymatic lysis buffer (20 mM Tris pH 8, 2 mM EDTA, 1.2 % (v/v) Triton X-100) were added to each pellet and incubated for 30 min at 37 °C. Purification of DNA was then performed using a DNeasy kit (Qiagen), according to the manufacturer's instructions: 25 µl of proteinase K and 200 µl buffer AL were added and mixed by vortexing. This was incubated at 70 ^{o}C for 30 min before the addition of 200 µl 100 % (v/v) ethanol. The resulting mixture was transferred into a DNeasy mini spin column and centrifuged in a microfuge at 10,500 x g for 1 min, discarding the flow through and collection tube. 500 µl buffer AW1 was then added, the column centrifuged at 10,500 x g for 1 min and the flow through and collection tube discarded. After this, 500 µl buffer AW2 was added and the column spun for 17,000 x g for 3 min. Finally, 100 µl sterile deionised water was added, incubated for 1 min at room temperature and then centrifuged at 10,500 x g for 1 min to elute the DNA.

2.3.2 Plasmid preparation

2.3.2.1 Plasmid preparation from *E. coli*

Cells were grown overnight in LB broth with addition of the appropriate antibiotics to maintain selective pressure. A 1.5 ml aliquot was removed and centrifuged at 17,000 x g for 2 min and the supernatant removed. Plasmid extraction and purification was then performed using a QIAprep Spin Miniprep kit (Qiagen) according to the manufacturer's instructions: 250 µl buffer P1 was added followed by 250 µl buffer P2, mixed by inversion and left to stand for 3 min. 350 µl buffer N3 was added to the mixture and vortexed thoroughly to produce a homogeneous

suspension which was then centrifuged at 17,000 x g for 10 min in a microfuge. The supernatant was transferred into spin columns with collection tubes and centrifuged at 17,000 x g for 1 min with flow through discarded. 500 µl PB buffer was added before centrifuging for a further 1 min at 17,000 x g, discarding the flow through. Finally, 750 µl PE buffer was added, centrifuging for 1 min at 17,000 x g, discarding the flow through, and then centrifuging for a further 1 min to remove any residual ethanol from the spin column. The plasmid DNA was eluted by adding 50 µl sterile deionised water, incubating at room temperature for 1 min and centrifuging at 17,000 x g for 1 min.

2.3.2.2 Plasmid preparation from S*. aureus*

Cells were grown overnight in BHI broth with addition of the appropriate antibiotics. A 3 ml aliquot was removed and centrifuged at 17,000 x g for 2 min and the supernatant removed. Cells were resuspended in 250 µl P1 lysis buffer from a QIAprep Spin Miniprep Kit (Qiagen) with the addition of 5 µl lysostaphin 5 mg/ml (Sigma) and incubated for 30 min at 37^{o}C. Plasmid extraction and purification was performed with the QIAprep Spin Miniprep kit as described above.

2.3.3 RNA preparation

Bacterial isolates were inoculated from overnight cultures at a 1:500 dilution and grown in BHI broth for 4 h, until mid exponential phase. 1 ml of RNA Protect (Qiagen) was added to 0.5 ml of each bacterial culture before pelleting the mixture by centrifugation at 5,200 x g for 10 min and removing the supernatant. Pellets were stored at -80 ^{o}C prior to extraction of RNA.

195 µl of TE buffer (10 mM Tris HCl, pH 8.0, 1 mM EDTA) and 5 µl lysostaphin 5 mg/ml (Sigma) were added to the pellets prior to extraction. The mixture was incubated at room temperature

for 20 min and vortexed regularly. RNA was extracted and purified using an RNeasy Mini kit (Qiagen) according to the manufacturer's instructions: 700 µl RLT buffer, containing 7 µl β-mercaptoethanol, was added to the mixture, mixed by vortexing and centrifuged at 13,000 x g for 2 min. The supernatant was decanted into a new tube and 500 µl 100 % ethanol (v/v) added before 600 µl aliquots were transferred to spin columns, centrifuging at 13,000 x g for 1 min after each aliquot was added. 700 µl buffer RW1 was then added and the column centrifuged at 13,000 x g for 1 min, discarding the flow through and collection tube. After this, 500 µl RPE was added, the column centrifuged at 13,000 x g for 1 min, a further 500 µl RPE added and the column centrifuged again at 13,000 x g for 2 min. To elute the RNA, the column was placed in a microfuge tube, 100 µl sterile RNAse free water (Qiagen) added and incubated at room temperature for 1 min before centrifuging at 13,000 x g for 1 min.

Before conversion to cDNA, RNA samples were treated with Turbo DNase (Ambion) according to the manufacturer's instructions: 11 µl x10 Turbo DNase buffer and 3 µl (2 U) Turbo DNase was added to 100 µl RNA sample and incubated at 37 ^{o}C for 30 min. The RNA was then re-purified with the RNeasy Mini kit as described above. The absence of genomic DNA was verified by PCR as described in 2.4.2, using the RNA preparation as template and a genomic DNA preparation as the positive control.

2.3.4 Purification of PCR products

PCR products were purified using a QIAquick spin column (Qiagen) according to the manufacturer's instructions: Binding buffer was added to PCR product at a ratio of 5 volumes to 1 and mixed by vortexing. The mixture was transferred to a spin column in a collection tube and centrifuged at 17,000 x g for 1 min, with the flow through discarded. 750 µl binding buffer was then added to the spin column, centrifuged at 17,000 x g for 1 min, discarding the flow through and then centrifuged at 17,000 x g for a further 1 min to remove any residual ethanol.

Finally, the column was transferred to a microfuge tube, 50 µl sterile deionised water added, incubated at room temperature for 1 min and centrifuged at 17,000 x g for 2 min to elute the DNA.

2.4 DNA manipulation techniques

2.4.1 Primer design

Primers were designed by analyzing the required amplification regions with Vector NTI software (Invitrogen). Predicted melting and annealing temperatures were calculated with the New England Biolabs Tm calculator (www.neb.com/tools-and-resources/interactive-tools/tm-calculator). Once designed, primer specificity was verified with a BLAST search (http://blast.ncbi.nlm.nih.gov/Blast.cgi).

Primers were synthesized by Sigma-Aldrich and stored at -20^{o}C as 10 µM working solutions or 100 µM stock solutions. For use in the promoter pull down experiments, forward primers were synthesized with 5' biotinylation. For use in site-directed mutagenesis, all primers were synthesized with 5' phosphorylation. For use in quantitative RT-PCR, primers were designed as previously published by Dumitrescu *et al* (Dumitrescu *et al*, 2011) and purified by polyacrylamide gel electrophoresis. The primers used for *agr* sequencing AgrC 5' B, AgrA 5' A, AgrB F, agrC R were originally designed by Traber *et al* (Traber *et al*, 2008).

Primers used in the study are listed in Table 2.4.

Table 2.4 Primers used in the study

Name	Sequence (5' to 3')	Application
AgrBDCAF	ACAACTCATCAACTATTTTCC	*agr* amplification
AgrBDCAR	GATTTACAATTGAATACGCCG	*agr* amplification
Pvl F	ATGTCCTTTCACTTTAATTTCATGAGTTTT	*pvl* testing
Pvl R	CATGCTACTAGAAGAACAACACACTATGG	*pvl* testing
AgrpromoR B	(B)ACAACTCATCAACTATTTTCC	Pulldown
AgrpromoR	TCTCTTTTGAAGATACGTGGC	Pulldown
PvlpromoF	TACTTATATTGCTAATAGTGG	Pulldown
PvlpromoF B	(B)TACTTATATTGCTAATAGTGG	Pulldown
PvlpromoR	ATTCTCAATATTGTTATCAGC	Pulldown
AgrD1234F	TATGCACCTGCAGCTACTAA	*agr* typing
AgrD1234R	TCATGACGGAACTTGCGC	*agr* typing
Agrfull F	GCAACGCGAAAATATACCTG	*agr* sequencing
Agrfull R	GCGTTGCTGCAATAGTGACA	*agr* sequencing
AgrC 5' B	AAAGAGATGAAATACAAACG	*agr* sequencing
AgrA 5' A	ATTAACAACTAGCCATAAGG	*agr* sequencing
AgrB F	AATAAAATTGACCAGTTTGC	*agr* sequencing
agrC R	GAATAATACCAATACTGCGAC	*agr* sequencing
AgrC-N267I-F	(P)AGACAATTTACAAATGAATGCTATAAAATTA	SDM
AgrC-N267I-R	(P)TTCATAGGTACAATAATTTTATTGAAATAAT	SDM
AgrC-Y251F-F	(P)CACTTTCAGAATTCATTCGAGAAGATGA	SDM
AgrC-Y251F-R	(P)TCGTTAAGATATTGACATAATCATGACG	SDM
AgrC-A343T-F	(P)GATAATGCAATTGAGACATCAACTGAAA	SDM
AgrC-A343T-R	(P)AAGAATAATACCAATACTGCGACTTAAATC	SDM
AgrC-I311T-F	(P)AAATGAATATTCCGACTAGTATCGAAATACC	SDM
AgrC-I311T-R	(P)CTTGTGCACGTAAAATTTTCGCAGTAAT	SDM
AgrC-L245A-F	(P)ATTATGTCAATATCGCAACGACACTTTCAG	SDM
AgrC- L245A-R	(P)CATGACGGAACTTGCGCA	SDM
AgrC-F264A-F	(P)GGCCTACGTGATTATGCTAATAAAAATATTGTACC	SDM
AgrC- F264A-R	(P)AGGCATGTCATCTTCTCGAATGTA	SDM
AgrC-N308A-F	(P)GCACAAGAAATGGCTATTCCGATTAGTATC	SDM
AgrC- N308A-R	(P)ACGTAAAATTTTCGCAGTAATTAAGCCTT	SDM
AgrC- T247I-F4	(P)TACTTTCAGAATACATTCGAGAA	SDM
AgrC- T247I-R4	(P)TCGTTAAGATATTGACATAATCAT	SDM
GyrB F	GGTGGCGACTTTGATCTAGC	qRT-PCR
GyrB R	TTATACAACGGTGGCTGTGC	qRT-PCR
LukS-PV F	AATAACGTATGGCAGAAATATGGATGT	qRT-PCR
LukS-PV R	CAAATGCGTTGTGTATTCTAGATCCT	qRT-PCR
RNAIII F	GGGATGGCTTAATAACTCATAC	qRT-PCR
RNAIII R	GGAAGGAGTGATTTCAATGG	qRT-PCR
EJM63	ATACGAATTCCCATGGCAACTATTTTCCATCACA	*agr* cloning
EJM65	ATCGGATCCGTTAACTGACTTTATTATC	*agr* cloning

(P) = 5' phosphorylation. (B) = 5' biotinylation. SDM = site directed mutagenesis. qRT-PCR = quantitative real time PCR.

2.4.2 PCR amplification

A high-fidelity DNA polymerase, Phusion (New England Biolabs), was used in all reactions.

Components of a standard 50 µl reaction, made up with sterile deionised water, were as follows:

5 x Phusion HF buffer	10 µl
dNTPs	200 µM each
Primers	0.5 - 1 µM each
Template	1 pg – 10 ng
Phusion DNA polymerase	1 U

PCR reactions were carried out on a T3000 ThermoCycler (Thistle Scientific). Standard settings used were:

1 cycle	Initial denaturation	98 ^{o}C	2 min
30 cycles	Denaturation	98 ^{o}C	10 s
	Annealing	55-69 ^{o}C	30 s
	Extension	98 ^{o}C	30 s per kb (2 min minimum)
1 cycle	Final extension	72 ^{o}C	2 min

PCR products were stored at -20 ^{o}C.

2.4.3 Agarose gel electrophoresis

DNA samples were separated by electrophoresis in 1.5 % (w/v) agarose gels made up with 1 x TAE buffer (40 mM Tris acetate, 2 mM EDTA ph 8.5). To enable visualization of DNA, ethidium bromide was added to the molten agarose at a final concentration of 0.4 µg/ml. Samples were

prepared in DNA loading buffer (Promega) and gels run in 1 x TAE at 100 V for 30 to 60 min. A 1 kb DNA ladder (Promega) was also run on the gel to enable comparison of DNA fragment size. After electrophoresis, bands were visualized using a UV transilluminator.

2.4.4 Ligation of PCR products

DNA Ligase enzyme (Invitrogen) was used for ligation as follows: 7 µl PCR product was mixed with 2 µl x 10 ligase buffer, 1 µl ligase enzyme and 10 µl sterile deionised water. The mixture was incubated at room temperature overnight before use.

2.4.5 Small scale DNA sequencing

Following purification of PCR products or preparation of plasmid, DNA was sent to Source Bioscience Life Sciences (Nottingham) for sequencing along with aliquots of the appropriate sequencing primers.

2.4.6 Sequence analysis

All sequence analysis and alignment, except for analysis of next generation sequencing data, was carried out using Vector NTI Advance 11.0 software (Invitrogen) with consensus sequences shown in yellow, partial matches in blue and non-consensus bases shown in white. GenBank reference sequences were obtained from the National Center for Biotechnology Information at www.ncbi.nlm.nih.gov. Reference sequences used are listed in Table 2.5. Next generation sequencing data was analysed as described in 2.8.

Table 2.5 *S. aureus* reference sequences used in this study

Name	Description	GenBank Accession ID
NCTC 8325	Laboratory MSSA, *agr* group 1 reference	CP000253.1
HO 5096 0412	HA-MRSA, SCC*mec* IV, representative of EMRSA-15	HE681097.1
MW2 (& ΦMW2)	CA-MRSA, SCC*mec* IV, *agr* group 3 reference	NC_003923.1
N315	HA-MRSA, SCC*mec* II, *agr* group 2 reference	BA000018.3
USA300 (& ΦSLT)	CA-MRSA, SCC*mec* IV	CP000255.1
ΦPVL	Prophage carrying the *pvl* gene	NC_012784
Φtp310-1	Prophage isolated from ST22 spa-310 strain	EF462197
Φtp310-3	Prophage isolated from ST22 spa-310 strain	EF462199

2.4.7 Molecular characterisation of clinical isolates

S. aureus agr types were determined by amplifying and sequencing *agrD* with *agrD1234F* and *agrD1234R* primers. The resulting sequences were aligned to reference strains of known *agr* type.

spa typing and Multi-Locus Sequence Typing (MLST) were carried out by Kome Otokunefor (Otokunefor *et al*, 2012).

2.4.8 Reverse transcriptase PCR

cDNA was synthesised from RNA samples with Superscript II reverse transcriptase (Invitrogen) according to the manufacturer's instructions: 10 µl RNA preparation (approximately 5 µg) was mixed with 1 µl dNTPs (10 mM) and incubated at 65 ^{o}C for 5 min before addition of 4 µl 5x first strand buffer and 2 µl 0.1 M DTT. This mixture was left at room temperature for 2 min before addition of 1 µl superscript II enzyme, made up to 20 µl total with sterile deionised water. The reaction mixture was heated to 25 ^{o}C for 10 min, 42 ^{o}C for 50 min and 70 ^{o}C for 10 min to generate the cDNA.

cDNA was cleaned up with a QIAquick PCR purification kit (Qiagen) as described in 2.3.4 and yields verified using a Nanodrop ND-1000 spectrophotometer (Labtech) testing for ssDNA at a wavelength range of 220 nm to 350 nm with an extinction coefficient of 33 ng-cm/µl. cDNA samples were stored at -20 ^{o}C prior to comparative gene quantification.

2.4.9 Quantitative real-time PCR

cDNA templates were amplified using a Power SYBR Green Master mix (Life Technologies Corporation) according to the manufacturer's instructions, with amplification recorded by an

AB7500 Real-time PCR System (Applied Biosystems). The PCR mixture for each well consisted of:

2 x SYBR Green Master mix	12.5 µl
Forward primer	0.75 µl
Reverse primer	0.75 µl
cDNA template	2 µl
Deionised water	9 µl

The primers for *gyrB* F, *gyrB* R, *lukS*-PV F, *lukS*-PV R, RNAIII F and RNAIII R (Table 2.4) were first tested using serial dilutions of a single cDNA template to ensure primers worked efficiently at a 1:1 ratio of forward to reverse primer.

Once primer efficiency had been established, comparative cycle threshold (CT) values were recorded for each combination of primer and template in triplicate. The comparative CT values were used to calculate relative expression of the target genes *lukS-PV* and *RNAIII*, with *gyrB* acting as a constitutively expressed control.

2.5 Transformation techniques

2.5.1 Transformation of *E. coli*

2.5.1.1 Preparation of *E. coli* electrocompetent cells

4 ml of overnight culture was placed in 400 ml LB and incubated at 37 ^{o}C with shaking to OD 0.4-0.6. The flask was placed on ice with occasional swirling for 20 min before centrifugation at 4000 x g, 4^{o}C for 10 min. After the supernatant was poured off, pellets were resuspended in 25 ml ice cold sterile water and spun again. This wash step was repeated twice before resuspension of the pellets in 10 % (v/v) glycerol in water. Aliquots were snap frozen in liquid nitrogen and stored at -80 ^{o}C.

2.5.1.2 Transformation of *E. coli* by electroporation

10 µl of plasmid or ligated PCR product was added to an aliquot of electrocompetent cells and transferred to a 1 mm electroporation cuvette, keeping cells on ice throughout. Electrical current was delivered at 200 Ω, 1.75 kV and 25 µF before addition of 1 ml LB broth. Cells were incubated for 1 h at 37 ^{o}C for recovery before plating 200 µl onto LB agar, containing the appropriate antibiotic for selection, and incubated at 37 ^{o}C overnight.

2.5.2 Transformation of *S. aureus*

2.5.2.1 Preparation of *S. aureus* electrocompetent cells

A single colony was placed in 500 ml BHI broth and grown for 14 h overnight at 37 °C with shaking. This was diluted to OD 0.1 in 500 ml BHI and grown to OD 0.4-0.6, allowing growth for no longer than 90 min at 37 °C with shaking. The resulting culture was split into 10 x 50 ml tubes and centrifuged for 10 min at 3,400 x g with supernatant discarded, before resuspension of the pellets in 25 ml deionised water and further centrifugation for 10 min at 3,400 x g. This wash step was repeated twice more, before resuspension of the pellets in 20 ml 10 % (v/v) glycerol in water. After centrifugation for 10 min at 3,400 x g, the pellets were re-suspended in 10 ml 10 % (v/v) glycerol and incubated for 30 min at room temperature. Following a final centrifugation, pellets were pooled and resuspended in the residual 10 % (v/v) glycerol left after decanting of the supernatant with 60 µl aliquots taken and frozen immediately at -80 °C.

2.5.2.2 Transformation of *S. aureus* by electroporation

5, 10 or 15 µl of plasmid preparation was added to a 50 µl aliquot of electrocompetent cells and transferred to a 1 mm electroporation cuvette. Electrical current was delivered at 100 Ω, 2.3k V and 25 µF before immediate addition of 1 ml BHI broth. Cells were incubated for 3 h at 37 °C for recovery before plating 200 µl onto BHI agar containing the selection antibiotic for growth at 37 °C overnight.

2.5.3 Phage transduction

The construction of *S. aureus* strains MY15 and MY20 by phage transduction was carried out by Maho Yokoyama as part of her MSc project, as described below.

A plasmid, pEJM6, was constructed by introducing the wild type group 1 *agr*P2*BDCA* genes, amplified with primers EJM63 and EJM65, onto the integrative plasmid pEJM5. pEJM6 was transformed into a chromosomal integration strain of *Staphylococcus aureus,* CYL12349, with selection for kanamycin resistance, resulting in integration of *agrP2BDCA* at an *attB*2 site on CYL12349.

Phage lysate was prepared from the CYL12349 intermediate strains by mixing 200 µl overnight culture with LK broth and phage buffer (1 mM $MgSO_4$, 4 mM $CaCl_2$, 50 mM Tris-HCl, 100 mM NaCl, 1 g/L gelatin powder in deionised water) in a 1:1 ratio. 500 µl Φ11 RN6390B lysate was added and the mixture incubated at 30 ^oC with shaking until clear.

Once prepared, the lysates were used to transduce the Δ*agr*::*agrP3-lux* bioreporter ROJ48 as follows; 1.8 ml LK broth, 10 µl 1 M $CaCl_2$, 200 µl overnight ROJ48 culture and 200-500 µl phage lysate were incubated for 45 min at 37 ^oC with shaking. 1 ml of 20 mM trisodium citrate was added to the mixture and incubated on ice for 5 min followed by centrifugation at 17,000 x g. for 2 min. The pellet obtained was resuspended in 1 ml 20 mM trisodium citrate and placed on ice for 2.5 h. 200 µl of the mixture was plated on tryptic soy agar containing 10 mM trisodium citrate and incubated at 37 ^oC. Following transduction, the resulting colonies of ROJ48 were confirmed to have the *agr*P2*BDCA* genes integrated at an ectopic chromosomal location, following phage integration, creating the *S. aureus* strain MY15.

MY20 was made by introducing AgrC-N267I into pEJM6 by site directed mutagenesis, to make pMYP3, before integrating onto CYL12349 and transduction with ROJ48 as described above.

2.6 Protein analysis

2.6.1 Exoprotein sample preparation

The desired *S. aureus* clinical isolates for analysis were inoculated into CYGP broth and grown overnight, unless otherwise stated. A volume equivalent to an OD_{600} of 5 was calculated using the formula: volume = $OD_{600}/5$. The calculated volume of culture was centrifuged at 17,000 x g for 5 min and the supernatant removed and filter sterilised. 100 % (w/v) trichloroacetic acid was added to the supernatant in a microfuge tube at a final concentration of 10 % (v/v), incubating on ice for 1 h. The mixture was centrifuged at 17,000 x g for 5 min and the supernatant discarded. 500 µl acetone was added to the microfuge tube and the tube vortexed thoroughly to disrupt the pellets. After centrifugation at 17,000 x g for 5 min, the pellets were washed with a further 500 µl acetone which was removed following centrifugation. The pellets were allowed to dry for 5 min in air, after which 40 µl SDS-PAGE buffer (Nupage) was added. Samples were heated to 80 ^{o}C for 3 min prior to loading.

2.6.2 SDS-PAGE

Routine SDS-PAGE was performed using a 12 % (w/v) acrylamide resolving gel consisting of:

30 % (w/v) acrylamide/Bis (BioRad)	4 ml
1.5 M Tris-HCl (pH 8.8)	2.5 ml
Deionised water	3.35 ml
10 % (w/v) SDS	100 µl
10 % (w/v) ammonium persulphate (APS)	100 µl
TEMED	15 µl

The APS and TEMED were added immediately before pouring, and a layer of isopropanol was added to the top of the gel after pouring.

Once the resolving gel had set, the isopropanol was removed and a stacking gel added, placing a comb on top immediately to create separate wells. The stacking gel consisted of:

30 % (w/v) acrylamide/Bis (BioRad)	0.83 ml
0.5 M Tris-HCl (pH 6.8)	0.62 ml
Deionised water	2.5 ml
10 % (w/v) SDS	50 µl
10 % (w/v) ammonium persulphate (APS)	50 µl
TEMED	5 µl

Once the stacking gel had set, the comb was removed and the gel placed in a Protean II (BioRad) gel-running tank filled with SDS-PAGE running buffer (14.4 g/L glycine, 3 g/L Tris base, 1 g/L SDS in deionised water). Samples (5 to 20 µl) were loaded into the wells, with purified LukF (provided by Charles Okolie, Microbiology, Centre for Biomolecular Sciences) and alpha-haemolysin (Sigma) used as positive controls. 10 µl of Novex Sharp protein standard (Invitrogen) was also loaded to determine protein sizes. Proteins were separated by electrophoresis at 150 V until the blue dye front of the sample buffer reached the base of the gel.

2.6.3 Coomassie blue staining

Proteins were visualized by staining with SimplyBlue™ Safe Stain (Novex) according to the manufacturer's instructions: Gels were first soaked in deionised water for 10 min, changing the water after 5 min. The gels were covered in the staining fluid and left for 1 h. Finally, gels were rinsed and left to destain in deionised water for a further h or until the protein bands could be clearly seen.

2.6.4 Immunoblots

Proteins were first separated by SDS-PAGE as described in 2.6.2. A BioTrace®NT nitrocellulose membrane (PALL life sciences, USA) was cut to the same size as the SDS-PAGE gel and protein transferred from gel to membrane using the BioRad II Mini-Cell and Electroblotting Module according to the manufacturer's instructions. Transfer was carried out in blotting buffer (14.4 g/L glycine, 3 g/L Tris, 1 g/L SDS in deionised water) at a fixed current of 140 mA for 1 h. The membrane was stained reversibly with Ponceau S solution (Sigma) to confirm successful protein transfer before proceeding to immunoblot. After rinsing with deionised water, the membrane was blocked in 5 % (w/v) skimmed milk in phosphate buffered saline (PBS pH 7.4) for 2 h or overnight.

Immunoblotting was performed by incubating the membrane with 1/1000 (v/v) anti-LukF or 1/2000 (v/v) anti-Hla mouse monoclonal antibodies (Prof. L. Durrant, School of Medicine, University of Nottingham), in 5 % (w/v) skimmed milk in PBS for 1 h. After 2 x 15 min washes with PBS Tween (PBS pH 7.4 with 0.05 % (v/v) Tween 20), the membrane was incubated in secondary antibody solution containing 1/3000 (v/v) protein A-Horseradish peroxidise conjugate (Sigma) in conjugate buffer (50 mM Tris, 100 mM NaCl pH 8.0) for 1 h.

Following 2 x 15 minute washes in conjugate buffer containing 0.05 % (v/v) Tween 20, the membrane was coated in ECL substrate (GE Healthcare) for 2 min and exposed to film (Amersham Hyperfilm ECL, GE Healthcare) in the dark room.

2.7 Promoter pull down experiments

2.7.1 Generation of biotinylated promoter probes by PCR

Biotin labeled primers (Table 2.4) were used to amplify the *pvl* and *agr* promoter regions by PCR. Ten 50 µl PCR reactions were used per sample which were then pooled and purified as described in 2.3.4 with elution in 200 µl sterile deionised water. The DNA concentration of the PCR product was not measured prior to use.

2.7.2 Preparation of lysed cell extracts

Bacterial cultures were grown overnight in 10 ml CYGP before 1:100 dilution into 400 ml of CYGP and incubated for 5 h with shaking. Cultures were centrifuged for 10 min at 3,400 x g to pellet the bacteria. Pellets were resuspended in 2 ml of lysis buffer (100 mM NaCl, 10 mM Tris-HCl pH 8, 1 mM EDTA, 0.05 % (v/v) Triton X-100) before addition of 40 µl of lysostaphin 5 mg/ml. After incubation for 1 h at 37 ^{o}C, the mixture was homogenised with a Precellys 24 homogenizer (Precellys) for 3 cycles, incubating on ice for 5 min between cycles. The lysate obtained was centrifuged at 13,000 x g for 10 min to remove any residual cell debris. 20 µl of 100 mM PMSF protease inhibitor (Invitrogen) and 50 µl salmon sperm DNA (Invitrogen) was added per 1ml of lysate.

2.7.3 Binding of proteins to the promoter fragments

Following preparation of lysed cell extract, 100 µl of Dynabeads (Invitrogen Dynabeads M-280 Streptavadin) were placed in a microfuge tube for each sample to be tested. Using a magnetic rack, the beads were washed with 1 ml wash buffer 2 X (2 M NaCl, 10 mM Tris-HCl pH 7.4, 1 mM EDTA) three times before resuspension in 200 µl of the biotinylated promoter PCR product for 30 min.

After three washes of the beads with 1 ml wash buffer 1 X (1 M NaCl, 5 mM Tris-HCl ph 7.4, 0.5 mM EDTA), 1 ml of lysed cell extract was added and incubated for 4 h at room temperature, or overnight. The beads were washed again for four times with 1 ml lysis buffer (100 mM NaCl, 10 mM Tris-HCl pH 8.0, 1 mM EDTA, 0.05 % (v/v) Triton X-100) before resuspension in 20 µl elution buffer (1.2 M NaCl, 10 mM Tris-HCl pH 8.0, 1 mM EDTA, 0.05 % (v/v) Triton X-100).

2.7.4 Separation and identification of promoter bound proteins

The eluted fraction was mixed with 20 µl SDS-PAGE loading buffer (NuPage, Invitrogen) and 20 µl loaded onto a 4-12 % precast SDS-PAGE gel (NuPage Novex, Invitrogen) in MES buffer (50 mM MES, 50 mM Tris base, 0.1 % (w/v) SDS, 1 mM EDTA pH 7.3) and run at 150 V for 1 h. After Coomassie blue staining, bands of interest were cut from the gel and sent to the Protein and Nucleic Acid Chemistry Laboratory (University of Leicester) for sequencing by mass spectrometry. Protein identifications were returned as a list of proteins in each gel band and a relative quantification given which accounts for % of spectra and protein molecular weight.

2.8 Construction of *agr* bioreporters and bioreporter assays

2.8.1 Construction of the group 1 and 3 *agr* bioreporters

An *agr*P3-*lux* bioreporter strain, ROJ48, was constructed previously by replacing the *agr* locus in RN4220 with an *agrP3-luxABCDE* promoter fusion and *ermB*, which confers resistance to erythromycin (Jensen *et al*, 2008).

Plasmids, based on pSKerm (conferring chloramphenicol and ampicillin resistance), were constructed with *agrCA* of either group 1 or 3 under the control of the *agrP2* promoter and used to transform ROJ48 to create the group 1 bioreporter ROJ143 (Jensen *et al*, 2008) and the group 3 bioreporter ROJ154 (Rasmus Jensen, unpublished).

2.8.2 Site-directed mutagenesis of the *agr* group 1 bioreporter

5' phosphorylated primers containing the desired point mutations in *agrC* (Table 2.4) were used to amplify the group 1 bioreporter plasmid pAgrC1agrA. PCR products were purified and ligated as described in 2.4.4 to create circularized plasmid. 10 µl of ligation product was transformed with TOP 10 *E. coli,* selecting for ampicillin resistance. Plasmid was prepared from a selection of successful transformants and sequenced to confirm the desired mutations were present. Plasmids with the correct sequence were transformed into ROJ48, selecting for chloramphenicol resistance, to create mutant bioreporters.

2.8.3 Bioluminescent reporter assay

Bioreporter strains were grown overnight at 37 ^{o}C in BHI medium with the addition of chloramphenicol 10 µg/ml to maintain the selective pressure on the plasmid. Cultures were diluted 1/50 and incubated for a further 4 h. 10 µl of reporter culture was placed into wells in a 96 well microtitre plate and 20 µl of either test culture supernatant or synthetic AIP was

added, with each sample tested in triplicate. Synthetic AIPs were used as positive controls, with medium only for negative controls. BHI containing chloramphenicol 10 µg/ml was added to each well, to a total volume of 200 µl, and the plate incubated in an Infinite 200 PRO microplate luminometer (Tecan) overnight. Light and OD_{600} were measured every 15 min over 12 h.

Data were plotted as relative light units per cell density (RLU/OD) over time in Excel (Microsoft Corp.). Peak values from each concentration of AIP were calculated and exported to PRISM2 program (GraphPad, San Diego, CA). An EC_{50} value was then generated for each reporter based on the variable slope sigmoidal dose response curve. All assays were conducted in triplicate.

2.8.4 Measurement of AIP production over the growth curve

1 ml of overnight culture from each test isolate was pelleted and washed 3 times in fresh BHI. Bacteria were inoculated at a 1:500 dilution in BHI and incubated at 37 ^{o}C with shaking. At fixed time points, 1 ml of culture was removed, centrifuged and the supernatant filter sterilised. Supernatants collected at several time points were analysed with the bioluminescent reporter assay, compared to a full dilution range of AIP. If there was sufficient AIP present in the supernatants to saturate the bioreporter, assays were repeated with serial dilutions of supernatant. Peak values of RLU/OD for each test supernatant were then compared with the values generated from the AIP standard curve in order to determine the AIP concentration present.

2.9 Whole genome sequencing analysis

Genomic DNA was prepared as described in 2.3.1 and sent to the DeepSeq Facility (University of Nottingham) where it was sequenced using a MiSeq benchtop sequencer (Illumina) with a 2x 150 bp paired end run.

The raw data was processed with the assistance of a Bioinformatician, Hardeep Naghra (Centre for Biomolecular Sciences, University of Nottingham).

Illumina reads were first mapped to the EMRSA-15 representative genome HO 5096 0412 (Holden *et al*, 2013) with the Burrows-Wheeler alignment tool (Li & Durbin, 2009) using the default settings.

Variants were then called with mpileup and bcftools (Li *et al*, 2009a) using default settings and filtering out base quality scores lower than 15. Single nucleotide polymorphisms (SNPs) with less than 5 reads were also removed.

The resulting analyses were produced in *.vcf format which could be analysed, along with the BWA alignments, using Artemis 14.0.0 software (Wellcome Trust Sanger Institute, Cambridge).

A *de novo* assembly was attempted with velvet de novo assembly software (Zerbino & Birney, 2008) to find any large unmapped reads. Unmapped reads were analysed with the Basic Local Alignment Search Tool (BLAST) at blast.ncbi.nlm.nih.gov (National Center for Biotechnology Information, United States).

3 Variable PVL production relates to *agr* activity

3.1 Introduction

3.1.1 Regulation of exotoxin production in *S. aureus*

The regulation of exotoxin virulence determinants in *S. aureus* relies on the activity of global regulators, predominantly *agr* and the Sar proteins, coordinated in response to environmental conditions by TCSs (Bronner *et al*, 2004). In addition, sigma factors interact with RNA polymerase to control regulator and virulence gene transcription in a growth or stress response dependent manner (Bronner *et al*, 2004). Gene promoter regions which are situated upstream of transcriptional and translational start codons contain sites for DNA binding proteins to bind and either stimulate or repress transcription (Arvidson & Tegmark, 2001). Furthermore, translation of mRNAs can be modified through the formation of complexes with regulator RNAs (Geisinger *et al*, 2006).

There are complex interactions between regulators; for example SarS is expressed during early exponential phase while *agr* activity is low, enhancing protein A expression, while during mid to late exponential phase, *agr* is highly expressed, repressing SarS and hence protein A expression while upregulating exotoxins (Arvidson & Tegmark, 2001).

As an exotoxin, PVL appears to conform to the established paradigm of exotoxin regulation in *S. aureus*, being positively regulated by *agr*. The precise nature by which *agr* and the other major regulators regulate the *pvl* genes, which are found on a prophage, is not fully known.

3.1.2 Variable *pvl* expression by clinical strains

Enhanced expression of *pvl* and other exotoxins has been observed by some clinical strains compared to others, particularly the CA-MRSA strain USA300 (Li *et al*, 2009b). The reasons

behind variable expression are unclear, although variations in *agr* activity are believed to be important. Whether higher concentrations of secreted PVL exacerbate the severity of infections is also not known, although there are some indications that this may be the case. Neutrophils either undergo apoptosis or necrosis through exposure to PVL in a concentration dependent manner (Genestier *et al*, 2005). Enhanced expression of *agr* and core virulence determinants by CA-MRSA was associated with reduced survival in a rabbit model (Li *et al*, 2010). While studying *in vitro* expression gives an indication of the potential of a strain for high level toxin expression, it should be borne in mind that this may not always correlate well with expression *in vivo* (Xiong *et al*, 2002).

While expression of PVL and other exotoxins has been well studied in CA-MRSA strains, particularly USA300, less attention has been paid to PVL MSSA strains which are likely to be more diverse, from a greater range of strain backgrounds and hence possess a highly heterogeneous phenotype.

3.1.3 Chapter Overview

1. A collection of clinical strains isolated in Nottingham were characterised by molecular and phenotypic methods including MLST and analysis of exotoxin production.
2. The variations in exotoxin production between strains were explored with reference to *agr*, investigating the impact of exogenous AIPs on PVL production.
3. A promoter pull down assay was developed and used to identify potential regulators binding to the *agr* and *pvl* gene promoters.
4. Sequence analysis of the gene promoters and whole *agr* locus sequence of selected strains was carried out to identify polymorphisms that could explain variable exotoxin production.
5. The genomes of two closely related MSSA type 22 strains, TS13 and TS14 with divergent PVL phenotypes were sequenced and compared with ST22 strain HO 5096 0412 which represents the widespread U.K. EMRSA-15 clone.

3.2 Results

3.2.1 Characterisation of a collection of PVL positive clinical isolates

A collection of PVL positive clinical isolates were characterised as a starting point for the study. Many of these isolates had been initially gathered from the Clinical Microbiology department at Queen's Medical Centre Nottingham as part of an MSc project. The aim was to gather strains that would represent a range of infections, sample types and patient demographics. Isolates were initially identified by the Clinical Microbiology laboratory from clinical samples as *S. aureus* based on colonial appearance, Gram staining, production of catalase and DNAse. This was confirmed by the laboratory through a further panel of metabolic tests, and antibiotic sensitivities ascertained by a disc diffusion method.

Twenty five strains were collected initially (TS 1-25), the majority (n=20) of which were PVL positive by PCR as previously tested by the Staphylococcus Reference Unit (Laboratory of Healthcare Associated Infection, Colindale). Characteristics of the PVL positive clinical isolates are summarized in Table 3.1. Clinical presentations included abscesses, infected skin ulcers, bacteraemia, pneumonia and carriage isolates. The patients' ages ranged from 3 to 89 years (mean 45.4) with 56% being male. Nearly all (92 %) of the strains were MSSA, reflecting both the local epidemiology at the time the strains were collected, and also the frequency of identification of a locally circulating PVL-positive MSSA with a characteristic antibiogram (gentamicin and trimethoprim resistant only). The majority of PVL positive strains were isolated from skin and soft tissue infections, predominantly from swabs submitted to the laboratory by general practitioners or hospital admissions units. Two strains (TS6 and TS9) were isolated from post-operative infections during a hospital ward-based outbreak. Strains TS1 and TS25 caused severe community acquired pneumonia, both resulting in admission to intensive care. Both of these cases of pneumonia had a history suggestive of preceding viral upper respiratory tract infection, although a respiratory virus could not be detected in either case.

The patient infected with TS1, a 30 year old lady, deteriorated rapidly following admission with haemoptysis, severe breathlessness and leucopenia. Despite early treatment with intravenous antibiotics, sedation and ventilation, she sadly died less than 72 h into her admission. Post mortem analysis of her lung tissue indicated she had died from a severe necrotizing pneumonia, most likely as a result of infection with PVL producing *S. aureus.* This clinical case shares a number of similarities with those described by Gillet and colleagues in their clinical case series of young immunocompetent patients with necrotizing pneumonia resulting from PVL positive *S. aureus* (Gillet *et al*, 2002).

3.2.1.1 Molecular characteristics of the strain collection

Once collected, the strains were genotyped by a number of methods to ascertain which of the isolates were more closely related to each other.

The PVL positive isolates had already been submitted to the Staphylococcus Reference Unit (Laboratory of Healthcare Associated Infection, Colindale) where they were tested for the presence of PVL and a number of other toxin genes, including *tst* and enterotoxins, by PCR. This data is included in Table 3.1.

3.2.1.1.1 Testing for the *lukSF* genes

Genomic DNA was prepared from all 25 isolates as described in 2.3.1 and presence or absence of the PVL genes was confirmed by PCR using the primers pvl F and pvl R (Table 2.4). This gave identical results to the reference laboratory; PCR with genomic DNA from the PVL negative controls TS3, TS4, TS10, TS11 and TS22 did not result in amplification whereas amplification occurred for DNA from the PVL positive isolates.

3.2.1.1.2 *agr* typing

The entire *agr* locus of each of the clinical isolates was amplified using the primers AgrBDCAF and AgrBDCAR (Table 2.4). The PCR product was sent for sequencing with the cross group AgrD primer AgrD1234F. Sequences were aligned with reference genomes representing different *agr* types; *S. aureus* NCTC 8325, N315 and MW2 for *agr* types 1, 2 and 3 respectively (see Table 2.5 for reference sequence descriptions). Depending on which reference genome each *agrD* gene sequence aligned to, the clinical isolates were assigned to one of the three *agr* groups. One isolate, TS3, which did not align to any of the references was found to encode the *agr* group 4 AIP and so was assigned to *agr* group 4. *agr* group 1 was the predominant group in the collection (n=13) followed by group 3 (n=6) and group 2 (n=5).

3.2.1.1.3 MLST and *spa* typing

A PCR based method for identifying the Multi-Locus Sequence Type (MLST) and *spa* type of each isolate was performed by Kome Otokunefor (Otokunefor *et al*, 2012). Seven housekeeping genes were amplified by PCR and sequenced before comparing the sequence data to the MLST database (http://saureus.mlst.net/) in order to assign each strain to a specific MLST type.

Shared sequence types occurred only within *agr* groups as expected. The divergence of *agr* groups is believed to have been an early event in the development of *S. aureus*, placing much of the divergence into strain types after this event (Wright *et al*, 2005b).

ST22/*agr*1 strains (n=10) were the most common of which 5 were the same *spa* type, t005. The ST22 group, all of which were only resistant to gentamicin and trimethoprim, appeared to represent the PVL positive gentamicin and trimethoprim resistant isolates which were being encountered frequently in the Clinical Microbiology laboratory at the time they were collected for the study (2008 to 2010).

Other common types were ST30/*agr*3 (n=4) and ST772/*agr*2 (n=3). There was no obvious pattern in the distribution of sequence types among the different clinical presentations (skin infections, pneumonia, bacteraemia, carriage) although the strain collection is too small to make valid statistical comparisons.

TS1 was found to have a previously unidentified sequence type ST1518.

3.2.1.2 Exotoxin Production

An important aim of the study was to find out how PVL toxin levels vary between clinical isolates. A monoclonal antibody directed against one of the two subcomponents of the PVL toxin, LukF, was available (Prof. L. Durrant, School of Medicine, University of Nottingham) and so was used to perform western blots against culture supernatants.

Every PVL positive clinical isolate in the collection was tested by performing western blots on exoprotein extracts from culture supernatants collected at several time points. Clinical isolates were inoculated into CYGP medium at a 1:1000 final concentration from overnight cultures, incubated at 37 ^{o}C with shaking at 250 rpm and supernatant collected at several time points. Proteins were precipitated from the supernatants and normalised as described in 2.6.1, separated by SDS-PAGE, transferred to a nitrocellulose membrane and western blots performed with the anti-LukF monoclonal antibody as described in 2.6.4. The level of PVL production was determined semi-quantitatively by comparing the band sizes on the western blots between isolates.

Some of the isolates produced a much greater quantity of PVL toxin than others (Figure 3.1). For some of the isolates, PVL toxin was barely detectable (Figure 3.2). As growth had been slow with a 1:1000 inoculum, the experiment was repeated with a 1:500 inoculum (Figure 3.3) which was used for all subsequent experiments.

As the quantities of PVL production by clinical strains could not be compared with precision they were classed as either 'low' (similar to TS12 and TS13), 'medium' (similar to TS1 and TS27) or 'high' (similar to TS14).

Although a fixed quantity of 100 ng LukF control protein was used for the initial comparisons of PVL exotoxin production between all of the TS clinical strains, several different concentrations of LukF control were used for subsequent experiments. The concentration of LukF used is indicated on the figures so that tentative comparisons can be made between immunoblots.

Alpha haemolysin (Hla) is a well characterised staphylococcal toxin controlled by *agr*. An antibody to Hla was also used to perform western blots on the same exoprotein preparations used for PVL detection to determine whether there was any correlation between the levels of PVL and Hla produced. Isolates which exhibited higher PVL production also showed higher levels of Hla (Figures 3.1, 3.3). This finding suggested that the differences noted in PVL production could be, at least in part, consequent on differential expression of *agr*.

Table 3.1 Characteristics of PVL positive clinical isolates

Name	Clinical details	*agr* type	Sequence type	*spa* type	Other genes of interest	LukF expression
TS1	Fatal necrotising pneumonia	1	ST1518	t1941		Medium
TS2	Thigh abscess	2	ST772	t657	*mecA, sea, sec, seg, sei*	Low
TS5	Axillary boil	2	ST772	t657	*sea, sec, seg, sei*	Low
TS6	Wound infection following hip surgery	1	ST22	t6642	*seg, sei*	High
TS7	Nasal carriage	3	ST30	t021	*sea, seg, sei*	Low
TS8	Facial abscess	2	ST772	t657	*sea, sec, seg, sei*	Low
TS9	Wound infection following hip surgery	1	ST22	t6642	*seg, sei*	High
TS12	Wound infection	3	ST30	t021	*seg, sei*	Low
TS13	Leg abscess	1	ST22	t005	*seg, sei*	Low
TS14	Leg ulcer	1	ST22	t005	*seg, sei*	High
TS15	Recurrent boils	3	ST30	t021	*seg, sei*	Low
TS16	Thigh abscess	3	ST30	t021	*sea, seg, sei*	Low
TS17	Nasal carriage	1	ST22	t852	*seg, sei*	High
TS18	Foot wound	1	ST22	t005	*seg, sei*	High
TS19	Back abscess	1	ST22	t310	*seg, sei*	High
TS20	Knee bursitis	1	ST22	t005	*seg, sei*	High
TS21	Empyema	3	ST88	t6769	*seg, sei*	Low
TS23	Cellulitis and bacteraemia in an IVDU	1	ST22	t6642	*seg, sei*	High
TS24	Cellulitis on foot and bacteraemia	1	ST22	t005	*seg, sei*	High
TS25	Severe pneumonia following a viral illness	3	ST1	t3342	*sed, seg, sei*	Low
TS27	Recurrent boils	1	CC8	t008	*mecA*	Medium
TS31	Necrotising pneumonia	1	NK	NK		High
TS32	Prostatic abscess	1	NK	NK		High
TS33	Bacteraemia associated with prostatic abscess	1	NK	NK		Low
NRS162	Not known	3	ST30	NK		Low
NRS255	Not known	3	CC80	NK	*mecA* (SCCmecIV)	Low

ST = sequence type. IVDU = intravenous drug user. NK = not known. *se* = staphylococcal enterotoxin.

Figure 3.1 Exotoxin production by TS1 and TS14 during growth

Immunoblot (A) probed with anti-LukF and anti-Hla (alpha haemolysin) antibodies and SDS-PAGE gel (B) showing exotoxin production during growth in CYGP medium. Each lane is labelled with the sampling time (h), which is also shown on a growth curve (C). TS14 produced much higher quantities of PVL and alpha haemolysin than TS1. The LukF control (500ng,*) forms oligomers seen on the SDS-PAGE gel as heavier bands (B). MW = Molecular Weight markers.

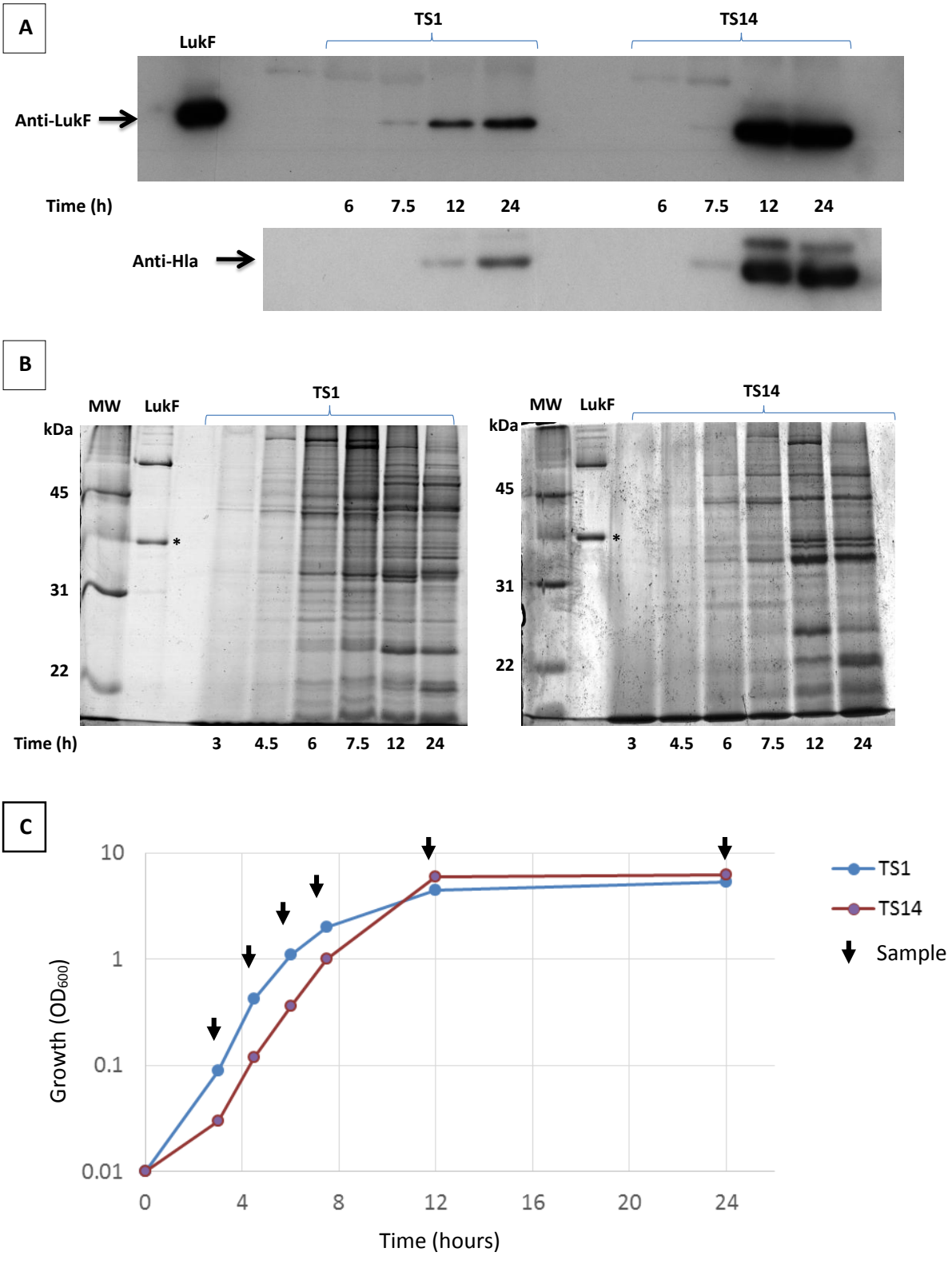

Figure 3.2 Exotoxin production by TS12, TS16, TS27, NRS162 and NRS255 during growth

Immunoblots (A) probed with anti-LukF antibodies showing exotoxin production during growth in CYGP medium. Each lane is labelled with sampling time (h), which is also shown on a growth curve (B). TS12, TS16, NRS162 and NRS255 all produced low quantities of PVL with TS27 showing moderate PVL production. 200 ng of LukF was used for the immunoblot with TS12 and TS16, with 10 ng of LukF used for the immunoblot with TS27, NRS162 and NRS255.

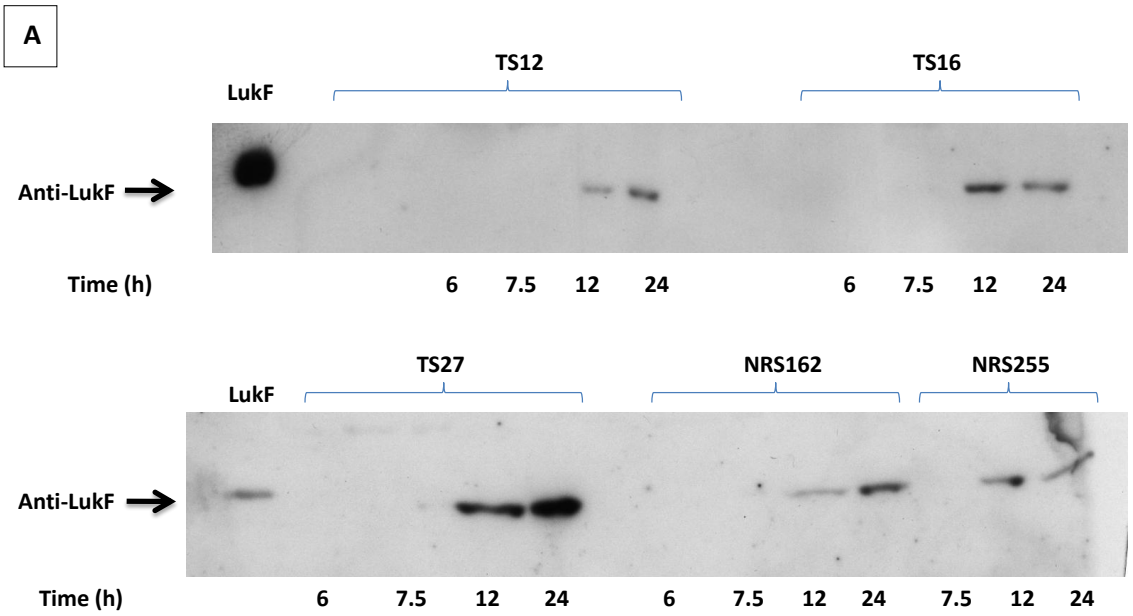

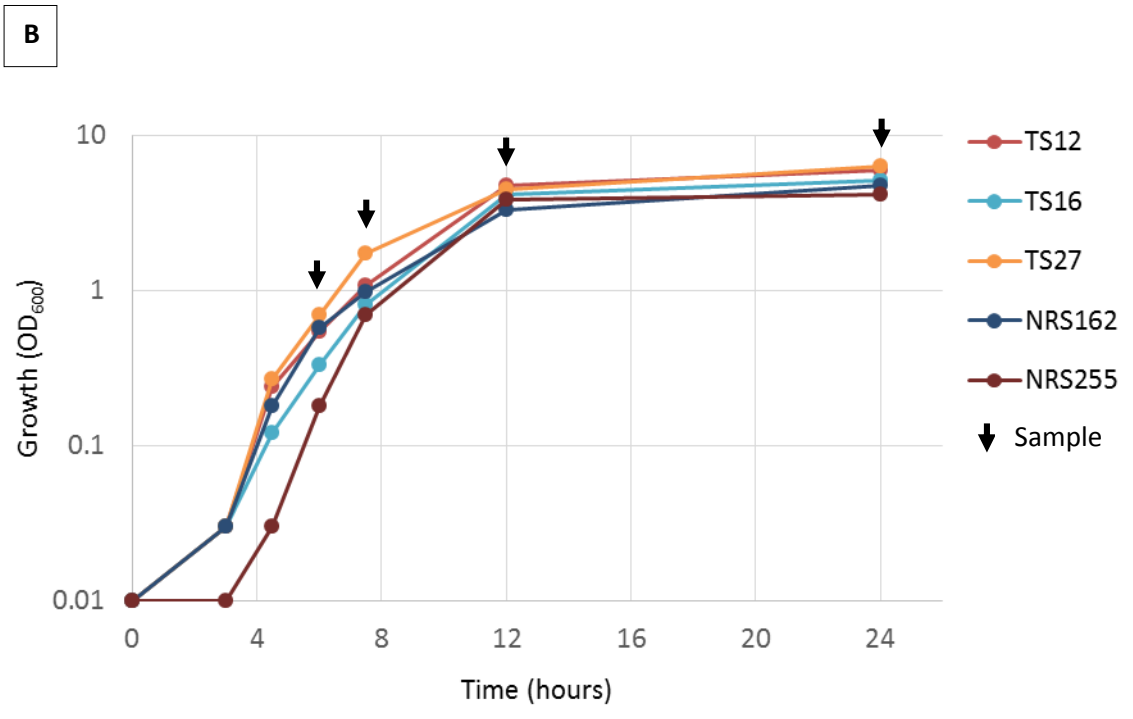

Figure 3.3 Exotoxin production by TS13 and TS14 during growth

Immunoblots (A) probed with anti-LukF and anti-Hla (alpha haemolysin) antibodies and SDS-PAGE gels (B) showing exotoxin production during growth in CYGP medium. Each lane is labelled with sampling time (h), which is also shown on a growth curve (C). TS14 produced higher quantities of both PVL and alpha haemolysin than TS13. 10 ng of LukF control was used. MW = Molecular Weight markers.

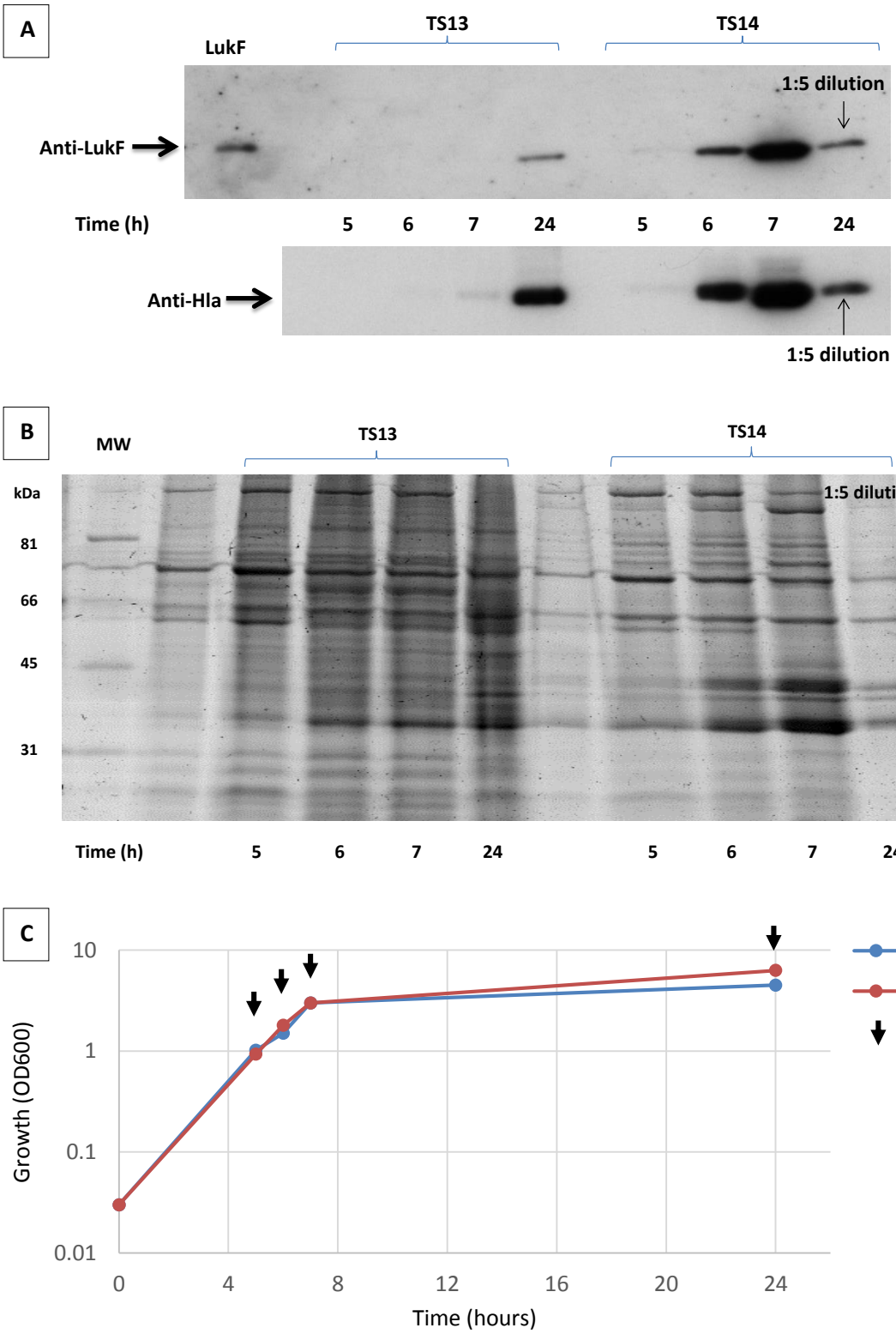

CYGP medium was used as previous work in the laboratory had shown it stimulated *agr* expression, making it easier to detect any toxins present in culture supernatants. Exoprotein extracts from a high (TS14) and a low level toxin (TS13) producer were tested in a variety of different growth media to determine the impact on toxin levels. Growth in CYGP clearly resulted in much higher toxin expression than the other growth media tested with toxin barely detectable in BHI, LB and TSB (Figure 3.4).

When comparing the pattern of high and low level toxin producers to the MLSTs and *agr* types (Table 3.1) it became apparent that the isolates producing the most toxin were all *agr* group 1 MLST 22 isolates. This was an interesting finding given the frequency that such isolates with a gentamicin and trimethoprim resistant antibiogram were being identified by the Clinical Microbiology laboratory as causing community-acquired skin and soft tissue infections. Of all of the *agr* group 1, MLST 22 isolates there was one exception, TS13, which appeared to be producing less PVL toxin than the others. Alpha haemolysin production was also lower possibly indicating reduced *agr* activity.

The other two groups of strains within the collection, ST30/*agr* 3 and ST772/*agr* 2, appeared to produce much less toxin than the ST22/*agr* 1 isolates. This gives the impression that strain background is an important determinant in the level of exotoxin expression although the numbers and diversity of strain types represented here are too small to draw any firm conclusions. Strain background has previously been noted to be an important determinant of toxin gene expression with the USA300 strain background reported to be associated with high level toxin expression (Li *et al*, 2009b).

Figure 3.4 PVL production varies depending on the growth medium used

Immunoblots (A) probed with anti-LukF antibodies and SDS-PAGE gels (B) showing exotoxin production during growth in BHI (1), CYGP (2), TSB (3) or LB (4) medium when incubated overnight at 37 °C. PVL production was highest in CYGP. 10 ng of LukF control was used on the gel. MW = Molecular Weight markers.

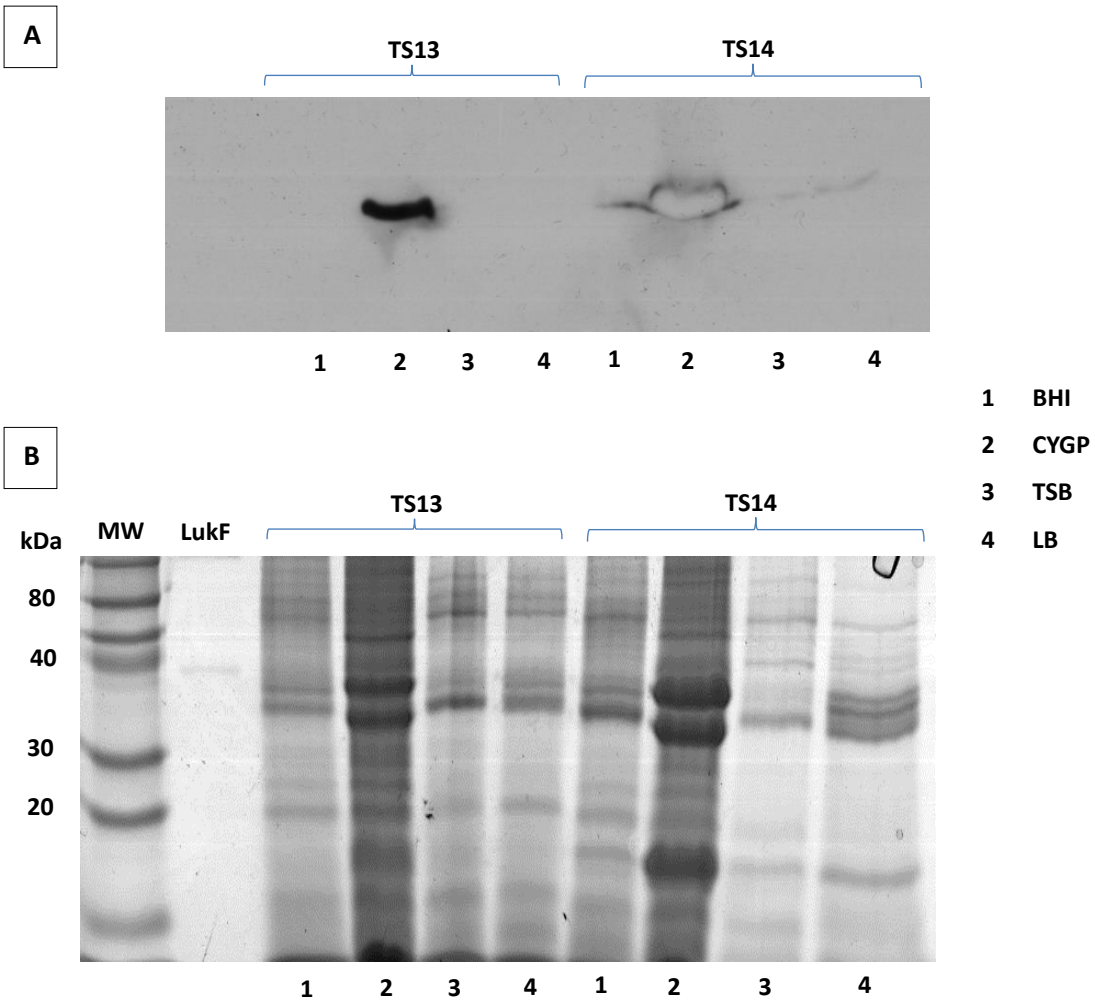

3.2.2 PVL expression can be modulated by exogenous autoinducing peptides

3.2.2.1 Stimulation of *agr* by exogenous AIP increases PVL production

The initial exotoxin analysis indicated that PVL production could be lower in some of the clinical isolates as a result of reduced *agr* activity. To investigate this possibility further, a selection of clinical isolates with low toxin production were cultured in the presence of the synthetic type specific AIP. AIP-1 and AIP-3 were both available having been synthesised by collaborators from the School of Pharmacy (Dr. Weng Chan, Centre for Biomolecular Sciences, University of Nottingham).

Exogenous synthetic AIP was added at a final concentration of 100 nM to cultures at the time of inoculation and incubated overnight in CYGP with shaking at 37 ^{o}C. TS13, the low producing ST22/*agr* 1 isolate, and several low producing group 3 isolates, including TS7, TS12, TS21 and TS25, all exhibited a marked increase in toxin production following addition of type specific AIP (Figure 3.5, data for TS7, 21 and 25 not shown).

In addition, if AIP-1 was not added to TS13 until mid-exponential phase of growth (t = 6 h), there was no increase in toxin production as compared to TS13 with no exogenous AIP-1 added (TS13 No AIP; Figure 3.5).

A further experiment was carried out by adding exogenous AIP-1 to TS13 at inoculation and by measuring toxin production at several time points during mid and late exponential and early stationary phase (t = 5.5 h, 7 h, 8.5 h) and overnight (t = 24 h). AIP-1 was also added to separate cultures at those time points during growth (t = 5.5 h, 7 h, 8.5 h). Toxin production was detectable from mid exponential phase if AIP-1 was added at the time of inoculation and increased markedly by stationary phase (Figure 3.6). However, AIP-1 added at any point from mid-exponential phase did not result in increased toxin production when measured at 24 h.

Figure 3.5 Activation and inhibition of *agr* by exogenous AIP alters PVL production

Immunoblot (A) probed with anti-LukF antibodies and SDS-PAGE gel (B) demonstrating the impact of exogenous type specific AIP or the cross-type AgrC antagonist (ala^5)AIP-1 to cultures either at inoculation (0 h) or during exponential phase (6 h). PVL production was increased when type specific AIP was added to TS12 and TS13 at 0 h but no effect was seen when AIP-1 was added to TS13 at 6 h. PVL toxin production was inhibited by the addition of (ala^5)AIP-1 at 0 h. Control lanes without activator or inhibitor are labelled as 'No AIP'. 2.5 µg of LukF control was used. Strains were grown in CYGP medium at 37 °C. MW = Molecular Weight markers.

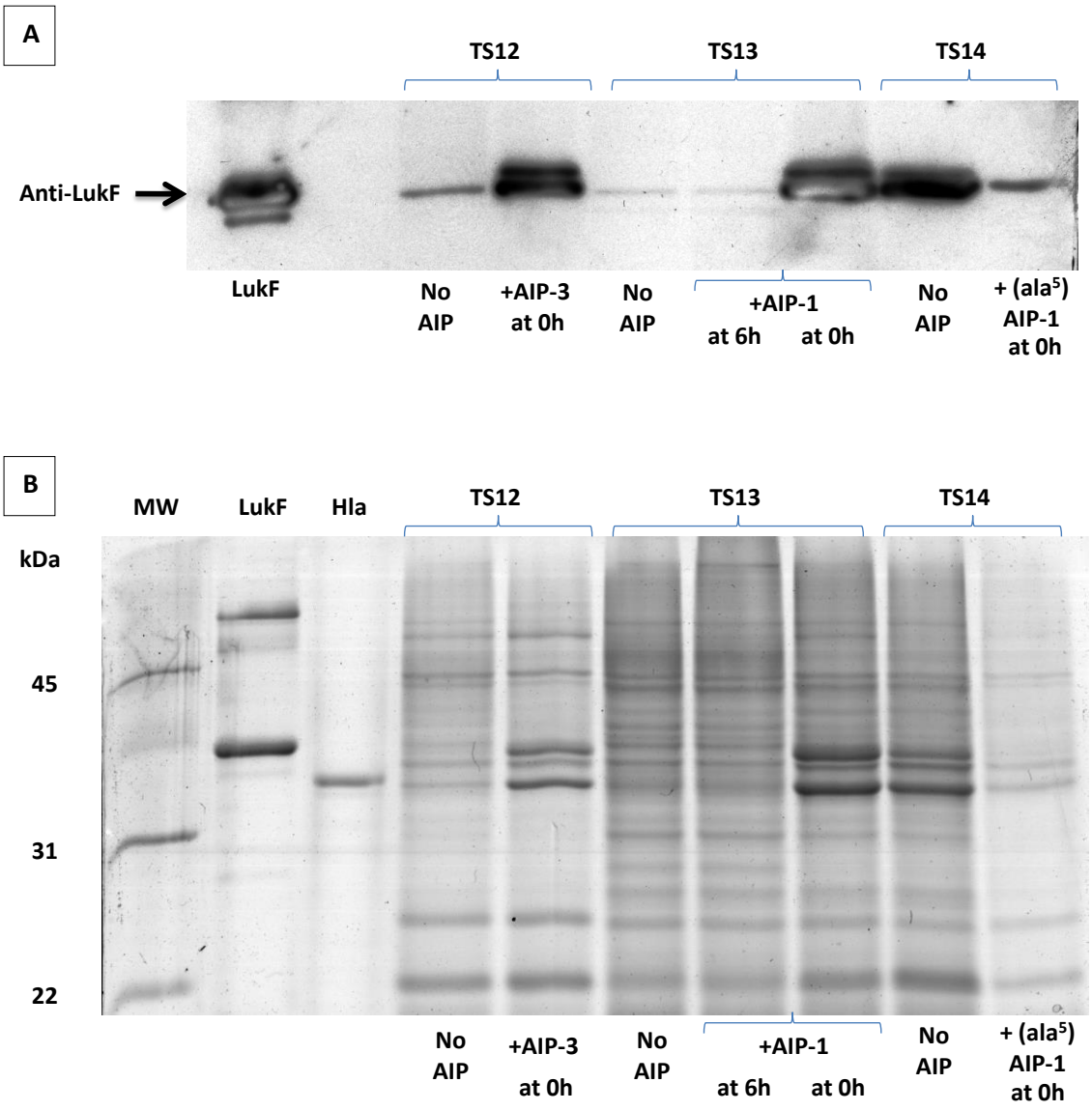

Figure 3.6 Timing of exogenous AIP addition effects PVL production

Immunoblot (A) probed with anti-LukF antibodies and SDS-PAGE gel (B) demonstrating the impact of exogenous type specific AIP at inoculation (0 h) or during exponential and stationary phase. Timing (h) of supernatant collection is shown above the blot and on the growth curve (C) with timing of AIP-1 addition below. The 24 h samples are shown on the gel (B). PVL toxin was barely detectable at 5.5 h even when *agr* was activated with exogenous AIP at 0 h, although high levels of PVL had been produced after 24 h. Adding AIP-1 to cultures at 5.5, 7 or 8.5 h did not result in high level PVL production when measured at 24 h. 20 ng of LukF control was used. Strains were grown in CYGP medium at 37 °C. MW = Molecular Weight markers.

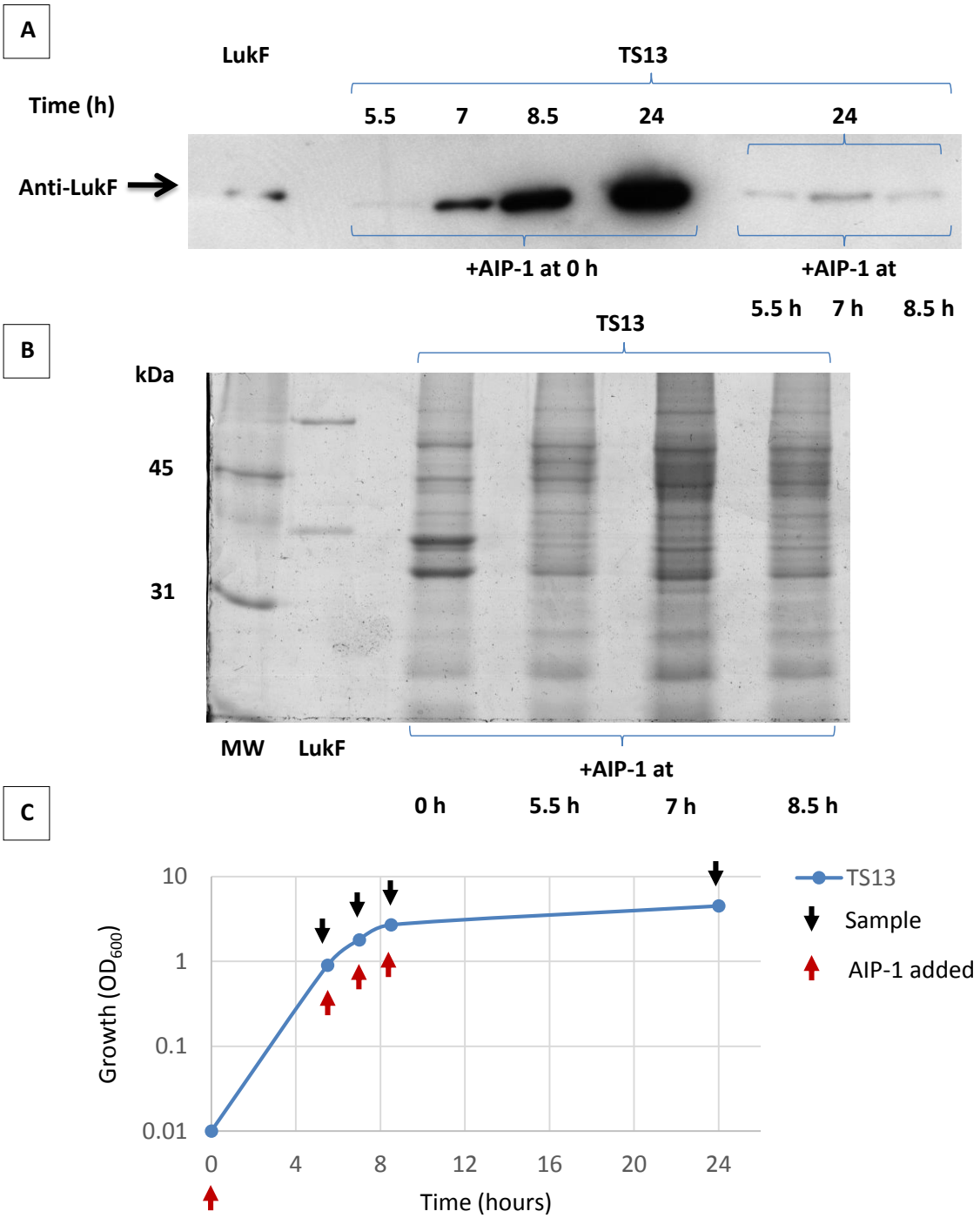

The observation that addition of exogenous AIP-1 significantly enhances toxin production if added at inoculation but not during exponential phase is an interesting one. This suggests a 'window period' during which external stimulation of *agr* dramatically influences the kinetics of the system, driving toxin production. During exponential phase, the system appears to be unresponsive to exogenous AIP, even though PVL production clearly continues during and after exponential phase if *agr* can be stimulated early enough. One possible explanation for this is that if *agr* activity is low going in to exponential phase, repressor proteins which would normally be repressed by *agr* such as SarS and Rot are expressed in higher quantities. These would then bind to the *agr* and toxin gene promoters and prevent significant toxin production from occurring, even if *agr* is stimulated subsequently.

3.2.2.2 *agr* inhibition reduces PVL expression

As PVL production appeared to be dependent, at least in part, on *agr* expression, experiments were conducted to determine whether PVL expression could be suppressed by the global *agr* inhibitor (ala^5)AIP-1 (McDowell *et al*, 2001).

Several of the isolates which displayed the highest toxin production (TS6, TS14, TS20) were grown overnight in CYGP with 100 nM (ala^5)AIP-1 added at inoculation. All of these displayed significant reductions in the amount of secreted PVL detected in the supernatants, although this did not prevent PVL expression altogether. An immunoblot of TS14 inhibition is shown in Figure 3.5. Identical results were seen if 300 nM or 600 nM of (ala^5)AIP-1 was added at inoculation (data not shown).

To determine whether the timing of inhibitor addition was important, 100nM (ala^5)AIP-1 was added to cultures of one of the high producing isolates, TS14, at inoculation or 2, 4 or 6 h post-inoculation. PVL production was reduced in the cultures where the inhibitor was added at

inoculation or 2 h into growth, but not if the inhibitor was added at 4 or 6 h where no differences were observed (Figure 3.7).

Figure 3.7 Inhibition of PVL production by the AgrC antagonist (ala^5)AIP-1 is time/growth phase dependent

Immunoblot (A) probed with anti-LukF antibodies and SDS-PAGE gel (B) demonstrating the impact of the AgrC antagonist (ala^5)AIP-1 at inoculation (0 h) or during growth. LukF is indicated with an arrow in B. Timing (h) of supernatant collection is shown above the bands and on the growth curve (C) with timing of AIP-1 addition below. PVL toxin production was inhibited if the AgrC antagonist was added at 0 or 2 h but not at 4 or 6 h into growth compared to the TS14 control (No AIP inhibitor added). All samples taken at 24 h. 10 ng of LukF control was used. Strains were grown in CYGP medium at 37 °C. MW = Molecular Weight markers.

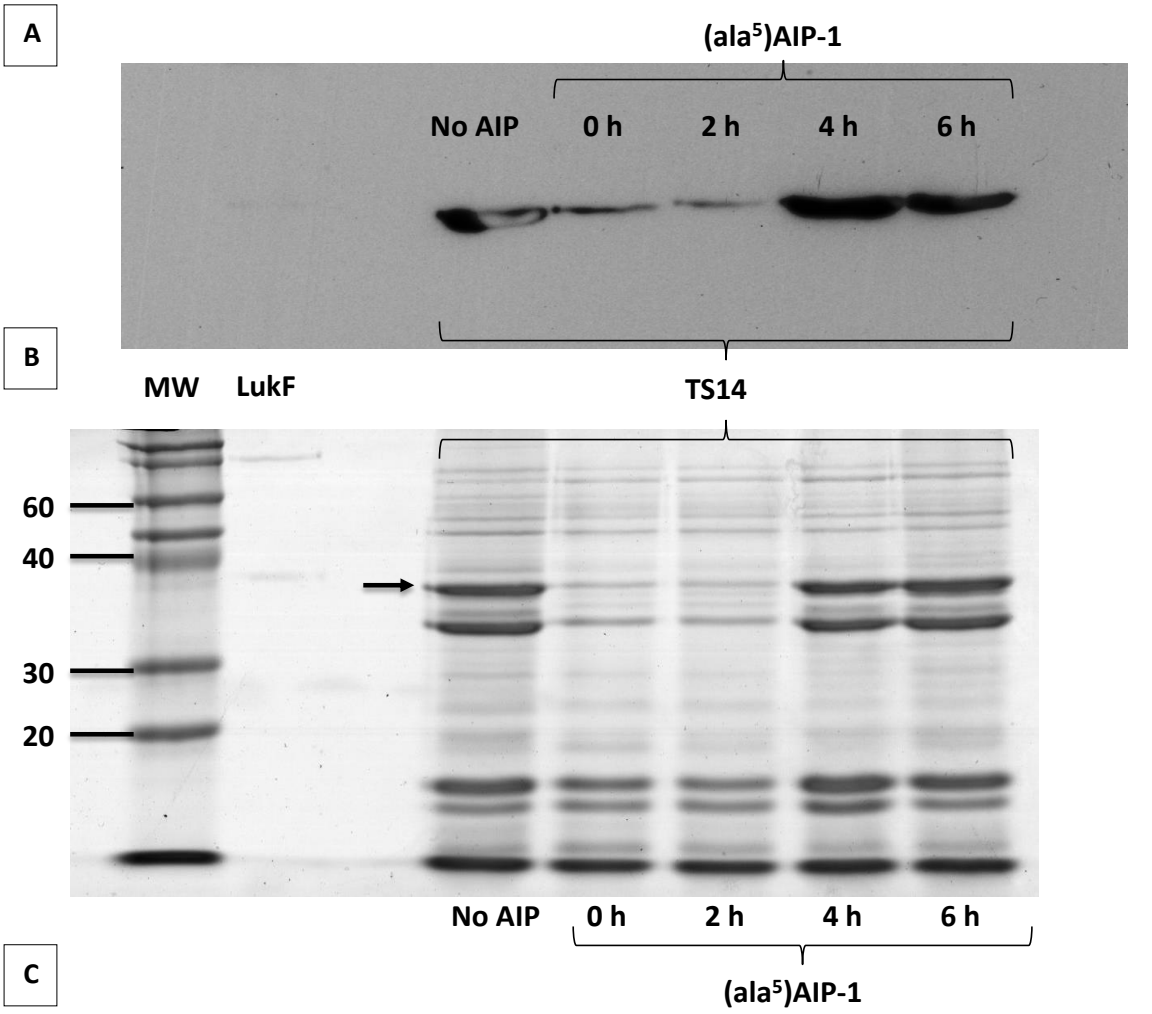

Anti-Staphylococcal beta-lactam antibiotics such as flucloxacillin are frequently used in clinical settings in the UK to treat presumed or confirmed infections with *S. aureus*. Culturing PVL producing *S. aureus* in the presence of sub-growth inhibitory concentrations of oxacillin results in an increase in PVL expression (Dumitrescu *et al*, 2007; Dumitrescu *et al*, 2011)

The low producing ST22/*agr* 1 isolate TS13 was grown in oxacillin to determine whether these clinical isolates used in this study responded similarly. TS13 was inoculated into CYGP containing 0.1, 0.25 or 1 µg/ml oxacillin and incubated for 24 h at 37 ^{o}C with shaking. Growth was markedly reduced in the presence of 0.25 and 1 µg/ml oxacillin but occurred normally in the presence of 0.1 µg/ml oxacillin. Western blotting of exoprotein extracts from the culture containing 0.1 µg/ml oxacillin revealed a significant increase in PVL production as compared with the control culture in a manner similar to that noted following the addition of exogenous AIP-1 (Figure 3.8). TS13 was also cultured overnight with both 0.1 µg/ml oxacillin and 100 nM (ala^{5})AIP-1 added at inoculation. In this case, toxin production was greater than baseline but much lower than if only oxacillin had been added. This appeared to indicate that the PVL production, even if enhanced by oxacillin, was still largely dependent on *agr*.

Figure 3.8 Sub inhibitory oxacillin enhances PVL production

Immunoblot (A) probed with anti-LukF antibodies and SDS-PAGE gel (B) demonstrating induction of PVL production by a sub inhibitory concentration of oxacillin (0.1 µg/ml) which can be partially inhibited by the AgrC antagonist (ala^5)AIP-1. Oxacillin and (ala^5)AIP-1 were added to cultures at the time of inoculation. TS13 was then incubated overnight in CYGP medium at 37 ^{o}C. A high quantity of LukF control was used for the immunoblot (>100 ng). A control lane is shown for TS13 without the addition of either oxacillin or inhibitor.

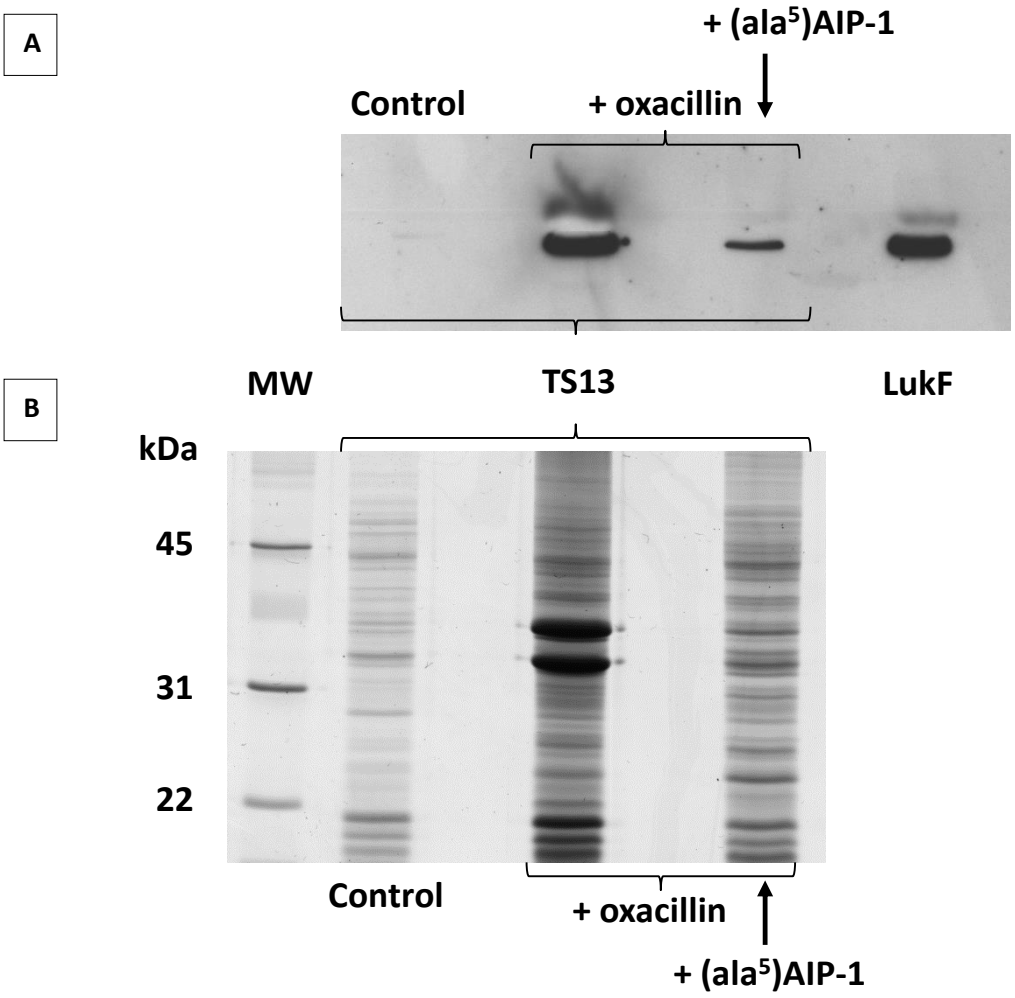

3.2.3 Analysis of *agr* and *pvl* promoter regions

3.2.3.1 Promoter sequence analysis for selected clinical strains

Mutations in promoter regions can result in altered gene expression. An 11 bp deletion in the promoter of Mga, a global regulator in *Streptococcus pyogenes*, resulted in reduced *mga* transcripts and attenuated virulence (Flores *et al*, 2013). Villaruz *et al* (2009) found a point mutation in the *agr*P2 promoter of a strain of *S. aureus* causing dysfunction of *agr* resulting in abnormally high protein A expression. This mutation occurred in one of the four putative AgrA binding sites of which two are present in both the *agr*P2 and *agr*P3 promoters (Koenig *et al*, 2004; Morfeldt *et al*, 1995). A separate binding region for SarA has also been proposed, covering the gap between *agr*P2 and *agr*P3 (Sterba *et al*, 2003).

To determine whether there were any obvious mutations/deletions/polymorphisms in important promoter regions that could explain the phenotypic variation observed, the *agr* and *pvl* promoter regions of selected clinical strains representing different *agr* groups and toxin expression phenotypes (TS1, TS2, TS3, TS12, TS13, TS14, TS25) were sequenced and compared with reference genomes.

3.2.3.1.1 Analysis of *agr* promoter sequences

Following amplification of the entire *agr* locus of selected strains with primers *agr*BDCAF and *agr*BDCAR, *agr* promoter regions were sequenced with primers *agr*BDCAF and *agr*promoR (Table 2.4). Promoter sequences were aligned to *S. aureus* N315 and the ST22 MRSA HO 5096 0412, which represents EMRSA-15 (Figure 3.9, Table 2.5). The *agr* group 3 reference genome MW2 was identical to N315 across the promoter region so was not included.

There were no SNPs in any of the AgrA or SarA binding regions of the clinical strains. The sequences of the low producing ST22/*agr* 1 strain TS13 and the high producing ST22/*agr* 1

strain TS14 were identical to each other, and also to HO 5096 0412, so *agr* promoter variation could not account for the phenotypic differences observed between them.

Compared with N315, TS1, TS3 and TS12 all had an A to T SNP at N315 base 2,079,278 in the penultimate base of the *agr*P3 promoter in the -10 RNA polymerase recognition site (Figure 3.9). Although TS3 is PVL negative, both TS1 and TS12 showed low expression of PVL toxin. Alpha haemolysin production was observed in TS1 and so it appears that *agr* is still functional in this strain. It is conceivable that this polymorphism could interfere with RNAIII transcription, particularly by weakening the association with RNA polymerase, although -10 and -35 recognition site sequences often vary by several bases while still retaining functionality (Zhang & Stewart, 2000).

TS13 and TS14 both had a C to A SNP in the middle of the *agr*P2 promoter at N315 base 2,079,373 (Figure 3.9). This substitution was also present in HO 5096 0412 and so appears to be a feature of this sequence type and therefore less likely to have any functional significance.

TS1 had a unique T to A SNP at base 2,079,375. As with the other SNPs, the functional significance is difficult to determine without a direct comparison to a similar strain without the change, but this was also outside of the AgrA consensus binding sites.

Figure 3.9 *agr* promoter sequences of selected strains aligned to reference genomes

Alignment of *agr* promoter regions for selected strains with the reference sequences for N315 and HO 5095 0412 (EMRSA-15). The *agr*P2 and *agr*P3 promoters are indicated, with the -10 and -35 RNA polymerase recognition sites, predicted transcription start sites and consensus sequences for AgrA binding marked. The SarA binding region is also shown between the two AgrA binding regions. The N315 Agr promoter sequence begins after N315 base 2,790,000 so, for example, the 230 position marked above the sequences corresponds to N315 2,790,230. The notable SNPs are A to T for TS1, TS3 and TS12 in the -10 region of the *agr*P3 promoter, and T to A for TS1 in the middle of the *agr*P2 promoter.

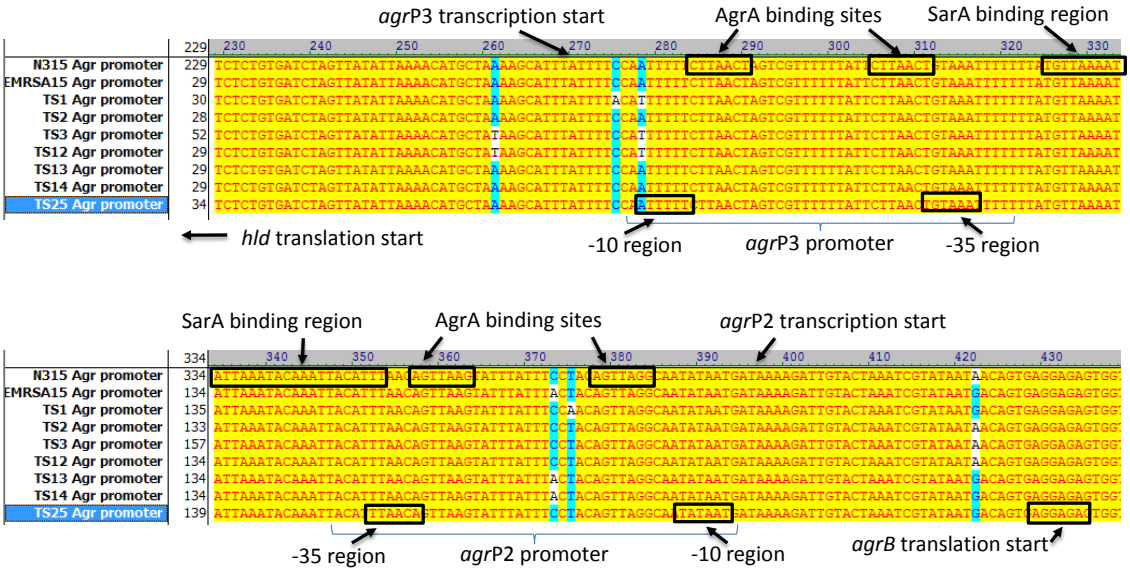

3.2.3.1.2 Analysis of *pvl* promoter sequences

Unlike the *agr* promoter, little is known about the *pvl* promoter. The promoter region is situated in the region upstream of *lukS*, between *lukS* and the next upstream coding region (a predicted phage amidase gene). Consensus sequences for a ribosomal binding site and RNA polymerase recognition sites have been previously identified in this region (Rahman *et al*, 1991).

The *pvl* promoter regions for the selected clinical strains were amplified and sequenced with the primers *pvl*promoF and *pvl*promoR (Table 2.4) and aligned to reference sequences for the three most common *pvl* encoding phages (ΦSLT, ΦMW2, ΦPVL) (Figure 3.10, Table 2.5). Another PVL phage sequence Φtp310-1 was also included in the analysis as it was first identified in an ST22 strain and therefore useful to compare to the ST22 strains TS6, TS13 and TS14.

Once this had been done, the promoter region was analysed by looking for conserved motifs. The -10 Pribnow box sequence TATAAT was identified as in the original analysis by Rahman *et al* (1991) and also 4 out of 6 bases of the -35 motif TTGACA, instead occurring as TTATCA (Figure 3.10). This gave a predicted region for RNA polymerase recognition and binding for *pvl* transcription, along with a predicted transcriptional start region. A predicted ribosomal binding site was also identified immediately upstream of the *lukS* coding sequence with a 4 out of 6 nucleotide match to the Shine-Dalgarno sequence (Shine & Dalgarno, 1974).

The SarA binding region previously described in *agr* by Sterba *et al* (2003) contained 29 bases. This base sequence was used to search in the region of the *pvl* promoter for any potential matches. Two regions each contained 19 of the 29 bases in the *agr* promoter SarA binding region and so were designated as potential SarA binding sites for *pvl* regulation (Figure 3.10). Both of these were downstream of the predicted *pvl* transcription start site and so could conceivably play a role in both transcriptional and post-transcriptional regulation.

Finally, Kumarevel *et al* (2009) reported a 24 base sequence which acts as a generic binding region for MarR-like helix-turn-helix (HTH) regulators, of which the Sar proteins, particularly MgrA, are representatives. This sequence was reported as TTTGCTATTGTTAACAATAGCAAA. Comparing this to the promoter sequences identified another region downstream of the predicted RNA polymerase binding site which was then designated as a generic HTH binding site (Figure 3.10).

Comparing the TS sequences, only one polymorphism was noted distinguishing the strains, a G to A polymorphism from ΦPVL present in TS2, TS6, TS12, TS13 and TS14 downstream of the predicted RNA polymerase binding region and between the two SarA binding regions. This polymorphism was also present in ΦSLT and Φtp310-1 and so, seemed likely to represent the differences in PVL phage types in these strains as opposed to acquired polymorphisms (Figure 3.10). The other two polymorphisms were unique to ΦPVL and ΦSLT respectively.

Figure 3.10 Analysis of the *pvl* promoter region

Alignment of *pvl* promoter regions for selected strains with the reference sequences for ΦPVL, ΦMW2, ΦSLT and Φtp310-1. The predicted *pvl* promoter region for RNA polymerase binding is marked, along with the -35 and -10 consensus sequences. Two predicted SarA binding sites were identified with a 19/29 base similarity to the region identified in *agr* by Sterba *et al* (2003). A further generic helix-turn-helix (HTH) regulatory binding site was identified with a 16/24 base similarity to a sequence described by Kumarevel *et al* (2009). The predicted ribosomal binding site is immediately upstream to the start of the *lukS* coding sequence and has a 4/6 base similarity to the Shine-Dalgarno sequence. The only nucleotide polymorphism distinguishing the TS strains was a G to A substitution present in TS2, TS6, TS13 and TS14, immediately after the first SarA binding site, which was also present in ΦSLT and Φtp310-1.

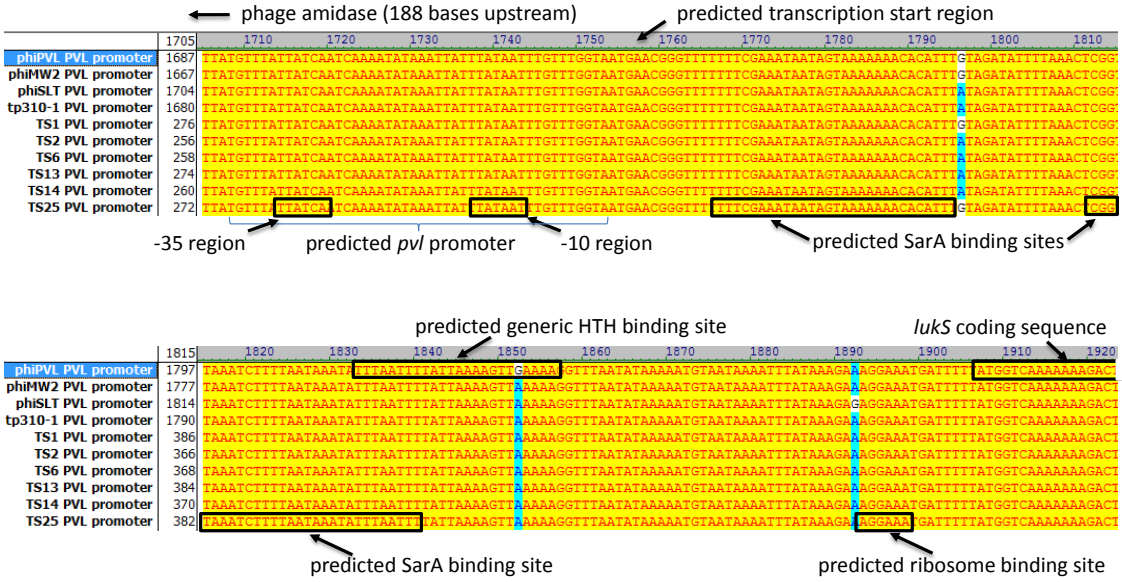

3.2.3.2 Development of the promoter pulldown technique in *S. aureus*

A number of regulatory proteins bind to the *agr* promoter to regulate gene expression including AgrA, SarA and other transcriptional regulators such as the repressor, Rot (Cheung *et al*, 2004; McNamara *et al*, 2000). While the expression of the *lukSF*-PV genes is regulated by *agr* (Bronner *et al*, 2000), there are no published data demonstrating direct binding of transcriptional regulators to the *pvl* promoter.

A promoter pulldown technique was developed to determine which regulatory proteins were binding to the *agr* and *pvl* promoters of selected clinical strains, and to see if there were any obvious differences between the protein binding patterns of the genotypically, apparently identical but phenotypically distinct TS13 and TS14. The pulldown technique relies on protein binding to biotinylated promoter fragments generated by PCR which can then be separated with streptavadin coated magnetic beads and any bound proteins eluted (Figure 3.11).

3.2.3.2.1 Verification that proteins bind selectively to the promoter fragments

The PVL negative TS3 strain was used as an initial test isolate to determine which proteins bound selectively to the *agr* promoter fragment and for later comparison with the PVL positive strains. Biotinylated *agr* promoter fragments were mixed with streptavadin-coated beads and incubated with TS3 cell lysate as described in section 2.7.3. Pooled PCR product from ten 50 µl reactions was used so that an excess of promoter DNA would be present. After incubation, the beads were separated from the lysate using a magnetic rack, washed and any residual proteins eluted (section 2.7.4). Both the eluent and original cell lysate were separated by SDS-PAGE and compared. Several discrete bands were present in the eluent compared to a dense smear of many mixed proteins in the lysate, confirming that selective binding had occurred.

Bands from the eluent lane of the SDS-PAGE gel were sent for Q-TOF protein sequencing. Sequencing results confirmed that AgrA and several Sar family proteins including SarA, SarS, SarR, SarX and SarV were bound to the *agr* promoter fragment. Other bound proteins included ribosomal proteins, translation initiation factors, DNA directed RNA polymerase and a DNA helicase, *ruvA* (Figure 3.12).

3.2.3.2.2 Confirmation that large cell volumes are required for the cell lysate

The protocol used for generating the cell lysate requires 400 ml of bacterial culture for a single experiment. To ensure that this volume was required for the PVL positive strains too and that the assay was not saturated with protein, the pull down experiment was performed again with another PVL negative strain TS10, using serial dilutions of cell lysate for the incubation step (section 2.7.3). The eluents derived from promoter fragments incubated with the diluted cell lysates contained lower protein concentrations, indicating that cell lysate protein concentrations were a limiting factor in the assay and that a large volume of bacterial culture was required (Figure 3.13).

Figure 3.11 The promoter pull down assay method

A diagrammatic representation of the promoter pull down assay. The *agr* promoter on the left and *pvl* promoter on the right were amplified by PCR before binding to magnetic beads. After mixing with concentrated lysed cell extract, the beads were separated from the mixture by a magnetic rack and the eluent analysed by SDS-PAGE. Gel bands were sent for protein sequencing to identify promoter bound products.

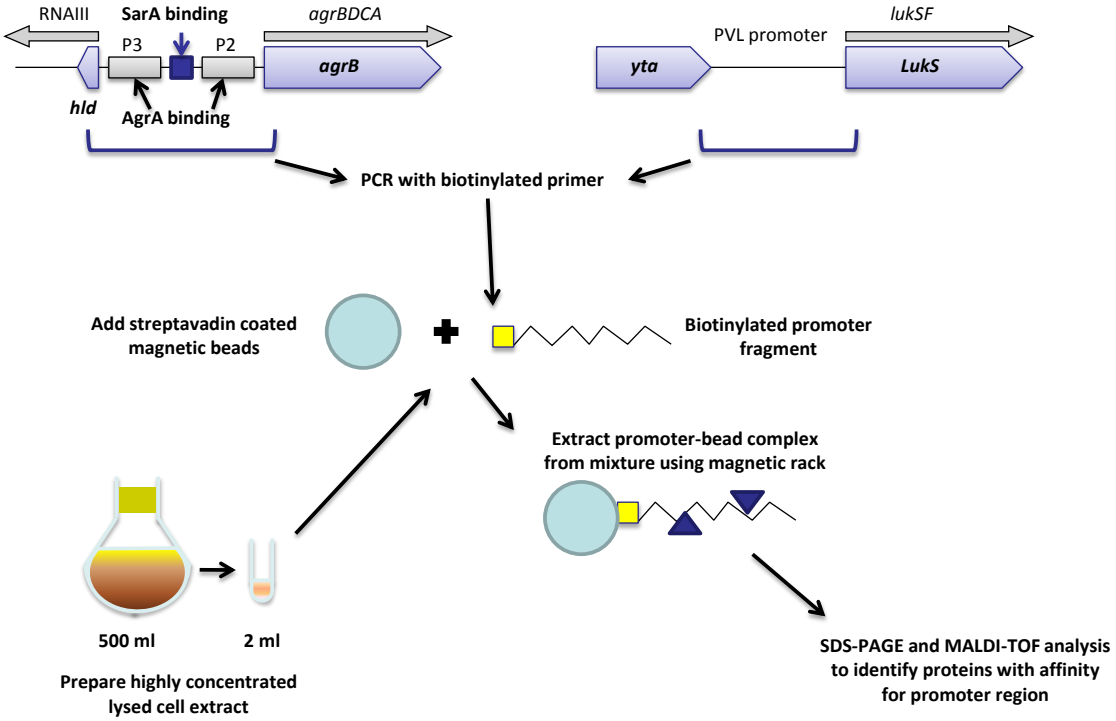

Figure 3.12 Pull down assay products from a PVL negative strain TS3

SDS-PAGE gel indicating eluted products from a promoter pull down assay using the TS3 *agr* promoter with lysed TS3 concentrated cell extract. Bands sent for sequencing (A to F) are indicated with arrows, with protein sequencing products shown in the boxes. Proteins are indicated by mass and identity, with the mass spectrometry quantification shown in brackets. The quantification is a relative value accounting for % of spectra and protein molecular weight. MW = molecular weight.

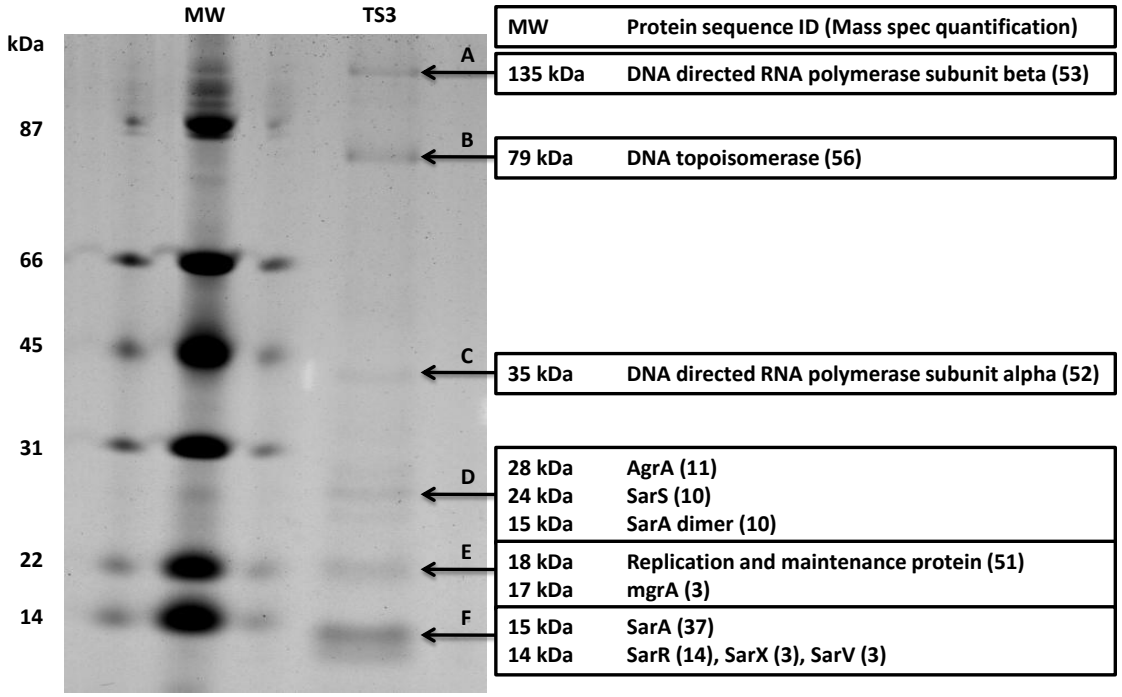

Figure 3.13 Effect of diluting the pull down cell extract on quantity of eluted protein

SDS-PAGE gel indicating eluted products from a promoter pull down assay using the TS10 *agr* promoter with lysed TS10 concentrated cell extract. Serial dilutions of cell extract were mixed with the biotinylated promoter to determine if the mixture was saturated with protein. A control without the addition of promoter was included for comparison. The dilutions indicate that reducing the cell extract concentration dramatically reduced the eluted product, confirming the need to use a large culture volume. MW = molecular weight.

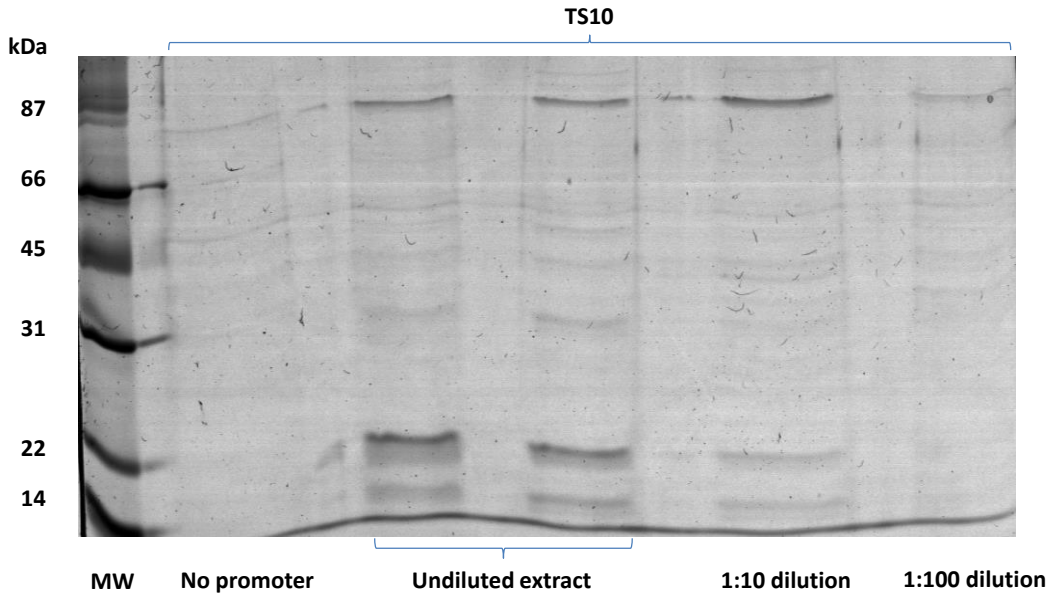

3.2.3.3 Identification and comparison of proteins bound to *pvl* and *agr* promoters

Three PVL positive strains were chosen for investigation of their *agr* and *pvl* promoter protein binding profiles. Strains TS13 and TS14 were chosen together with TS12 - a representative of *agr* group 3 which shows very low PVL toxin product.

Many of the Sar proteins were identified as binding to both the *agr* and *pvl* promoters of all three isolates tested, particularly SarS and SarA. AgrA was bound to all of the *agr* promoter fragments but none of the *pvl* promoter fragments indicating that specific binding was occurring (Figure 3.14 and 3.15). The proteins bound to the *agr* promoters were similar to that seen previously in TS3.

Other proteins of interest bound to the promoter fragments included Rot, MgrA and another transcriptional regulator, TcaR. All of the proteins bound to the *pvl* promoter fragments and giving clear bands on the SDS-PAGE gel were known transcriptional regulators.

Although the assay was intended as a qualitative measure of promoter protein binding, peptide fragment quantifications were compared to look for possible variations. When comparing the profiles of TS12 and TS13, there were no striking differences between them. There was a visible difference in profiles of TS13 and TS14 with fainter bands around 30 kDa in size for TS14. This could be explained by less SarS protein bound to the TS14 promoters than for TS13. From the protein bands sequenced, the amount of Rot bound to the TS14 promoters was also lower than TS13. SarS and Rot are both exotoxin repressors and are associated with repressed *agr* activity. The differences observed could reflect global differences therefore in the *agr* function of TS13 and TS14.

Figure 3.14 Pull down products bound to the *agr* and *pvl* promoters of TS12 and TS13

SDS-PAGE gel indicating eluted products from a promoter pull down assay using the TS12 and TS13 *agr* and *pvl* promoters with lysed concentrated cell extract. Bands sent for sequencing (A1 to C4) are indicated with arrows, with protein sequencing products shown in the boxes. Protein products are indicated by mass and identity, with the mass spectrometry quantification shown after the gel band label. The quantification is a relative value accounting for % of spectra and protein molecular weight. SarS, SarA, Rot and other Sar proteins bound to all the promoters. AgrA was only identified from the *agr* promoters. MgrA was identified binding to the *pvl* promoter only, although the corresponding *agr* bands were fainter and so not sent for sequencing. MW = molecular weight.

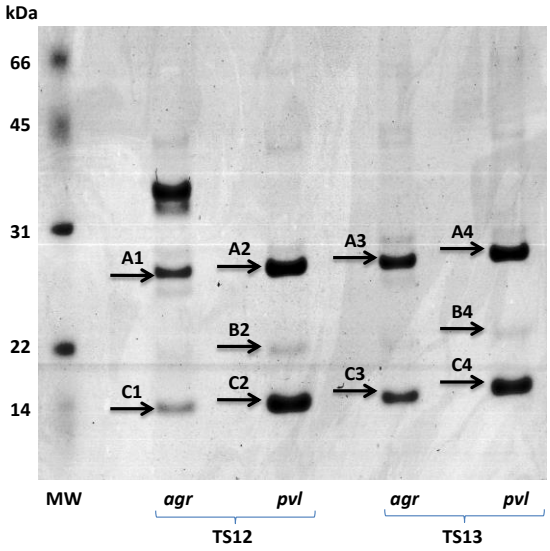

MW	Protein ID	Gel Band: Mass spec quantification
30 kDa	SarS	A1: 119, A2: 139, A3: 112, A4: 209 B2: 52, B4: 35
28 kDa	AgrA	A1: 24, A3: 20 C1: 22, C3: 14
20 kDa	Ferritin	B2: 7, B4: 11
19 kDa	Rot	B2: 11, B4: 9 C1: 20, C2: 71, C3: 34, C4: 66
18 kDa	TcaR	B2: 30, B4: 27
17 kDa	MgrA	B2: 121, B4: 113
15 kDa	SarA	B2: 19, B4: 12 C1: 106, C2: 152, C3: 129, C4: 120
14 kDa	SarX SarV SarR	C1: 13, C2: 10, C3: 11, C4: 8 C1: 11, C2: 9, C3: 12, C4: 17 C1: 33, C2: 33, C3: 54, C4: 61

Figure 3.15 Pull down products bound to the *agr* and *pvl* promoters of TS13 and TS14

SDS-PAGE gel indicating eluted products from a promoter pull down assay using the TS13 and TS14 *agr* and *pvl* promoters with lysed concentrated cell extract. Bands sent for sequencing (A1 to C4) are indicated with arrows, with protein sequencing products shown in the boxes. Protein products are indicated by mass and identity, with the mass spectrometry quantification shown after the gel band label. The quantification is a relative value accounting for % of spectra and protein molecular weight. SarS, SarA, Rot and other Sar proteins bound to all the promoters. AgrA was only identified from the *agr* promoters. SarS and Rot quantities are highlighted in red as these appeared to differ between TS13 and TS14. MW = molecular weight.

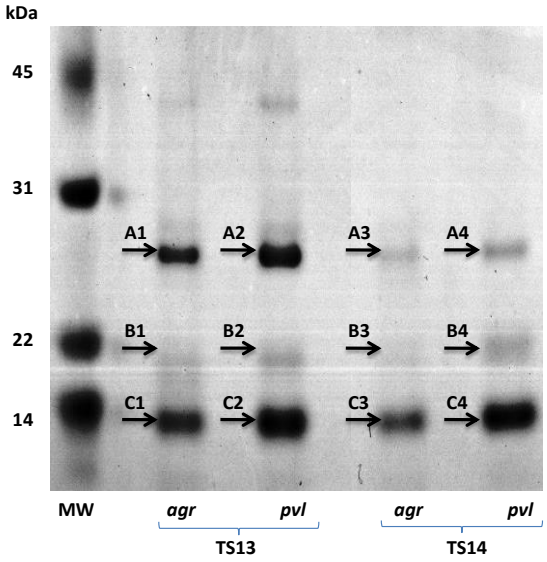

MW	Protein ID	Gel Band: Mass spec quantification
30kDa	SarS	A1: 137, A2: 255, A3: 78, A4: 95
28kDa	AgrA	A1: 25, A3: 51
19kDa	Rot	C1: 41, C2: 81, C3: 8, C4: 19
18kDa	TcaR	B1: 8, B2: 33, B3: 13, B4: 18
17kDa	MgrA	B1: 51, B2: 138, B3: 54, B4: 77
15kDa	SarA	C1: 157, C2: 146, C3: 106, C4: 112
14kDa	SarR	C1: 66, C2: 74, C3: 40, C4: 49
14kDa	SarV	C1: 15, C2: 21, C3: 8, C4: 10
14kDa	SarX	C1: 13, C2: 10, C3:7, C4:7

3.2.3.4 Comparison of *agr* and *pvl* gene expression by qRT-PCR

From the immunoblotting data presented in section 3.2.1.2, TS14 clearly produced more PVL and alpha haemolysin than TS13. This phenotype suggested global differences in toxin gene expression, possibly due to differences in *agr*. It was unclear from these data whether this was due to differences in toxin gene transcription, translation or even secretion.

To obtain a clearer indication of the source of the observed differences, expression of the *agr* and *pvl* genes by TS13 and TS14 respectively were compared directly by a SYBR green-based quantitative real time PCR assay (section 2.4.9). TS13 and TS14 were grown in CYGP broth and cultures harvested in exponential phase (n = 3, t = 4.5 h). Following RNA extraction and cDNA synthesis, cDNA samples were tested in triplicate. The *pvl* and *agr* genes were amplified using the primers RNAIII F and R and *lukS*-PV F and R with the *gyrB* gene acting as a constitutive control, amplified with the primers *gyrB* F and R (Table 2.4).

PCR cycle threshold (CT) was used to quantify each gene in the cDNA samples. *agr* and *pvl* gene quantities were adjusted based on the *gyrB* value in order to account for variations in total cDNA between samples. As *pvl* and *agr* gene expression was higher in TS14 than TS13, relative quantities (RQ) of each gene were expressed as a multiple of the average gene quantification for TS13. All analyses were performed using the AB7500 Real-time PCR System software (Applied Biosystems). RQs were calculated with a range for the minimum to maximum 95 % confidence levels (Figure 3.16). Compared with an RQ of 1.0 (0.8 to 1.3) for TS13 *agr* expression, mean TS14 *agr* expression was over tenfold higher with an RQ of 11.3 (7.0 to 18.4) ($p<0.05$). Expression of the *pvl* genes was also much higher for TS14 than TS13 with an RQ of 59.7 (37.8 to 94.1) for TS14 compared to an RQ of 1 (0.8 to 1.3) for TS13 ($p<0.01$).

These data suggest that PVL toxin gene expression by TS14 is clearly higher than TS13 due to differences in *pvl* transcription. As with staphylococcal toxins such as alpha-haemolysin, the regulation of *pvl* by *agr* is probably mediated by RNAIII expression, which acts indirectly through

altering the translation of other regulators (Geisinger *et al*, 2006). RNAIII expression was over tenfold higher in TS14 than TS13. Because of the downstream impact a difference in RNAIII expression would have on the translation of many of the global regulators such as Rot, SarS, SarA and SarR, this could account for the large difference in *pvl* gene transcription observed here.

Figure 3.16 qRT-PCR results for RNAIII and *pvl* gene transcription by TS13 and TS14

Quantification of *lukF-PV* and RNAIII gene expression (calculated as RQ – see section 2.4.9) in TS13 and TS14 grown to mid-exponential phase in CYGP medium at 37°C. Expression of *lukF-PV* was 59.7-fold higher and RNAIII expression 11.3-fold higher in TS14 than TS13. Error bars indicate the 95% confidence intervals.

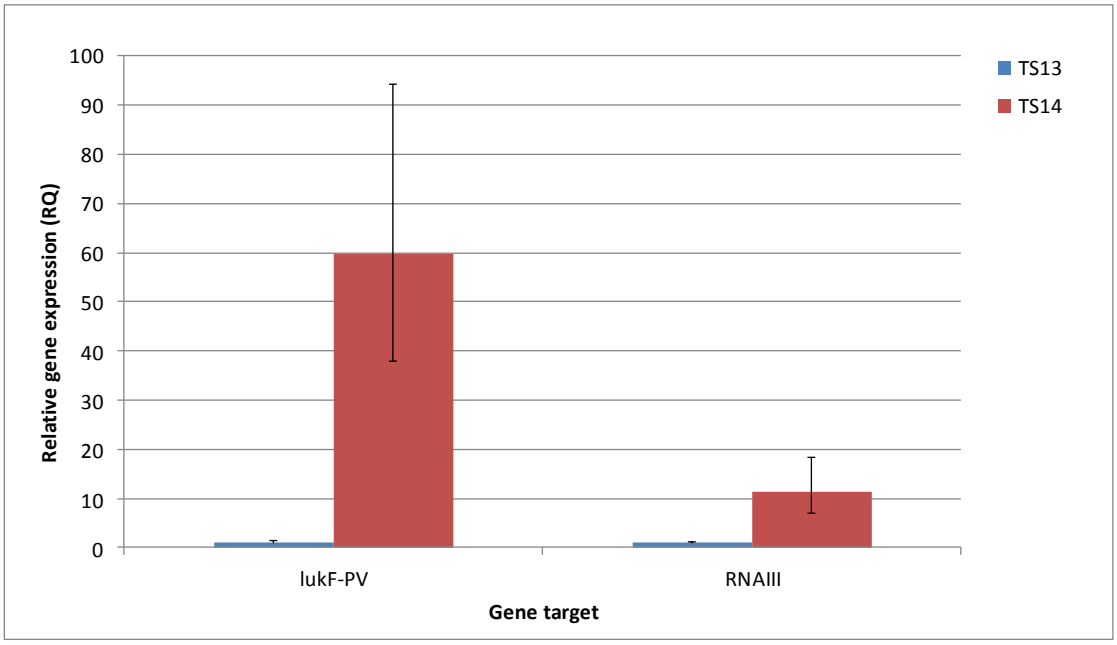

3.2.4 Analysis of full *agr operon* sequences

As differences in *agr* expression had been observed between strains TS13 and TS14 which could have important phenotypic implications, but could not be explained by changes in the promoter sequences, the analysis was extended to the entire *agr* P2 locus for this and other selected clinical isolates.

To ensure full sequencing coverage of *agr*BDCA in both directions, several sequencing primers were used as follows: AgrBDCAF, AgrB F, AgrD1234F, AgrC 5' B, AgrA 5' A, AgrBDCAR, Agrfull R and AgrC R (Table 2.4).

3.2.4.1 Analysis of *agr* group 1 sequences

The *agr* locus of *S. aureus* NCTC 8325 (Table 2.5) was used as a reference for the wild type group 1 sequence. When compared to this sequence there were 30 SNPs in TS14 spread over all four *agr*P2 genes, including 2 in the intergenic region between *agrD* and *agrC.* These substitutions resulted in 5 amino acid substitutions in the AgrB protein: I49L, I90L, F106P, V119I and L152F of which 3/5 were conservative (Figure 3.17A). One substitution, Y251F, was noted in AgrC (Figure 3.17B). No nonsense mutations, insertions, deletions or frame shifts were found. The AgrD and AgrA protein sequences were identical to the wild type. As the reference sequence for the ST22 EMRSA15 strain HO 5096 0412 was available (Table 2.5), this was also compared with TS14 and was found to be identical across the entire *agr* locus. This suggests that the changes identified are likely to result from *agr* mutations which have occurred during the divergence of this sequence type.

3.2.4.1.1 Identification of a non-synonymous *agrC* polymorphism in TS13

The *agr* genes of several other ST22 isolates in the collection, TS6, TS9, TS13 and TS17, were sequenced. The TS6, TS9 and TS17 sequences were all identical to TS14, but TS13 was found to have a single nucleotide change in *agrC.* This was a C to T substitution resulting in a change to the AgrC amino acid sequence: N267I (Figure 3.17B). Changing the residue at this position from asparagine to isoleucine results in the replacement of an amino functionality with a short carbon chain, reducing polarity and increasing hydrophobicity.

The first 205 amino acids of AgrC are understood to form the transmembrane spanning domains, responsible for receiving and recognizing AIP (Jensen *et al*, 2008). The other domain of the protein, from amino acid 205 to 430, forms the cytoplasmic domain which is phosphorylated at the H239 residue in response to activation by AIP (George Cisar *et al*, 2009). The N267I substitution may therefore impact on either phosphorylation or the interaction with and phosphotransfer to AgrA, and so could explain the differences observed in *agr* expression between TS13 and TS14.

Figure 3.17 Alignment of the AgrB and AgrC amino acid sequences for TS13 and TS14

Amino acid alignments demonstrating the variations in AgrB (A) and AgrC (B) sequences for TS13 and TS14 compared to the reference sequences NCTC 8325 and HO 5096 0412 (representing EMRSA-15). Variations from NCTC 8325 are marked with arrows. TS13 and TS14 have 5 predicted amino acid variations from NCTC 8325 in AgrB and 1 predicted variation, Y251F, in AgrC. All of these are present in EMRSA-15. TS13 also has a predicted N267I amino acid substitution which is not present in any of the other sequences.

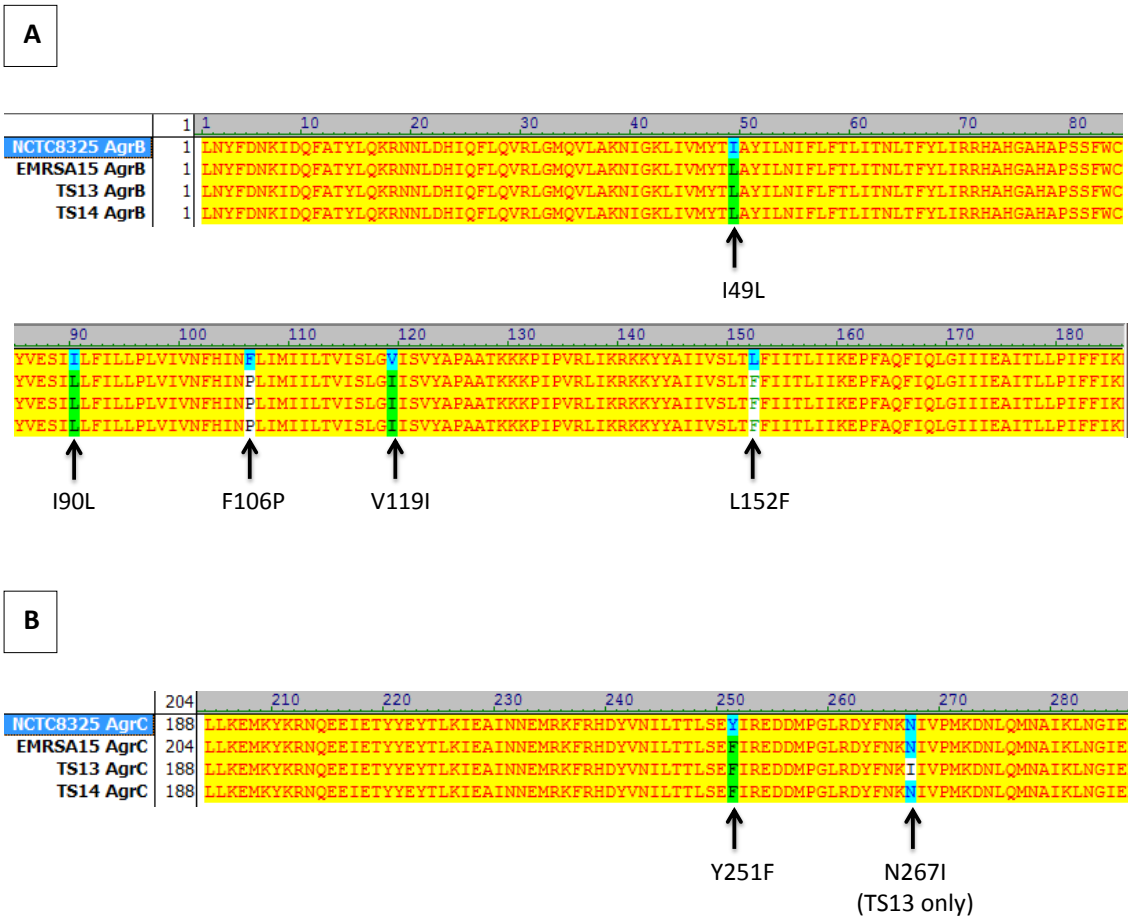

3.2.4.1.2 Amino acid sequence changes in *S. aureus* TS1 AgrBDCA

TS1 was isolated from a case of fatal necrotizing pneumonia and was found to have a unique MLST. Because of these interesting characteristics, the TS1 *agr* locus was also sequenced to look for *agr* variations from the *agr* group 1 laboratory reference strain NCTC 8325 (Table 2.5).

TS1 differed significantly from NCTC 8325, with 126 SNPs across *agrBDCA*. The TS1 sequence had many more amino acid substitutions than any of the other group 1 clinical isolates or reference strains used for comparison. As with the other group 1 strains, no nonsense mutations, insertions, deletions or frame shifts were noted.

Nucleotide polymorphisms in TS1 *agrB* resulted in 14 predicted AgrB amino acid substitutions, of which 4 were also present in EMRSA-15, including: K38V, Y67F, I90L, V98L, I99V, F106P, I115T, L117I, V119I, S121A, K142R, Y143N, T151I and L152F (Figure 3.18A). 4 of these 15 substitutions: V98L, I99V, K142R and T151I were also present in the MW2 *agr* group 3 sequence, leaving 7 which were unique to TS1. The AgrD amino acid sequence was identical to the wild type.

TS1 has 10 amino acid substitutions in the group 1 AgrC when compared with NCTC 8325: V42G, S44T, Y100F, S109N, I127L, T141S, P142S, N308S, S321T and S322R (Figure 3.18B). 4 of these 10 substitutions: V42G, Y100F, S321T and S322R were also present in MW2, leaving 6 which were unique to TS1. There was also a single substitution in AgrA: D194N.

The large amount of variation in TS1 presumably reflects its divergent sequence type. It is unclear why some of the changes seen here are also found in *agr* group 3. It may be that these reflect common mutations with insignificant functional consequences, given that *agr* appears to function in TS1 which produces measurable amounts of alpha haemolysin and PVL toxin. An alternative hypothesis may be that the development of the *agr* locus in TS1 diverged from the

rest of the group 1 isolates further back in time, perhaps retaining some residues that were originally common to group 1 and group 3.

Figure 3.18 Alignment of the AgrB and AgrC amino acid sequences for TS1

Amino acid alignments demonstrating the variations in AgrB (A) and AgrC (B) sequences for TS1 compared to the reference sequences NCTC 8325 and HO 5096 0412 (representing EMRSA-15). Variations from NCTC 8325 are marked with arrows and variations also shown as red circles on the AgrC diagram (C). TS1 has 14 predicted amino acid variations from NCTC 8325 in AgrB and 10 predicted variations in AgrC. TS1 residues which are identical to EMRSA-15 are labelled with E, and those identical to MW2 labelled with M. AgrC variations which are in regions with particular functional importance, the surface loops or the cytoplasmic region, are marked with small arrows on the AgrC diagram (C).

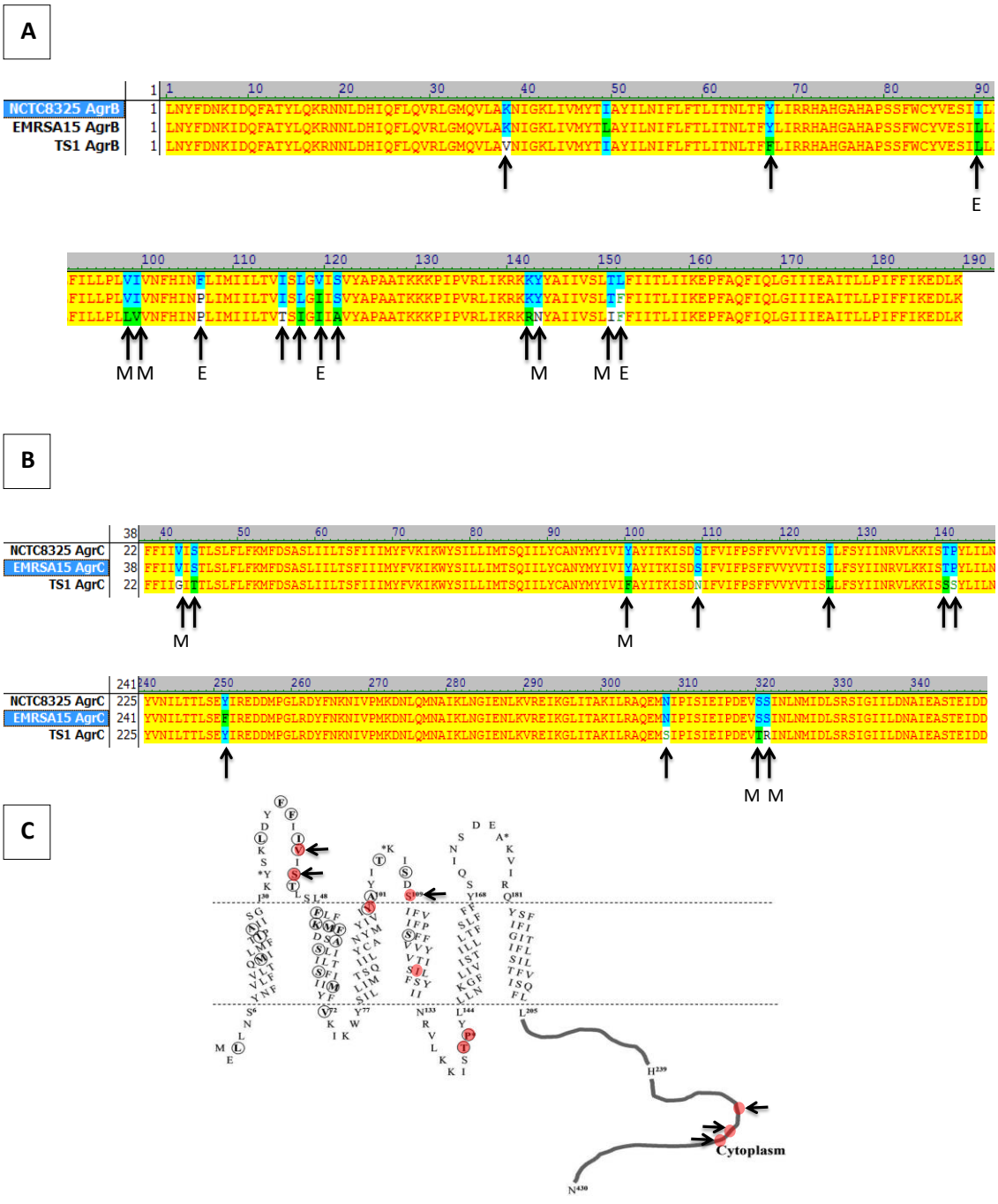

3.2.4.2 Analysis of *agr* group 3 sequences

The finding of the AgrC N267I substitution in TS13 focused attention on the potential for mutations that may interfere with AgrC phosphorylation and phosphotransfer to AgrA. To determine whether there were similar mutations occurring in any of the group 3 isolates, most of which produced much less PVL toxin than the group 1 isolates, the *agrC* and *agrA* genes of several isolates were sequenced and compared with a group 3 reference sequence MW2 (Table 2.5).

The only predicted amino acid variations identified arising from non-synonymous nucleotide polymorphisms in these genes included an I87T AgrC substitution in TS7, an L156F AgrC substitution in TS25 and a K136R AgrA substitution in TS21 (Figure 3.19). The AgrC variations were both in the transmembrane regions of the membrane spanning portion of AgrC, rather than occurring in the receptor loops.

The portion of AgrA, in which the TS21 K136R substitution occurs, is in a LytR-like DNA binding domain believed to be important for binding of AgrA to the *agr* promoter, rather than interaction with AgrC (Nikolskaya & Galperin, 2002). This variation could conceivably interfere with the DNA binding function of AgrA, resulting in reduced *agr* expression.

Figure 3.19 Alignment of the AgrC and AgrA amino acid sequences for *agr* group 3 strains

Amino acid alignments demonstrating the variations in AgrC (A) and AgrA (B) sequences for *agr* group 3 strains compared to the reference MW2. Variations from MW2 are marked with arrows. Predicted variations from MW2 are: TS7 AgrC I87T, TS25 AgrC L156F and TS21 K136R. Both of the AgrC variations occur in predicted transmembrane domains whereas the AgrA K136R change in TS21 occurs in a DNA binding region, predicted to interact with the *agr* promoter.

A

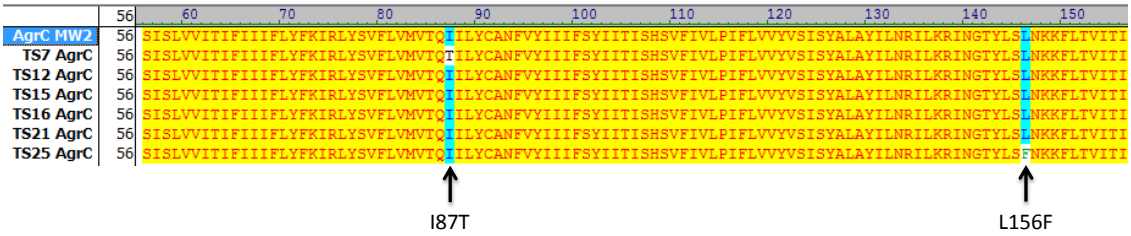

B

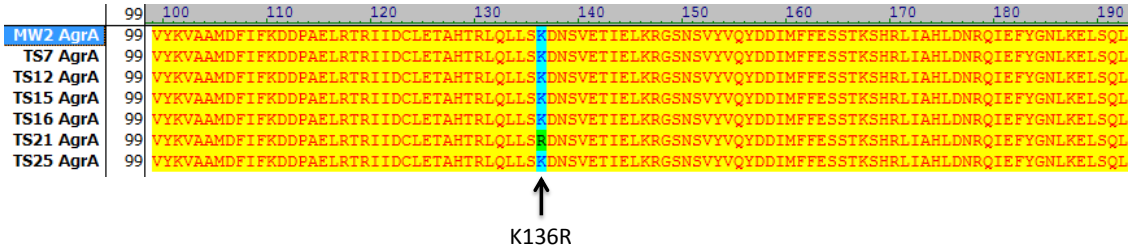

3.2.5 Whole genome sequence analysis of TS13 and TS14

3.2.5.1 Generation of sequencing data

The *agr* loci of TS13 and TS14 differed by only an N267I change in AgrC possibly accounting for their phenotypic differences. Although the isolates appeared to be quite similar genotypically, having the same *spa* type and MLST, the amount of genome wide variation between them was unknown. Based on the clinical and patient information available when the isolates were collected, there was no immediate obvious relationship between the two strains. PVL positive isolates with trimethoprim and gentamicin resistance were frequently identified by the clinical laboratory at the time the strains were collected, so these may represent a locally circulating strain type. Similar PVL positive ST22 isolates had been detected previously in a study of *S. aureus* strains received by the Staphylococcus Reference Unit (Holmes *et al*, 2005).

To gain additional information about this lineage and to enable a more complete comparison to be made between TS13 and TS14, whole genome sequences were obtained for both isolates. This was carried out at the DeepSeq facility (University of Nottingham) by an Illumina MiSeq benchtop sequencer generating 150 bp paired end reads, and the data made available in Illumina FASTQ format. 2,091,482 reads were generated for TS13 and 2,642,626 reads for TS14. Based on a genome size of approximately 3 Mb, with 300 bases per read, this represents approximately 200 times coverage for TS13 and 260 times coverage for TS14. 96.0% of the reads were reported as having a quality score (Q) greater than 30 indicating that good quality sequences had been obtained. A brief *de novo* assembly was also performed by the Illumina BaseSpace software to aid in selection of a reference genome.

The *de novo* assembly returned 344 contigs for TS13 and 257 contigs for TS14 of which 41 of the TS13 contigs and 38 of the TS14 contigs were larger than 10 kb. The largest contigs were 232 kb and 267 kb for TS13 and TS14 respectively.

3.2.5.2 Selection of a reference genome

A complete *de novo* genome construction for TS13 and TS14 was not attempted as additional sequence data would have been required. Instead, the sequence data generated was used to map both isolates individually to a reference genome. Once comparisons had been made between each isolate and the reference, the differences noted could be compared for TS13 and TS14.

The three largest contigs from TS13 and TS14 were compared to publically available genome sequences by BLAST searches to find the closest matches in available reference genomes (Table 3.2).

Strain HO 5096 0412 was returned as the closest match for all 6 of the contigs analyzed, with 99 % identity and 99 % coverage for all but 1 of the contigs. HO 5096 0412 is an MLST22 MRSA representative of EMRSA-15, one of the two major HA-MRSA clones in the UK (see Table 2.5 for reference source). The genome sequencing and analysis was performed by the Sanger Institute (Wellcome Trust, Cambridge). A reconstruction of the ST22-A lineage, which includes the data from HO 5096 0412, was reported by Holden *et al* (2013). Although this isolate is PVL negative and MRSA positive, unlike TS13 and TS14, it appeared to be the closest match available among the whole genome sequences deposited in GenBank, and also had the advantage of being included in a study comparing different strains of the ST22 lineage.

HO 5096 0412 was therefore selected as the reference genome for the next stage of the analysis.

Table 3.2 Results for BLAST search of the largest TS13 and TS14 contigs

The nucleotide sequences for the 3 largest contigs each from an initial *de novo* assembly of TS13 and TS14 were compared by BLAST search with publically available *S. aureus* sequence data at www.ncbi.nlm.nih.gov. The closest match for each contact is shown along with % coverage and identity. The ST22 MRSA strain HO 5096 0412 (Genbank identifier HE681097.1) was returned as the closest match for all 6 contigs. Contig size represents number of nucleotides.

Strain	Contig size	Closest match	Query cover	Identity	Genbank ID
TS13	232,249	HO 5096 0412	99 %	99 %	HE681097.1
	188,271	HO 5096 0412	99 %	99 %	HE681097.1
	173,732	HO 5096 0412	99 %	99 %	HE681097.1
TS14	267,231	HO 5096 0412	97 %	99 %	HE681097.1
	188,094	HO 5096 0412	99 %	99 %	HE681097.1
	173,578	HO 5096 0412	99 %	99 %	HE681097.1

3.2.5.3 Alignment of TS13 and TS14 to HO 5096 0412

The paired end reads from TS13 and TS14 were mapped to the HO 5096 0412 FASTA file obtained from GenBank using the Burrows Wheeler alignment tool (Li & Durbin, 2009).

The TS13 reads covered 98.5% of the HO 5096 0412 genome at least once, with an average coverage of 222.8 reads. The TS14 reads had a coverage of 97.6%, with an average coverage of 281.5 reads. Artemis 14.0.0 (Wellcome Trust Sanger Institute) was used to visualize how the sequencing reads aligned with the reference genome so that the specific regions where gaps occurred could be identified.

Unsurprisingly, a large gap occurred in mapping the genomic region between 33 Kb and 57 Kb on the reference genome, representing SCC*mec* (Figure 3.20A). TS13 and TS14 are both MSSA strains so are likely to be missing the SCC*mec* region altogether. HO 5096 0412 has SCC*mec* IVh which contains a type-2 *ccr* gene complex and class-B *mec* gene complex. Within the class-B *mec* gene complex are two transposases, IS431 and IS1272 (Ma *et al*, 2002). Both of these transposases were the only genes within the SCC*mec* region associated with mapped reads from TS13 and TS14, presumably reflecting the presence of similar transposases elsewhere on the chromosomes of these strains.

Other gaps in the mapping were identified as follows:

A 15 kb gap was identified between nucleotides at 1,360 kb and 1,375 kb on the reference genome, which appeared to reflect an unidentified mobile genetic element which TS13 and TS14 do not possess (Figure 3.20B). BLAST searching of genes within this element indicated it could be an ICE6013-like element, first identified by Smyth and Robinson (2009), which possess integrative and conjugative functions but no obvious virulence determinants.

The region between 1,520 kb and 1,565 kb on HO 5096 0412 has a phage inserted, designated ΦSa2 $_{\text{HO 5096 0412}}$, which is defined by the presence of a *Bcg*I-like restriction enzyme (Holden *et*

al, 2013). TS13 and TS14 did not appear to carry this enzyme, suggesting a different phage inserted at this site (Figure 3.21A). The phages encoding *lukSF-PV* nearly all insert at this phage site, ΦSa2 (Goerke *et al*, 2009), and so it would be expected that the PVL positive TS13 and TS14 strains would have a different phage here to the PVL negative HO 5096 0412.

Gaps were noted sporadically throughout the second phage region on the reference genome between 2,040 kb and 2,090 kb which is known to contain a phage, designated ΦSa3 $_{\text{HO 5096 0412}}$, encoding Staphylokinase and the immune evasion proteins CHIPS and SCIN (Holden *et al*, 2013). The uneven mapping of the TS13 and TS14 reads suggested that a different but related phage was inserted at this site (Figure 3.21B). Reads mapped well to the genes for CHIPS, SCIN and Staphylokinase (*sak)* so it seemed likely that this related phage also contains the immune evasion complex (IEC) comprising these genes (de Haas *et al*, 2004).

Apart from the regions described above, TS13 and TS14 mapped to the rest of the reference genome. Other regions of interest which HO 5096 0412 is known to possess and appear to be shared with TS13 and TS14 included the enterotoxins *seg* and *sei*, gamma haemolysin, fibronectin binding protein A (*fnbpA*), and a Tn554 like transposon which encodes a β-lactamase.

Figure 3.20 TS13 and TS14 are missing mobile genetic elements present in HO 5096 0412

Alignment of sequence reads for TS13 and TS14 with HO 5096 0412 in the region of SCC*mec* (A) and a transposon at reference position 1,360 kb (B). Coverage is indicated by the graphs for TS13 and TS14 which represent number of reads matching each position. Gaps in the graphs indicate there were no reads matching this portion of the reference genome. TS13 and TS14 had reads matching the two transposons IS431 and IS1272 but did not appear to possess SCC*mec*, with no reads matching *mecA*. TS13 and TS14 also appeared to be missing an unidentified mobile genetic element (MGE) shown in B.

Figure 3.21 TS13 and TS14 carry different phages to HO 5096 0412

Alignment of sequence reads for TS13 and TS14 with HO 5096 0412 in the two phage insertion sites for ΦSa2 $_{HO\ 5096\ 0412}$ (A) and ΦSa3 $_{HO\ 5096\ 0412}$ (B). Coverage is indicated by the graphs for TS13 and TS14 which represent number of reads matching each position. Gaps in the graphs indicate there were no reads matching this portion of the reference genome. The *bcgI*-like restriction enzyme which is a defining feature of ΦSa2 $_{HO\ 5096\ 0412}$ was not present in TS13 and TS14 (A). TS13 and TS14 had reads matching the immune evasion complex (IEC) containing CHIPs and Staphylokinase, but had gaps elsewhere in the ΦSa3 $_{HO\ 5096\ 0412}$ sequence (B).

3.2.5.4 SNP calling and comparison of TS13 and TS14 genomes

Once mapped, single nucleotide polymorphisms (SNPs) occurring between the test strains and the reference genome were called using the mpileup and bcftools software (Li *et al*, 2009a), excluding bases with less than 5 times coverage or a quality score less than 13, indicating an unreliable base read, and indels. Because the reference genome phages appeared to be different to the test strains, SNPs called in these regions were also excluded from the analysis.

After filtering, a combined total of 835 SNPs were found in TS13 and TS14 when compared with HO 5096 0412. Of these, 118 were exclusive to TS14 and 75 were exclusive to TS13, leaving 642 SNPs in common between the two strains (Figure 3.22).

A script, written by Hardeep Naghra, was used to compare the SNPs loci to the coding sequence annotations for HO 5096 0412. SNPs were then filtered according to their likely impact on gene products. 434 SNPs were identified which were likely to change the amino acid sequence of gene products (non-synonymous) while 204 were found which would not (synonymous). This left 197 SNPs which were found to be in non-coding regions of the genome.

Analysis was then focused on the 434 non-synonymous SNPs identified in TS13 and TS14. Of these, 78 were exclusive to TS13 and 64 to TS14, leaving 292 in common. The SNPs exclusive to TS13 and TS14 along with their affected gene products are listed in Appendix 7.1 and 7.2.

Changes of interest exclusive to TS13 included the A to T substitution in *agrC* at location 2,108,636 of the reference and a G to T substitution in a putative staphylococcal accessory regulator, CDS 23970, at location 2,589,488. BLAST searching of the base sequence of this regulatory gene revealed this to be *sarU*.

Changes of interest exclusive to TS14 included a C to T substitution in coding sequence 5930 at position 691,792, annotated as being an AraC family regulatory protein.

The SNP comparison between the two strains indicates that they are very closely related. Excluding the phage regions, the 193 unique SNPs between them represent less than 0.01 % of the total genome.

As the phenotypic analysis focused on differences in *agr* expression, further analysis was carried out to determine whether any of the other genes encoding Sar proteins contained SNPs. Not all of the Sar protein genes were annotated on the HO 5096 0412 genome so this required BLAST searching with individual Sar protein gene sequences to identify the matching coding sequences for each one. The results of this analysis are shown in Table 3.3.

Four coding SNPs were identified which were all non-synonymous changes. In addition to the *agrC* and *sarU* changes in TS13 already mentioned above, two additional substitutions were identified in both TS13 and TS14 in the *saeS* gene and another in *sarU*.

Figure 3.22 Genome map summarising the TS13 and TS14 sequence analysis

Comparison of the TS13 and TS14 sequence data with the reference genome HO 5096 0412. The coding sequences (CDS) for HO 5096 0412 are shown as forward sequences, blue, and reverse sequences, purple. Single nucleotide polymorphisms (SNPs) occurring in TS13 and TS14 are shown in red. Significant differences between the TS strains and HO 5096 0412 are indicated, including the lack of SCC*mec* and the presence of difference phages. Potentially important SNPs in regulatory genes are listed on the right with a summary of the SNPs which occur in both TS13 and TS14, or exclusively in one or the other, shown in the bottom right.

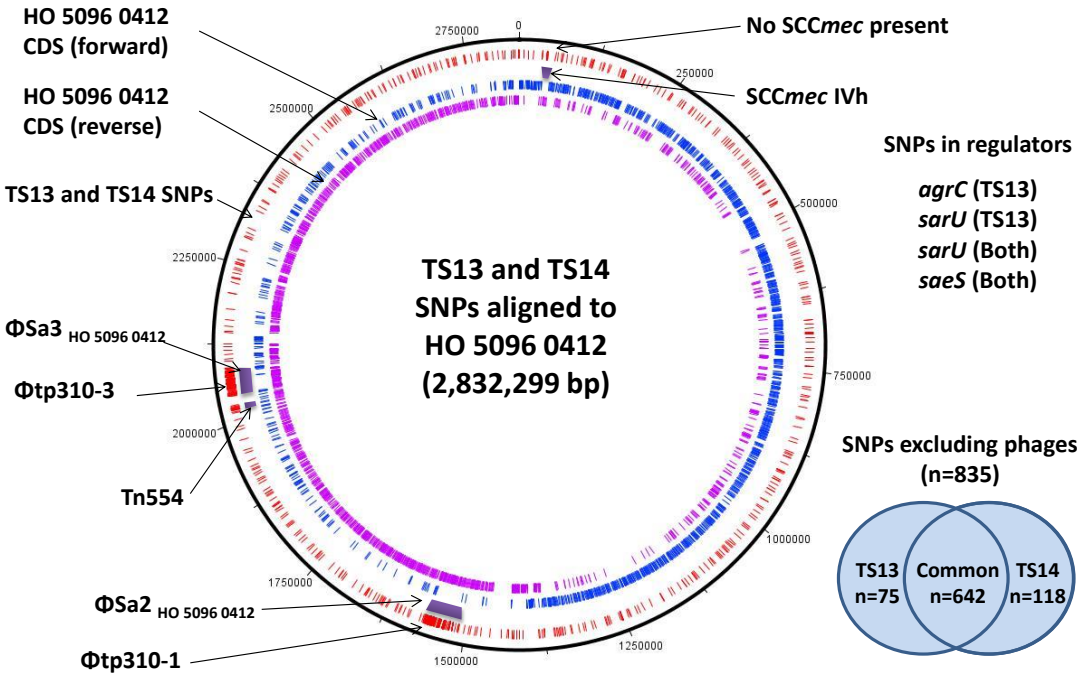

Table 3.3 Summary of SNPs occurring in selected genes known to be involved in staphylococcal exotoxin regulation

The coding sequence annotation identifier each gene is labelled with in the HO 5096 0412 Genbank file is shown in the 2nd column, with the base ranges marked for these genes in the 3rd column. The nucleotide position in HO 5096 0412 that SNPs occur in are shown along with the polymorphism in column 4, indicating whether this SNP occurs in TS13 only or in both TS13 and TS14. The final column indicates the predicted amino acid substitution that would occur as a consequence of the SNP.

Gene	Coding Sequence ID	Base range	SNP	Substitution
sarS	SAEMRSA15_00780	100174..100926	no	
sarA	SAEMRSA15_05440	640499..640873	no	
sarX	SAEMRSA15_05940	692834..693259	no	
mgrA	SAEMRSA15_06120	708245..708688	no	
saeS	SAEMRSA15_06310	728125..729180	728161 T to C BOTH	I341M
saeR	SAEMRSA15_06320	729180..729866	no	
rot	SAEMRSA15_16700	1851896..1852396	no	
agrC	SAEMRSA15_19460	2107837..2109129	2108636 A to T TS13	N267I
sigB	SAEMRSA15_19740	2148019..2148789	no	
sarV	SAEMRSA15_21650	2344373..2344723	no	
sarR	SAEMRSA15_21920	2366747..2367094	no	
sarY	SAEMRSA15_21940	2367912..2368655	no	
sarZ	SAEMRSA15_22850	2465242..2465688	no	
sarT	SAEMRSA15_23960	2588442..2588801	no	
sarU	SAEMRSA15_23970	2589089..2589865	2589392 T to C BOTH	C102R
			2589488 G to T TS13	D134Y

3.2.5.5 Identity of genetic material not mapping to the reference genome

The genome mapping approach used enabled SNPs to be identified within the core genome. To determine whether there were other significant portions of genetic material from TS13 and TS14 which did not map to the reference sequence, the *de novo* sequences were aligned to HO 5096 0412 by Hardeep Naghra (Centre for Biomolecular Sciences). Aligned contigs were filtered out, leaving only those contigs which did not align to the reference genome. This left 7 contigs for TS13 and 5 contigs for TS14 which were over 1 kb in length.

These unaligned contigs were used in BLAST searches in order to try and identify their contents. Table 3.4 summarises the results of these searches and indicates their most likely components.

Two patterns emerged from these data. The first was the large number of hits against phages designated tp310 which are unpublished but recorded in the database as occurring in ST22 strains of *S. aureus*. Hits against *S. aureus* genomes for these fragments occurred in regions where phage was inserted into the genome, presumed to be similar or identical to tp310 phages.

The other hits of interest were to plasmids, one each for TS13 and TS14. The pSAP076A plasmid matching the TS13 contig appeared to mostly contain heavy metal ion transporters and it was unclear whether any of these represented antibiotic resistance genes. The pSK77 plasmid, however, which matched one of the TS14 contigs, encoded a dihydrofolate reductase and an aminoglycoside phosphotransferase in the region matching the contig. These enzymes are known to confer resistance to trimethoprim and gentamicin respectively which could therefore explain the antibiotic resistance phenotype of the strains (gentamicin and trimethoprim resistant only).

Table 3.4 BLAST search data for unaligned contigs of TS13 and TS14

TS13 and TS14 contigs were aligned to HO 5096 0412 and remaining unaligned contigs filtered for further analysis. BLAST searching with these contigs yielded the following matches. Contigs are identified by source, either TS13 or TS14, and size in base pairs. The first 3 matches for each contig are shown where the first letter 'g' indicates a genome sequence, 'p' a plasmid sequence and 'Φ' a phage sequence. Conclusions were drawn about the potential contents of each contig based on reviewing the annotation data available from the BLAST sequence results. The majority of the matches were to phage fragments similar to Φtp310 phages, previously found in ST22 strains but unpublished. A large (33 kb) contig was also identified in TS13 representing a plasmid, although antibiotic resistance genes could not be identified in the annotation data for the plasmid matches. Also of note, a 5.5 kb contig in TS14 which contained antibiotic resistance genes for trimethoprim and gentamicin.

Source	Size (bp)	Match 1	Match 2	Match 3	Contents
TS13	33096	pSAP076A	pSAP102A	pSAP075A	Plasmid borne heavy metal transporters
	27593	g04-02981	gJH1	gJH9	Phage terminase
	9462	g55/2053	Φtp310-3	gED133	Parts of Φtp310-3
	7178	Φtp310-3	g55/2053	gM1	Parts of Φtp310-3
	4316	gBmb9393	gMSSA476	gMW2	Phage integrase
	3472	g11819-97	Φtp310-3	Φtp310-1	Parts of Φtp310 phages
	3006	gJKD6008	pSK77	pSAP068A	Transposases
TS14	17397	g 55/2053	Φtp310-3	Φtp310-1	Parts of Φtp310 phages
	6748	Φtp310-3	g55/2053	gNCTC8325	Parts of Φtp310-3
	5494	pSK77	pLW043	gJKD6008	Dihydrofolate reductase (trimethoprim resistance), Aminoglycoside phosphotransferase (gentamicin resistance)
	3608	Φtp310-3	gM013	gSA957	Parts of Φtp310-3
	3555	gSA957	gM913	gNCTC8325	Phage fragments, other hypothetical proteins

3.2.5.6 Identification of TS13 and TS14 phages

The best characterised phages which encode PVL include ΦPVL, ΦMW2 and ΦSLT, all of which insert at a genomic location around 1.5 Mb, occupied by ΦSa2 $_{HO\ 5096\ 0412}$ on the reference genome. PCR based phage typing of TS13 and TS14 had already been carried out by Kome Otokunefor and identified both as having ΦPVL (Otokunefor *et al*, 2012).

The large number of hits of unaligned contigs to Φtp310 phages raised the possibility that TS13 and TS14 have a PVL encoding phage which is related to ΦPVL but has a greater similarity to Φtp310 phages. The reference sequence for the Φtp310-1 phages includes the sequences for *lukSF-PV*, whereas Φtp310-3 does not, therefore alignments of TS13 and TS14 to ΦPVL and Φtp310-1 were carried out initially.

Mapping the sequences for TS13 and TS14 against the reference sequence for ΦPVL showed uneven mapping over the first 17 kb of the phage and again towards the final portion between 37 and 44 kb. There appeared to be even mapping over *lukSF-PV* (Figure 3.23A).

By contrast, sequence mapping for Φtp310-1 showed consistent coverage over the whole phage, indicating a greater likelihood of this phage type being present in TS13 and TS14 rather than ΦPVL (Figure 3.23B).

As many of the contigs matched specifically against Φtp310-3, TS sequences were also mapped against the reference sequence for this phage. The sequences aligned without gaps, indicating TS13 and TS14 encode a phage with a high degree of similarity to Φtp310-3 (Figure 3.24). This phage encodes staphylokinase and the immunomodulatory proteins CHIPS and SCIN and so is also more likely to be present in the TS strains than ΦSa3 $_{HO\ 5096\ 0412}$ at the 2.1 mb phage insertion site.

Without a full *de novo* construction of these two strains, any integrated phages could not be characterised with certainty. Based on a combination of the contig matches and phage

alignment however, it seems that TS13 and TS14 probably carry both the PVL positive Φtp310-1 and the IEC encoding Φtp310-3.

Figure 3.23 PVL phage alignments for TS13 and TS14

Alignment of sequence reads for TS13 and TS14 with ΦPVL (A) and Φtp310-1 (B). Coverage is indicated by the graphs for TS13 and TS14 which represent number of reads matching each position. Gaps in the graphs indicate there were no reads matching this portion of the reference genome. The sequence mapping for TS13 and TS14 to ΦPVL contained gaps (A) whereas the mapping to Φtp310-1 did not (B).

Figure 3.24 Alignment of TS13 and TS14 to Φtp310-3

Alignment of sequence reads for TS13 and TS14 with Φtp310-3. Coverage is indicated by the graphs for TS13 and TS14 which represent number of reads matching each position. Gaps in the graphs indicate there were no reads matching this portion of the reference genome. TS13 and TS14 sequences mapped well to Φtp310-3, which encodes the immune evasion complex (IEC), indicating this phage type is probably present in the TS strains. SCIN = Staphylococcal complement inhibitor. CHIPS = chemotaxis inhibitory protein.

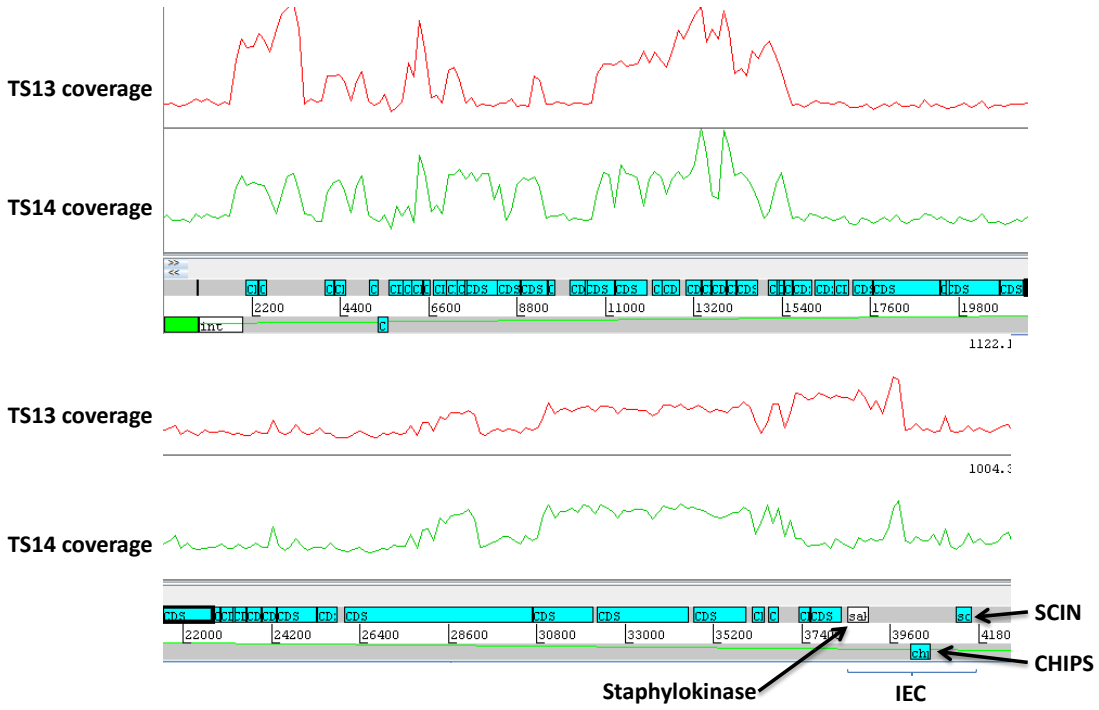

3.2.5.7 Summary of functionally relevant differences

The whole genome sequence analyses for TS13 and TS14 were summarised in Figure 3.22. As the likely identity of the phages is known, these are labelled as Φtp310-1 and Φtp310-3 alongside ΦSa2 $_{HO\ 5096\ 0412}$, and ΦSa3 $_{HO\ 5096\ 0412}$ respectively. This confirms that TS13 and TS14 are PVL positive, and also that they carry the immune evasion complex genes.

The TS strains did not possess SCC*mec,* as expected. Although gentamicin and trimethoprim resistance genes were only identified in a contig from TS14 and not TS13, it seems likely that TS13 also possesses these genes given they are both resistant to gentamicin and trimethoprim.

In terms of potentially important polymorphisms in regulators, SNPs in *agrC* and *sarU* in TS13 were identified. Also, in both strains, another SNP in *sarU* and one in *saeS* were also present. These are discussed in more detail later (Section 3.3.4.4).

3.3 Discussion

3.3.1 Why does PVL production vary between clinical isolates?

Large variations in PVL production were noted *in vitro* between the clinical isolates tested. Taken together, the data from the alpha haemolysin western blots, *agr* activation and inhibition experiments and pull-down assays indicate that variable expression of global regulators, particularly *agr*, probably explains the majority of this variation.

In the strains tested, there was no clear correlation between the amount of PVL produced and the severity of clinical infections. Most of the high producing ST22 strains caused skin and soft tissue infections, with the cases of severe pneumonia being caused by strains from other lineages which produced much less toxin. The numbers are obviously too small to draw any firm conclusions, but the limited numbers tested do not support the theory that severe infections are always caused by strains which are high PVL producers *in vitro*.

The MSSA ST22 lineage was highly represented, and despite some variations in *spa* profiles between isolates, levels of PVL production were similar within this lineage. There are reports of CA-MRSA lineages, notably USA300, which are associated with high level toxin expression mediated by *agr* (Li *et al*, 2010). In a study of a very successful locally circulating strain ST93 CA-MRSA in Australia, 58 ST93 isolates were found to have similar phage profiles and *lukSF-PV* expression (Coombs *et al*, 2012).

There may be a number of reasons why production of PVL and other toxins is similar within lineages. This is most likely to reflect historic acquisition of point mutations or horizontal gene transfer. Point mutations in global gene regulators or two-component systems which coordinate environmental responses could give lineages distinct patterns of toxin expression.

One possible explanation for the enhanced *agr* and toxin expression of USA300 is a mutation in the *pknB* gene, a kinase involved in cell wall metabolism, which resulted in reduced

expression of *sigB* and increased expression of *agr* (Tamber *et al*, 2010). This however is at variance with another study of a *sigB* mutant which showed hyper production of alpha haemolysin and elevated SarA expression (Cheung *et al*, 1999). In addition to enhanced *agr* expression, the *agr* regulon was also reported to be altered in USA300 such that higher than expected expression of toxin genes including alpha haemolysin (*hla)* and *lukSF-PV* resulted. The mechanism for this was not clear but speculated to involve non coding RNAs (Cheung *et al*, 2011).

Mutations in toxin repressor genes could influence toxin gene expression both directly and indirectly through binding to the promoters of global regulators such as *agr* and *sarA*. Rot was originally identified from a strain harbouring a Rot-inactivating mutation which showed upregulation of toxins (McNamara *et al*, 2000).

Horizontal gene transfer could alter global regulation by bringing in repressor genes or increasing the overall metabolic load on the bacteria. *psm-mec* carried by certain SCC*mec* types was found to bind to AgrA mRNA and suppress translation (Kaito *et al*, 2013).

Finally, differences in *agr* activity could be inherently different between *agr* groups. RNAIII expression was noted to be higher in *agr* group 1 as compared to groups 2 and 3 which could partly explain differences in toxin expression between lineages belonging to different *agr* groups (Geisinger *et al*, 2012).

In the context of variable PVL production, before considering specific findings in the clinical strains studied which could explain the variations it is clearly important to examine how PVL is regulated. As differences between strains probably largely revolve around expression of global regulators, understanding the role of *agr* is key.

3.3.2 How is PVL production regulated?

3.3.2.1 The role of *agr* in regulating PVL production

It has been known for some time that *agr* plays a role in regulation of *pvl* gene expression. *agr* and *sarA* mutants display markedly reduced transcription of *pvl* as measured by RT-PCR (Bronner *et al*, 2000). Comparing RNAIII and *pvl* transcription by the low PVL producing TS13 and high PVL producing TS14 strains demonstrated a ~60-fold difference in *pvl* expression with a ~10-fold difference in RNAIII expression. This could either indicate that *agr* is only playing a partial role in determining the differences in exotoxin gene expression between the strains or that because *agr* influences the expression of several regulators, the final effect on exotoxin expression is amplified.

In the strains studied, alpha haemolysin production was highest in the strains which also produced high levels of PVL toxin, suggesting shared global regulation of both exotoxins in these strains. Similarly when exogenous AIP was added to cultures at time of inoculation, overnight exotoxin expression of both alpha haemolysin and PVL were much higher. This gives a clearer indication of the importance of *agr* in upregulating PVL production. Conversely, the AgrC antagonist (ala5)AIP-1 inhibited PVL production in the strains tested if added early enough to cultures.

The results above are perhaps not surprising given that *pvl* expression is known to be at least in part dependent on *agr*. The unexpected findings were that the timing of addition of exogenous activators or inhibitors is crucial in determining whether they effect PVL production or not. TS13, the low producing isolate, responded to exogenous AIP-1 but only if this was added early enough. Once the bacteria had entered exponential phase, adding 100 nM of exogenous AIP-1 did not appear to have an appreciable effect on toxin production. There was a similar effect observed with the *agr* inhibitor (ala^5)AIP-1 which no longer appeared to be effective in inhibiting PVL production by TS14, the high producing strain, once 4 h had elapsed

from inoculation. These findings, taken together, indicate a 'window period' during which directly modulating *agr* with exogenous peptides influences exotoxin production, but once this window period has elapsed, *agr* inhibition or activation no longer has an appreciable impact on exotoxin production. From measuring PVL production over time in selected isolates, it seems that most of the PVL is produced after exponential phase outside of the window period identified, so the unresponsiveness to late addition of the AgrC antagonist is not because the PVL has already been produced and secreted.

RNAIII, the effector mRNA of the *agr* system, is well characterised as influencing translation by forming complexes with other mRNAs as opposed to directly influencing transcription (Geisinger *et al*, 2006). Comparing gene expression in TS13 and TS14 showed a large enough difference to account for differences in exotoxin production without any additional regulation at the translational or post-translational levels. In terms of the role of *agr* in regulating *pvl* gene transcription, this was hypothesised to be due to regulatory proteins whose translation is regulated by RNAIII binding directly to the *pvl* promoter.

3.3.2.2 What do the promoter pull down experiments reveal about *pvl* regulation?

The promoter pull down experiments were designed to identify the regulatory proteins which interact directly with the *pvl* promoter. The *agr* promoter was included in the analysis for comparison. The identification of AgrA binding to the *agr* but not the *pvl* promoter indicated specific regulator-protein binding interactions were occurring. The portion of AgrA that interacts with promoters contains a LytR type DNA binding domain (Nikolskaya & Galperin, 2002). This has been shown to bind to other promoters besides *agr*P2 (Queck *et al*, 2008), particularly in PSM regulation, but does not appear to interact with the *pvl* promoter.

Consistent results were observed between the isolates tested in terms of the regulators identified binding to the promoters. Some of the products such as the ribosomal subunit proteins, the DNA topoisomerase and gyrase represent generic DNA binding proteins which are not acting as regulators. The Sar family of transcriptional regulators bound to all of the promoters in significant amounts, particularly SarA, SarS and SarR. MgrA and Rot, other helix-turn-helix regulators from the same family were also observed binding to both *agr* and *pvl* promoters. The involvement of these regulators makes perfect sense from the point of view of transcriptional regulation of *pvl*.

From comparisons with the regulation of other toxins, SarA is likely to be an important factor in upregulating *pvl* expression, itself being upregulated by *agr*. As mentioned previously, a SarA mutant demonstrated a marked reduction in *pvl* expression (Bronner *et al*, 2000). By contrast, SarS, SarR and Rot are likely to act as transcriptional repressors. SarS has been previously identified as binding to the *hla* and *agr* promoters, with knockout mutants demonstrating it has a strong repressive effect, itself being repressed by *agr* and SarA (Tegmark *et al*, 2000). MgrA is known to regulate *spa* and *hla* gene transcription in both an *agr* dependent and independent fashion. (Ingavale *et al*, 2005). It appears that this regulator may also play a role in regulating *pvl* gene transcription. MgrA seems to act in concert with *agr* with similar regulator effects and so is likely to have a positive effect on *pvl* gene transcription (Luong *et al*, 2006).

Another protein which was identified binding to both *pvl* and *agr* promoters was TcaR, which shares sequence homology with the other MarR-like transcriptional regulators and is known to be a positive regulator of SarS (McCallum *et al*, 2004). Based on this, it would seem possible that TcaR could act to repress PVL toxin production either act directly through binding to the *pvl* promoter, or indirectly by upregulating SarS.

The pulldown assay was not set up to be a quantitative assay, however large differences in SarS and Rot binding were observed between the low PVL producing TS12 and TS13 and the high

PVL producing TS14. This could reflect differences in the production of these regulators contingent on differences in *agr* function. As an excess of promoter DNA was used, some of the bound protein products identified may not be functionally relevant. Quantifying and optimising the quantity of promoter DNA required for the assay would be one approach to attempt to distinguish high affinity from low affinity binding. Heterodimer complexes combining different Sar subunits could also be another factor further complicating the interactions between promoter and regulator which would not have been identified in this assay.

The involvement of a number of transcriptional activators and repressors in regulating *pvl* gene expression may explain the 'window effect' discussed above as it would explain the importance of determining *agr* expression as early as possible. The regulatory proteins would be transcribed and translated during exponential phase of growth, and so their production would be determined by RNAIII levels. Once produced, it may be too late to significantly alter their production by stimulating or inhibiting *agr* such that a significant downstream impact on exotoxin gene expression would not be observed.

3.3.2.3 Environmental and other factors influencing PVL production

Activating and inhibiting *agr* affected PVL production. In addition, well characterised staphylococcal transcriptional regulators known to play a role in regulating gene expression were identified binding to the *pvl* promoter. Two other additional factors which may influence PVL production were briefly investigated; exposure to sub-inhibitory concentrations of antibiotic and the growth medium.

Adding a sub-inhibitory concentration of oxacillin to the low producing TS13 resulted in much higher production of PVL, consistent with previous reports (Dumitrescu *et al*, 2008). In a follow up paper, Dumitrescu *et al* (2011) analysed the upregulation of *pvl* gene expression in the

presence of several antibiotics by RT-PCR. They found that affinity of the antibiotics for PBP1 was essential, with non-selective oxacillin and PBP1 selective imipenem demonstrating a clear effect, but PBP2 and PBP3 specific antibiotics ineffective. By comparing knockout mutants of the regulators Rot, SarA, Agr and SaeRS, they were able to show that Rot and SarA were essential for the induction effect, whereas Agr and SaeRS were not.

Growing TS13 in the presence of both oxacillin and (ala5) AIP-1 resulted in an observable reduction in PVL toxin production compared to oxacillin alone, indicating that the induction effect does not operate independently of *agr* even if it is mediated by upstream effects on SarA and Rot.

The exotoxin upregulation observed in the presence of certain beta-lactam antibiotics has been put forward previously as a drawback to using these for treatment in situations where toxin production plays a major role in pathogenesis; upregulation of alpha haemolysin by oxacillin has been known for some time (Ohlsen *et al*, 1998). The upregulation of shiga toxin by quinolones in *E. coli* is another example of an undesirable antibiotic effect (Kimmitt *et al*, 1999). The exact mechanism for the beta-lactam effect is unknown, although, as mentioned above appears to involve both PBP-mediated effects and global regulators. In a recent study of CA-MRSA, *agr* repression was observed in the presence of oxacillin, believed to be mediated by induction of PBP2a (Rudkin *et al*, 2013). Surprisingly, although Agr-mediated PSM production was reduced, the expression of both alpha-haemolysin and PVL were increased as observed in the studies mentioned above. Hence it is not clear if this is an effect that is specific to CA-MRSA, which have been shown to constitutively express lower levels of PBP2a than other MRSA strains carrying the larger *mec* cassettes such as type II (Rudkin *et al*, 2012). As only USA300 and USA400 were tested in the study, it is also possible that the *agr* repression observed is strain dependent because of mutations in key regulators involved in stress responses, such as the PknB kinase mutation in USA300 (Tamber *et al*, 2010). At the present time there does not

appear to be any conclusive data besides *in vitro* experiments to support the hypothesis that the use of beta-lactam antibiotics to treat PVL and other exotoxin associated infections worsens outcome due to induction of elevated toxins.

Growth medium is known to influence expression of toxins and global regulators in *S. aureus*. Addition of yeast extract to defined media, the use of rich media and low pH all increase *agr* and alpha haemolysin expression (Jassim *et al*, 1989; Regassa & Betley, 1992). A brief comparison of PVL production by TS13 and TS14 in selected growth media demonstrated that growth in CYGP medium resulted in the highest production of PVL. BHI appeared to support slightly higher production of PVL by TS14 than TSB or LB. This is broadly consistent with other reports of the impact of growth medium on PVL; *pvl* expression was observed to be 100 fold higher in a medium containing yeast extract and casamino acids, similarly to CYGP, than in BHI medium (Bronner *et al*, 2000). *pvl* expression in CCY medium, another medium containing both yeast extract and casamino acids, was noted to be much higher than in TSB and BHI media (Malachowa *et al*, 2011). The presence of yeast extract and casamino acids might favour metabolic pathways which are associated with stimulation of *agr* expression, or perhaps result in metabolic byproducts which change the culture environment thereby upregulating *agr*.

The potential role for environmental factors in determining gene expression is important as this could explain the severity of certain types of infections. Necrotising pneumonia is thought to involve a feedback cycle of neutrophil attraction and destruction, leading to the release of inflammatory mediators and further tissue damage (Diep *et al*, 2010). Conditions of inflammation and contact with neutrophils could be potential factors that enhance PVL production *in vivo*, contributing to pathogenesis and explaining any mismatch between *in vitro* expression and *in vivo* severity. A study that compared *pvl* expression in drained abscess pus to *in vitro* expression found that higher *in vivo* expression could be only partially explained by

higher *agr* expression. The mismatch in expression was hypothesised to be due to *in vivo* neutrophil exposure (Loughman *et al*, 2009).

There are a few other potential factors involved in regulating PVL which were not explored in this study. There appears to be strain and phage dependent variation in enhanced PVL production in response to induction, with USA300 having defective prophage excision (Wirtz *et al*, 2009). This could be implicated in the response to antibiotics, perhaps also explaining the potentially strain dependent nature of antibiotic induction effects. Although there is no definitive evidence in the literature to suggest that the type of PVL phage determines expression, PVL haplotypes with variations in the gene sequence have been associated with different lineages (Chen *et al*, 2013). PVL phages are also known to integrate into different sites depending on the strain background, and this could conceivably influence gene expression (Boakes *et al*, 2011a).

In summary, PVL production is heavily influenced by *agr* activity and appears to be also regulated by the Sar family of global regulators. Environmental factors are important including exposure to antibiotics and the growth media used. Addition of the AgrC antagonist (ala5)AIP-1 inhibits PVL toxin production if added early enough in growth raising the possibility that AgrC antagonists could have a role to play in reducing the severity of PVL and other toxin associated infections (Chan *et al*, 2004). However, the narrow *in vitro* window period in which these inhibitors are effective may be a significant drawback, as in many clinical situations bacterial growth is likely to be well established before a patient is symptomatic, with a further delay to presentation and treatment. Further studies of the impact *agr* inhibitors *in vivo* is required.

3.3.3 Do the promoter and *agr* variations explain the variable PVL production?

In an attempt to explain the observed differences in PVL production between the clinical isolates, *pvl* and *agr* promoter and operon-wide *agr* sequence analysis was performed. The *agr* promoter sequence polymorphisms identified occurred in regions where the functional significance is not known. Some of these polymorphisms, particularly the C to A substitution in *agr*P2 found in TS13, TS14 and HO 5096 0412, are probably conserved in certain lineages without functional significance. Importantly, no polymorphisms were identified in the AgrA DNA-binding regions, a point mutation in which was previously found to cause a marked reduction in *agr* expression (Koenig *et al*, 2004; Villaruz *et al*, 2009). *agr*P2 and *agr*P3 can still activate in an AgrA-independent manner although much less effectively (Reynolds & Wigneshweraraj, 2011).

Even less is known about the *pvl* promoter, and this made it difficult to draw any firm conclusions from the sequence data. As already described, the three promoter sequence polymorphisms which were identified were present across several strains with all of the ST22 strains TS6, TS13 and TS14 having identical sequences. It appears as though the polymorphisms probably reflect different PVL phage types and in the absence of clear patterns between those and PVL production, they were not taken forward for further analysis. While it seems plausible that *pvl* promoter mutations could occur which significantly reduce *pvl* production, these would be unlikely to impact on global regulation or expression of other toxins in a manner that would explain the expression patterns observed in the clinical strains. This is in contrast with staphylococcal proteases which appear to be key mediators of secretion and accumulation of several other virulence factors including PVL and alpha haemolysin (Kolar *et al*, 2013).

The analysis of the complete *agr* operon in selected strains identified many variations from the reference sequences, particularly in TS1 which appears to be from an unusual strain background. Without recreating each of these in a reporter system it is difficult to determine

what impact they may have on *agr* expression and hence exotoxin production. One of the drawbacks of this diverse collection of strains is that there are insufficient numbers representing each of the different strain types to build up a clear picture of which nucleotide substitutions are associated with particular backgrounds. Fortunately, there were a large enough number of ST22 strains to draw attention to the lower PVL production of TS13. Comparing the ST22 sequences then confirmed that the observed *agr* polymorphisms were common to all of the isolates except that observed in the TS13 *agrC* cytoplasmic domain region. This mutation clearly warranted further study and will be investigated and discussed in more detail in the next chapter. There are a number of other *agrC* cytoplasmic domain region mutations reported in the literature as occurring in clinical isolates which have impaired *agr* functionality (Somerville *et al*, 2002; Traber *et al*, 2008).

While little is known about the specific functions of different regions of the AgrC cytoplasmic domain, other parts of the AgrC protein have been better characterised, particularly the AgrC AIP binding domain. This is predicted to have three surface loops which are important for AIP binding and recognition (Jensen *et al*, 2008). While the ST22 isolates and the *agr* group 3 isolates tested did not have any predicted amino acid substitutions in these loops, TS1 had three; V42G, S44T and S109N, all of which could potentially impair receptor functionality.

While no polymorphisms were found in the *agrD* sequences, some were observed in *agrB* which could potentially effect AgrD processing and therefore AIP production. As TS1 produces both PVL and alpha haemolysin it seems likely that *agr* is functioning and that some AIP is being produced however.

Finally, there were two polymorphisms in *agrA* which were predicted to change the amino acid sequences of the LytR-like DNA binding region, AgrA K136R in TS21 and AgrA D194N in TS1. As there were no other isolates with a similar strain background or identical changes to compare

these two, they were not investigated further, but could conceivably impact on AgrA binding to DNA.

3.3.4 What do the whole genome sequences reveal about the ST22 strains?

3.3.4.1 How do TS13 and TS14 compare with other reported *S. aureus* genomes?

There were several reasons for selecting TS13 and TS14 for whole genome sequencing. The ST22 PVL MSSA strains were the most heavily represented in the strain collection and appeared to be the PVL strain most commonly identified by the clinical laboratory at the time the strains were collected. Furthermore, the genotypic similarity but phenotypic incongruence of TS13 and TS14 presented a unique opportunity to study naturally occurring differences which impacted significantly on exotoxin production.

There are other reports in the literature about PVL producing ST22 strains, predominantly focusing on CA-MRSA strains as opposed to MSSA. A PVL positive ST22 SCC*mec*IV strain which was also resistant to gentamicin and trimethoprim caused an outbreak in a neonatal unit in Australia (Pinto *et al*, 2013). The strain appeared to be highly transmissible and caused several severe infections with 2 fatalities over a 7 month period. In the UK, the *Staphylococcus* Reference Unit reported that CC22 strains, including the HA-MRSA EMRSA15, have caused significant public health problems. They studied PVL positive CA-MRSAs which were identified as belonging to CC22 by PFGE and found that the majority were *spa* type t005, carried SCC*mec*IVc and ΦPVL and were resistant to gentamicin and trimethoprim (Boakes *et al*, 2011b). The authors also observed that EMRSA-15 is epidemiologically distinct from the CC22 PVL positive strains. From comparison with their data it seems that TS13 and TS14 are very closely related to these PVL CA-MRSAs – the ST22 PVL MSSAs probably represent a reservoir of circulating strains that SCC*mec* acquisition events could occur in. Alternatively, loss of *mec* elements has been speculated to occur such that successful circulating CA-MRSAs revert back into MSSAs when selective pressure is lacking. A study in the United States identified CC8 MSSA strains which bore close similarity to USA300, having the same R variant PVL phage and

sequence type (Brown *et al*, 2012). Phages are often acquired, lost and transferred between lineages (McCarthy *et al*, 2012).

When compared with the publicly available genome sequence data by BLAST searching, the reference genome HO 5096 0412 was the closest available match to TS13 and TS14. HO 5096 0412 is representative of EMRSA-15, one of the two predominant HA-MRSA clones established in the UK. In an analysis of the development of EMRSA-15 within the ST22 lineage, Holden *et al* (2013) traced the divergence of the ST22-A cluster of which EMRSA-15 is a member. EMRSA-15 and relatives are genetically distinct from non-ST22-A strains, having acquired SCC*mec*IVh as a defining event for this cluster. In addition, a large proportion of the clade, designated ST22-A2, have a point mutation conferring resistance to fluoroquinolones and most have the *ermC* gene conferring resistance to erythromycin. ST22-A strains carrying the *pvl* genes have not been identified so far, possibly because they already have a phage inserted at the ΦSa2 site which encodes a *Bcg*I-like restriction enzyme.

TS13 and TS14 do not have any of the defining features of the ST22-A group and this is again consistent with the notion that they are non-ST22-A strains, more closely related to the ST22 PVL CA-MRSAs analysed by Boakes *et al* (2011), probably representing the pool from which *mec* acquisition could occur (Figure 3.25).

Figure 3.25 The hypothetical development of PVL positive ST22 MRSA

ST22-MSSA *spa* type t005 strains may have acquired a PVL phage, creating a pool of successful, circulating PVL MSSA strains which subsequently acquired SCC*mec* elements on numerous occasions. Adapted from Boakes *et al* (2011b)

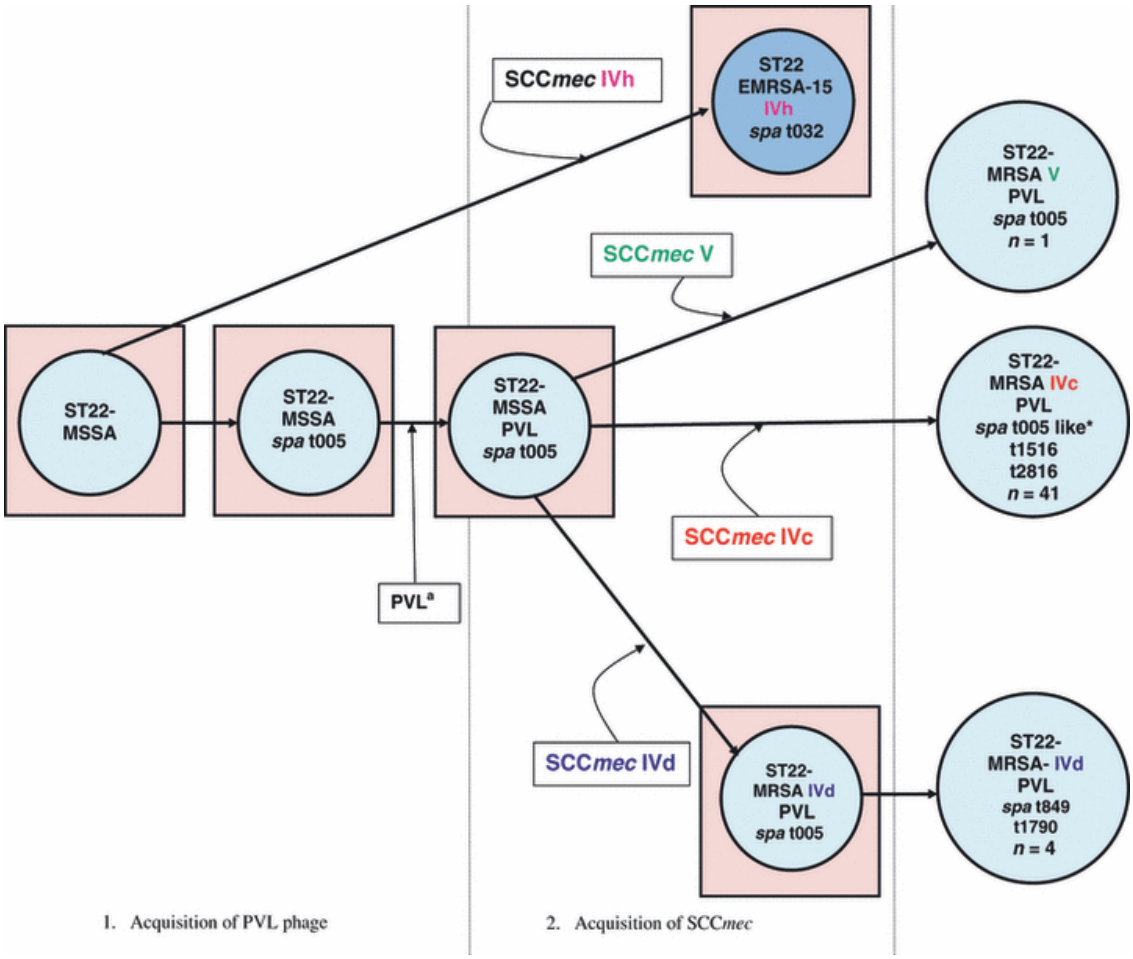

3.3.4.2 What does the sequence analysis reveal about the virulence of TS13 and TS14?

Genome wide comparison of TS13 and TS14 to HO 5096 0412 confirmed a number of virulence factors which were present in all of the strains. The presence of the immune evasion complex (IEC) carried on the phage integrated at ΦSa3 is potentially important. The IEC includes the immunomodulators CHIPS, SCIN and staphylokinase (SAK) which confer the bacteria with a significant advantage in avoiding phagocytosis. CHIPS, the chemotaxis inhibitory protein, interferes with activation of neutrophils by complement signaling while SCIN, the staphylococcal complement inhibitor, prevents the formation of C3b on the bacterial cell surface by blocking C3 convertase (van Wamel *et al*, 2006). SAK is understood to interfere with the innate immune system in various ways to inhibit opsonisation (Rooijakkers *et al*, 2005b).

The combination of several virulence factors that inhibit phagocytosis with the production of PVL is likely to be potent as this would provide synergistic benefit for both evading and destroying neutrophils before they can prevent bacterial invasion.

In addition to these phage-encoded virulence determinants, the expected collection of core genome encoded genes were also present which promote epithelial surface binding and colonization including the fibronectin binding protein A (*fnbpA*), clumping factors A and B (*clfA* and *clfB)* and collagen binding protein (*cna)*.

In terms of exotoxins, TS13 and TS14 were already known to carry two of the enterotoxin genes, *seg* and *sei*, and while beta-haemolysin is inactivated by the presence of the *hlb* converting phage inserted at ΦSa3, genes for alpha, delta and gamma-haemolysin were present.

As expected, TS13 and TS14 did not have an SCC*mec* element which was confirmed by the observation that sequences from these strains did not map to the HO 5096 0412 SCC*mec*IVh sequence. All of the strains did, however, appear to have the Tn554-like transposon which encodes a beta-lactamase and confers resistance to penicillin. The aminoglycoside transferase

and dihydrofolate reductase conferring resistance to gentamicin and trimethoprim respectively were identified through plasmid fragment analysis. Gentamicin resistance is unlikely to be of much benefit in the community as aminoglycoside antibiotics are usually only administered intravenously in hospitals. Trimethoprim resistance may be of greater benefit to the bacteria in colonising certain patient groups as this is a widely used first line to treat uncomplicated urinary tract infections.

The disadvantage in a comparative genome analysis as conducted here instead of a complete *de novo* genome reconstruction is that virulence factors which are encoded by the test strains but not the reference strain may be missed. Analysing the larger unmapped contigs with BLAST searches was carried out to identify any larger mobile genetic elements that may not have been picked up in the direct comparative analysis, but smaller elements such as transposons may not have been identified.

3.3.4.3 Phage identification

Identifying the specific phages carried by TS13 and TS14 was difficult due to the reasons described above – these were the regions of the genomes that differed the most from HO 5096 0412.

Phages in S. *aureus* are tailed, termed *Caudoviridae*, and are generally of the subtype *Siphoviridae*, being about 40 kb in size (Goerke *et al*, 2009). Distinct patterns of phage clustering are seen by sequence type as phage insertion appears to be restricted by lineage. The ordering of genes within the *Siphoviridae* phages are as follows: lysogeny (including integrase), replication, packaging, head, tail and lysis (Deghorain & Van Melderen, 2012). Virulence genes are found at either end of the phage sequence, presumably because these were originally 'picked up' by the phages during integration into other lineages or species and subsequently carried as part of the phage genetic material. Staphylococcal phages are classified according to the integrase genes which also define where they integrate on the staphylococcal chromosome (Xia & Wolz, 2013).

There appear to be two phages in TS13 and TS14, with the PVL and IEC phages integrating at the second and third phage integration site respectively. Nearly all of the known PVL encoding phages integrate at ΦSa2 (Goerke *et al*, 2009). HO 5096 0412 has a different phage at this site which encodes the *Bcg*I-like restriction enzyme but not PVL. PCR based phage typing had indicated that TS13 and TS14 were both carrying ΦPVL, although the sequencing reads did not align consistently with this phage. Based on the unaligned fragment analysis and the comparison of TS mapping to ΦPVL and Φtp310-1, it seems that Φtp310-1 is the closest match. This phage has a type 2 integrase, so would integrate at the ΦSa2 insertion site as expected, and also carries the *pvl* genes (Xia & Wolz, 2013). Without a complete *de novo* strain construction this cannot be conclusively determined.

The beta haemolysin converting phage integrating at the ΦSa3 site, rendering the strains *hlb* negative, appears to be similar to that in HO 5096 0412 as already discussed. *hlb* converting phages occur more commonly in colonising strains, perhaps because of the advantage the IEC confers against the innate immune system (Goerke *et al*, 2009). As already discussed, Φtp310-3 appears to be the best match for the phages present at ΦSa3 in TS13 and TS14, carrying the three genes of the IEC and having a type 3 phage integrase (Xia & Wolz, 2013).

3.3.4.4 Does the whole genome sequencing data explain the phenotypic differences?

One of the principal reasons for analysing the genome sequences of these strains was to determine whether any other explanations could be found for their differing exotoxin production phenotypes.

The survey of staphylococcal regulators which included the Sar family, *rot*, *mgrA*, *saeRS* and *agr* revealed SNPs in *saeS* and *sarU* in addition to the change already identified in *agrC.*

Holden *et al* (2013) produced a comparison of gene polymorphisms which distinguish the ST22-A clade from non-ST22-A strains. The supplementary data for their paper, Table S3, lists the SNPs that differentiate ST22-A from non-ST22-A strains, which should encompass TS13 and TS14. The substitution identified in *saeS* is included in this list, indicating that this SNP likely occurred during the development of the ST22-A lineage and that TS13 and TS14 have the original s*aeS* sequence.

The function of SarU is described by Manna and Cheung (2003) as a SarA homolog which regulates *agr* expression in conjunction with SarT (Manna & Cheung, 2003). A *sarT* mutant showed increased transcription of *sarU* indicating that SarT is likely activating as a transcriptional repressor of *sarU.* A *sarU* mutant showed reduced expression of RNAII and RNAIII.

Both TS13 and TS14 were predicted to have a C102R amino acid substitution in SarU compared to HO 5096 0412. The reference sequence for SarU in GenBank (Accession ID AFD54311.1) however, also has an arginine at residue 102 so it appears as though this change is not unique to TS13 and TS14 and may reveal a mutation from the wild type acquired by HO 5096 0412.

TS13 also has an aspartate to tyrosine substitution D134Y in SarU. As SarU is known to be a positive regulator of *agr*, a mutation in SarU could conceivably result in reduced *agr* expression and the resulting phenotype associated with TS13 as compared to TS14. A change of aspartate

to tyrosine could potentially have a functional impact on the protein, substituting a carboxyl group for a phenol group. SarU binding was not observed in significant quantities to the *agr* promoter during the promoter pulldown experiments so it is not possible to conclude whether SarU had failed to bind in TS13 as compared to TS14. Transcriptional profiling of *sarU* by RT-PCR may provide more information, however if this mutation impacted the translation or subsequent functioning of SarU rather than transcription, no difference would be observed.

Based on the whole genome sequencing data, it appeared that the AgrC N267I and SarU D134Y substitutions were the best candidates for explaining the phenotypic differences observed in TS13 and TS14. This observation mandated further exploration of the functional impact of AgrC cytoplasmic domain mutations, such as that identified in TS13, including reconstruction of this and other mutations in a different *S. aureus* strain background.

3.3.5 Key Findings

1. In a collection of PVL positive clinical isolates from Nottingham, large variations in PVL production were noted.
2. MLST 22 PVL positive MSSA isolates were the largest subgroup and all showed high levels of toxin production except for one isolate, TS13.
3. PVL production could be stimulated by exogenous AIP or repressed by an AgrC competitive antagonist (ala^{5})AIP-1 if these were added early enough during growth.
4. Promoter pull down assays demonstrated (i) the binding of Sar family proteins to the *agr* and *pvl* promoters, particularly SarA, SarR and SarS but also MgrA and Rot and (ii) the lack of AgrA-binding directly to the *pvl* promoter.
5. Analysis of promoter and *agr* locus sequences did not give a clear indication as to why differences in PVL production occurred between strains except for the presence of a single nucleotide polymorphism in the *agrC* gene of the low PVL producer TS13.
6. Expression of *agr* and *pvl* is lower in TS13 than the high PVL producer TS14 when measured by RT-PCR.
7. Whole genome sequence analysis of TS13 and TS14 revealed they both carry the immune evasion complex in addition to the PVL genes and are very similar genetically.
8. The predicted amino acid substitutions in TS13 AgrC N267I and SarU D134Y are the best candidates for explaining the differences in exotoxin expression between TS13 and TS14.

4 Agr kinetics and *agrC* cytoplasmic domain polymorphisms

4.1 Introduction

4.1.1 *agr* polymorphisms in clinical strains

There are numerous reports of *agr* dysfunction in clinical *S. aureus* strains, with mutations identified throughout the locus from the promoter regions, as previously discussed, to those impacting on AIP processing (*agrB*), AIP recognition (*agrC*) and signal transduction (*agrC* and *agrA*) (Somerville *et al*, 2002; Traber *et al*, 2008; Villaruz *et al*, 2009). These mutations are usually described as resulting in an *agr* null phenotype with no observable haemolytic activity, and involve amino acid substitutions, deletions resulting in frame shifts or premature stop codons.

The *agrC* SNPs investigated in this chapter were all found in the cytoplasmic domain region of *agrC.* The receptor domain has been reasonably well characterized (although the three dimensional structure has not been elucidated), with transmembrane domains and loops predicted, and the consequences of substituting specific amino acids analysed (Jensen *et al*, 2008). By contrast, the cytoplasmic domain has not been studied in detail. The function of several key residues was investigated by George Cisar *et al* (2009) by using a dual plasmid expression system to analyse AgrC dimerisation. AgrC H239 is phosphorylated following dimerisation by a kinase domain on the dimer counterpart, in which G394 and G396 appear to be important. Replacing both the glycines in the kinase domain with alanine inactivated AgrC.

The impact of several *agrC* SNPs, including that found in TS13, was investigated here through site specific mutagenesis of an *agr* group 1 bioreporter and the implications for our understanding of *agrC* structure discussed.

4.1.2 Analysis of *agr* kinetics

The data for exogenous AIP activation of exotoxin production presented in the previous chapter indicate that timing of AIP production is important. Exotoxin production in *S. aureus* is already known to be growth phase dependent, with late exponential phase representing a key population density for exotoxin expression (Tegmark *et al*, 2000).

In light of these findings, clinical isolates were analysed for AIP production over the growth curve, comparing those with and without *agrC* cytoplasmic mutations. This was intended to provide further evidence as to the importance of a window period during exponential phase in which *agr* must be activated for high level exotoxin production to occur.

Aside from *agr* sequence variation, the presence of specific *SCCmec* elements has also been shown to determine *agr* expression and hence exotoxin production (Rudkin *et al*, 2012). The impact on *agr* kinetics of deleting the *mecA* gene from an HA-MRSA strain was investigated to determine whether changes in *agr* kinetics could be a universal marker for altered *agr* function.

4.1.3 Chapter Overview

1. Selected clinical isolates were assayed for AIP production over the growth curve to identify any differences in Agr kinetics between strains with varying phenotypes.
2. Deleting *mecA* from a HA-MRSA strain was demonstrated to affect *agr* kinetics.
3. The *agrC* polymorphism in TS13 and several other *agrC* polymorphisms associated with large reductions in exotoxin expression were introduced into a bio reporter to assess the impact on AgrC function.
4. The N267I amino acid substitution in TS13 was introduced into a neutral background with a complete auto induction circuit and demonstrated to delay *agr*P3 activation.

4.2 Results

4.2.1 Kinetics of AIP production

4.2.1.1 AIP production as a function of growth in TS13 and TS14

Having identified the *agrC* mutation in TS13, a series of experiments were conducted to determine whether it impacts on the onset of AIP-1 production in TS13 compared with TS14. This is particularly relevant in the context of the earlier series of western blots demonstrating that exogenous AIP-1 must be added to TS13 before late-exponential growth (∼OD 1 in CYGP medium) otherwise only low level toxin production occurs. The hypothesis was that accumulation of AIP-1 in TS13 had not reached a sufficient concentration by this key point.

Overnight cultures of TS13 and TS14 were inoculated at a final concentration of 1:1000 in CYGP and broth and grown for 6 h until exponential phase. After centrifugation, supernatants from these cultures were assayed for AIP-1 using the group 1 *agr*P3-*lux* bioreporter ROJ143 which has the *agrP2C1A* genes on a plasmid and so does not produce AIP-1 but will respond to exogenous AIP, producing light (Jensen *et al*, 2008). The assay was performed as described in section 2.8.3. Light output was measured on a luminometer and expressed as relative light units divided by the bioreporter optical density (RLU/OD).

The TS14 supernatant collected at 6 h activated the bioreporter; giving a peak RLU/OD of 294.7 compared to the background luminescence peak of 38.3 if no supernatant was added. The 6 h TS13 supernatant did not activate the reporter however, with a peak RLU/OD of 33.0, similar to the background luminescence. The lower limit of detection of AIP-1 in supernatant, which is diluted 1:10, is 10 nM based on a minimum concentration of AIP-1 required to activate the reporter of 1 nM. The TS13 AIP-1 concentration at 6 h must therefore have been less than 10 nM.

To give a clearer picture of the differences in the onset and accumulation of AIP, this experiment was repeated, using BHI as bacterial growth is faster and higher population densities are reached, and using a higher starting inoculum of 1:500. Cell pellets from overnight cultures were washed 3 times in BHI prior to inoculation to ensure there was no carryover of residual AIP. Cultures were set up in triplicate. After a 2 h incubation, 500 µl volumes of culture were removed every 30 min until stationary phase and the supernatant assayed for AIP-1. Compared to CYGP where AIP-1 was previously undetectable in TS13 supernatants at 6 h (~OD 2), in BHI AIP-1 was detected in TS13 from 4 h (OD 5.0) onwards, reflecting the faster growth and higher cell densities.

To quantify AIP-1 production over time, the response of ROJ143 to serial dilutions of a known concentration of AIP-1 was also measured. RLU/OD values for known concentrations of AIP-1 were compared with RLU/OD values for the test supernatants and the original AIP-1 concentrations of the cultures calculated (Figure 4.1).

AIP-1 was undetectable at 3 h (OD 1.1) in both TS13 and TS14, however at 4 h (OD 5.0), TS14 AIP-1 concentration was 125 nM (+/- 52.3) compared to 12.8 nM (+/- 3.5) for TS13. An hour later (TS13 OD 8.0, TS14 OD 7.0), TS13 AIP-1 concentration had increased to 246 nM (+/- 50.4) but TS14 AIP-1 concentration had already peaked at 941 nM (+/- 127). In addition to the delay observed in AIP-1 production by TS13, final AIP-1 concentration in stationary phase (t = 6 h, TS13 OD 11.0, TS14 OD 10.5) was approximately half in TS13 compared with TS14 at 546 nM (+/- 32.3) compared with 1050 nM (+/- 40.2) ($p<0.0001$).

From these data it seems that AIP-1 production by TS13 is delayed by about 1 h under these growth conditions and that the final AIP-1 concentration achieved in stationary phase is also lower. This raises the hypothesis that the mutation in AgrC could potentially impact on the efficiency of autophosphorylation and subsequent phosphotransfer to AgrA in response to AIP-1 receptor activation. Even with the *agr* autoinduction loop still functioning, the reduction in

efficiency could be sufficient to delay the time taken to drive up AIP-1 production resulting in lower overall levels of signal molecule and hence toxins.

A delay in AIP-1 reaching concentrations of over 100 nM by only 1-2 h could be important because the critical period in exponential phase when RNAIII levels determine the translation of other staphylococcal regulators, particularly Rot, would be missed (Geisinger *et al*, 2006). Although TS13 *agr* is clearly active by late exponential and early stationary phase, it is possible that by this point many of the toxin repressors such as SarS, Rot and SarR have already been produced in sufficient quantities to prevent high level toxin production from occurring.

Figure 4.1 AIP-1 production by TS13 and TS14 as a function of growth

Comparison of AIP-1 production by TS13 and TS14 throughout growth. TS13 unlike TS14 has an AgrC N267I amino acid substitution. AIP-1 concentrations (solid lines) were determined by assaying culture supernatants with a bio-reporter. Growth curves (dotted lines) show the transition from late exponential to stationary phase at about 4 h (OD 5.0), at which point AIP-1 was detectable in TS14 supernatants. The AIP-1 concentration in the TS14 supernatants is almost double that of TS13 at stationary phase (TS13 OD 11.0, TS14 OD 10.5). Error bars indicate standard deviations based on testing triplicate culture supernatants.

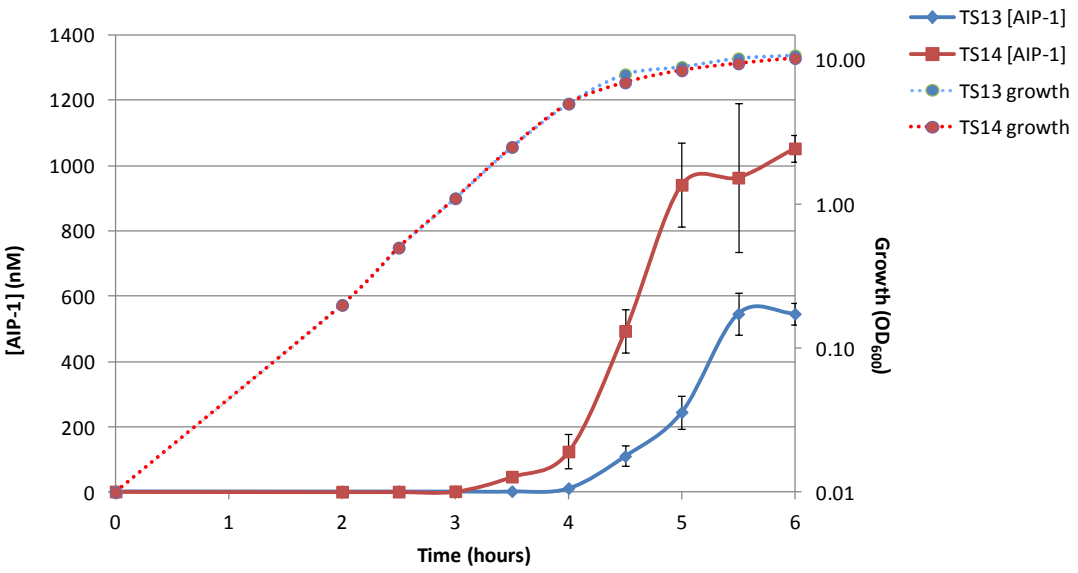

4.2.1.2 AIP production by other clinical isolates with AgrC cytoplasmic mutations

Additional, naturally occurring AgrC cytoplasmic domain mutations were identified by Dr Ruth Massey at the University of Bath in a large group of genetically related PVL negative ST239 clinical isolates from Turkey. These strains were being evaluated as as part of a larger study to test the feasibility of using genome wide association study to predict staphylococcal virulence. Hence, they presented an opportunity to broaden the investigation of *agrC* cytoplasmic mutations.

4.2.1.2.1 AIP production by strains with I311T and A343T AgrC amino acid substitutions

Compared with the NCTC8325 group 1 *agrC* sequence, some of the ST239 strains had a T to C base change resulting in an I311T amino acid substitution in AgrC. Many of these strains were found to be highly lytic in their T-cell assay (Ruth Massey, personal communication), although a subgroup of strains with reduced lysis was also found to have a G to A base change resulting in an A343T substitution in AgrC. The T-cell assay involves incubating T cells with bacterial supernatant for 10 minutes and measuring cell death (Collins *et al*, 2010). It therefore represents the overall activity of several cytolytic exotoxins.

AIP-1 production by two of these strains, IU12, which has the I311T change, and HU24 which has both I311T and A343T, were compared by repeating the same experiment performed with TS13 and TS14 (Figure 4.2). AIP-1 production was delayed in both of these strains with AIP barely detectable by 8 h (OD 9.0) in HU24 at 52.1 nM (+/- 7.8) but with a significantly higher concentrations in IU12 (OD 8.0) supernatant at 463 nM (+/- 92.3) ($p<0.01$).

The delay observed in both of these strains may be a factor of the strain background, or could result from the I311T change. The very low AIP-1 production by HU24 would be in keeping with

a greater functional impact of the double substitution I311T-A343T than that observed in TS13 with N267I.

Figure 4.2 AIP-1 production by HU24 and IU12 as a function of growth

HU24 and IU12 both have an AgrC I311T amino acid substitution, while HU24 also has an additional AgrC A343T substitution. AIP-1 concentrations (solid lines) were determined by assaying culture supernatants with a bioreporter. Growth curves (dotted lines) show the transition from late exponential to stationary phase at about 5 h. AIP-1 was first detectable in IU12 supernatants at 6 h (OD 5.5) and concentrations increased markedly after that to ~10 fold greater than HU24 at 8 h (IU12 OD 8.0, HU24 OD 9.0). Error bars indicate standard deviations based on testing culture supernatants in triplicate.

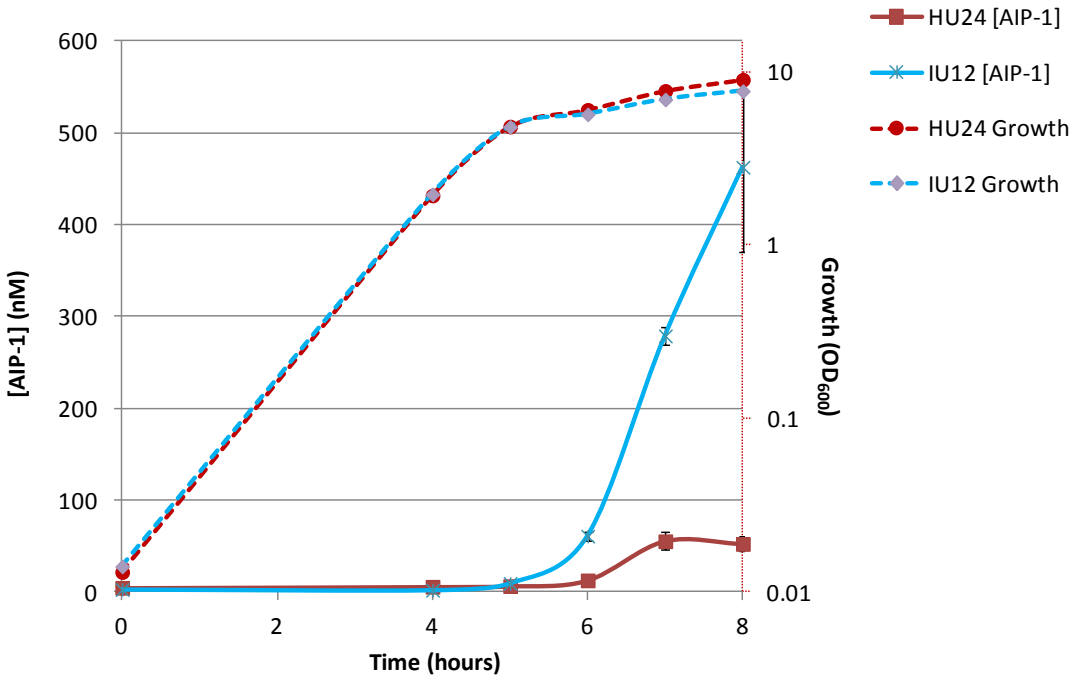

4.2.1.2.2 AIP production by strains differing by a T247I AgrC amino acid substitution

Among the ST239 strains in the Bath University collection were two very closely related strains ICP5014 and ICP5062 which differed across their genomes by only 111 nucleotides, one of which conferred a T247I AgrC amino acid substitution. When tested in the T-cell assay (Ruth Massey, personal communication), the ICP5062 strain with the T247I change was less cytolytic with only 4 % T cell death compared to 85 % for ICP5014.

When AIP-1 concentrations were assayed over the growth curve as above, ICP5014 produced moderate amounts of AIP-1 compared with the other strains tested previously, with AIP-1 detectable by 4 h (OD 3.5) at 46.8 nM (+/- 15.1), rising to a concentration of 607 nM (+/- 115) by 7 h (OD 6.5) (Figure 4.3). ICP5062 on the other hand, barely produced any AIP-1 over the time frame tested, with a significantly lower AIP-1 concentration at 7 h (OD 7.0) of 53.4 nM (+/- 6.0) ($p<0.01$).

These findings are consistent with T247I having a significant impact on *agr* function, probably accounting for the large reduction in T cell cytolysis observed for ICP5062 as compared with ICP5014.

Figure 4.3 AIP-1 productionby ICP5014 and ICP5062 as a function of growth

ICP5062 but not ICP5014 has an AgrC T247I amino acid substitution. AIP-1 concentrations (solid lines) were determined by assaying culture supernatants with a bioreporter. Growth curves (dotted lines) show the transition from late exponential to stationary phase at about 4 h. AIP-1 was first detectable in ICP5014 supernatants at 4 h (OD 3.5) with concentrations peaking at around 600 nM by 7 h (OD 6.5), more than 10-fold higher than ICP5062 AIP-1 concentrations at the same time point (7h, OD 7.0). Error bars indicate standard deviations based on testing triplicate culture supernatants.

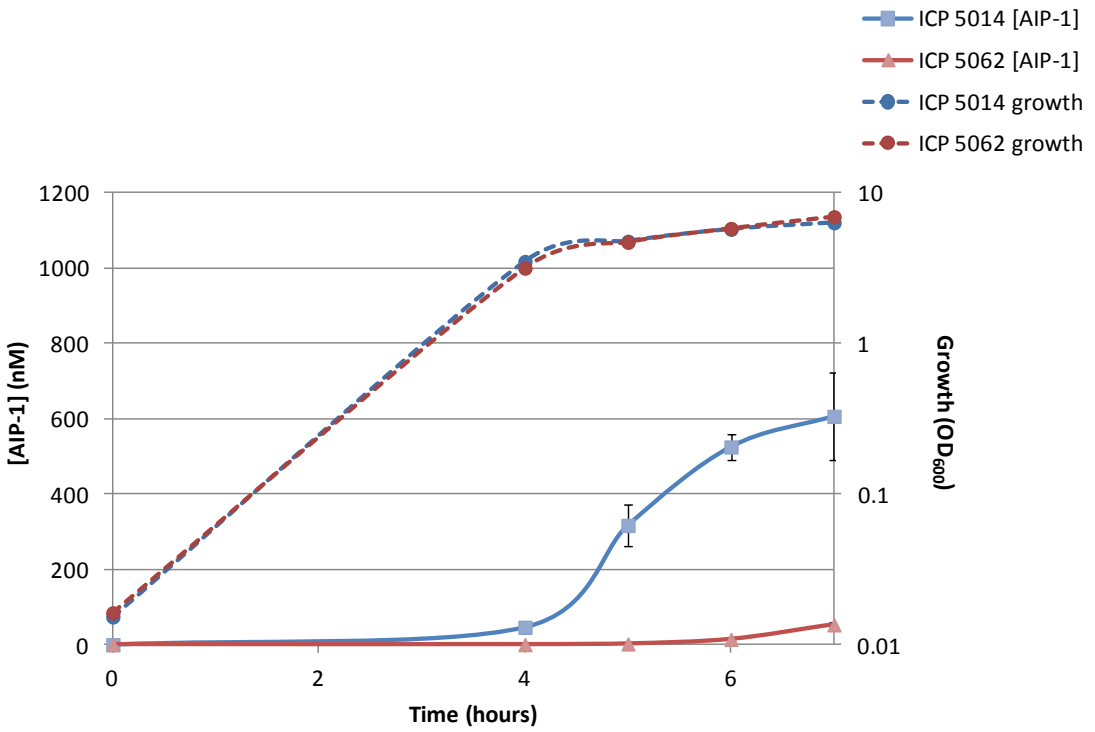

4.2.1.3 Impact of *mecA* on AIP production

Studying AIP-1 production by strains with *agrC* cytoplasmic domain SNPs demonstrated delays in AIP-1 production. This raised the question as to whether differences in *agr* kinetics, the timing and concentration of AIP-1 produced, may be a broader marker of differential in *agr* activity.

Rudkin *et al* (2012) had previously shown that deleting the *mecA* gene enhanced the T cell cytolytic activity of a HA-MRSA strain BH1CC by upregulating *agr* expression, although the precise mechanism for this effect was not fully understood. By externally treating the cell wall of whole BH1CC cells with lysostaphin, a similar increase in cytolysis was observed and therefore hypothesized that the modified cell wall present in HA-MRSA strains could impact on the capacity for AIP to access and bind to the cell membrane.

The HA-MRSA BH1CC used in this study and isogenic Δ*mecA* mutant were tested for AIP-1 production during growth, to see if the differences in *agr* expression previously identified in terms of RNAIII expression and cytolysis were matched by changes in *agr* kinetics. BH1CC Δ*mecA* produced AIP-1 earlier than BH1CC (4.5 h, OD 4.5), resulting in a higher concentration by stationary phase (6h, OD 7.0) of 373 nM (+/- 26.5) compared with BH1CC (6h, OD 7.5) which had a concentration of 144 nM (+/- 39.6) ($p<0.01$) (Figure 4.4).

This finding is consistent with the enhanced *agr* expression and T-cell lysis observed by Rudkin *et al* (2012) following the deletion of the *mecA* gene. Whatever the mechanism by which the activity of MecA is interfering with *agr* expression it would appear that AIP-1 production is consequently delayed and reduced.

Figure 4.4 AIP-1 production by BH1CC and BH1CC Δ*mecA* as a function of growth

AIP-1 concentrations (solid lines) were determined by assaying culture supernatants with a bioreporter. Growth curves (dotted lines) show the transition from late exponential to stationary phase at about 4 h. AIP-1 was first detectable in BH1CC Δ*mecA* supernatants at 4.5 h (OD 4.5) with concentrations peaking at ~375 nM by 6 h (OD 7.0), more than double those found in BH1CC at the same time point (6h, OD 7.5). Error bars indicate standard deviations based on testing triplicate culture supernatants.

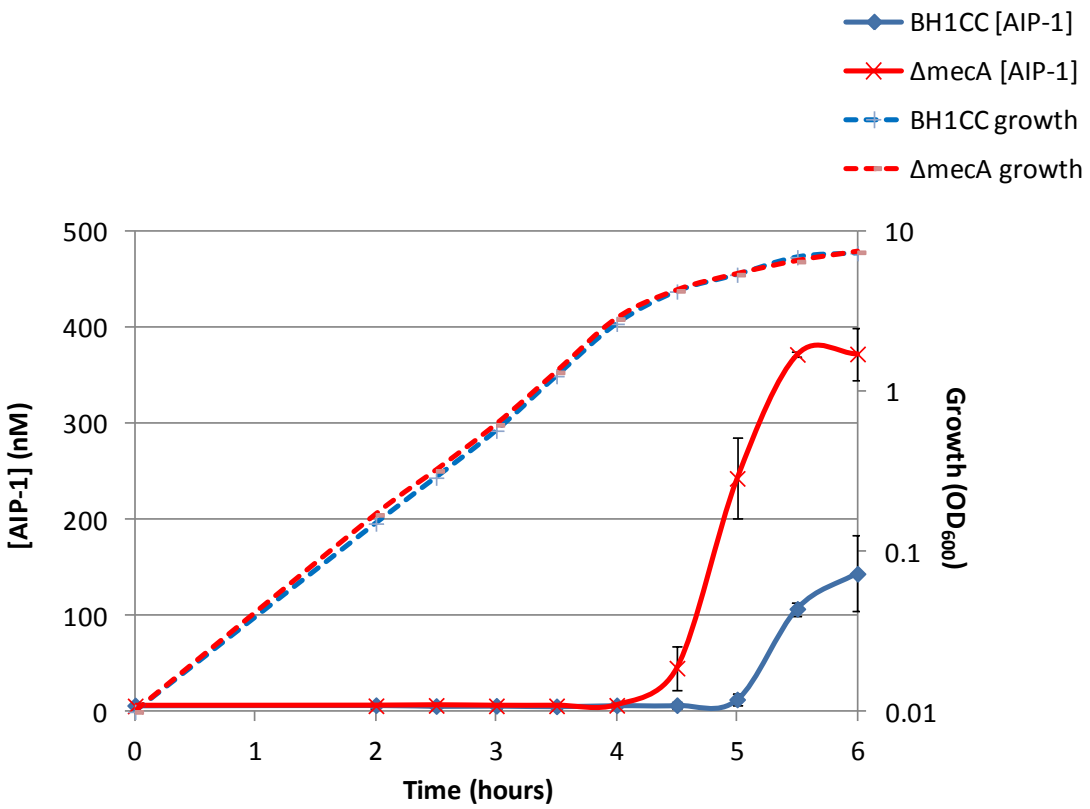

Table 4.1 Kinetics of AIP production by clinical strains

Summary of AIP production profiles of paired clinical strains analysed throughout growth. Strains are shown with corresponding AgrC mutations in brackets. The timing when AIP was first detected is indicated with the mean final AIP concentrations shown in nM (+/- standard deviation). Growth rate (μ) was calculated as ln2/doubling time (h) during exponential phase.

Strain (AgrC substitution)	**Peak OD**	**Growth rate (h^{-1})**	**Time of AIP induction (h)**	**Final AIP concentration (nM)**
TS14	10.5	1.54	3.5	1050 (+/- 40.2)
TS13 (N267I)	11.0	1.54	4.5	564 (+/- 32.3)
IU12 (I311T)	8.0	1.24	6.0	463 (+/- 92.3)
HU24 (I311T/A343T)	9.0	1.25	7.0	52.1 (+/- 7.8)
ICP5014	6.5	1.36	4.0	607 (+/- 115)
ICP5062 (T247I)	7.0	1.32	7.0	53.4 (+/- 6.0)
BH1CC	7.5	1.48	5.5	144 (+/- 39.6)
BH1CC Δ*mecA*	7.0	1.45	4.5	373 (+/- 26.5)

4.2.2 Analysis of functional impact of AgrC mutations

4.2.2.1 Site directed mutagenesis of the Agr group 1 bioreporter

While it was clear that the clinical strains tested with AgrC cytoplasmic mutations showed differences in the AIP production profiles, it was not possible to be certain whether the AgrC substitutions were responsible, wholly or partly, for the observed phenotype. The presence of an autoinduction circuit could also mask the impact of the mutations, or conversely may amplify the effect of small reductions in AgrC sensitivity to AIP and signal transduction efficiency.

To attempt to elucidate more precisely the functional impact of the AgrC mutations identified so far, site directed mutagenesis was performed on the plasmid, encoding *agrP2CA,* carried by the group 1 *agr*P3-*lux* bioreporter (Jensen *et al*, 2008). This bioreporter is responsive to AIP-1 but does not produce AIP, enabling reductions in signal response to be quantified directly. Phosphorylated primers containing the required base substitutions (Table 2.4) were used to amplify the *agrP2CA* plasmid before transformation back into the ROJ48 reporter strain which has an *agr*P3-lux fusion in place of the *agr* locus (section 2.8.2).

The mutated reporters were incubated with serial dilutions of AIP-1 and bioluminescence values used to generate EC_{50} values which could be compared with the wild type group 1 reporter.

4.2.2.2 Functional impact of AgrC mutations found in TS13 and TS14

When compared to *S. aureus* NCTC8325, TS13 and TS14 were both found to have a Y251F AgrC substitution, with only TS13 harbouring the N267I change.

To determine whether either or both of these substitutions would impact on AgrC function, three reporters were made; one with AgrC-N267I only, one with AgrC-Y251F and one with both AgrC-N267I and AgrC-Y251F.

The AgrC-Y251F mutation, when introduced into ROJ48, resulted in little difference compared with the control with EC_{50}s of 2.8 nM (+/- 1.2 nM) and 3.4 nM (+/- 0.6 nM) ($p>0.05$) respectively (Figure 4.5). The AgrC-N267I mutation however exhibited a significant, ~3-fold reduction in sensitivity to AIP-1 with an EC_{50} value of 9.6 nM (+/- 1.6 nM) ($p<0.01$) (Figure 4.6A). Although the AgrC-Y251F-N267I reporter also had reduced sensitivity with an EC_{50} of 9.3 nM (+/- 1.8 nM) ($p<0.01$), this did not differ significantly from the EC_{50} for AgrC-N267I ($p>0.05$) (Figure 4.6B).

In summary, the AgrC-N267I appears sufficient to cause an approximately three-fold reduction in reporter sensitivity, while AgrC-Y251F had no effect.

Figure 4.5 Functional impact of a Y251F substitution on AgrC functionality

Sigmoidal dose response curves demonstrating the sensitivity to AIP-1 of the *agr* group 1 AgrC bioreporter and AgrC1 Y251F mutant reporter. The response to serial dilutions of AIP-1 was measured as RLU divided by bioreporter OD. To account for background luminescence, and variations in the maximum light output between assays and bioreporters, the raw data (A) were also normalized (B). This was achieved by subtracting background luminescence and adjusting values so that the peak of the sigmoidal dose response curve was 100. The difference between reporter sensitivity for AgrC1 and AgrC1 Y251F is not significant. Graphs represent one assay. EC_{50} values were calculated from triplicate assays +/- standard deviation.

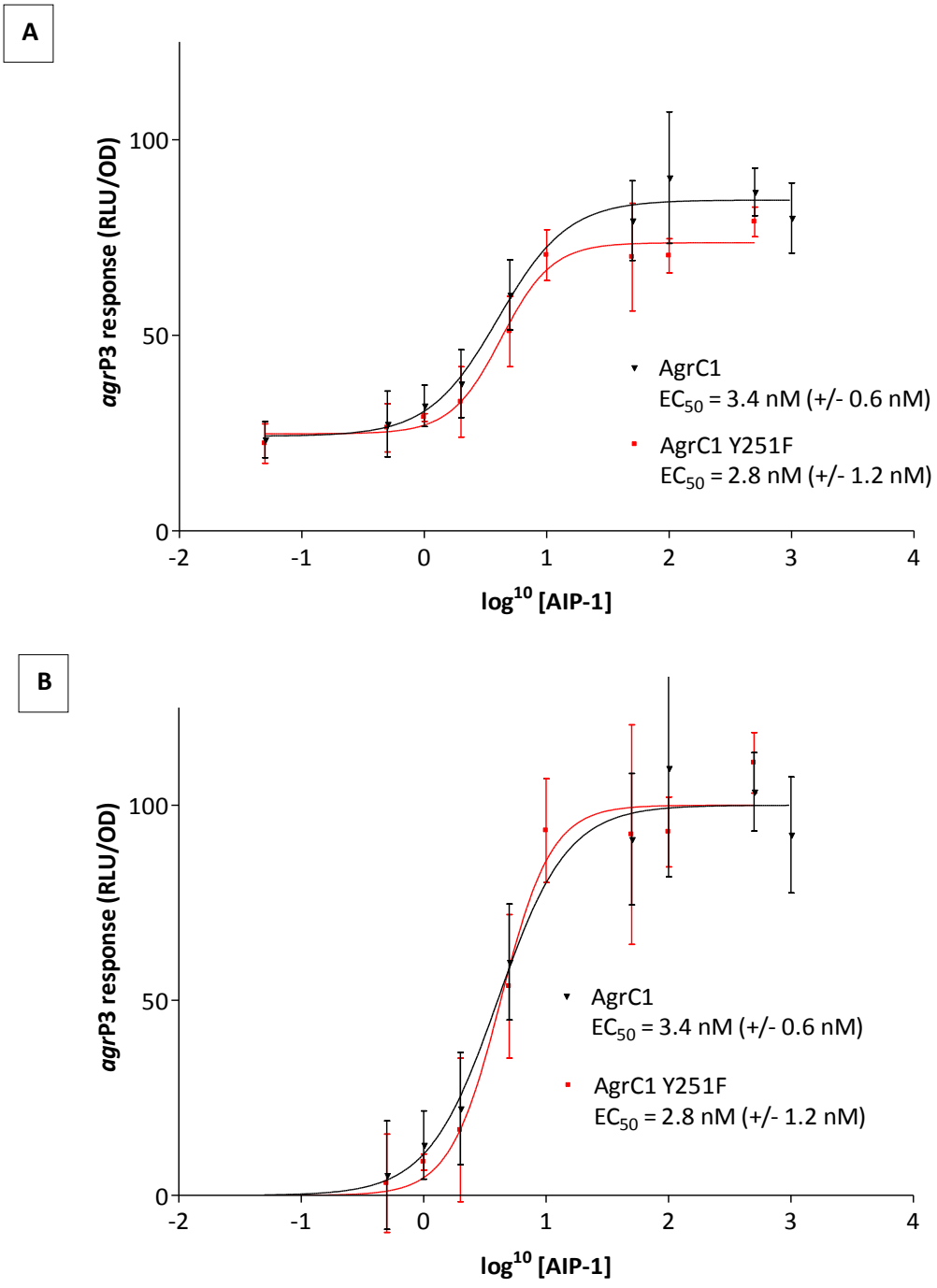

Figure 4.6 Functional impact of N267I and Y251F-N267I substitutions on AgrC activity

The response to serial dilutions of AIP-1 was measured as RLU divided by bio-reporter OD. Data were normalized as described in Figure 4.5. The difference between reporter sensitivity for AgrC1 and AgrC1 N267I was significant ($p<0.01$) (A) but not that between AgrC1 N267I and AgrC1 N267I-Y251F was not (B). Graphs represent one assay. EC_{50} values were calculated from triplicate assays +/- standard deviation.

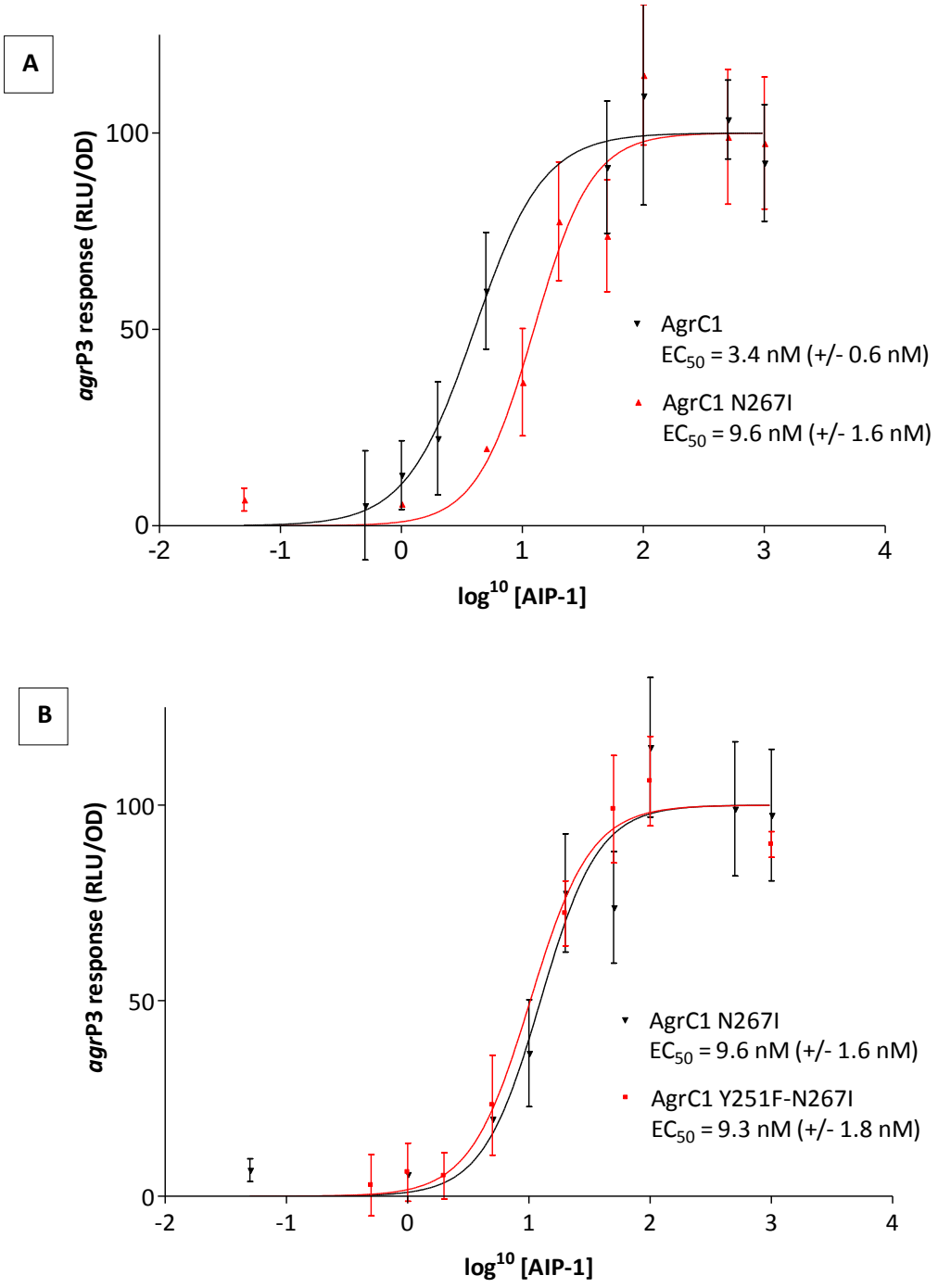

4.2.2.3 Functional impact of AgrC mutations found in the ST239 lineage strains

As described in Section 4.2.1.2, a study of a collection of Turkish ST239 clinical isolates at Bath University identified a group of strains with an AgrC I311T substitution, an example being IU12, with a subgroup of these, like HU24, also having an AgrC A343T substitution. Three different reporters were made by site directed mutagenesis, introducing each mutation individually and in combination.

The AgrC-A343T substitution in ROJ48 surprisingly was as sensitive as the *agr* group 1 control with an EC_{50} of 2.8 nM (+/- 0.8 nM) ($p>0.05$) (Figure 4.7A). Compared with an EC_{50} value of 3.4 nM (+/- 0.6 nM) for the control reporter, the AgrC-I311T substitution resulted in an ~6-fold reduction in sensitivity to AIP-1 with an EC_{50} value of 20.9 nM (+/- 0.6 nM) ($p<0.01$) (Figure 4.7B).

Testing the combined AgrC-I311T-A343T mutant, however, revealed an even greater effect than I311T alone with an EC_{50} of 38.1 nM (+/- 1.7 nM) ($p<0.01$) (Figure 4.7B), giving a greater than ten-fold reduction in reporter sensitivity as compared with the control.

The observations show that not only could the amino acid residues modified give cumulative effects, , but that certain combinations of mutation might be required in order to confer any functional impact at all. This may suggest that that these two residues are in close proximity in the folded protein, perhaps on different strands of a loop structure (or on two different but spatially close loops).

AgrC T247I was identified in ICP5062 as described in Section 4.2.1.2. This substitution resulted in an EC_{50} value of 22.9 nM (+/- 2.6 nM) (Figure 4.9), also significantly different to the AgrC group 1 control reporter ($p<0.01$).

Figure 4.7 Functional impact of C I311T and A343T substitutions on AgrC functionality

The response to serial dilutions of AIP-1 was measured as RLU divided by bio-reporter OD. Data were normalized as described in Figure 4.5. The difference between reporter sensitivity for AgrC1 and AgrC1 A343T was not significant ($p>0.05$) (A). AgrC1 I311T had reduced sensitivity compared to AgrC1 ($p<0.01$) but greater sensitivity than AgrC1 I311T-A343T ($p<0.01$) (B). Graphs represent one assay. EC_{50} values were calculated from triplicate assays +/- standard deviation.

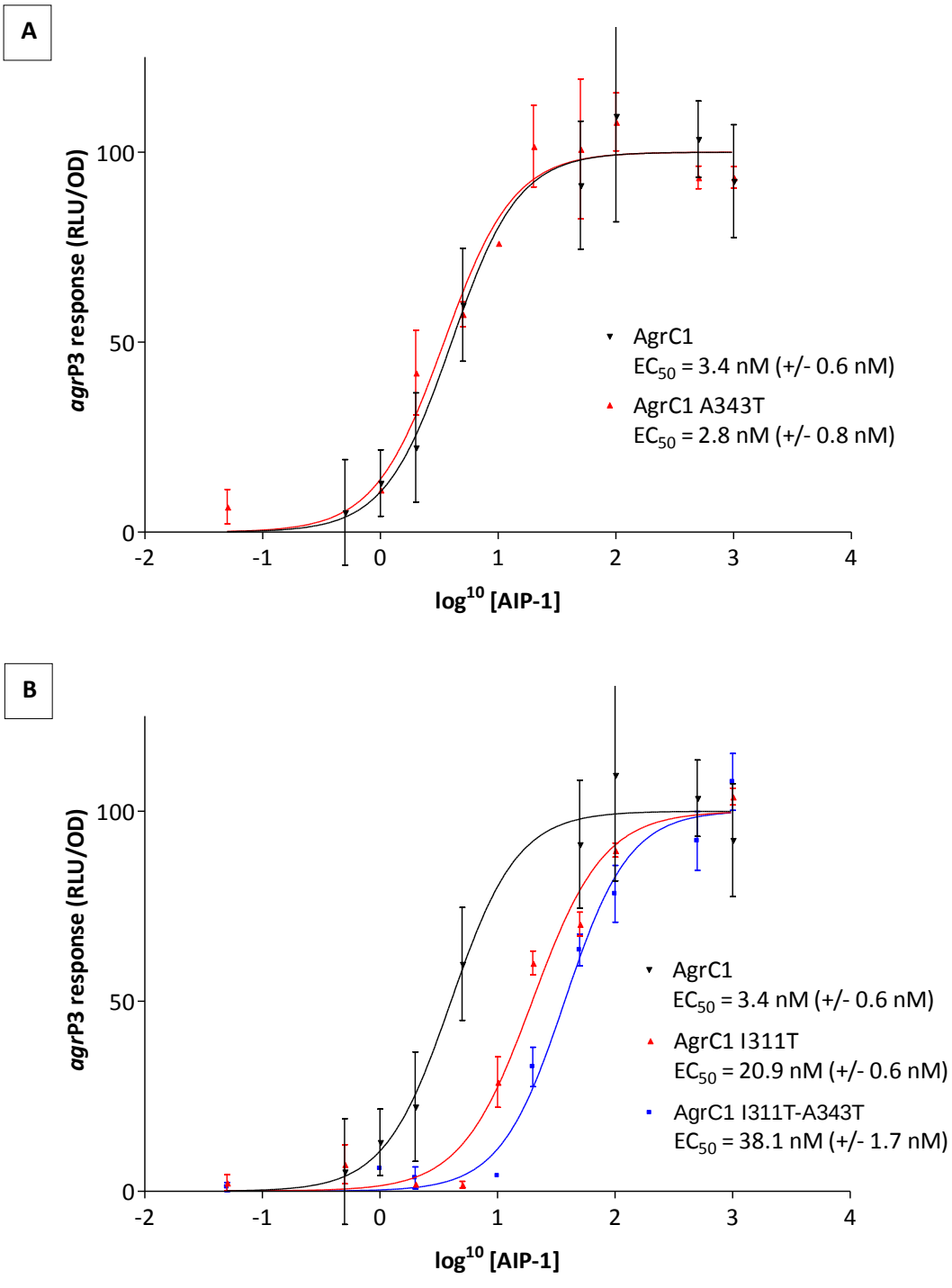

Figure 4.8 Functional impact of a T247I substitution on AgrC functionality

The response to serial dilutions of AIP-1 was measured as RLU divided by bio-reporter OD. Data were normalized as described in Figure 4.5. The difference between reporter sensitivity for AgrC1 and AgrC1 T247I was significant ($p<0.01$). Graphs represent one assay. EC_{50} values were calculated from triplicate assays +/- standard deviation.

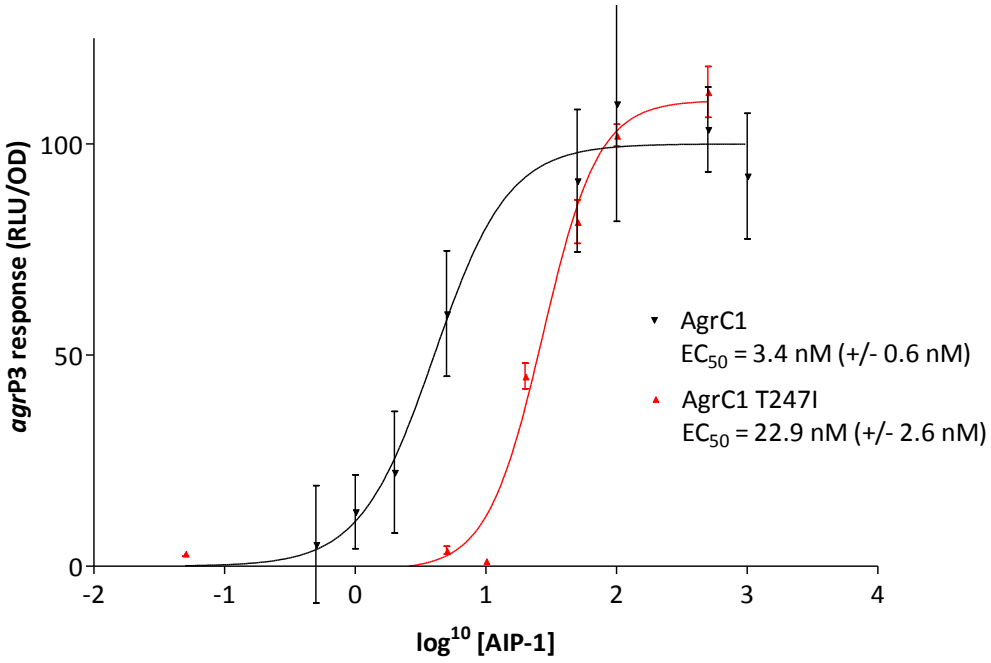

4.2.2.4 Functional impact of other selected AgrC mutations

There are a number of other reports in the literature of cytoplasmic AgrC mutations occurring in clinical strains which show altered to *agr* functionality. Changes reported included L245S and T399P (Traber *et al*, 2008), F264A (Shopsin *et al*, 2008) and G394A (Somerville *et al*, 2002). Other reported mutations resulted in either frame shifts or premature stop codons.

As L245 and F264 are close to N267, two different AgrC mutants were made for these residues, replacing them both with alanine. Each of these substitutions had a significant impact on reporter sensitivity (Figure 4.9) with EC_{50} values of 8.0 nM (+/- 2.1 nM) for L245A ($p<0.05$) and 8.3 nM (+/- 1.3 nM) for F264A ($p<0.01$) respectively.

An N308S substitution had been identified in TS1, close to the I311T substitution already tested. An AgrC-N308A reporter was made and tested to see if the asparagine was important for function but was found to make no difference to reporter sensitivity, resulting in an EC_{50} value of 2.7 nM (+/- 0.9 nM) ($p<0.05$) (Figure 4.10).

A summary of all of the EC_{50} values for the AgrC cytoplasmic mutations is shown in Table 4.2.

Figure 4.9 Functional impact of L245A and F264A substitutions on AgrC functionality

The response to serial dilutions of AIP-1 was measured as RLU divided by bio-reporter OD. Data were normalized as described in Figure 4.5. The difference between reporter sensitivity for AgrC1 and AgrC1 L245A (A) was significant ($p<0.05$) as was the difference between AgrC1 and AgrC1 F264A (B) ($p<0.01$). Graphs represent one assay. EC_{50} values were calculated from triplicate assays +/- standard deviation.

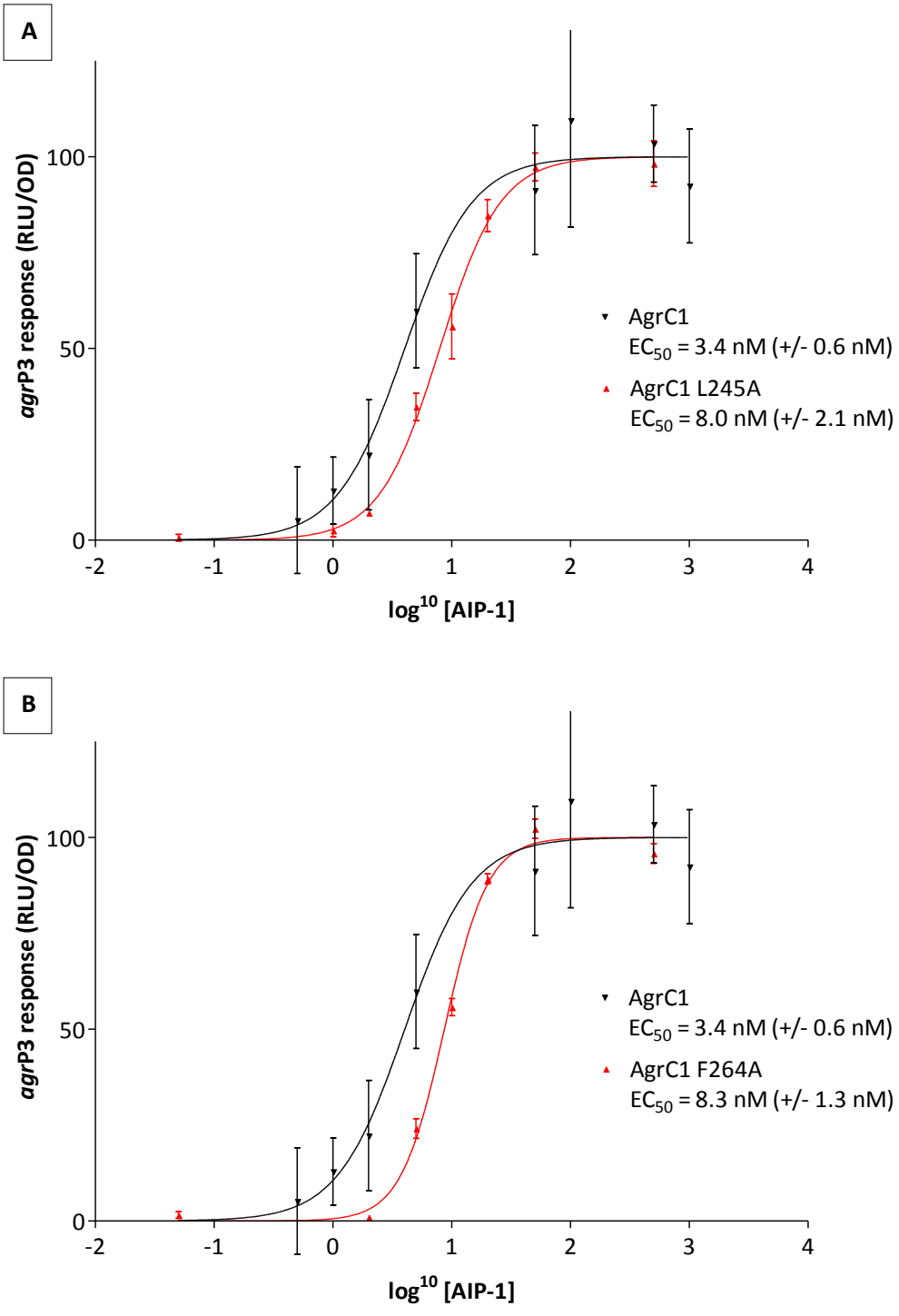

Figure 4.10 Functional impact of N308A substitutions on AgrC functionality

The response to serial dilutions of AIP-1 was measured as RLU divided by bioreporter OD. Data were normalized as described in Figure 4.5. The difference between reporter sensitivity for AgrC1 and AgrC1 N308A was not significant ($p>0.05$). Graphs represent one assay. EC_{50} values were calculated from triplicate assays +/- standard deviation.

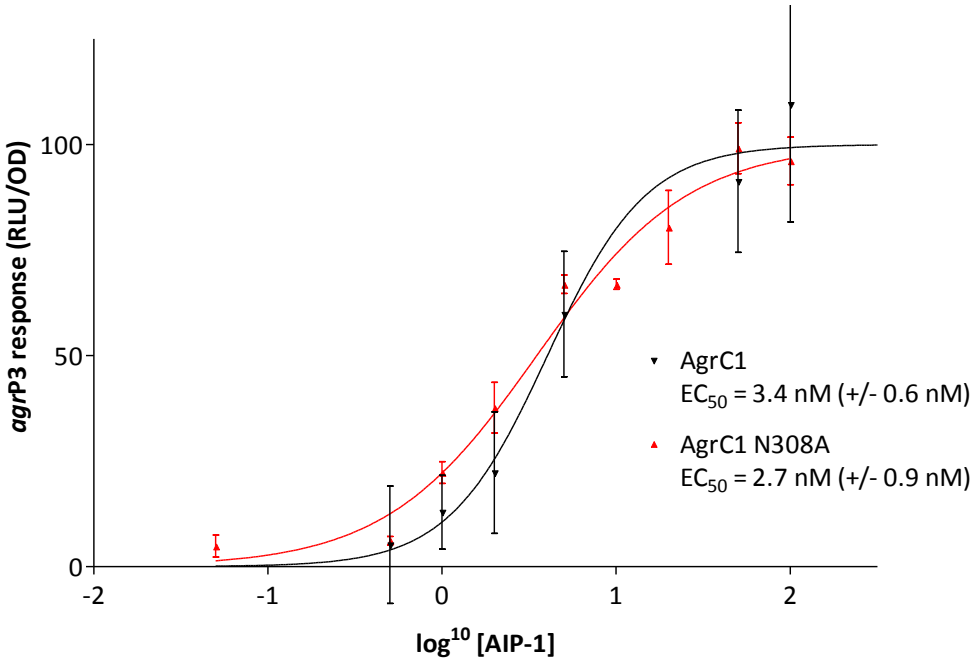

Table 4.2 Summary of functional impact of AgrC cytoplasmic domain mutations

Response to AIP-1 by the Group 1 AgrC bioreporter and AgrC mutants expressed as the concentration of AIP-1 required for 50 % activation (EC_{50}). EC_{50} values given are the mean value for 3 separate assays plus the standard deviation (SD). Statistical significance is shown in comparison with the group 1 AgrC control reporter. Amino acid substitutions, alone or in combination, which were present in clinical strains and associated with reduced or null exotoxin phenotype are shown in red. The AgrC T247I (EC_{50}=22.9 nM) and AgrC I311T-A343T (EC_{50}=38.1 nM) reporters showed the greatest reduction in sensitivity. Sources for the original mutations are given as either the TS strain collection (Table 2.2), the ST239 Turkish isolates (Table 2.2) or other published studies.

AgrC mutation	EC_{50} (nM)	SD	Significance	Source
Group 1 AgrC	3.4	0.6		
Y251F	2.8	1.2	p>0.05	TS13/14
N267I	9.6	1.6	p<0.01	TS13
Y251F/N267I	9.3	1.8	p<0.01	TS13
I311T	20.9	0.6	p<0.01	ST239
A343T	2.8	0.8	p>0.05	ST239
I311T/A343T	38.1	1.7	p<0.01	ST239
T247I	22.9	2.6	p<0.01	ST239
L245A	8	2.1	p<0.05	Traber *et al* (2008)
F264A	8.3	1.3	p<0.01	Shopsin *et al* (2008)
N308A	2.7	0.9	p>0.05	TS1

4.2.2.5 Impact of key *agrC* mutations on *agr* autoinduction

All of the data gathered on AgrC cytoplasmic domain mutations so far used a plasmid-based reporter system incapable of AIP synthesis. Although the reduction in sensitivity observed for AgrC-N267I was significant, it was conceivable that the impact would be magnified when placed in the context of an autoinduction circuit.

A chromosomal *agr* group 1 reporter strain MY15 had previously been constructed by Maho Yokoyama (Centre of Biomolecular Sciences) by inserting the *agrP2BDCA* genes into an ectopic chromosomal site of an integration strain and transducing this into the *agrP3-lux* reporter ROJ48 (section 2.5.3). MY15 both produces and responds to AIP, producing light when *agr*P3 is activated. MY20 was also constructed by introducing the appropriate SNP into *agrC,* resulting in AgrC-N267I.

To compare the light production profiles of these strains, reflecting the timing of *agr* activation as a result of their native AIP-1 production, both strains were incubated over a 20 h period in 96 well plates with luminescence recorded at 20 min intervals (Figure 4.11A). MY15, encoding the NCTC8325 reference *agrC* sequence, showed measurable bioluminescence by 6 h, which continued to rise over the following 12 h. *agr*P3 activation in MY20, harbouring the AgrC-N267I mutation, did not show measurable bioluminescence until 14 h, a delay of 8 h. While this delay was much greater than that observed in the clinical strain TS13, this is likely to reflect a reduced overall efficiency of the *agr* autoinduction circuit when placed in an ectopic chromosomal location, with a delay also seen in the control reporter.

When both strains were grown under the same conditions in the presence of 100 nM AIP-1, added at inoculation, early activation was observed in both MY15 and MY20, although MY20 activation was still slightly higher up to 16 h (Figure 4.11B). The AgrC antagonist (ala^{5})AIP-1 abolished *agr*P3 activation by both MY15 and MY20.

Figure 4.11 *agr* autoinduction is delayed in a chromosomal AgrC-N267I reporter

*agr*P3 activation of bioluminescent reporters expressed as RLU per OD over 20 h. Bioreporters consist of an *agr*P3-lux fusion, with the *agr*P2 locus inserted at an ectopic chromosomal mutation to allow the introduction of the N267I AgrC substitution. A negative control without the *agr*P2 locus is shown, with no light output, compared with a reporter with the NCTC8325 *agrC* sequence activating around 6 h (AgrC1) and an AgrC1-N267I mutant reporter activating around 14 h (A). While the AgrC antagonist (ala^5) AIP-1 abolished *agr*P3 activation, addition of exogenous AIP-1 resulted in early activation, at around 2 to 4 h, for both the AgrC1 and AgrC1-N267I reporters (B).

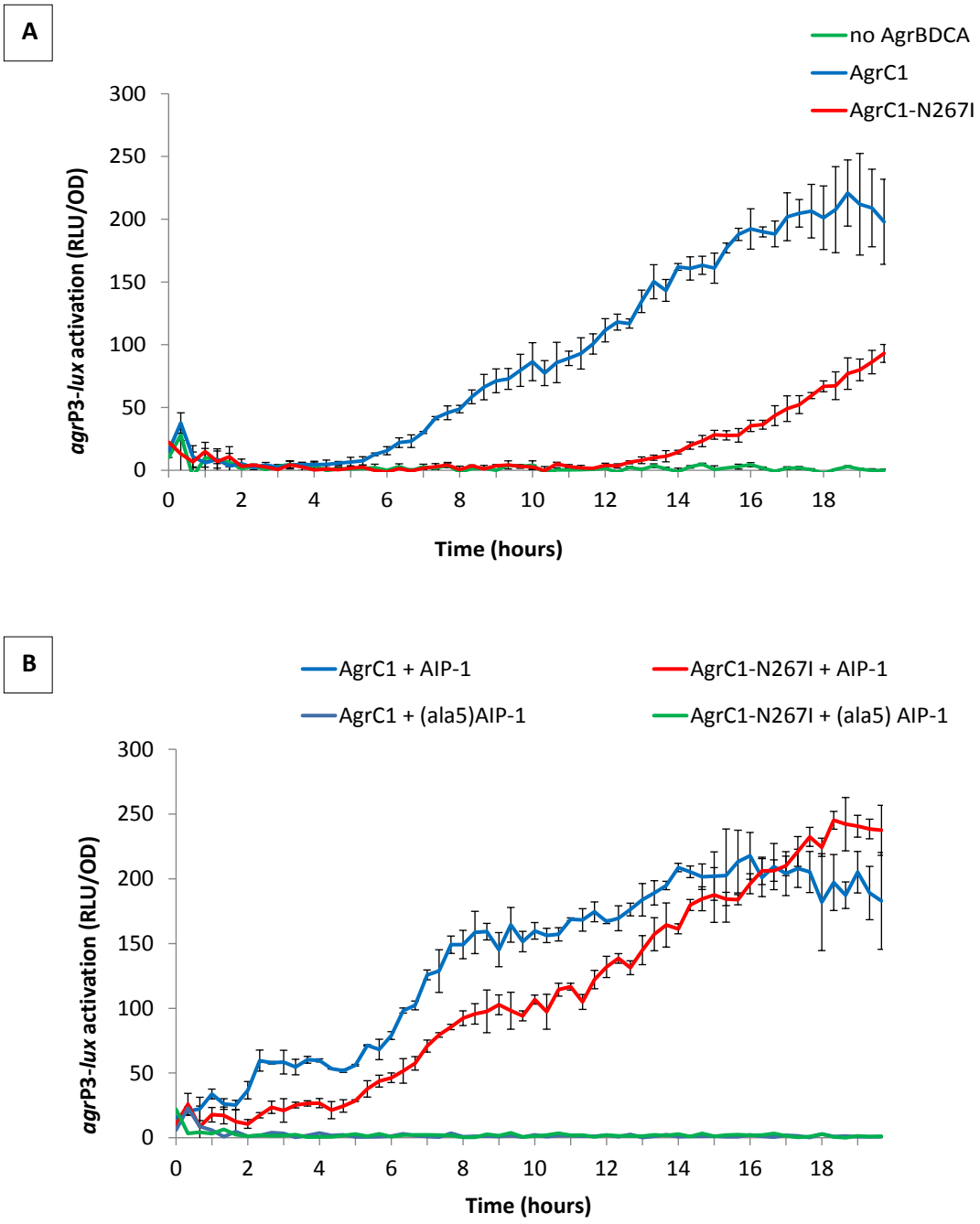

4.3 Discussion

4.3.1 Variable exotoxin production and AIP production kinetics

The direct comparison of TS13 and TS14 was the ideal natural experiment to investigate differences in *agr* function underlying variable exotoxin expression.

Serial collection of culture supernatants through exponential to stationary phase revealed a delay of about 1 h in the production of AIP-1 by TS13 as compared to TS14 with a lower final AIP-1 concentration reached by TS13 in stationary phase. Given the differences in *agr* expression already identified by the RT-PCR analysis, this result was in good agreement.

As there were no other genotypically matched but phenotypically variable pairs of isolates in the strain collection, other strains with predicted AgrC substitutions and large phenotypic differences were sought for comparison.

HU24 and IU12 were two ST239 strains which had been identified with collaborators at Bath University as having identical *agr* sequences except for a predicted A343T AgrC substitution. While IU12 was highly lytic in a T-cell assay indicating production of high levels of exotoxin production, particularly haemolysins and phenol soluble modulins, HU24 demonstrated lytic activity that was around 20-fold lower. As with the TS isolates, there was a marked difference between these two strains in AIP-1 production. While IU12 was approaching a 100 nM AIP-1 concentration at 6 h, HU24 had barely reached this by 7 h and 1 h later the AIP-1 concentration did not change.

The other pair of ST239 isolates identified with significant phenotypic differences (4 % compared with 85 % T cell lysis) were ICP5014 and ICP5062, with ICP 5062 harbouring a predicted T247I AgrC substitution. The variation in AIP-1 production between these strains was the most marked with a delay of at least 3 h by ICP5062 which had a barely detectable concentration of AIP-1 when measured well into stationary phase.

While the delays observed here were only 1 h for the first 2 comparisons, the exogenous AIP addition experiments indicated that the concentration of AIP present going into exponential phase is a crucial determinant of global exotoxin production. Whether the delay or eventual peak of AIP-1 production is a bigger factor in determining the downstream regulatory effects is not clear.

The *agr* system exhibits classical quorum sensing such that activation is primarily due to changes in cell density, which can occur during growth and also due to changes in the environment. It may be, therefore, that a mismatch between AIP concentration and bacterial population density defines exotoxin production such that low AIP concentration in the presence of high bacterial population density results in low exotoxin production.

A recent report analysing AIP-1 production from culture supernatants by mass spectrometry found that in USA300, AIP-1 was detectable from about 4 h, although they estimated the concentration at this point to be 1 µM, much higher than the ∼125 nM detected in TS14 at 4 h (Junio *et al*, 2013). This could be because USA300 produces much higher levels of AIP-1 than the strains tested here, in keeping with higher levels of *agr* expression. Alternatively, the MS-based method may be much more sensitive than the *lux*-based bio reporter assay. As seen here, AIP-1 concentrations in USA300 increased rapidly following initial detection to around 8 µM in early stationary phase although continued to increase slowly to a final peak of 12 µM at 16 h. As the experimental data presented here was predominantly intended to give an indication of differences in the initial AIP production timing, AIP-1 concentrations were not studied beyond early stationary phase. Through comparison of culture supernatants taken from stationary phase, Junio *et al* were also able to show that AIP-1 concentrations correlated with red blood cell lysis in several different strain backgrounds, particularly for USA300 and COL. However, when comparing a number of CC45 strains, poor correlation was observed with some isolates that only produced lower levels of AIP-1 still showing marked (75 %) lysis of red blood cells. It

is interesting to note that this study did not investigate the timing of AIP-1 production between these strain types to see if this was a better predictor of haemolytic activity.

Differences in the timing of *agr* expression have been linked to exotoxin gene expression by other investigators. A study of the timing of *agr* expression compared the effect of variations in *agr* sequence between the four *agr* groups on RNAIII and exotoxin gene expression using transcriptional reporter fusions (Geisinger *et al*, 2012). Of note, RNAIII expression occurred at a much earlier time point when controlled by the group 1 *agr* locus as compared with group 3. Earlier RNAIII expression was associated with higher expression of *hla* and *pvl* but lower expression of *spa* and *rot*. Four of the group 3 isolates from the strain collection TS12, TS16, NRS162 and NRS255 were briefly tested for AIP-3 production with the group 3 bio reporter ROJ154 but AIP could not be detected until 12 h of growth. As it was unclear if this was comparable with the group 1 bioreporter data or simply due to reduced sensitivity of the group 3 bioreporter, the data was not included in this thesis. None of the group 3 isolates in the clinical strain collection exhibited high level PVL production however, so this effect may well be genuine and in keeping with the study by Geisinger *et al* (2012).

4.3.2 Causes and consequences of changes in AIP production kinetics

In the study by Geisinger *et al* (2012), the authors explained differences in the timing of *agr* expression in terms of polymorphisms between groups in important functional regions, particularly in *agrB* and *agrC*. The strains studied here all harboured polymorphisms in the *agrC* gene which were predicted to alter the amino acid sequence. This raises the obvious mechanistic question as to whether changes in the AgrC amino acid sequence could delay the autoinduction circuit resulting in slower accumulation of AIP and consequently delayed activation of *agr*P3.

As AIP autoinduction depends on a positive feedback circuit, introducing inefficiencies in the system could potentially have a marked and cumulative impact on quorum sensing. Accumulation of AIP would occur slowly at first, accelerating as higher concentrations were reached. Limiting this initial accumulation could have an amplified impact on autoinduction potentially causing the delays observed here. This will be discussed in more detail in the context of the data generated by introducing AgrC mutations into the bioreporter ROJ48 strain background.

The delays in AIP production by the strains tested occur during late exponential or early stationary phase. RNAIII expression is essential for post-exponential *hla* expression but also, when RNAIII was placed under the control of an inducible promoter and expressed at various time points, delays in expression during late exponential phase resulted in large increases in *spa* expression (Vandenesch *et al*, 1991). As *spa* expression is heavily dependent on the transcriptional regulator SarS, which also represses toxin gene transcription, this is a potentially important indicator that the transition from exponential to stationary phase is pivotal in determining the timing of virulence gene expression in *S. aureus*.

As discussed previously, the other potentially important transcriptional regulator which is translationally repressed by RNAIII is Rot through RNAIII to *rot* mRNA complex formation

(Geisinger *et al*, 2006). The effect of Rot on exotoxin expression is significant; deleting *rot* partially restored toxin expression in an *agr* null mutant (McNamara *et al*, 2000). Carrying out a greater range of experiments studying the precise timing when exogenous AIP addition no longer impacts exotoxin expression would clarify the window period. Furthermore, employing RT-PCR to study *rot* and *sar* gene expression over time may yield even greater insight into the window period, identifying exactly when exotoxin repressor mRNA is present in high levels.

4.3.3 The role of *mecA* in reducing AIP production

Rudkin *et al* (2012) had previously observed that deleting *mecA* in a HA-MRSA strain BH1CC enhanced virulence in a mouse model. They were able to demonstrate that *mecA* expression reduced *agr* expression and hypothesised this was related to changes in the cell wall which interfered with AIP signaling/autoinduction. Reducing the cell walls with lysostaphin abolished the differences in *agr* expression between BH1CC and the BH1CC Δ*mecA* mutant. This raises the possibility that PBP2a alters the cell wall architecture in some way, perhaps interfering with AIP access to the cell membrane. This could in turn delay autoinduction and lead to lower final AIP concentrations.

Comparing AIP-1 production between the strains used in their study demonstrated that AIP-1 was both delayed in BH1CC and less than half of the overall concentration in early stationary phase when compared to the BH1CC Δ*mecA* mutant. This is consistent with their data and lends more weight to the overall hypothesis that AIP production, either the time to reach a threshold concentration or the final level reached at stationary phase, could be used as an indication of *agr* activity and consequently virulence factor expression.

While alterations in penicillin binding protein activity and hence cell wall architecture may mediate this effect, other researchers have speculated that SCC*mec* may alter global gene regulation through other mechanisms. Psm-*mec* was noted to repress *agr* activity by directly inhibiting translation of AgrA (Kaito *et al*, 2013). The effect noted by Rudkin *et al* appeared to occur regardless of whether the entire SCC*mec* element or just the *mecA* gene was deleted, suggesting a specific role for *mecA*. Interestingly, *mecA* was observed to be constitutively expressed at higher levels in BH1CC as compared to CA-MRSA strains suggesting the existence of another mechanism for the enhanced virulence of CA-MRSA.

The finding of reduced AIP production in BH1CC is consistent with the experimental data presented by Junio *et al* (2013). As discussed previously, they found that AIP-1 production was higher in USA300 than HA-MRSA strains and associated with superior red cell lysis.

Delays in AIP production resulting from the presence of the *mecA* element indicates that factors upstream of *agr* can produce this effect and this phenomenon is not just a consequence of polymorphisms in *agr*. This also underlies the association between delayed and reduced AIP production, reduced *agr* activity, lower production of exotoxins and reduced toxin associated virulence.

4.3.4 Mutation of the cytoplasmic domain of AgrC

4.3.4.1 Do the *agrC* polymorphisms explain the attenuated exotoxin expression?

The marked differences in PVL and alpha haemolysin production between TS13 and TS14 despite their genotypic similarities pointed to the possibility of a pivotal mutation in a global regulator. The *agrC* polymorphism in TS13 that was predicted to result in an asparagine to isoleucine substitution at the 267th amino acid residue of AgrC remained the best candidate to explain this change after whole genome analysis. Expression of RNAIII in exponential phase was noted to be 10-fold lower in TS13 by qRT-PCR and AIP production was delayed by 1 h. Introduction of this *agrC* SNP into the group 1 bioreporter by site directed mutagenesis resulted in a ~3-fold rise in EC_{50}, representing a fall in sensitivity to AIP-1. Although this effect was small, this could explain the differences in exotoxin phenotype and Agr kinetics. As the autoinduction loop depends on a positive feedback effect, a small reduction in efficiency when AIP concentration is low may result in a bigger delay in the amplification loop.

Mutagenesis of the membrane spanning receptor domain of AgrC has previously shown that key residues in loops 1 and 2 are important for AIP binding and recognition (Jensen *et al*, 2008). Introducing mutations into these residues also resulted in increases in the AgrC EC_{50} in response to AIP. While the AgrC receptor is fairly well characterised in terms of transmembrane spanning regions, loops and key residues, little is currently known about the structure or key functional residues of the AgrC cytoplasmic domain.

As the plasmid based AIP reporter does not produce endogenous AIP and therefore does not represent a strain with an intact autoinduction circuit, the N267I AgrC substitution was introduced into a bioreporter harbouring the Agr P2 locus at an ectopic site, with the *agr*P3 promoter fused to *lux*. When light output was compared with an identical bioreporter without the N267I substitution, a clear delay in onset was observed, providing further evidence that the change was probably sufficient to explain the change in *agr* kinetics. It therefore seems likely

that the phenotypic variation observed between TS13 and the other ST22 strains in the original collection of clinical isolates can be accounted for by this *agrC* polymorphism. This underlines the importance of the cytoplasmic region domain of *agrC* as pivotal to global gene regulation in *S. aureus*.

Paired strains with marked differences in exotoxin expression and other *agrC* polymorphisms were also analysed by introducing the substitutions found in these strains into the bioreporter. Both I311T and T247I had an even bigger impact on the sensitivity of AgrC with EC_{50} values greater than 20 nM compared with the control EC_{50} of 3.4 nM. The T247I AgrC substitution is therefore also likely to explain the phenotypic variation observed between ICP5014 and ICP5062 with exotoxin dependent lysis being potent in ICP5014 but barely apparent in ICP5062 which harbours the AgrC substitution.

Comparing the data for I311T, A343T and the double mutant presents a slightly more complicated picture. When comparing ST239 strains that were highly lytic to those that were not, the *agrC* SNP resulting in A343T was associated with reduced lysis. When A343T was introduced alone into the bioreporter, there was no apparent difference from the control reporter. All of the ST239 strains analysed in this cluster harbour the *agrC* SNP resulting in I311T, suggesting this was a common feature of this clade. Despite this substitution, which would be expected to result in impaired *agr* activity, some of the strains were still highly lytic in the T-cell assay. Hence it may be that other changes in global regulation in these strains compensates for a baseline reduction in the efficiency of AgrC such that *agr* functionality is preserved. Introducing A343T into the bioreporter containing the I311T substitution did however result in the biggest increase in EC_{50} to ~38 nM. This suggests that these residues are interacting in some way, possibly within a single loop or between two regions of the polypeptide that are in contact with each other. The difference in EC_{50} between the I311T and

the I311T-A343T mutant strains would be sufficient to explain the phenotypic differences seen within this subgroup of strains.

Finally, two AgrC residues which were reported in the literature to potentially result in reduction in exotoxin production were L245 and F264. These were both replaced with alanine to determine whether these residues are important for AgrC function. Both resulted in small but significant reductions in receptor sensitivity, which are in keeping with the original reports (Shopsin *et al*, 2008; Traber *et al*, 2008).

4.3.4.2 How do the polymorphisms relate to AgrC function?

While the AgrC cytoplasmic domain has not been well characterised, histidine kinase signal transducers like it occur throughout the bacterial kingdom with key regions conserved between species (Grebe & Stock, 1999). AgrC is understood to form a dimer, enabling trans-autophosphorylation of the histidine at residue 239 by a kinase domain in the dimer pair located at the end of the cytoplasmic region around residues 394 and 396 (George Cisar *et al*, 2009). Modification of several residues around H239, particularly R238, have been reported to result in constitutive activation of AgrC (Geisinger *et al*, 2009). Type 1 histidine kinases have been relatively well characterised with five conserved 'boxes' recognized including the 'H box' containing the histidine, but also X, N, D and G boxes (Grebe & Stock, 1999). AgrC is classified as a type 10 histidine kinase, having H, N and G boxes but no X or D box (see Figure 4.12). While the H box is important for autophosphorylation as already discussed and the G box probably represents the kinase, the N box may play a role in ATP binding prior to trans-autophosphorylation. Highlighting the AgrC amino acid substitutions analysed in this study in relation to the functional regions indicates that many of them fall in the less well conserved regions of unknown functionality. T247I occurs quite close to the histidine and so could potentially interfere with phosphorylation, perhaps explaining the large impact this appears to have on transduction efficiency. N267I on the other hand, is situated between the H and N boxes and so it is unclear whether this affects ATP binding or phosphorylation directly, or protein structure in some other way. Both T247I and N267I are in a region predicted to form a large coiled-coil dimerisation domain so could conceivably interfere with dimerization prior to trans-autophosphorylation (George Cisar *et al*, 2009). As I311T and A343T are both close to the N box, it is conceivable that they interfere with the structure of this region, perhaps impairing ATP binding. Mutations in the G box at AgrC residues 394 and 399 have been reported in the literature and it is likely then that these impair the functionality of the kinase, reducing the

efficiency of phosphotransfer to AgrA (Somerville *et al*, 2002; Traber *et al*, 2008). Whether phosphotransfer depends on direct interaction and binding of AgrC to AgrA is not known.

There would be several potential ways of investigating further the functionality of AgrC. One possibility would be to set up a bacterial two hybrid binding assay to look at the interaction between the cytoplasmic region of AgrC and AgrA. Amino acids could then be substituted in the AgrC fragment to determine whether they interfere with the AgrC-AgrA interaction. Alternatively, an expanded programme of alanine scanning may give a clearer picture of essential and non-essential residues in regions of interest. Finally, comprehensive *in silico* modelling of the predicted AgrC three-dimensional structure may indicate where the loops and residue to residue interactions occur and therefore explain why some of the substitutions tested here have more of an impact than others.

Figure 4. 12 Position of mutations compared to functionally important regions of AgrC

AgrC is divided into a transmembrane sensor domain and a cytoplasmic histidine kinase domain as shown in A. The cytoplasmic domain has been further subdivided into a dimerisation and histidine phosphotransfer domain (DHp) and a catalytic/ATP binding subdomain (CA) containing the kinase. The DHp subdomain is predicted to form a coiled α-helical structure which is important for dimerisation, with a supercoiled region around the H239 marked with a grey rectangle underneath the H box (George Cisar *et al*, 2009).

An alignment of histidine phosphate kinases (HPKs) is shown in B, demonstrating the similarity in the key functional H, N and G boxes between type 10 HPKs along with the sequences of divergent HPKs found in *E. coli*. The H box histidine is phosphorylated by the G box kinase.

The locations of the cytoplasmic domain amino acid substitutions which attenuate AgrC function, both investigated in this study and reported in the literature, are marked on the structural map (green arrows) and the alignment (blue lines). F264A, N267I and I311T fall outside of the functional boxes but may have an impact on dimerisation.

A and B are both adapted from George Cisar *et al* (2009).

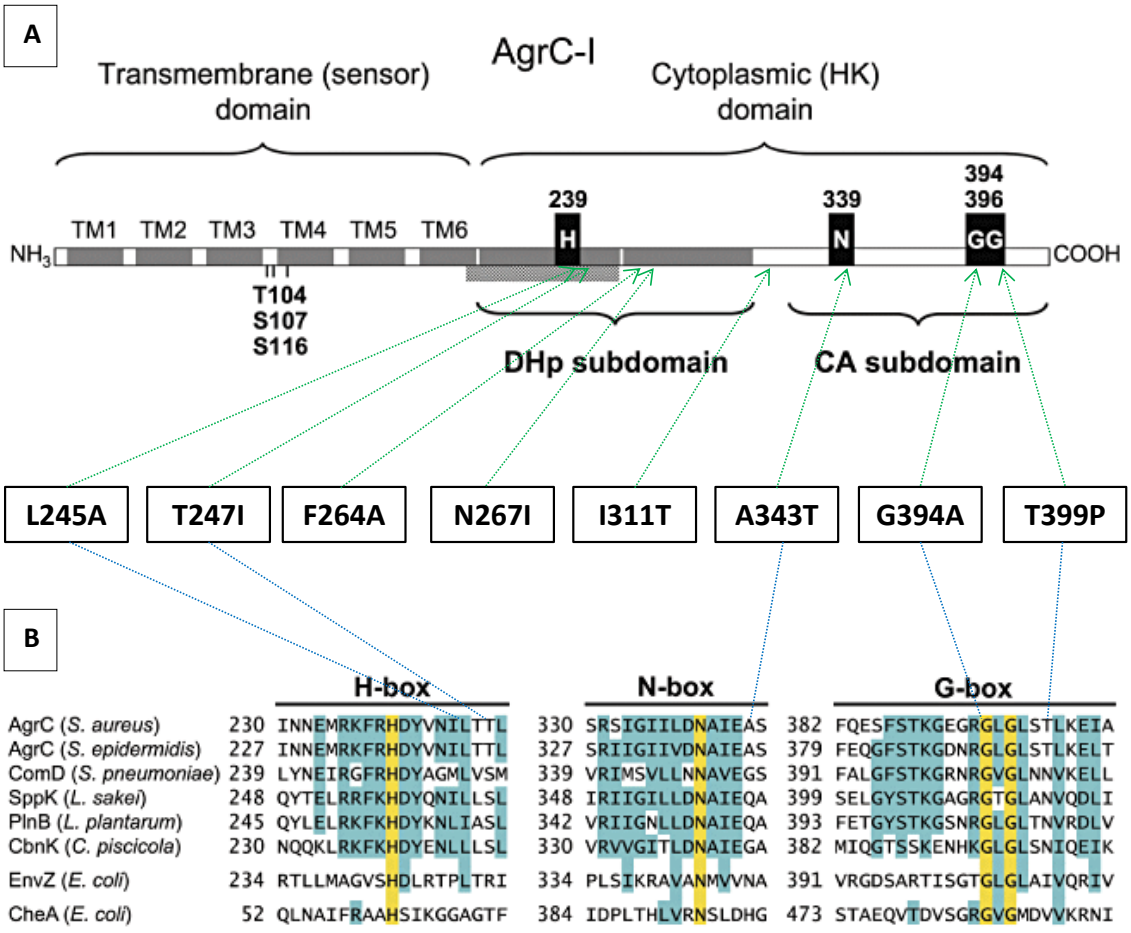

4.3.4.3 What is the significance of *agrC* polymorphisms in clinical isolates?

While it appears that *agrC* SNPs occur naturally, both within clades and spontaneously in single isolates, raising the question as to why these changes occur and whether they could be adaptive.

Isolates with a defective Agr system as a consequence of SNPs, premature stop codons and frame shifts have been identified in clinical samples, usually mixed with isolates in which Agr is fully functional (Traber *et al*, 2008). *agr* mutants occur during the course of an infection, for example within abscesses, and in this comparatively more stable environment than, for example, the bloodstream, appear to have a survival advantage over non-mutants (Schwan *et al*, 2003). The TS13 clinical strain harbouring the AgrC N267I substitution was isolated from abscess pus. In the context of chronic infection, such as in the cystic fibrosis lung, *agr* appears to become less and less important, with the inevitable consequence of accumulating *agr* mutations (Goerke & Wolz, 2004).

Shopsin *et al* (2008) identified isolates from family members with identical *agr* mutations, suggesting *agr* mutation does not prevent transmission. They also observed a greater incidence of *agr* mutation in hospital strains, suggesting that the hospital environment may be more favourable to their emergence. If a fully functional Agr system is required for breaching the physical barriers of the host and overcoming the innate immune system but also represents a fitness burden, it is perhaps not surprising that Agr-impaired strains would more easily spread in hospitals in the context of immunocompromised hosts. A follow up study of HA-MRSA strains by Shopsin *et al* (2010) indicated however that the majority of *agr* mutants are sporadic and did not appear to spread beyond the initial host or close contacts suggesting they are primarily adaptive for host survival not spread.

One *agr* mutation identified in an epidemic strain is the AgrC G55R substitution in the CC30 EMRSA-16 strain which, accompanied with a frame shift in the alpha haemolysin gene, appears

to attenuate exotoxin-associated virulence (DeLeo *et al*, 2011). This indicates that, as expected, the success of epidemic HA-MRSA clones depends primarily on colonisation and antibiotic resistance as opposed to an aggressive virulent phenotype.

Quorum sensing mutations have also been identified in other Gram positive pathogens, for example *Enterococcus faecalis*. Teixeira *et al* (2012) found a mutation in the sensor domain of FsrC, analogous to AgrC, predicted to truncate the ATPase sensor domain. The strain in which the mutation occurred had markedly reduced gelatinase expression compared to similar strains without the mutation.

Most of the aforementioned studies of Agr dysfunction have focused solely on a haemolysin positive or negative phenotype as observed on blood agar. The clinical isolates studied here were characterised by a number of methods including an assay for AIP production kinetics, western blots of exotoxin production for the TS strains and T-cell lysis assays for the ST239 strains. The advantage of this approach is that it identified subtler changes in Agr function which did not fit into the recognised paradigm of Agr positive and Agr negative. Rather, there appears to be a continuum of Agr functionality where the autoinduction system can remain intact, but with reduced exotoxin production as a consequence of *agrC* SNPs. This could give an added advantage to the strains acquiring these mutations as they would retain the capacity to respond dynamically to growth and environmental changes, while expending fewer resources on exotoxin production once successfully established within the host.

While the TS strains were collected directly from the clinical laboratory and stored at -80 ^{o}C, the acquisition of mutations before this cannot be excluded, as isolates in the clinical laboratory are routinely subcultured at least once before storage. Somerville *et al* (2002) passaged *S. aureus* isolates several times before *agr* sequencing and found that *agrC* and intergenic *agrC-agrA* mutations were common.

The dramatic difference in phenotype between TS13 and TS14 as the result of a single base change in *agrC* highlights the importance of this region of the *agr* locus in determining exotoxin expression. The potential implications of this are two-fold. The first is that in building up a picture of which AgrC residues are essential for normal Agr functionining, it should be possible to identify strains which are predicted to have reduced exotoxin expression directly from sequence data. The second is that AgrC to AgrA signal transduction, and more broadly staphylococcal signal transduction, are essential for virulence regulation and therefore present an attractive target for the design of novel antivirulence drugs. A signal transduction blocker with broader spectrum would interfere with multiple cellular processes and also potentially have activity beyond *S. aureus*, but with sufficient specificity to avoid toxicity to eukaryotic cells.

4.3.5 Does high level expression matter *in vivo*?

As alluded to previously, the study of exotoxin expression *in vitro* raises questions about the relevance to clinical infections *in vivo.* One aspect of this debate is how representative *in vitro* exotoxin production is to that found *in vivo.* Another is whether high level exotoxin production *in vivo* determines severity or not. Finally, while exotoxin production may be critical to the pathogenesis of certain types of infection, particularly those involving abscess formation, it may be less critical or even counterproductive in the course of other infections.

Several animal studies have confirmed that strains such as USA300 with high level expression of *agr in vitro* are more virulent than other strains with lower *agr* expression (Li *et al*, 2010). Cheung *et al* (2011) observed that alpha haemolysin transcript levels correlated with abscess size. Varshney *et al* (2010) demonstrated that strains which produced more PVL *in vitro* caused larger skin abscesses with more inflammation. As this study was performed using a mouse model, it is debatable whether they were observing a PVL-dependent effect or rather a broader effect of increased *agr* expression, probably mediated by a combination of exotoxins.

The mismatch between *in vitro* and *in vivo* expression observed by Loughman *et al* (2009) was hypothesised to be related to the interaction between human neutrophils and staphylococci. Staphylococci may be able to bypass *agr* and *sar* dependent expression pathways through the upregulation of *saeRS* in response to environmental factors. This was observed in a strain specific manner by Goerke *et al* (2001). *saeRS* mediated exotoxin expression may ensure high level toxin expression in response to environmental triggers regardless of *agr* activity *in vitro*. It has also been noted that RNAIII can be activated in a time, density and tissue specific manner, independently of RNAII (Xiong *et al*, 2002).

AIP-1 is known to be gradually inactivated *in vitro* by the oxidation of the methionine thioether side-chain to form a methionyl sulphoxide with around 60% of AIP-1 inactivated at 14 h (McDowell *et al*, 2001). This rate of oxidation could be similar *in vivo*, or could be enhanced by

environmental conditions. In addition, AIP-1 may be inactivated by other enzymes, bound to plasma proteins or diluted by fluid movement, as would undoubtedly occur in the bloodstream.

In terms of whether high level exotoxin production determines severity, it was interesting to note that TS1, which caused a fatal nectrotising pneumonia, was not a high level toxin producer. Boakes *et al* (2012) compared PVL production by ELISA with strain background and type of clinical presentation (pneumonia, skin and soft tissue infection, bacteraemia), finding a correlation with strain background but not presentation. They concluded that the amount of PVL produced is unimportant in determining severity. The difficulty with this approach is that different clinical presentations are not really indicators of severity but rather distinct syndromes, probably with varying importance of exotoxin. For example, the majority of cases of PVL pneumonia could be caused by nasal colonisation strains, with severe inflammation facilitated by preceding viral infections. In addition, the huge variety of host factors which could determine outcome cannot be accounted for when viewing clinical severity retrospectively. Animal models are probably the only way to investigate this potential phenomenon effectively.

Genestier *et al* (2005) observed concentration dependent neutrophil lysis *in vitro* with a transition from controlled apoptosis to frank necrosis occurring at high PVL concentrations. It may be that once a critical concentration of toxin is reached, neutrophils are lysed effectively and any additional PVL above this does not confer any further advantage. Whether this concentration is easily reached *in vivo* is not currently known.

Investigating *in vivo* exotoxin expression could be achieved through a number of means, although is likely to be technically challenging. Reporter gene fusions would be one potential method and have previously been employed to show distinct expression profiles of staphylococcal genes *in vitro* versus *in vivo*, although not in real time (Cheung *et al*, 2004). Measuring RNA transcript levels would be another approach as employed in clinical samples by Loughman *et al* (2009) generating information on multiple genes at once, or even the whole

RNA transcriptome. While a reporter gene fusion method could potentially generate real time data in live animals using PET, SPECT and luminescence recording, RNA work would inevitably require animal sacrifice however, preventing dynamic, temporal data recording.

4.3.6 Key Findings

1. AIP production was delayed by ~1 h in TS13 and 50% that of TS14.
2. ST239 strains with reduced exotoxin production and the AgrC substitutions I311T or T247I also demonstrated delayed AIP production compared with genetically related strains without these changes.
3. Comparing a HA-MRSA BH1CC with an isogenic *mecA* deletion mutant indicated that the presence of *mecA* delays and reduces overall AIP production.
4. Introducing AgrC N267I into the plasmid based group 1 bioreporter raised the EC_{50} in response to AIP-1 while AgrC Y251F had no effect.
5. The combined presence of AgrC I311T and A343T substitutions, or AgrC T247I had the greatest impact on AgrC function.
6. Several other potentially important AgrC residues identified by other studies of *agr* dysfunction were investigated. This demonstrated an observable impact of substituting AgrC L245 and F264 for alanine.
7. Introducing AgrC N267I onto a chromosomally encoded *agr* bioreporter with a fully functional autoinduction circuit delayed *agr*P3 activation.

5 Conclusions

The starting point for this study was the analysis of a collection of PVL producing *S. aureus* strains isolated from patients in Nottingham. While the collection was never intended to be a comprehensive study of locally circulating PVL strain types, ST22 *agr* group 1 and ST30 *agr* group 3 strains made up the majority of those investigated. ST30 *agr* group 3 PVL MSSA strains have been identified spreading worldwide (Rasigade *et al*, 2010) and both groups are common in the UK (Holmes *et al*, 2005). A comparison of these strains revealed a wide variation in PVL production between lineages, which appears to be due primarily to differences in *agr* activity. Based on the observation that USA300, the most notorious of CA-MRSA clones, is a high level PVL producer, it is possible that the success of the ST22 MSSAs in Nottingham was in part related to their high level exotoxin production. By contrast, TS1 was not a high level toxin producer and appears to be unrelated to any of the successful staphylococcal lineages in the UK. Nonetheless, this strain was responsible for a fatal necrotising pneumonia, possibly indicating the importance of host factors in determining the severity of PVL associated infections, and the mismatch between strain transmissibility and potential for causing severe disease.

PVL production in the Nottingham strain collection was regulated by *agr*. The addition of exogenous autoinducing peptides or the competitive AgrC antagonist (ala^{5})AIP-1 demonstrated that *agr* activation and inhibition has a major role to play in determining the final level of PVL production achieved. The AIP concentration required for *agr* activation must be present before a critical cell population density is reached equivalent to mid-exponential growth. Further investigation of the *pvl* promoter indicated potential binding sites for staphylococcal regulators, particularly the SarA protein family, which was confirmed via promoter pull down experiments.

Hence PVL production is subject to multiple levels of regulation involving these well characterised staphylococcal regulators acting directly at the *pvl* promoter as well as via *agr*. The similarities between PVL and alpha haemolysin regulation, and evidence of PVL overexpression *in vivo* (Loughman *et al*, 2009) lends weight to the hypothesis that PVL expression could occur through both *agr*-dependent and *agr*-independent mechanisms.

The comparison of TS13, a low PVL producing *spa* t005 ST22 MSSA, with the high PVL producing *spa* t005 ST22 TS14 presented a useful natural experiment to investigate why PVL production might vary within lineages. Studying the whole genomes sequences of these isolates also gave additional insights into how the ST22 MSSAs compared to similar staphylococcal strains.

TS13 and TS14 differ by around 190 SNPs in their core genome which indicates they are closely related. Apart from the phage differences, they shared many of the core genome features found the UK epidemic MRSA clone EMRSA-15, with the most important differences being the lack of an SCC*mec* element and the presence of the PVL encoding phage Φtp310-1. The combination of the IEC, found on Φtp310-3, and PVL production is likely to confer a significant advantage in terms of overcoming the innate immune defenses to *S. aureus* which is highly dependent on phagocytosis by neutrophils.

The finding of a SNP in TS13 *agrC* conferring an N267I substitution probably explains the phenotypic difference observed between these strains, based on the importance of *agr* in determining PVL production, and the differences in both RNAIII and *pvl* transcription observed between them. The D134Y substitution in TS13 SarU could also be a contributing factor, although this was not tested.

Given the large number of SNPs varying between the two isolates, and the possibility that there is other genetic material distinguishing them which could not be identified, the predicted

impact of the N267I substitution in AgrC cannot be confirmed from the sequence data and requires biological investigation. The response to AIP-1 was reduced by the AgrC N267I substitution, lending further weight to the hypothesis that it was responsible for the low producing PVL phenotype seen in TS13. As the clinical isolates were difficult to manipulate, the AgrC N267I mutation could not be repaired in TS13 or introduced into TS14. Instead, AgrC N267I was introduced into a chromosomal *agr* bio reporter, resulting in a delay in AIP autoinduction. As TS13 was also observed to exhibit a delay in the initial production and lower final concentrations of AIP compared to TS14, the conclusion was that slight reductions in AgrC efficiency resulted in delayed AIP autoinduction. This, in turn, reduced AIP concentrations around the critical cell population density in exponential phase resulting in reduced PVL concentrations.

To show this was not an isolated occurrence, other clinical strains with naturally occurring *agrC* cytoplasmic mutations were also studied and found to have delayed, reduced AIP production associated with reduced exotoxin levels. These *agrC* mutations also caused reductions in the sensitivity of AgrC to AIP-1 when evaluated in agr biosensor strains carrying the mutation. Furthermore, comparing a *mecA* deletion mutant of a HA-MRSA BH1CC indicated that other factors influencing *agr* expression can also alter the kinetics of AIP production in a similar way.

This study also explored variations in exotoxin production between clinical isolates, regulation of PVL production and the impact of naturally occurring *agrC* cytoplasmic mutations on *agr* kinetics and exotoxin production. An important question underlying all of this is the role of PVL in determining pathogenesis, in particular whether the level of PVL production is a major factor in determining the severity of infections. While there is some indication that the level of PVL production is important *in vivo,* further investigation of this would be best served by analysis of real time gene expression in animal models relevant to PVL.

The ‘window effect’ during which the level of PVL production can be activated or inhibited by addition of exogenous peptides is one of the more interesting findings and would require further study to characterise completely. More experiments could be done to determine the exact OD or point during growth when the bacteria no longer respond to exogenous peptide, how strain and growth medium dependent this effect is, and whether using high doses of AIP or (ala^{5})AIP-1 overcomes the lack of response observed after the window period.

An initial analysis of the *pvl* promoter region by studying the promoter sequence and developing the pulldown technique gave fresh insight into how *pvl* is regulated. Experiments could be conducted with fragments of the *pvl* promoter, to confirm whether Sar proteins will bind to the predicted region between the putative RNA polymerase recognition sites and the start of the coding sequence. Comparisons of other low and high producing strains from other lineages, and analysis of promoter binding profiles at different time points, in different conditions and in the presence of activators and inhibitors of *agr* would also be valuable.

Finally, the cytoplasmic domain region of *agrC* was found to be of crucial importance for exotoxin expression, and appears to be vulnerable to mutation *in vivo*. A thorough analysis of this region to determine its 3-dimensional structure and key functional residues would yield important information which could be exploited in a number of ways. Understanding the molecular interactions required for signal transduction could lead to the development of novel anti-virulence agents, potentially with a broader spectrum of activity. Furthermore, if residues can be identified which are essential for unimpaired AgrC functionality, thereby reliably reducing exotoxin expression if mutated, this could contribute towards efforts in predicting staphylococcal virulence from sequence data.

Advances in genome sequencing have provided the research community with huge volumes of data, however interpreting and making use of this data in a clinical setting still presents a formidable challenge. This study demonstrates how through careful investigation of clinical

strains, phenotypic and genome sequencing data can be analysed side by side to guide mechanistic analysis. By bridging the gap between genomics and functionality, the anticipation is that the Clinical Microbiology service of the future will be able to provide users with timely, clinically relevant information about virulence and resistance based on genome sequencing data, which will in turn guide treatment and infection control.

6 Bibliography

Abdelnour A, Arvidson S, Bremell T, Rydén C, Tarkowski A (1993) The accessory gene regulator (*agr*) controls *Staphylococcus aureus* virulence in a murine arthritis model. *Infect Immun* **61:** 3879-3885

Arvidson S, Tegmark K (2001) Regulation of virulence determinants in *Staphylococcus aureus*. *Int J Med Microbiol* **291:** 159-170

Bae IG, Tonthat GT, Stryjewski ME, Rude TH, Reilly LF, Barriere SL, Genter FC, Corey GR, Fowler VG (2009) Presence of genes encoding the panton-valentine leukocidin exotoxin is not the primary determinant of outcome in patients with complicated skin and skin structure infections due to methicillin-resistant *Staphylococcus aureus*: results of a multinational trial. *J Clin Microbiol* **47:** 3952-3957

Barrios López M, Gómez González C, Orellana M, Chaves F, Rojo P (2013) *Staphylococcus aureus* abscesses: methicillin-resistance or Panton-Valentine leukocidin presence? *Arch Dis Child* **98:** 608-610

Bennett CM, Coombs GW, Wood GM, Howden BP, Johnson LE, White D, Johnson PD (2013) Community-onset *Staphylococcus aureus* infections presenting to general practices in South-eastern Australia. *Epidemiol Infect***:** 1-11

Beynon RP, Bahl VK, Prendergast BD (2006) Infective endocarditis. *BMJ* **333:** 334-339

Beyrouthy R, Hamze M, Hleis S, Mallat H, Dabboussi F (2012) Panton-Valentine leukocidin producing *Staphylococcus aureus* nasal carriage, in North-Lebanon. *Med Mal Infect* **43:** 386-390

Boakes E, Kearns AM, Badiou C, Lina G, Hill RL, Ellington MJ (2012) Do differences in Panton-Valentine leukocidin production among international methicillin-resistant *Staphylococcus aureus* clones affect disease presentation and severity? *J Clin Microbiol* **50:** 1773-1776

Boakes E, Kearns AM, Ganner M, Perry C, Hill RL, Ellington MJ (2011a) Distinct bacteriophages encoding Panton-Valentine leukocidin (PVL) among international methicillin-resistant *Staphylococcus aureus* clones harboring PVL. *J Clin Microbiol* **49:** 684-692

Boakes E, Kearns AM, Ganner M, Perry C, Warner M, Hill RL, Ellington MJ (2011b) Molecular diversity within clonal complex 22 methicillin-resistant *Staphylococcus aureus* encoding Panton-Valentine leukocidin in England and Wales. *Clin Microbiol Infect* **17:** 140-145

Boyce JM, Causey WA (1982) Increasing occurrence of methicillin-resistant *Staphylococcus aureus* in the United States. *Infect Control* **3:** 377-383

Boyle-Vavra S, Daum RS (2007) Community-acquired methicillin-resistant *Staphylococcus aureus*: the role of Panton-Valentine leukocidin. *Lab Invest* **87:** 3-9

Bronner S, Monteil H, Prévost G (2004) Regulation of virulence determinants in *Staphylococcus aureus*: complexity and applications. *FEMS Microbiol Rev* **28:** 183-200

Bronner S, Stoessel P, Gravet A, Monteil H, Prévost G (2000) Variable expressions of *Staphylococcus aureus* bicomponent leucotoxins semiquantified by competitive reverse transcription-PCR. *Appl Environ Microbiol* **66:** 3931-3938

Brown ML, O'Hara FP, Close NM, Mera RM, Miller LA, Suaya JA, Amrine-Madsen H (2012) Prevalence and sequence variation of panton-valentine leukocidin in methicillin-resistant and methicillin-susceptible *Staphylococcus aureus* strains in the United States. *J Clin Microbiol* **50:** 86-90

Brunskill EW, Bayles KW (1996) Identification of LytSR-regulated genes from *Staphylococcus aureus*. *J Bacteriol* **178:** 5810-5812

Bubeck Wardenburg J, Bae T, Otto M, Deleo FR, Schneewind O (2007) Poring over pores: alpha-hemolysin and Panton-Valentine leukocidin in *Staphylococcus aureus* pneumonia. *Nat Med* **13:** 1405-1406

Bubeck Wardenburg J, Palazzolo-Ballance AM, Otto M, Schneewind O, DeLeo FR (2008) Panton-Valentine leukocidin is not a virulence determinant in murine models of community-associated methicillin-resistant *Staphylococcus aureus* disease. *J Infect Dis* **198:** 1166-1170

Burlak C, Hammer CH, Robinson MA, Whitney AR, McGavin MJ, Kreiswirth BN, Deleo FR (2007) Global analysis of community-associated methicillin-resistant *Staphylococcus aureus* exoproteins reveals molecules produced in vitro and during infection. *Cell Microbiol* **9:** 1172-1190

Chan WC, Coyle BJ, Williams P (2004) Virulence regulation and quorum sensing in staphylococcal infections: competitive AgrC antagonists as quorum sensing inhibitors. *J Med Chem* **47:** 4633-4641

Chen L, Chavda KD, Solanki M, Mediavilla JR, Mathema B, Schlievert PM, Kreiswirth BN (2013) Genetic variation among Panton-Valentine leukocidin-encoding bacteriophages in *Staphylococcus aureus* clonal complex 30 strains. *J Clin Microbiol* **51:** 914-919

Cheng AG, DeDent AC, Schneewind O, Missiakas D (2011) A play in four acts: *Staphylococcus aureus* abscess formation. *Trends Microbiol* **19:** 225-232

Cheung AL, Bayer AS, Zhang G, Gresham H, Xiong YQ (2004) Regulation of virulence determinants *in vitro* and *in vivo* in *Staphylococcus aureus*. *FEMS Immunol Med Microbiol* **40:** 1-9

Cheung AL, Chien YT, Bayer AS (1999) Hyperproduction of alpha-hemolysin in a *sig*B mutant is associated with elevated SarA expression in *Staphylococcus aureus*. *Infect Immun* **67:** 1331-1337

Cheung AL, Eberhardt KJ, Chung E, Yeaman MR, Sullam PM, Ramos M, Bayer AS (1994) Diminished virulence of a *sar-/agr-* mutant of *Staphylococcus aureus* in the rabbit model of endocarditis. *J Clin Invest* **94:** 1815-1822

Cheung AL, Koomey JM, Butler CA, Projan SJ, Fischetti VA (1992) Regulation of exoprotein expression in *Staphylococcus aureus* by a locus (*sar*) distinct from *agr*. *Proc Natl Acad Sci U S A* **89:** 6462-6466

Cheung AL, Nishina KA, Trotonda MP, Tamber S (2008) The SarA protein family of *Staphylococcus aureus*. *Int J Biochem Cell Biol* **40:** 355-361

Cheung AL, Projan SJ (1994) Cloning and sequencing of *sar*A of *Staphylococcus aureus*, a gene required for the expression of *agr*. *J Bacteriol* **176:** 4168-4172

Cheung GY, Wang R, Khan BA, Sturdevant DE, Otto M (2011) Role of the accessory gene regulator *agr* in community-associated methicillin-resistant *Staphylococcus aureus* pathogenesis. *Infect Immun* **79:** 1927-1935

Chi CY, Lin CC, Liao IC, Yao YC, Shen FC, Liu CC, Lin CF (2013) Panton-Valentine Leukocidin Facilitates the Escape of *Staphylococcus aureus* From Human Keratinocyte Endosomes and Induces Apoptosis. *J Infect Dis*

Chien Y, Cheung AL (1998) Molecular interactions between two global regulators, *sar* and *agr*, in *Staphylococcus aureus*. *J Biol Chem* **273:** 2645-2652

Clauditz A, Resch A, Wieland KP, Peschel A, Götz F (2006) Staphyloxanthin plays a role in the fitness of *Staphylococcus aureus* and its ability to cope with oxidative stress. *Infect Immun* **74:** 4950-4953

Coia JE, Duckworth GJ, Edwards DI, Farrington M, Fry C, Humphreys H, Mallaghan C, Tucker DR, Chemotherapy JWPotBSoA, Society HI, Association ICN (2006) Guidelines for the control and

prevention of meticillin-resistant *Staphylococcus aureus* (MRSA) in healthcare facilities. *J Hosp Infect* **63 Suppl 1:** S1-44

Collins J, Rudkin J, Recker M, Pozzi C, O'Gara JP, Massey RC (2010) Offsetting virulence and antibiotic resistance costs by MRSA. *ISME J* **4:** 577-584

Coombs GW, Goering RV, Chua KY, Monecke S, Howden BP, Stinear TP, Ehricht R, O'Brien FG, Christiansen KJ (2012) The molecular epidemiology of the highly virulent ST93 Australian community *Staphylococcus aureus* strain. *PLoS One* **7:** e43037

Crowe SA, Døssing LN, Beukes NJ, Bau M, Kruger SJ, Frei R, Canfield DE (2013) Atmospheric oxygenation three billion years ago. *Nature* **501:** 535-538

Crémieux AC, Dumitrescu O, Lina G, Vallee C, Côté JF, Muffat-Joly M, Lilin T, Etienne J, Vandenesch F, Saleh-Mghir A (2009) Panton-valentine leukocidin enhances the severity of community-associated methicillin-resistant *Staphylococcus aureus* rabbit osteomyelitis. *PLoS One* **4:** e7204

Cunha BA (2005) Methicillin-resistant *Staphylococcus aureus*: clinical manifestations and antimicrobial therapy. *Clin Microbiol Infect* **11 Suppl 4:** 33-42

de Haas CJ, Veldkamp KE, Peschel A, Weerkamp F, Van Wamel WJ, Heezius EC, Poppelier MJ, Van Kessel KP, van Strijp JA (2004) Chemotaxis inhibitory protein of *Staphylococcus aureus*, a bacterial antiinflammatory agent. *J Exp Med* **199:** 687-695

Deghorain M, Van Melderen L (2012) The Staphylococci phages family: an overview. *Viruses* **4:** 3316-3335

Del Giudice P, Bes M, Hubiche T, Blanc V, Roudière L, Lina G, Vandenesch F, Etienne J (2011) Panton-Valentine leukocidin-positive *Staphylococcus aureus* strains are associated with follicular skin infections. *Dermatology* **222:** 167-170

DeLeo FR, Kennedy AD, Chen L, Bubeck Wardenburg J, Kobayashi SD, Mathema B, Braughton KR, Whitney AR, Villaruz AE, Martens CA, Porcella SF, McGavin MJ, Otto M, Musser JM, Kreiswirth BN (2011) Molecular differentiation of historic phage-type 80/81 and contemporary epidemic *Staphylococcus aureus*. *Proc Natl Acad Sci U S A* **108:** 18091-18096

Denison AM, Deleon-Carnes M, Blau DM, Shattuck EC, McDougal LK, Rasheed JK, Limbago BM, Zaki SR, Paddock CD (2013) Molecular Characterization of *Staphylococcus aureus* and Influenza Virus Coinfections in Patients with Fatal Pneumonia. *J Clin Microbiol*

Diep BA, Afasizheva A, Le HN, Kajikawa O, Matute-Bello G, Tkaczyk C, Sellman B, Badiou C, Lina G, Chambers HF (2013) Effects of linezolid on suppressing *in vivo* production of staphylococcal

toxins and improving survival outcomes in a rabbit model of methicillin-resistant *Staphylococcus aureus* necrotizing pneumonia. *J Infect Dis* **208:** 75-82

Diep BA, Chan L, Tattevin P, Kajikawa O, Martin TR, Basuino L, Mai TT, Marbach H, Braughton KR, Whitney AR, Gardner DJ, Fan X, Tseng CW, Liu GY, Badiou C, Etienne J, Lina G, Matthay MA, DeLeo FR, Chambers HF (2010) Polymorphonuclear leukocytes mediate *Staphylococcus aureus* Panton-Valentine leukocidin-induced lung inflammation and injury. *Proc Natl Acad Sci U S A* **107:** 5587-5592

Dinges MM, Orwin PM, Schlievert PM (2000) Exotoxins of *Staphylococcus aureus*. *Clin Microbiol Rev* **13:** 16-34, table of contents

Dohin B, Gillet Y, Kohler R, Lina G, Vandenesch F, Vanhems P, Floret D, Etienne J (2007) Pediatric bone and joint infections caused by Panton-Valentine leukocidin-positive *Staphylococcus aureus*. *Pediatr Infect Dis J* **26:** 1042-1048

Dubrac S, Boneca IG, Poupel O, Msadek T (2007) New insights into the WalK/WalR (YycG/YycF) essential signal transduction pathway reveal a major role in controlling cell wall metabolism and biofilm formation in *Staphylococcus aureus*. *J Bacteriol* **189:** 8257-8269

Dumitrescu O, Badiou C, Bes M, Reverdy ME, Vandenesch F, Etienne J, Lina G (2008) Effect of antibiotics, alone and in combination, on Panton-Valentine leukocidin production by a *Staphylococcus aureus* reference strain. *Clin Microbiol Infect* **14:** 384-388

Dumitrescu O, Boisset S, Badiou C, Bes M, Benito Y, Reverdy ME, Vandenesch F, Etienne J, Lina G (2007) Effect of antibiotics on *Staphylococcus aureus* producing Panton-Valentine leukocidin. *Antimicrob Agents Chemother* **51:** 1515-1519

Dumitrescu O, Choudhury P, Boisset S, Badiou C, Bes M, Benito Y, Wolz C, Vandenesch F, Etienne J, Cheung AL, Bowden MG, Lina G (2011) Beta-lactams interfering with PBP1 induce Panton-Valentine leukocidin expression by triggering *sar*A and *rot* global regulators of *Staphylococcus aureus*. *Antimicrob Agents Chemother* **55:** 3261-3271

Duncan JL, Cho GJ (1971) Production of staphylococcal alpha toxin. I. Relationship between cell growth and toxin formation. *Infect Immun* **4:** 456-461

Edwards AM, Massey RC (2011) How does *Staphylococcus aureus* escape the bloodstream? *Trends Microbiol* **19:** 184-190

Ellington MJ, Perry C, Ganner M, Warner M, McCormick Smith I, Hill RL, Shallcross L, Sabersheikh S, Holmes A, Cookson BD, Kearns AM (2009) Clinical and molecular epidemiology of ciprofloxacin-susceptible MRSA encoding PVL in England and Wales. *Eur J Clin Microbiol Infect Dis* **28:** 1113-1121

Errington J (2013) L-form bacteria, cell walls and the origins of life. *Open Biol* **3:** 120143

Eshwara VK, Munim F, Tellapragada C, Kamath A, Varma M, Lewis LE, Mukhopadhyay C (2013) *Staphylococcus aureus* bacteremia in an Indian tertiary care hospital: observational study on clinical epidemiology, resistance characteristics, and carriage of the Panton-Valentine leukocidin gene. *Int J Infect Dis* **17:** e1051-1055

Falord M, Mäder U, Hiron A, Débarbouillé M, Msadek T (2011) Investigation of the *Staphylococcus aureus* GraSR regulon reveals novel links to virulence, stress response and cell wall signal transduction pathways. *PLoS One* **6:** e21323

Felden B, Vandenesch F, Bouloc P, Romby P (2011) The *Staphylococcus aureus* RNome and its commitment to virulence. *PLoS Pathog* **7:** e1002006

Flores AR, Olsen RJ, Wunsche A, Kumaraswami M, Shelburne SA, Carroll RK, Musser JM (2013) Natural variation in the promoter of the gene encoding the Mga regulator alters host-pathogen interactions in group a Streptococcus carrier strains. *Infect Immun* **81:** 4128-4138

Foster TJ (2005) Immune evasion by staphylococci. *Nat Rev Microbiol* **3:** 948-958

Foster TJ, Höök M (1998) Surface protein adhesins of *Staphylococcus aureus*. *Trends Microbiol* **6:** 484-488

Fournier B, Hooper DC (2000) A new two-component regulatory system involved in adhesion, autolysis, and extracellular proteolytic activity of *Staphylococcus aureus*. *J Bacteriol* **182:** 3955-3964

Freeman ZN, Dorus S, Waterfield NR (2013) The KdpD/KdpE two-component system: integrating K^+ homeostasis and virulence. *PLoS Pathog* **9:** e1003201

Geiger T, Goerke C, Mainiero M, Kraus D, Wolz C (2008) The virulence regulator Sae of *Staphylococcus aureus*: promoter activities and response to phagocytosis-related signals. *J Bacteriol* **190:** 3419-3428

Geisinger E, Adhikari RP, Jin R, Ross HF, Novick RP (2006) Inhibition of *rot* translation by RNAIII, a key feature of *agr* function. *Mol Microbiol* **61:** 1038-1048

Geisinger E, Chen J, Novick RP (2012) Allele-dependent differences in quorum-sensing dynamics result in variant expression of virulence genes in *Staphylococcus aureus*. *J Bacteriol* **194:** 2854-2864

Geisinger E, Muir TW, Novick RP (2009) *agr* receptor mutants reveal distinct modes of inhibition by staphylococcal autoinducing peptides. *Proc Natl Acad Sci U S A* **106:** 1216-1221

Genestier AL, Michallet MC, Prévost G, Bellot G, Chalabreysse L, Peyrol S, Thivolet F, Etienne J, Lina G, Vallette FM, Vandenesch F, Genestier L (2005) *Staphylococcus aureus* Panton-Valentine leukocidin directly targets mitochondria and induces Bax-independent apoptosis of human neutrophils. *J Clin Invest* **115:** 3117-3127

George Cisar EA, Geisinger E, Muir TW, Novick RP (2009) Symmetric signalling within asymmetric dimers of the *Staphylococcus aureus* receptor histidine kinase AgrC. *Mol Microbiol* **74:** 44-57

Gillaspy AF, Hickmon SG, Skinner RA, Thomas JR, Nelson CL, Smeltzer MS (1995) Role of the accessory gene regulator (*agr*) in pathogenesis of staphylococcal osteomyelitis. *Infect Immun* **63:** 3373-3380

Gillet Y, Issartel B, Vanhems P, Fournet JC, Lina G, Bes M, Vandenesch F, Piémont Y, Brousse N, Floret D, Etienne J (2002) Association between *Staphylococcus aureus* strains carrying gene for Panton-Valentine leukocidin and highly lethal necrotising pneumonia in young immunocompetent patients. *Lancet* **359:** 753-759

Goerke C, Fluckiger U, Steinhuber A, Zimmerli W, Wolz C (2001) Impact of the regulatory loci *agr*, *sar*A and *sae* of *Staphylococcus aureus* on the induction of alpha-toxin during device-related infection resolved by direct quantitative transcript analysis. *Mol Microbiol* **40:** 1439-1447

Goerke C, Pantucek R, Holtfreter S, Schulte B, Zink M, Grumann D, Bröker BM, Doskar J, Wolz C (2009) Diversity of prophages in dominant *Staphylococcus aureus* clonal lineages. *J Bacteriol* **191:** 3462-3468

Goerke C, Wolz C (2004) Regulatory and genomic plasticity of *Staphylococcus aureus* during persistent colonization and infection. *Int J Med Microbiol* **294:** 195-202

Grebe TW, Stock JB (1999) The histidine protein kinase superfamily. *Adv Microb Physiol* **41:** 139-227

Gresham HD, Lowrance JH, Caver TE, Wilson BS, Cheung AL, Lindberg FP (2000) Survival of *Staphylococcus aureus* inside neutrophils contributes to infection. *J Immunol* **164:** 3713-3722

Griffiths E, Gupta RS (2004) Signature sequences in diverse proteins provide evidence for the late divergence of the Order Aquificales. *Int Microbiol* **7:** 41-52

Grkovic S, Brown MH, Hardie KM, Firth N, Skurray RA (2003) Stable low-copy-number *Staphylococcus aureus* shuttle vectors. *Microbiology* **149:** 785-794

Harbarth S, Rutschmann O, Sudre P, Pittet D (1998) Impact of methicillin resistance on the outcome of patients with bacteremia caused by *Staphylococcus aureus*. *Arch Intern Med* **158:** 182-189

Hershow RC, Khayr WF, Smith NL (1992) A comparison of clinical virulence of nosocomially acquired methicillin-resistant and methicillin-sensitive *Staphylococcus aureus* infections in a university hospital. *Infect Control Hosp Epidemiol* **13:** 587-593

Hidron AI, Low CE, Honig EG, Blumberg HM (2009) Emergence of community-acquired meticillin-resistant *Staphylococcus aureus* strain USA300 as a cause of necrotising community-onset pneumonia. *Lancet Infect Dis* **9:** 384-392

Higgins J, Loughman A, van Kessel KP, van Strijp JA, Foster TJ (2006) Clumping factor A of *Staphylococcus aureus* inhibits phagocytosis by human polymorphonuclear leucocytes. *FEMS Microbiol Lett* **258:** 290-296

Hiramatsu K (1995) Molecular evolution of MRSA. *Microbiol Immunol* **39:** 531-543

Hiron A, Falord M, Valle J, Débarbouillé M, Msadek T (2011) Bacitracin and nisin resistance in *Staphylococcus aureus*: a novel pathway involving the BraS/BraR two-component system (SA2417/SA2418) and both the BraD/BraE and VraD/VraE ABC transporters. *Mol Microbiol* **81:** 602-622

Holden MT, Hsu LY, Kurt K, Weinert LA, Mather AE, Harris SR, Strommenger B, Layer F, Witte W, de Lencastre H, Skov R, Westh H, Zemlicková H, Coombs G, Kearns AM, Hill RL, Edgeworth J, Gould I, Gant V, Cooke J, Edwards GF, McAdam PR, Templeton KE, McCann A, Zhou Z, Castillo-Ramírez S, Feil EJ, Hudson LO, Enright MC, Balloux F, Aanensen DM, Spratt BG, Fitzgerald JR, Parkhill J, Achtman M, Bentley SD, Nübel U (2013) A genomic portrait of the emergence, evolution, and global spread of a methicillin-resistant *Staphylococcus aureus* pandemic. *Genome Res* **23:** 653-664

Holland HD (2006) The oxygenation of the atmosphere and oceans. *Philos Trans R Soc Lond B Biol Sci* **361:** 903-915

Holmes A, Ganner M, McGuane S, Pitt TL, Cookson BD, Kearns AM (2005) *Staphylococcus aureus* isolates carrying Panton-Valentine leucocidin genes in England and Wales: frequency, characterization, and association with clinical disease. *J Clin Microbiol* **43:** 2384-2390

Holzinger D, Gieldon L, Mysore V, Nippe N, Taxman DJ, Duncan JA, Broglie PM, Marketon K, Austermann J, Vogl T, Foell D, Niemann S, Peters G, Roth J, Löffler B (2012) *Staphylococcus*

aureus Panton-Valentine leukocidin induces an inflammatory response in human phagocytes via the NLRP3 inflammasome. *J Leukoc Biol* **92:** 1069-1081

Hongo I, Baba T, Oishi K, Morimoto Y, Ito T, Hiramatsu K (2009) Phenol-soluble modulin alpha 3 enhances the human neutrophil lysis mediated by Panton-Valentine leukocidin. *J Infect Dis* **200:** 715-723

Horsburgh MJ, Aish JL, White IJ, Shaw L, Lithgow JK, Foster SJ (2002) sigmaB modulates virulence determinant expression and stress resistance: characterization of a functional *rsb*U strain derived from *Staphylococcus aureus* 8325-4. *J Bacteriol* **184:** 5457-5467

Ibarra JA, Pérez-Rueda E, Carroll RK, Shaw LN (2013) Global analysis of transcriptional regulators in *Staphylococcus aureus*. *BMC Genomics* **14:** 126

Ingavale S, van Wamel W, Luong TT, Lee CY, Cheung AL (2005) Rat/MgrA, a regulator of autolysis, is a regulator of virulence genes in *Staphylococcus aureus*. *Infect Immun* **73:** 1423-1431

Ito T, Katayama Y, Hiramatsu K (1999) Cloning and nucleotide sequence determination of the entire mec DNA of pre-methicillin-resistant *Staphylococcus aureus* N315. *Antimicrob Agents Chemother* **43:** 1449-1458

Janzon L, Löfdahl S, Arvidson S (1989) Identification and nucleotide sequence of the delta-lysin gene, hld, adjacent to the accessory gene regulator (*agr*) of *Staphylococcus aureus*. *Mol Gen Genet* **219:** 480-485

Jassim S, Salt WG, Stretton RJ (1989) In vitro studies of haemolysis by some staphylococci grown in chemically defined media. *J Appl Bacteriol* **67:** 511-520

Jensen RO, Winzer K, Clarke SR, Chan WC, Williams P (2008) Differential recognition of *Staphylococcus aureus* quorum-sensing signals depends on both extracellular loops 1 and 2 of the transmembrane sensor AgrC. *J Mol Biol* **381:** 300-309

Jeong DW, Cho H, Jones MB, Shatzkes K, Sun F, Ji Q, Liu Q, Peterson SN, He C, Bae T (2012) The auxiliary protein complex SaePQ activates the phosphatase activity of sensor kinase SaeS in the SaeRS two-component system of *Staphylococcus aureus*. *Mol Microbiol* **86:** 331-348

Ji G, Beavis R, Novick RP (1997) Bacterial interference caused by autoinducing peptide variants. *Science* **276:** 2027-2030

Ji G, Beavis RC, Novick RP (1995) Cell density control of staphylococcal virulence mediated by an octapeptide pheromone. *Proc Natl Acad Sci U S A* **92:** 12055-12059

Jin T, Zhu YL, Li J, Shi J, He XQ, Ding J, Xu YQ (2013) Staphylococcal protein A, Panton-Valentine leukocidin and coagulase aggravate the bone loss and bone destruction in osteomyelitis. *Cell Physiol Biochem* **32:** 322-333

Johnson AP (1998) Antibiotic resistance among clinically important gram-positive bacteria in the UK. *J Hosp Infect* **40:** 17-26

Johnstone P, Matheson AS (2013) An invisible enemy: Panton-Valentine leukocidin *Staphylococcus aureus* on deployed troops. *J R Nav Med Serv* **99:** 9-12

Joshi GS, Spontak JS, Klapper DG, Richardson AR (2011) Arginine catabolic mobile element encoded *spe*G abrogates the unique hypersensitivity of *Staphylococcus aureus* to exogenous polyamines. *Mol Microbiol* **82:** 9-20

Junio HA, Todd DA, Ettefagh KA, Ehrmann BM, Kavanaugh JS, Horswill AR, Cech NB (2013) Quantitative analysis of autoinducing peptide I (AIP-I) from *Staphylococcus aureus* cultures using ultrahigh performance liquid chromatography-high resolving power mass spectrometry. *J Chromatogr B Analyt Technol Biomed Life Sci* **930C:** 7-12

Kaito C, Saito Y, Ikuo M, Omae Y, Mao H, Nagano G, Fujiyuki T, Numata S, Han X, Obata K, Hasegawa S, Yamaguchi H, Inokuchi K, Ito T, Hiramatsu K, Sekimizu K (2013) Mobile genetic element SCC*mec*-encoded *psm-mec* RNA suppresses translation of *agr*A and attenuates MRSA virulence. *PLoS Pathog* **9:** e1003269

Kaltsas A, Guh A, Mediavilla JR, Varshney AK, Robiou N, Gialanellia P, Henry M, Levi MH, Fries BC (2011) Frequency of panton-valentine leukocidin-producing methicillin-sensitive Staphylococcus strains in patients with complicated skin and soft tissue infection in bronx, new york. *J Clin Microbiol* **49:** 2992-2995

Kaneko J, Kimura T, Narita S, Tomita T, Kamio Y (1998) Complete nucleotide sequence and molecular characterization of the temperate staphylococcal bacteriophage phiPVL carrying Panton-Valentine leukocidin genes. *Gene* **215:** 57-67

Katayama Y, Ito T, Hiramatsu K (2000) A new class of genetic element, staphylococcus cassette chromosome *mec*, encodes methicillin resistance in *Staphylococcus aureus*. *Antimicrob Agents Chemother* **44:** 1549-1555

Kawada-Matsuo M, Yoshida Y, Zendo T, Nagao J, Oogai Y, Nakamura Y, Sonomoto K, Nakamura N, Komatsuzawa H (2013) Three distinct two-component systems are involved in resistance to the class I bacteriocins, Nukacin ISK-1 and nisin A, in *Staphylococcus aureus*. *PLoS One* **8:** e69455

Khanafer N, Sicot N, Vanhems P, Dumitrescu O, Meyssonier V, Tristan A, Bès M, Lina G, Vandenesch F, Gillet Y, Etienne J (2013) Severe leukopenia in *Staphylococcus aureus*-

necrotizing, community-acquired pneumonia: risk factors and impact on survival. *BMC Infect Dis* **13:** 359

Kimmitt PT, Harwood CR, Barer MR (1999) Induction of type 2 Shiga toxin synthesis in Escherichia coli O157 by 4-quinolones. *Lancet* **353:** 1588-1589

Kinkel TL, Roux CM, Dunman PM, Fang FC (2013) The *Staphylococcus aureus* SrrAB two-component system promotes resistance to nitrosative stress and hypoxia. *MBio* **4:** e00696-00613

Kleerebezem M, Quadri LE, Kuipers OP, de Vos WM (1997) Quorum sensing by peptide pheromones and two-component signal-transduction systems in Gram-positive bacteria. *Mol Microbiol* **24:** 895-904

Klevens RM, Morrison MA, Nadle J, Petit S, Gershman K, Ray S, Harrison LH, Lynfield R, Dumyati G, Townes JM, Craig AS, Zell ER, Fosheim GE, McDougal LK, Carey RB, Fridkin SK, Investigators ABCsAM (2007) Invasive methicillin-resistant *Staphylococcus aureus* infections in the United States. *JAMA* **298:** 1763-1771

Kobayashi SD, Malachowa N, Whitney AR, Braughton KR, Gardner DJ, Long D, Bubeck Wardenburg J, Schneewind O, Otto M, Deleo FR (2011) Comparative analysis of USA300 virulence determinants in a rabbit model of skin and soft tissue infection. *J Infect Dis* **204:** 937-941

Koenig RL, Ray JL, Maleki SJ, Smeltzer MS, Hurlburt BK (2004) *Staphylococcus aureus* AgrA binding to the RNAIII-*agr* regulatory region. *J Bacteriol* **186:** 7549-7555

Kolar SL, Ibarra JA, Rivera FE, Mootz JM, Davenport JE, Stevens SM, Horswill AR, Shaw LN (2013) Extracellular proteases are key mediators of *Staphylococcus aureus* virulence via the global modulation of virulence-determinant stability. *Microbiologyopen* **2:** 18-34

Kreiswirth BN, Löfdahl S, Betley MJ, O'Reilly M, Schlievert PM, Bergdoll MS, Novick RP (1983) The toxic shock syndrome exotoxin structural gene is not detectably transmitted by a prophage. *Nature* **305:** 709-712

Kumarevel T, Tanaka T, Umehara T, Yokoyama S (2009) ST1710-DNA complex crystal structure reveals the DNA binding mechanism of the MarR family of regulators. *Nucleic Acids Res* **37:** 4723-4735

Labandeira-Rey M, Couzon F, Boisset S, Brown EL, Bes M, Benito Y, Barbu EM, Vazquez V, Höök M, Etienne J, Vandenesch F, Bowden MG (2007) *Staphylococcus aureus* Panton-Valentine leukocidin causes necrotizing pneumonia. *Science* **315:** 1130-1133

Lei MG, Cue D, Alba J, Junecko J, Graham JW, Lee CY (2012) A single copy integration vector that integrates at an engineered site on the *Staphylococcus aureus* chromosome. *BMC Res Notes* **5:** 5

Li H, Durbin R (2009) Fast and accurate short read alignment with Burrows-Wheeler transform. *Bioinformatics* **25:** 1754-1760

Li H, Handsaker B, Wysoker A, Fennell T, Ruan J, Homer N, Marth G, Abecasis G, Durbin R, Subgroup GPDP (2009a) The Sequence Alignment/Map format and SAMtools. *Bioinformatics* **25:** 2078-2079

Li M, Cheung GY, Hu J, Wang D, Joo HS, Deleo FR, Otto M (2010) Comparative analysis of virulence and toxin expression of global community-associated methicillin-resistant *Staphylococcus aureus* strains. *J Infect Dis* **202:** 1866-1876

Li M, Diep BA, Villaruz AE, Braughton KR, Jiang X, DeLeo FR, Chambers HF, Lu Y, Otto M (2009b) Evolution of virulence in epidemic community-associated methicillin-resistant *Staphylococcus aureus*. *Proc Natl Acad Sci U S A* **106:** 5883-5888

Li M, Du X, Villaruz AE, Diep BA, Wang D, Song Y, Tian Y, Hu J, Yu F, Lu Y, Otto M (2012) MRSA epidemic linked to a quickly spreading colonization and virulence determinant. *Nat Med* **18:** 816-819

Lina G, Jarraud S, Ji G, Greenland T, Pedraza A, Etienne J, Novick RP, Vandenesch F (1998) Transmembrane topology and histidine protein kinase activity of AgrC, the *agr* signal receptor in *Staphylococcus aureus*. *Mol Microbiol* **28:** 655-662

Lipinska U, Hermans K, Meulemans L, Dumitrescu O, Badiou C, Duchateau L, Haesebrouck F, Etienne J, Lina G (2011) Panton-Valentine leukocidin does play a role in the early stage of *Staphylococcus aureus* skin infections: a rabbit model. *PLoS One* **6:** e22864

Liu Y, Manna AC, Pan CH, Kriksunov IA, Thiel DJ, Cheung AL, Zhang G (2006) Structural and function analyses of the global regulatory protein SarA from *Staphylococcus aureus*. *Proc Natl Acad Sci U S A* **103:** 2392-2397

Loughman JA, Fritz SA, Storch GA, Hunstad DA (2009) Virulence gene expression in human community-acquired *Staphylococcus aureus* infection. *J Infect Dis* **199:** 294-301

Luong TT, Dunman PM, Murphy E, Projan SJ, Lee CY (2006) Transcription Profiling of the *mgr*A Regulon in *Staphylococcus aureus*. *J Bacteriol* **188:** 1899-1910

Löffler B, Hussain M, Grundmeier M, Brück M, Holzinger D, Varga G, Roth J, Kahl BC, Proctor RA, Peters G (2010) *Staphylococcus aureus* panton-valentine leukocidin is a very potent cytotoxic factor for human neutrophils. *PLoS Pathog* **6:** e1000715

Ma XX, Ito T, Tiensasitorn C, Jamklang M, Chongtrakool P, Boyle-Vavra S, Daum RS, Hiramatsu K (2002) Novel type of staphylococcal cassette chromosome *mec* identified in community-acquired methicillin-resistant *Staphylococcus aureus* strains. *Antimicrob Agents Chemother* **46:** 1147-1152

Malachowa N, Whitney AR, Kobayashi SD, Sturdevant DE, Kennedy AD, Braughton KR, Shabb DW, Diep BA, Chambers HF, Otto M, DeLeo FR (2011) Global changes in *Staphylococcus aureus* gene expression in human blood. *PLoS One* **6:** e18617

Manna AC, Cheung AL (2003) sarU, a sarA homolog, is repressed by SarT and regulates virulence genes in *Staphylococcus aureus*. *Infect Immun* **71:** 343-353

Matsuhashi M, Song MD, Ishino F, Wachi M, Doi M, Inoue M, Ubukata K, Yamashita N, Konno M (1986) Molecular cloning of the gene of a penicillin-binding protein supposed to cause high resistance to beta-lactam antibiotics in *Staphylococcus aureus*. *J Bacteriol* **167:** 975-980

Matsuo M, Kato F, Oogai Y, Kawai T, Sugai M, Komatsuzawa H (2010) Distinct two-component systems in methicillin-resistant *Staphylococcus aureus* can change the susceptibility to antimicrobial agents. *J Antimicrob Chemother* **65:** 1536-1537

Mayville P, Ji G, Beavis R, Yang H, Goger M, Novick RP, Muir TW (1999) Structure-activity analysis of synthetic autoinducing thiolactone peptides from *Staphylococcus aureus* responsible for virulence. *Proc Natl Acad Sci U S A* **96:** 1218-1223

McCallum N, Bischoff M, Maki H, Wada A, Berger-Bächi B (2004) TcaR, a putative MarR-like regulator of sarS expression. *J Bacteriol* **186:** 2966-2972

McCarthy AJ, Witney AA, Lindsay JA (2012) *Staphylococcus aureus* temperate bacteriophage: carriage and horizontal gene transfer is lineage associated. *Front Cell Infect Microbiol* **2:** 6

McDowell P, Affas Z, Reynolds C, Holden MT, Wood SJ, Saint S, Cockayne A, Hill PJ, Dodd CE, Bycroft BW, Chan WC, Williams P (2001) Structure, activity and evolution of the group I thiolactone peptide quorum-sensing system of *Staphylococcus aureus*. *Mol Microbiol* **41:** 503-512

McNamara PJ, Bayer AS (2005) A *rot* mutation restores parental virulence to an *agr*-null *Staphylococcus aureus* strain in a rabbit model of endocarditis. *Infect Immun* **73:** 3806-3809

McNamara PJ, Milligan-Monroe KC, Khalili S, Proctor RA (2000) Identification, cloning, and initial characterization of *rot*, a locus encoding a regulator of virulence factor expression in *Staphylococcus aureus*. *J Bacteriol* **182:** 3197-3203

Melzer M, Eykyn SJ, Gransden WR, Chinn S (2003) Is methicillin-resistant *Staphylococcus aureus* more virulent than methicillin-susceptible *S. aureus*? A comparative cohort study of British patients with nosocomial infection and bacteremia. *Clin Infect Dis* **37:** 1453-1460

Meunier O, Falkenrodt A, Monteil H, Colin DA (1995) Application of flow cytometry in toxinology: pathophysiology of human polymorphonuclear leukocytes damaged by a pore-forming toxin from *Staphylococcus aureus*. *Cytometry* **21:** 241-247

Moran GJ, Krishnadasan A, Gorwitz RJ, Fosheim GE, McDougal LK, Carey RB, Talan DA, Group EINS (2006) Methicillin-resistant *S. aureus* infections among patients in the emergency department. *N Engl J Med* **355:** 666-674

Morfeldt E, Taylor D, von Gabain A, Arvidson S (1995) Activation of alpha-toxin translation in *Staphylococcus aureus* by the trans-encoded antisense RNA, RNAIII. *EMBO J* **14:** 4569-4577

Niemann S, Ehrhardt C, Medina E, Warnking K, Tuchscherr L, Heitmann V, Ludwig S, Peters G, Löffler B (2012) Combined action of influenza virus and *Staphylococcus aureus* panton-valentine leukocidin provokes severe lung epithelium damage. *J Infect Dis* **206:** 1138-1148

Nikolskaya AN, Galperin MY (2002) A novel type of conserved DNA-binding domain in the transcriptional regulators of the AlgR/AgrA/LytR family. *Nucleic Acids Res* **30:** 2453-2459

Nimmo GR, Coombs GW (2008) Community-associated methicillin-resistant *Staphylococcus aureus* (MRSA) in Australia. *Int J Antimicrob Agents* **31:** 401-410

Novick RP (2003) Autoinduction and signal transduction in the regulation of staphylococcal virulence. *Mol Microbiol* **48:** 1429-1449

Novick RP, Jiang D (2003) The staphylococcal *sae*RS system coordinates environmental signals with *agr* quorum sensing. *Microbiology* **149:** 2709-2717

Novick RP, Projan SJ, Kornblum J, Ross HF, Ji G, Kreiswirth B, Vandenesch F, Moghazeh S (1995) The *agr* P2 operon: an autocatalytic sensory transduction system in *Staphylococcus aureus*. *Mol Gen Genet* **248:** 446-458

Novick RP, Ross HF, Projan SJ, Kornblum J, Kreiswirth B, Moghazeh S (1993) Synthesis of staphylococcal virulence factors is controlled by a regulatory RNA molecule. *EMBO J* **12:** 3967-3975

O'Hara FP, Amrine-Madsen H, Mera RM, Brown ML, Close NM, Suaya JA, Acosta CJ (2012) Molecular characterization of *Staphylococcus aureus* in the United States 2004-2008 reveals the rapid expansion of USA300 among inpatients and outpatients. *Microb Drug Resist* **18:** 555-561

O'Neill E, Pozzi C, Houston P, Humphreys H, Robinson DA, Loughman A, Foster TJ, O'Gara JP (2008) A novel *Staphylococcus aureus* biofilm phenotype mediated by the fibronectin-binding proteins, FnBPA and FnBPB. *J Bacteriol* **190:** 3835-3850

Ohlsen K, Ziebuhr W, Koller KP, Hell W, Wichelhaus TA, Hacker J (1998) Effects of subinhibitory concentrations of antibiotics on alpha-toxin (*hla*) gene expression of methicillin-sensitive and methicillin-resistant *Staphylococcus aureus* isolates. *Antimicrob Agents Chemother* **42:** 2817-2823

Otokunefor K, Sloan T, Kearns AM, James R (2012) Molecular characterization and panton-valentine leucocidin typing of community-acquired methicillin-sensitive *Staphylococcus aureus* clinical isolates. *J Clin Microbiol* **50:** 3069-3072

Otter JA, Havill NL, Boyce JM, French GL (2009) Comparison of community-associated methicillin-resistant *Staphylococcus aureus* from teaching hospitals in London and the USA, 2004-2006: where is USA300 in the UK? *Eur J Clin Microbiol Infect Dis* **28:** 835-839

Otto M (2013) Community-associated MRSA: what makes them special? *Int J Med Microbiol* **303:** 324-330

Panton P, Came M, Valentine F (1932) Staphylococcal Toxin. *Lancet* **1:** 506-508

Pasquale TR, Jabrocki B, Salstrom SJ, Wiemken TL, Peyrani P, Haque NZ, Scerpella EG, Ford KD, Zervos MJ, Ramirez JA, File TM, Group I-HS (2013) Emergence of methicillin-resistant *Staphylococcus aureus* USA300 genotype as a major cause of late-onset nosocomial pneumonia in intensive care patients in the USA. *Int J Infect Dis* **17:** e398-403

Peterson PK, Verhoef J, Sabath LD, Quie PG (1977) Effect of protein A on staphylococcal opsonization. *Infect Immun* **15:** 760-764

Pietiäinen M, François P, Hyyryläinen HL, Tangomo M, Sass V, Sahl HG, Schrenzel J, Kontinen VP (2009) Transcriptome analysis of the responses of *Staphylococcus aureus* to antimicrobial peptides and characterization of the roles of *vra*DE and *vra*SR in antimicrobial resistance. *BMC Genomics* **10:** 429

Pinto AN, Seth R, Zhou F, Tallon J, Dempsey K, Tracy M, Gilbert GL, O'Sullivan MV (2013) Emergence and control of an outbreak of infections due to Panton-Valentine leukocidin positive, ST22 methicillin-resistant *Staphylococcus aureus* in a neonatal intensive care unit. *Clin Microbiol Infect* **19:** 620-627

Pope SD, Roecker AM (2007) Vancomycin for treatment of invasive, multi-drug resistant *Staphylococcus aureus* infections. *Expert Opin Pharmacother* **8:** 1245-1261

Pragman AA, Yarwood JM, Tripp TJ, Schlievert PM (2004) Characterization of virulence factor regulation by SrrAB, a two-component system in *Staphylococcus aureus*. *J Bacteriol* **186:** 2430-2438

Qazi SN, Counil E, Morrissey J, Rees CE, Cockayne A, Winzer K, Chan WC, Williams P, Hill PJ (2001) *agr* expression precedes escape of internalized *Staphylococcus aureus* from the host endosome. *Infect Immun* **69:** 7074-7082

Qiu R, Pei W, Zhang L, Lin J, Ji G (2005) Identification of the putative staphylococcal AgrB catalytic residues involving the proteolytic cleavage of AgrD to generate autoinducing peptide. *J Biol Chem* **280:** 16695-16704

Que YA, Haefliger JA, Piroth L, François P, Widmer E, Entenza JM, Sinha B, Herrmann M, Francioli P, Vaudaux P, Moreillon P (2005) Fibrinogen and fibronectin binding cooperate for valve infection and invasion in *Staphylococcus aureus* experimental endocarditis. *J Exp Med* **201:** 1627-1635

Queck SY, Jameson-Lee M, Villaruz AE, Bach TH, Khan BA, Sturdevant DE, Ricklefs SM, Li M, Otto M (2008) RNAIII-independent target gene control by the *agr* quorum-sensing system: insight into the evolution of virulence regulation in *Staphylococcus aureus*. *Mol Cell* **32:** 150-158

Rahman A, Izaki K, Kato I, Kamio Y (1991) Nucleotide sequence of leukocidin S-component gene (*lukS*) from methicillin resistant *Staphylococcus aureus*. *Biochem Biophys Res Commun* **181:** 138-144

Rasigade JP, Laurent F, Lina G, Meugnier H, Bes M, Vandenesch F, Etienne J, Tristan A (2010) Global distribution and evolution of Panton-Valentine leukocidin-positive methicillin-susceptible *Staphylococcus aureus*, 1981-2007. *J Infect Dis* **201:** 1589-1597

Recsei P, Kreiswirth B, O'Reilly M, Schlievert P, Gruss A, Novick RP (1986) Regulation of exoprotein gene expression in *Staphylococcus aureus* by *agar*. *Mol Gen Genet* **202:** 58-61

Regassa LB, Betley MJ (1992) Alkaline pH decreases expression of the accessory gene regulator (*agr*) in *Staphylococcus aureus*. *J Bacteriol* **174:** 5095-5100

Reynolds J, Wigneshweraraj S (2011) Molecular insights into the control of transcription initiation at the *Staphylococcus aureus agr* operon. *J Mol Biol* **412:** 862-881

Rooijakkers SH, Ruyken M, Roos A, Daha MR, Presanis JS, Sim RB, van Wamel WJ, van Kessel KP, van Strijp JA (2005a) Immune evasion by a staphylococcal complement inhibitor that acts on C3 convertases. *Nat Immunol* **6:** 920-927

Rooijakkers SH, van Wamel WJ, Ruyken M, van Kessel KP, van Strijp JA (2005b) Anti-opsonic properties of staphylokinase. *Microbes Infect* **7:** 476-484

Rudkin JK, Edwards AM, Bowden MG, Brown EL, Pozzi C, Waters EM, Chan WC, Williams P, O'Gara JP, Massey RC (2012) Methicillin resistance reduces the virulence of healthcare-associated methicillin-resistant *Staphylococcus aureus* by interfering with the *agr* quorum sensing system. *J Infect Dis* **205:** 798-806

Rudkin JK, Laabei M, Edwards AM, Joo HS, Otto M, Lennon KL, O'Gara JP, Waterfield NR, Massey RC (2013) Oxacillin alters the toxin expression profile of Community Associated-MRSA. *Antimicrob Agents Chemother*

Rutherford ST, Bassler BL (2012) Bacterial quorum sensing: its role in virulence and possibilities for its control. *Cold Spring Harb Perspect Med* **2**

Rybak MJ, Lomaestro BM, Rotschafer JC, Moellering RC, Craig WA, Billeter M, Dalovisio JR, Levine DP (2009) Therapeutic monitoring of vancomycin in adults summary of consensus recommendations from the American Society of Health-System Pharmacists, the Infectious Diseases Society of America, and the Society of Infectious Diseases Pharmacists. *Pharmacotherapy* **29:** 1275-1279

Saenz HL, Augsburger V, Vuong C, Jack RW, Götz F, Otto M (2000) Inducible expression and cellular location of AgrB, a protein involved in the maturation of the staphylococcal quorum-sensing pheromone. *Arch Microbiol* **174:** 452-455

Sakoulas G, Moellering RC (2008) Increasing antibiotic resistance among methicillin-resistant *Staphylococcus aureus* strains. *Clin Infect Dis* **46 Suppl 5:** S360-367

Sakwinska O, Kuhn G, Balmelli C, Francioli P, Giddey M, Perreten V, Riesen A, Zysset F, Blanc DS, Moreillon P (2009) Genetic diversity and ecological success of *Staphylococcus aureus* strains colonizing humans. *Appl Environ Microbiol* **75:** 175-183

Saïd-Salim B, Dunman PM, McAleese FM, Macapagal D, Murphy E, McNamara PJ, Arvidson S, Foster TJ, Projan SJ, Kreiswirth BN (2003) Global regulation of *Staphylococcus aureus* genes by Rot. *J Bacteriol* **185:** 610-619

Schlag S, Fuchs S, Nerz C, Gaupp R, Engelmann S, Liebeke M, Lalk M, Hecker M, Götz F (2008) Characterization of the oxygen-responsive NreABC regulon of *Staphylococcus aureus*. *J Bacteriol* **190:** 7847-7858

Schwan WR, Langhorne MH, Ritchie HD, Stover CK (2003) Loss of hemolysin expression in *Staphylococcus aureus agr* mutants correlates with selective survival during mixed infections in murine abscesses and wounds. *FEMS Immunol Med Microbiol* **38:** 23-28

Shallcross LJ, Fragaszy E, Johnson AM, Hayward AC (2013) The role of the Panton-Valentine leucocidin toxin in staphylococcal disease: a systematic review and meta-analysis. *Lancet Infect Dis* **13:** 43-54

Sharma-Kuinkel BK, Mann EE, Ahn JS, Kuechenmeister LJ, Dunman PM, Bayles KW (2009) The *Staphylococcus aureus* LytSR two-component regulatory system affects biofilm formation. *J Bacteriol* **191:** 4767-4775

Shine J, Dalgarno L (1974) The 3'-terminal sequence of Escherichia coli 16S ribosomal RNA: complementarity to nonsense triplets and ribosome binding sites. *Proc Natl Acad Sci U S A* **71:** 1342-1346

Shopsin B, Drlica-Wagner A, Mathema B, Adhikari RP, Kreiswirth BN, Novick RP (2008) Prevalence of *agr* dysfunction among colonizing *Staphylococcus aureus* strains. *J Infect Dis* **198:** 1171-1174

Shopsin B, Eaton C, Wasserman GA, Mathema B, Adhikari RP, Agolory S, Altman DR, Holzman RS, Kreiswirth BN, Novick RP (2010) Mutations in *agr* do not persist in natural populations of methicillin-resistant *Staphylococcus aureus*. *J Infect Dis* **202:** 1593-1599

Sina H, Ahoyo TA, Moussaoui W, Keller D, Bankolé HS, Barogui Y, Stienstra Y, Kotchoni SO, Prévost G, Baba-Moussa L (2013) Variability of antibiotic susceptibility and toxin production of *Staphylococcus aureus* strains isolated from skin, soft tissue, and bone related infections. *BMC Microbiol* **13:** 188

Skaar EP, Humayun M, Bae T, DeBord KL, Schneewind O (2004) Iron-source preference of *Staphylococcus aureus* infections. *Science* **305:** 1626-1628

Smyth DS, Robinson DA (2009) Integrative and sequence characteristics of a novel genetic element, ICE6013, in *Staphylococcus aureus*. *J Bacteriol* **191:** 5964-5975

Somerville GA, Beres SB, Fitzgerald JR, DeLeo FR, Cole RL, Hoff JS, Musser JM (2002) In vitro serial passage of *Staphylococcus aureus*: changes in physiology, virulence factor production, and *agr* nucleotide sequence. *J Bacteriol* **184:** 1430-1437

Spaan AN, Henry T, van Rooijen WJ, Perret M, Badiou C, Aerts PC, Kemmink J, de Haas CJ, van Kessel KP, Vandenesch F, Lina G, van Strijp JA (2013) The staphylococcal toxin Panton-Valentine Leukocidin targets human C5a receptors. *Cell Host Microbe* **13:** 584-594

Sterba KM, Mackintosh SG, Blevins JS, Hurlburt BK, Smeltzer MS (2003) Characterization of *Staphylococcus aureus* SarA binding sites. *J Bacteriol* **185:** 4410-4417

Stevens DL, Ma Y, Salmi DB, McIndoo E, Wallace RJ, Bryant AE (2007) Impact of antibiotics on expression of virulence-associated exotoxin genes in methicillin-sensitive and methicillin-resistant *Staphylococcus aureus*. *J Infect Dis* **195:** 202-211

Stock JB, Ninfa AJ, Stock AM (1989) Protein phosphorylation and regulation of adaptive responses in bacteria. *Microbiol Rev* **53:** 450-490

Sueke H, Shankar J, Neal T, Winstanley C, Tuft S, Coates R, Horsburgh MJ, Kaye S, Group MO (2013) *lukSF-PV* in *Staphylococcus aureus* keratitis isolates and association with clinical outcome. *Invest Ophthalmol Vis Sci* **54:** 3410-3416

Sun J, Zheng L, Landwehr C, Yang J, Ji Y (2005) Identification of a novel essential two-component signal transduction system, YhcSR, in *Staphylococcus aureus*. *J Bacteriol* **187:** 7876-7880

Tamber S, Schwartzman J, Cheung AL (2010) Role of PknB kinase in antibiotic resistance and virulence in community-acquired methicillin-resistant *Staphylococcus aureus* strain USA300. *Infect Immun* **78:** 3637-3646

Tegmark K, Karlsson A, Arvidson S (2000) Identification and characterization of SarH1, a new global regulator of virulence gene expression in *Staphylococcus aureus*. *Mol Microbiol* **37:** 398-409

Teixeira N, Santos S, Marujo P, Yokohata R, Iyer VS, Nakayama J, Hancock LE, Serror P, Silva Lopes MeF (2012) The incongruent gelatinase genotype and phenotype in *Enterococcus faecalis* are due to shutting off the ability to respond to the gelatinase biosynthesis-activating pheromone (GBAP) quorum-sensing signal. *Microbiology* **158:** 519-528

Thakker M, Park JS, Carey V, Lee JC (1998) *Staphylococcus aureus* serotype 5 capsular polysaccharide is antiphagocytic and enhances bacterial virulence in a murine bacteremia model. *Infect Immun* **66:** 5183-5189

Thurlow LR, Joshi GS, Clark JR, Spontak JS, Neely CJ, Maile R, Richardson AR (2013) Functional modularity of the arginine catabolic mobile element contributes to the success of USA300 methicillin-resistant *Staphylococcus aureus*. *Cell Host Microbe* **13:** 100-107

Torres VJ, Stauff DL, Pishchany G, Bezbradica JS, Gordy LE, Iturregui J, Anderson KL, Dunman PM, Joyce S, Skaar EP (2007) A *Staphylococcus aureus* regulatory system that responds to host heme and modulates virulence. *Cell Host Microbe* **1:** 109-119

Traber KE, Lee E, Benson S, Corrigan R, Cantera M, Shopsin B, Novick RP (2008) *agr* function in clinical *Staphylococcus aureus* isolates. *Microbiology* **154:** 2265-2274

Ulrich M, Bastian M, Cramton SE, Ziegler K, Pragman AA, Bragonzi A, Memmi G, Wolz C, Schlievert PM, Cheung A, Döring G (2007) The staphylococcal respiratory response regulator SrrAB induces *ica* gene transcription and polysaccharide intercellular adhesin expression, protecting *Staphylococcus aureus* from neutrophil killing under anaerobic growth conditions. *Mol Microbiol* **65:** 1276-1287

van Wamel WJ, Rooijakkers SH, Ruyken M, van Kessel KP, van Strijp JA (2006) The innate immune modulators staphylococcal complement inhibitor and chemotaxis inhibitory protein of *Staphylococcus aureus* are located on beta-hemolysin-converting bacteriophages. *J Bacteriol* **188:** 1310-1315

Vandenesch F, Kornblum J, Novick RP (1991) A temporal signal, independent of *agr*, is required for *hla* but not *spa* transcription in *Staphylococcus aureus*. *J Bacteriol* **173:** 6313-6320

Vandenesch F, Lina G, Henry T (2012) *Staphylococcus aureus* hemolysins, bi-component leukocidins, and cytolytic peptides: a redundant arsenal of membrane-damaging virulence factors? *Front Cell Infect Microbiol* **2:** 12

Vandenesch F, Naimi T, Enright MC, Lina G, Nimmo GR, Heffernan H, Liassine N, Bes M, Greenland T, Reverdy ME, Etienne J (2003) Community-acquired methicillin-resistant *Staphylococcus aureus* carrying Panton-Valentine leukocidin genes: worldwide emergence. *Emerg Infect Dis* **9:** 978-984

Varshney AK, Martinez LR, Hamilton SM, Bryant AE, Levi MH, Gialanella P, Stevens DL, Fries BC (2010) Augmented production of Panton-Valentine leukocidin toxin in methicillin-resistant and methicillin-susceptible *Staphylococcus aureus* is associated with worse outcome in a murine skin infection model. *J Infect Dis* **201:** 92-96

Villaruz AE, Bubeck Wardenburg J, Khan BA, Whitney AR, Sturdevant DE, Gardner DJ, DeLeo FR, Otto M (2009) A point mutation in the *agr* locus rather than expression of the Panton-Valentine leukocidin caused previously reported phenotypes in *Staphylococcus aureus* pneumonia and gene regulation. *J Infect Dis* **200:** 724-734

Vourli S, Vagiakou H, Ganteris G, Orfanidou M, Polemis M, Vatopoulos A, Malamou-Ladas H (2009) High rates of community-acquired, Panton-Valentine leukocidin (PVL)- positive methicillin-resistant S. aureus (MRSA) infections in adult outpatients in Greece. *Euro Surveill* **14**

Voyich JM, Otto M, Mathema B, Braughton KR, Whitney AR, Welty D, Long RD, Dorward DW, Gardner DJ, Lina G, Kreiswirth BN, DeLeo FR (2006) Is Panton-Valentine leukocidin the major virulence determinant in community-associated methicillin-resistant *Staphylococcus aureus* disease? *J Infect Dis* **194:** 1761-1770

Vuong C, Kocianova S, Yao Y, Carmody AB, Otto M (2004) Increased colonization of indwelling medical devices by quorum-sensing mutants of *Staphylococcus epidermidis in vivo*. *J Infect Dis* **190:** 1498-1505

Vuong C, Saenz HL, Götz F, Otto M (2000) Impact of the *agr* quorum-sensing system on adherence to polystyrene in *Staphylococcus aureus*. *J Infect Dis* **182:** 1688-1693

Wang R, Braughton KR, Kretschmer D, Bach TH, Queck SY, Li M, Kennedy AD, Dorward DW, Klebanoff SJ, Peschel A, DeLeo FR, Otto M (2007) Identification of novel cytolytic peptides as key virulence determinants for community-associated MRSA. *Nat Med* **13:** 1510-1514

Wertheim HF, Melles DC, Vos MC, van Leeuwen W, van Belkum A, Verbrugh HA, Nouwen JL (2005) The role of nasal carriage in *Staphylococcus aureus* infections. *Lancet Infect Dis* **5:** 751-762

Wertheim HF, Walsh E, Choudhurry R, Melles DC, Boelens HA, Miajlovic H, Verbrugh HA, Foster T, van Belkum A (2008) Key role for clumping factor B in *Staphylococcus aureus* nasal colonization of humans. *PLoS Med* **5:** e17

Williams P, Camara M, Hardman A, Swift S, Milton D, Hope VJ, Winzer K, Middleton B, Pritchard DI, Bycroft BW (2000) Quorum sensing and the population-dependent control of virulence. *Philos Trans R Soc Lond B Biol Sci* **355:** 667-680

Winzer K, Williams P (2001) Quorum sensing and the regulation of virulence gene expression in pathogenic bacteria. *Int J Med Microbiol* **291:** 131-143

Wirtz C, Witte W, Wolz C, Goerke C (2009) Transcription of the phage-encoded Panton-Valentine leukocidin of *Staphylococcus aureus* is dependent on the phage life-cycle and on the host background. *Microbiology* **155:** 3491-3499

Withers H, Swift S, Williams P (2001) Quorum sensing as an integral component of gene regulatory networks in Gram-negative bacteria. *Curr Opin Microbiol* **4:** 186-193

Witte W (2004) International dissemination of antibiotic resistant strains of bacterial pathogens. *Infect Genet Evol* **4:** 187-191

Wolkewitz M, Frank U, Philips G, Schumacher M, Davey P, Group BS (2011) Mortality associated with in-hospital bacteraemia caused by *Staphylococcus aureus*: a multistate analysis with follow-up beyond hospital discharge. *J Antimicrob Chemother* **66:** 381-386

Wright JS, Jin R, Novick RP (2005a) Transient interference with staphylococcal quorum sensing blocks abscess formation. *Proc Natl Acad Sci U S A* **102:** 1691-1696

Wright JS, Traber KE, Corrigan R, Benson SA, Musser JM, Novick RP (2005b) The *agr* radiation: an early event in the evolution of staphylococci. *J Bacteriol* **187:** 5585-5594

Xia G, Wolz C (2013) Phages of *Staphylococcus aureus* and their impact on host evolution. *Infect Genet Evol*

Xiong YQ, Van Wamel W, Nast CC, Yeaman MR, Cheung AL, Bayer AS (2002) Activation and transcriptional interaction between *agr* RNAII and RNAIII in *Staphylococcus aureus in vitro* and in an experimental endocarditis model. *J Infect Dis* **186:** 668-677

Zerbino DR, Birney E (2008) Velvet: algorithms for de novo short read assembly using de Bruijn graphs. *Genome Res* **18:** 821-829

Zhang S, Stewart GC (2000) Characterization of the promoter elements for the staphylococcal enterotoxin D gene. *J Bacteriol* **182:** 2321-2325

Zhao C, Liu Y, Zhao M, Yu Y, Chen H, Sun Q, Jiang W, Han S, Xu Y, Chen M, Cao B, Wang H (2012) Characterization of community acquired *Staphylococcus aureus* associated with skin and soft tissue infection in Beijing: high prevalence of PVL+ ST398. *PLoS One* **7:** e38577

7 Appendices

7.1 Non-synonymous SNPs found in TS13 only

A complete list of SNPs which were unique to TS13 and resulted in coding sequence changes (section 3.2.5.4). The location numbers indicate the base position on the reference strain HO 5096 0412 with both the reference base and TS13 variant shown. The coding sequence ID from the reference annotation is in column 4 with the annotated gene name (if known) in column 5 and description in column 6.

Location	Reference	TS13	Coding Sequence ID	Gene product	Description
116754	G	A	920	-	putative_membrane_protein
116755	G	A	920	-	putative_membrane_protein
182155	G	A	1480	argJ	putative_arginine_biosynthesis_bifunctional_protein
296240	G	A	2370	-	putative_membrane_protein
303593	G	A	2420	-	putative_membrane_protein
352330	C	G	2880	-	putative_PTS_multidomain_regulator
413095	G	A	3490	-	hypothetical_protein
440311	G	T	3770	-	putative_NADH-Ubiquinone/plastoquinone_(complex_I)_protein
458517	C	T	3960	-	LysR-family_regulatory_protein
499087	G	A	4280	-	putative_peptidyl-tRNA_hydrolase
546662	G	A	4570	-	conserved_hypothetical_protein
594078	T	C	4930	-	conserved_hypothetical_protein
637356	G	A	5400	-	putative_hydrolase
676430	C	G	5800	-	putative_membrane_protein
714778	C	T	6180	-	putative_membrane_protein

736167	T	C	6410	-	putative_para-aminobenzoate_synthetase_component
933720	A	G	8230	-	putative_oligopeptide_transport_system_permease_protein_(pseudogene)
1044535	C	T	9260	pdhD	dihydrolipoamide_dehydrogenase
1074548	G	A	9580	isdB	iron-regulated_heme-iron_binding_protein_(pseudogene)
1243331	T	C	11110	-	conserved_hypothetical_protein
1253375	A	G	11200	-	transposase_(fragment)
1256697	A	G	11240	-	putative_pyruvate_flavodoxin/ferredoxin_oxidoreductase
1314907	A	G	11870	-	putative_membrane_protein
1322367	T	A	11930	-	putative_exonuclease
1384978	G	C	12500	-	ABC_transporter_ATP-binding_protein
1449776	C	T	12970	ebh	very_large_surface_anchored_protein_(pseudogene)
1481909	C	A	13120	-	putative_exported_protein
1605227	T	A	14460	-	conserved_hypothetical_protein
1606147	G	A	14470	accC	biotin_carboxylase_subunit_of_acetyl-CoA_carboxylase
1638949	A	G	14840	-	conserved_hypothetical_protein,_pseudogene
1663284	A	T	15070	-	putative_membrane_protein
1713713	T	A	15560	tgt	queuine_tRNA-ribosyltransferase
1827886	T	C	16530	-	putative_aminopeptidase
1853199	C	T	16710	-	transposase
1881489	T	G	16990	pckA	phosphoenolpyruvate_carboxykinase
1883817	C	A	17020	-	conserved_hypothetical_protein
1924033	G	A	17480	-	putative_membrane_protein
1995463	C	A	18090	putP	high_affinity_proline_permease
2007441	A	G	18180	-	transposase_(fragment)
2007881	C	A	18190	-	transposase_(fragment)
2007902	T	C	18190	-	transposase_(fragment)
2017193	C	T	18280	-	isochorismatase_family_protein
2027595	T	A	18370	-	Tn554-related,_transposase_B

2035006	C	T	18470	-	putative_ABC_transporter_ATP-binding_protein
2038477	T	C	18510	-	hypothetical_protein
2108636	A	T	19460	agrC	autoinducer_sensor_protein
2160133	G	A	19870	kdpA	putative_potassium-transporting_ATPase_a_chain
2293253	G	A	21030	-	hypothetical_protein
2405583	G	A	22290	hutU	urocanate_hydratase
2424120	G	A	22480	-	hypothetical_protein
2492551	A	T	23120	-	transport_system_membrane_protein
2509829	G	A	23280	-	transposase_(fragment)
2509877	G	A	23280	-	transposase_(fragment)
2510039	A	G	23280	-	transposase_(fragment)
2540395	T	G	23510	-	putative_carboxylesterase
2584539	G	T	23940	-	putative_membrane_protein
2586266	C	T	23950	sasG	LPXTG_surface_protein_(pseudogene)
2586704	A	G	23950	sasG	LPXTG_surface_protein_(pseudogene)
2589488	G	T	23970	-	putative_staphylococcal_accessory_regulator
2595084	G	A	24010	gntP	putative_gluconate_permease
2597763	T	C	24030	gntR	gluconate_operon_transcriptional_repressor
2608565	G	T	24120	-	ABC_transporter_ATP-binding_protein
2614629	G	T	24170	-	putative_dioxygenase
2639555	G	A	24450	-	LysR-family_regulatory_protein
2645865	A	G	24510	clpL	putative_ATP-dependent_protease_ATP-binding_subunit_ClpL
2664626	G	T	24660	-	putative_glycosyltransferase
2666092	C	T	24670	-	putative_phytoene_dehydrogenase_related_protein
2737433	G	A	25350	clfB	fibrinogen_and_keratin-10_binding_surfaced_anchored_protein
2737646	T	C	25350	clfB	fibrinogen_and_keratin-10_binding_surfaced_anchored_protein
2737658	A	G	25350	clfB	fibrinogen_and_keratin-10_binding_surfaced_anchored_protein
2737661	A	G	25350	clfB	fibrinogen_and_keratin-10_binding_surfaced_anchored_protein

2737673	G	A	25350	clfB	fibrinogen_and_keratin-10_binding_surfaced_anchored_protein
2737685	A	G	25350	clfB	fibrinogen_and_keratin-10_binding_surfaced_anchored_protein
2791513	A	G	25750	icaB	intercellular_adhesion_protein_B
2810175	T	C	25930	cna	collagen_adhesin_precursor
2810187	A	G	25930	cna	collagen_adhesin_precursor
2810190	T	C	25930	cna	collagen_adhesin_precursor
2810331	C	T	25930	cna	collagen_adhesin_precursor

7.2 Non-synonymous SNPs found in TS14 only

A complete list of SNPs which were unique to TS14 and resulted in coding sequence changes (section 3.2.5.4). The location numbers indicate the base position on the reference strain HO 5096 0412 with both the reference base and TS14 variant shown. The coding sequence ID from the reference annotation is in column 4 with the annotated gene name (if known) in column 5 and description in column 6.

Location	Reference	TS14	Coding Sequence ID	Gene product	Description
36913	G	T	270	-	putative_transposase
68139	A	T	520	-	TetR_family_regulatory_protein
68141	A	C	520	-	TetR_family_regulatory_protein
131435	T	C	1070	-	binding-protein-dependent_transport_system_membrane_component
166233	G	A	1380	-	putative_lipoprotein
168047	T	G	1400	-	conserved_hypothetical_protein,_pseudogene
271844	C	T	2160	-	hypothetical_protein
284663	G	A	2260	bglA	6-phospho-beta-glucosidase
361479	C	A	2960	-	putative_membrane_protein
382759	A	G	3160	-	putative_membrane_protein
540747	C	T	4520	radA	putative_DNA_repair_protein
561505	A	G	4720	rpsL	30S_ribosomal_protein_S12
688820	G	A	5910	-	putative_exported_protein
691792	C	T	5930	-	AraC_family_regulatory_protein
704056	A	C	6090	bacA	putative_undecaprenol_kinase
720120	C	T	6250	-	putative_phosphofructokinase
742346	G	A	6460	-	ABC_transporter_ATP-binding_protein
787395	C	T	6850	uvrA	excinuclease_ABC_subunit_A

878668	A	G	7770	mnhF	Na+/H+_antiporter_subunit
886859	G	A	7860	-	NADH:flavin_oxidoreductase_/_NADH_oxidase_family_protein
963079	G	A	8500	prfC	peptide_chain_release_factor_3
1015251	C	T	9000	purL	putative_phosphoribosylformylglycinamidine_synthase_II
1125117	C	T	10100	-	conserved_hypothetical_protein
1143560	A	G	10270	-	glyoxalase/bleomycin_resistance_protein/dioxygenase_superfamily_protein_(pseudogene)
1158601	G	A	10410	-	conserved_hypothetical_protein
1224943	G	T	10970	polC	DNA_polymerase_III_PolC-type
1228731	C	T	10990	nusA	putative_N_utilization_substance_protein_A
1253708	C	A	11200	-	transposase_(fragment)
1271854	G	A	11360	-	putative_hydrolase
1351231	A	T	12150	trpE	anthranilate_synthase_component_I
1432637	C	T	12970	ebh	very_large_surface_anchored_protein_(pseudogene)
1567552	G	A	13480	-	hypothetical_protein,_pseudogene
1589216	C	G	14310	-	glyoxalase/bleomycin_resistance_protein/dioxygenase_superfamily_protein
1652227	A	G	14990	dnaJ	chaperone_protein
1673889	T	C	15210	-	hypothetical_phage_protein
1686714	G	C	15360	alaS	putative_alanyl-tRNA_synthetase
1705223	C	T	15510	relA	GTP_pyrophosphokinase
1851017	C	A	16680	-	conserved_hypothetical_protein
1883618	C	T	17020	-	conserved_hypothetical_protein
1916224	G	A	17390	trap	signal_transduction_protein
2162741	G	T	19880	kdpD	sensor_kinase_protein
2177589	T	C	20030	tenA	transcriptional_activator
2178861	C	T	20040	-	putative_exported_protein
2235170	A	G	20620	mtlA	PTS_system,_mannitol-specific_IIBC_component
2240552	C	G	20660	fmtB	putative_surface_anchored_protein
2249903	T	C	20690	-	putative_membrane_protein

2477430	G	A	22960	narG	nitrate_reductase_alpha_chain
2529128	T	C	23420	-	hypothetical_protein
2586650	C	T	23950	sasG	LPXTG_surface_protein_(pseudogene)
2592008	C	A	23990	fnbA	fibronectin-binding_protein_FnbA
2632747	A	G	24370	-	transposase_(pseudogene)
2634271	A	G	24410	glcB	PTS_system,_glucose-specific_IIABC_component
2650324	T	C	24550	-	putative_transport_protein
2657496	G	A	24600	copA	putative_copper_importing_ATPase_A
2673509	T	C	24730	-	putative_membrane_protein
2682118	G	A	24840	-	alcohol_dehydrogenase
2702279	T	G	25060	ldh2	L-lactate_dehydrogenase_2
2737436	T	G	25350	clfB	fibrinogen_and_keratin-10_binding_surfaced_anchored_protein
2810244	G	A	25930	cna	collagen_adhesin_precursor
2810302	G	C	25930	cna	collagen_adhesin_precursor
2810622	G	A	25930	cna	collagen_adhesin_precursor
2810673	A	G	25930	cna	collagen_adhesin_precursor
2810748	G	A	25930	cna	collagen_adhesin_precursor
2810781	A	G	25930	cna	collagen_adhesin_precursor